

Marshall University

Marshall Digital Scholar

Theses, Dissertations and Capstones

2018

Targeted Limb Heating Augments the Actions of IGF1 in the Growth Plate and Increases Bone Elongation in Growing Mice

Holly Lyn Racine
tamski@marshall.edu

Follow this and additional works at: <https://mds.marshall.edu/etd>



Part of the [Animal Experimentation and Research Commons](#), [Animal Sciences Commons](#), [Musculoskeletal, Neural, and Ocular Physiology Commons](#), and the [Physiology Commons](#)

Recommended Citation

Racine, Holly Lyn, "Targeted Limb Heating Augments the Actions of IGF1 in the Growth Plate and Increases Bone Elongation in Growing Mice" (2018). *Theses, Dissertations and Capstones*. 1326.
<https://mds.marshall.edu/etd/1326>

This Dissertation is brought to you for free and open access by Marshall Digital Scholar. It has been accepted for inclusion in Theses, Dissertations and Capstones by an authorized administrator of Marshall Digital Scholar. For more information, please contact zhangj@marshall.edu, beachgr@marshall.edu.

TARGETED LIMB HEATING AUGMENTS THE ACTIONS OF IGF1 IN THE GROWTH
PLATE AND INCREASES BONE ELONGATION IN GROWING MICE

A dissertation submitted to
the Graduate College of
Marshall University
In partial fulfillment of
the requirements for the degree of
Doctor of Philosophy
in Biomedical Sciences

by

Holly Lyn Racine

Approved by

Dr. Maria A Serrat, Committee Chairperson

Dr. Richard Egleton

Dr. John Kopchick

Dr. Travis Salisbury

Dr. Monica Valentovic

Marshall University
December 2018

APPROVAL OF DISSERTATION

We, the faculty supervising the work of Holly Lyn Racine, affirm that the dissertation, *Targeted Limb Heating Augments the Actions of IGF1 in the Growth Plate and Increases Bone Elongation in Growing Mice*, meets the high academic standards for original scholarship and creative work established by the Biomedical Sciences program and the Graduate College of Marshall University. This work also conforms to the editorial standards of our discipline and the Graduate College of Marshall University. With our signatures, we approve the manuscript for publication.

Dr. Maria Serrat	 Committee Chairperson	8/6/2018 Date
Dr. Richard Egleton	 Committee Member	8/6/18 Date
Dr. John Kopchick	 Committee Member	8-15-18 Date
Dr. Travis Salisbury	 Committee Member	8/6/18 Date
Dr. Monica Valentovic	 Committee Member	AUG 6, 2018 Date

© 2018
Holly Lyn Racine
ALL RIGHTS RESERVED

DEDICATION

I would like to dedicate this work to my family who have supported me through the continuous ups and down along the journey to earn my PhD. I am thankful for my grandmother, Punky, she was always a call away to be my human thesaurus when I hit a mental roadblock in my writing. I would also like to specifically thank my mother, and best friend, she was there to listen to both my frustrations and excitement, provide professional advice, and also aided in giving me the time I needed to focus on my work (in other words, entertained my children). I am especially grateful to my husband Christopher. He guided me through it all and was always my biggest cheerleader. Last but not least, I want to dedicate this work to my daughters, Teegan and Milena, although I didn't know it at the time, everything I've worked for is for the two of them.

ACKNOWLEDGMENTS

I would like to thank Maria Serrat for being inspirational in this area of research and establishing the unilateral heating model fundamental to my study. I am also grateful to my colleagues, G. Ion and C. Meadows that were instrumental to the unilateral heating trials and assisting with data collection. I would also like to thank the VA Medical Center and CEB staff for their support throughout this project. I am grateful to Dr. Howard and the Marshall Animal Resource Facility for animal husbandry, assistance with equipment setup, and room temperature monitoring. This work was aided by the use of the facilities at the Huntington, West Virginia VA medical center. Research was made possible by the National Institute of Arthritis and Musculoskeletal and Skin Diseases of the National Institutes of Health (1R15AR067451-01). The content is solely the responsibility of the author and does not necessarily represent the official views of the National Institutes of Health.

TABLE OF CONTENTS

Approval of Dissertation.....	ii
Dedication.....	iv
Acknowledgments.....	v
List of Tables.....	xii
List of Figures.....	xiv
Abstract.....	xvii
Chapter I: In Depth Review into Longitudinal Bone Growth.....	1
1.1 Postnatal Longitudinal Bone Growth Through Endochondral Ossification.....	1
1.1.1 Endochondral Ossification and Growth Plate Morphology.....	1
1.1.2 Differential Growth of Long Bones.....	4
1.1.3 Age Comparison of Mouse and Man.....	6
1.1.4 Limb Length Discrepancy.....	10
1.2 Regulation of Growth Plate During Postnatal Linear Growth.....	14
1.2.1 Endocrine Regulation of Linear Growth.....	14
1.2.2 Autocrine/Paracrine Regulation of Linear Growth.....	15
1.3 Growth Hormone and Insulin-Like Growth Factor Regulate Linear Growth.....	16
1.3.1 Evolution of the Somatomedin Hypothesis.....	16
1.3.2 IGF Induced Signaling Pathway.....	21
1.3.3 GH and IGF1 Distinct and Overlapping Functions on Linear Growth.....	23

1.3.4	GH and IGF1 Treatment of Hormonal Deficiencies.....	24
1.4	IGF1 as a Primary Mediator of Longitudinal Bone Growth.....	26
1.4.1	Function of Locally Expressed IGF1.....	26
1.4.2	IGF1 Antagonists.....	28
1.5	Regulation of Linear Growth by Temperature.....	33
1.5.1	Temperature Regulates Linear Growth in Nature.....	33
1.5.2	Temperature Regulates Linear Growth in Laboratory Setting.....	33
1.5.3	Unilateral Heating Model Enhances Bone Lengthening.....	34
1.5.4	Potential Function of IGF1 in Heat-Enhanced Linear Growth.....	35
1.6	Role of Vasculature in Promoting Longitudinal Bone Growth.....	36
1.6.1	Vascular Supply of the Growth Plate.....	36
1.6.2	Transport of Systemic IGF1 into the Growth Plate.....	38
1.6.3	Chondrocyte Expression of Angiogenic Factors.....	39
1.7	Scope of Current Work.....	40
Chapter II: Functional Impact of Targeted Limb Heating in Mice.....		44
2.1	Introduction.....	44
2.2	Material and Methods.....	45
2.2.1	Animals and Experimental Design.....	45
2.2.2	Tibial Radiographs.....	49
2.2.3	Hindlimb Weight Bearing.....	51
2.2.4	Tissue Collection.....	51
2.2.5	Tibial Elongation Rate Analysis and Long Bone Measurements.....	52
2.2.6	Statistical Analysis and Sample Size.....	53

2.3 Results.....	54
2.3.1 Unilateral Heating Parameters.....	54
2.3.2 Bone Length and Tibial Elongation Rate.....	54
2.3.3 Hindlimb Weight Bearing.....	57
2.4 Discussion.....	59
2.5 Conclusion.....	60
Chapter III: Chondrocyte Proliferation and Hypertrophy in Tibial Growth Plates	
Increases After 7 Days of Targeted Limb Heating.....	62
3.1 Introduction.....	62
3.2 Material and Methods.....	63
3.2.1 Animals and Experimental Design.....	63
3.2.2 Tissue Collection.....	66
3.2.3 Tibial Elongation Rate Analysis and Long Bone Measurements.....	66
3.2.4 Growth Plate Morphometry.....	67
3.2.5 Immunohistochemistry.....	68
3.2.6 Statistical Analysis and Sample Size.....	71
3.3 Results.....	71
3.3.1 Unilateral Heating Parameters.....	71
3.3.2 Bone Length and Tibial Elongation Rate.....	74
3.3.3 Growth Plate Morphometry.....	77
3.3.4 PCNA Expression.....	80
3.4 Discussion.....	82
3.5 Conclusion.....	85

Chapter IV: Subcutaneous Injections of Low Dose IGF1 in Conjunction with Targeted Limb Heating Can Augment Heat-Enhanced Bone Growth.....	87
4.1 Introduction.....	87
4.2 Material and Methods.....	89
4.2.1 Animals and Experimental Design.....	89
4.2.2 Tissue Collection and Sample Analysis.....	92
4.2.3 Immunohistochemistry.....	92
4.2.4 Statistical Analysis and Sample Size.....	92
4.3 Results.....	93
4.3.1 Unilateral Heating Parameters.....	93
4.3.2 Length of Long Bones and Tibial Elongation Rate.....	96
4.3.3 Growth Plate Morphometry.....	100
4.3.4 PCNA Expression.....	103
4.3.5 IGF1R and pIGF1R Expression in Proliferating Chondrocytes.....	105
4.4 Discussion.....	108
4.5 Conclusion.....	115
Chapter V: IGF1 Is Essential For Heat-Enhanced Bone Elongation.....	116
5.1 Introduction.....	116
5.2 Material and Methods.....	118
5.2.1 Animals and Experimental Design.....	118
5.2.2 Tissue Collection and Sample Analysis.....	121
5.2.3 Immunohistochemistry.....	121
5.2.4 Statistical Analysis.....	121

5.3 Results.....	122
5.3.1 Unilateral Heating Parameters.....	122
5.3.2 Length of Long Bones and Tibial Elongation Rate.....	124
5.3.3 Growth Plate Morphometry.....	127
5.3.4 PCNA Expression.....	127
5.3.5 IGF1R, pIGF1R and pAkt Expression.....	131
5.3.6 <i>GHR</i> ^{-/-} Growth Parameters.....	137
5.4 Discussion.....	140
5.5 Conclusion.....	145
Chapter VI: Differential Limb Length is Maintained Throughout Skeletal Development	
After End of Treatment.....	146
6.1 Introduction.....	146
6.2 Material and Methods.....	147
6.2.1 Animals and Experimental Design.....	147
6.2.2 Tissue Collection and Long Bone Measurements.....	150
6.2.3 Statistical Analysis.....	150
6.3 Results.....	150
6.3.1 Unilateral Heating Parameters.....	150
6.3.2 Length of Long Bones Following 7 Days of Heating.....	154
6.3.3 Length of Long Bones Following 14 Days of Heating.....	157
6.4 Discussion.....	159
6.5 Conclusion.....	161

Chapter VII: Thermal Imaging Reveals Temperature Retention in Hindlimbs of Mice After Targeted Intermittent Limb Heating.....	163
7.1 Introduction.....	163
7.2 Material and Methods.....	164
7.2.1 Infrared Thermal Imaging.....	164
7.2.2 Statistical Analysis and Sample Size.....	167
7.3 Results.....	167
7.3.1 Temperature Retention in Hindlimbs Post-Heating.....	167
7.4 Discussion.....	170
7.5 Conclusion.....	174
Chapter VIII: Concluding Remarks and Future Directions.....	175
References.....	184
Appendix A: Institutional Review Board Approval.....	215
Appendix B: List of Abbreviations.....	216
Appendix C: Curriculum Vitae.....	219

LIST OF TABLES

Table 1	Mouse Models With Disrupted IGF1 Regulation.....	18
Table 2	Summary Of IGF1 Antagonists In Inhibiting Overall Growth.....	31
Table 3	Comparison of Hindlimb Weight Bearing and Tibial Length Measured by X-Rays.....	56
Table 4	List of Primary Antibodies and Secondary Antibody Kits Used in the Study.....	70
Table 5	Comparison of Non-Treated and Heat-Treated Sides of Saline-Injected Experimental Mice Bone Parameters.....	75
Table 6	Comparison of Growth Plate Morphometry Between Non-Treated and Heat-Treated Sides of Saline-Injected Experimental Mice.....	78
Table 7	Comparison of Non-Treated And Heat-Treated Sides of IGF1-Injected Experimental Mice Bone Parameters.....	98
Table 8	Comparison of Growth Plate Morphometry Between Non-Treated and Heat-Treated Sides of IGF1-Injected Experimental Mice.....	101
Table 9	Comparison of Non-Treated and Heat-Treated Expression of Markers for IGF1 Activation In Proliferative Zone of Tibial Growth Plates in Saline and IGF1-Injected Mice.....	106
Table 10	Comparison of Non-Treated and Heat-Treated Bone Parameters of 4-Week Old Saline- and JB1-Injected Mice Following 7 Days of Heat-Treatment.....	125

Table 11	Comparison of Non-Treated and Heat-Treated Expression of PCNA in Proliferative Zone of Tibial Growth Plates in Saline and JB1-Injected Mice.....	128
Table 12	Comparison of Non-Treated and Heat-Treated Expression of Markers for IGF1 Activation in Proliferative Zone of Tibial Growth Plates in Saline and JB1-Injected Mice.....	133
Table 13	Comparison of Non-Treated and Heat-Treated Expression of Markers for IGF1 Activation in Hypertrophic Zone of Tibial Growth Plates in Saline and JB1-Injected Mice.....	134
Table 14	Comparison of Non-Treated and Heat-Treated Bone Parameters of 5-Week Old Wild-Type and <i>GHR</i> ^{-/-} Mice.....	138
Table 15	Comparison of Mass Between Heat-Treatment Groups at The Start of Treatment and at Skeletal Maturity.....	152
Table 16	Comparison of Non-Treated and Heat-Treated Sides of Experimental Mice Bone Parameters Following 7 Days of Limb Heating.....	155
Table 17	Comparison of Non-Treated and Heat-Treated Sides of Experimental Mice Bone Parameters Following 14 Days of Limb Heating.....	158
Table 18	Summary of Concluding Remarks.....	182
Table 19	Summary of Future Directions.....	183

LIST OF FIGURES

Figure 1	Diagram of a Growth Plate.....	2
Figure 2	Developmental Stages During Postnatal Linear Bone Growth Compared Between Mouse and Man.....	8
Figure 3	GH/IGF1 Axis in Postnatal Limb Elongation.....	20
Figure 4	IGF1 Induced Intracellular Signaling Pathway.....	22
Figure 5	JB1 Blocks IGF1R Signaling.....	32
Figure 6	Diagram of the Unilateral Heating Method.....	48
Figure 7	Radiographs Collected Before and After Unilateral Heat-Treatment.....	50
Figure 8	Extremities are Lengthened on the Heat-Treated Side	55
Figure 9	Increase In Weight Bearing and Tibial Elongation Rate are Correlated After 7 Days of Unilateral Heat-Treatment.....	58
Figure 10	Unilateral Heating Schematic	65
Figure 11	Majority of Body Mass Gained During 14 Days of Unilateral Heat- Treatment Occurs During the First 7 Days.....	73
Figure 12	Extremities are Lengthened on the Heat-Treated Side	76
Figure 13	When Normalized to Total Proximal Tibial Growth Plate Height, PZ is Reduced on the Heat-Treated Side and HZ is Enlarged.....	79
Figure 14	Expression of PCNA, Marker for Cell Proliferation, Increased with Heat- Treatment in the PZ of the Proximal Tibial Growth Plate.....	81
Figure 15	Unilateral Heating Schematic	91
Figure 16	Overall Change in Mass was not Impacted by IGF1 Injections at Either Length of Heat-Treatment.....	95

Figure 17	Extremities are Lengthened on the Heat-Treated Sides when Injected with Saline and IGF1.....	99
Figure 18	Proximal Tibial Growth Plate Morphometry After Administration of Low Dose IGF1 with Targeted Heating.....	102
Figure 19	Expression of PCNA in the PZ of Proximal Tibial Growth Plates After Administration of Low Dose IGF1 with Targeted Heating.....	104
Figure 20	Heat-Induced Effect on IGF1 Activity in the PZ of the Tibial Growth Plate with IGF1 Administration.....	107
Figure 21	Unilateral Heating Schematic	120
Figure 22	Total Body Mass Gained in Mice Treated for 7 days from 3-4 weeks of Age did not Differ Between Saline Controls and JB1-Injected Mice.....	123
Figure 23	Heat-Enhanced Growth Effects are Attenuated when IGF1 is Blocked..	126
Figure 24	Expression of PCNA in the PZ of Proximal Tibial Growth Plates Decreased when IGF1 is Blocked.....	129
Figure 25	Expression of Markers of IGF1 Activation Decreases in Heat-Treated Proximal Tibial Growth Plates when IGF1 is Inhibited.....	135
Figure 26	Heat-Induced Effect on IGF1 Activity in the Tibial Growth Plate is Evident in the PZ and HZ.....	136
Figure 27	Extremities of Growth-Hormone Receptor Knockout (<i>GHR</i> ^{-/-}) Mice are not Lengthened with Unilateral Heat-Treatment.....	139
Figure 28	Unilateral Heating Schematic	149

Figure 29	Mass did not Differ Between Non-Treated Controls, Heat-Treated Saline Control Mice, and Heat-Treated IGF1-Injected Mice at Either Duration of Limb Heating.....	153
Figure 30	Extremities Remained Longer on the Heat-Treated Sides at Skeletal Maturity when Limb Heating was Coupled with IGF1 Administration.....	156
Figure 31	Infrared Thermal Imaging Schematic.....	166
Figure 32	Thermal Imaging Shows Hindlimb Surface Temperature Remains Elevated up to 4 Hours Post-Heating.....	169
Figure 33	Expression of VEGF and CD31 Appeared to Increase in the Growth Plate on the Heat-Treated Sides.....	173
Figure 34	Diagram Summarizes the Action of Important Factors in the Different Zones of the Growth Plate.....	180

ABSTRACT

Bone elongation disorders can lead to painful musculoskeletal disabilities in adulthood. Existing treatment options to correct left-right asymmetry in limb length include invasive surgeries and/or drug regimens. These are often only partially effective. Previous studies in weanling mice have shown that a daily application of mild heat (40°C) to limbs on one side of the body could be used to noninvasively enhance bone elongation. However, the impact of heat-treatment on bone at the cellular level remains elusive. The epiphyseal growth plate, the band of cartilage located at each end of long bones, is the main site of longitudinal growth and is regulated by local and systemic growth factors. Insulin-like growth factor 1 (IGF1) is the major regulator of growth and controls bone elongation by promoting chondrocyte proliferation and hypertrophy. The objective of this study was to build upon an established method of targeted limb heating to determine how heat-treatment influences IGF1 action in the growth plate. This study tests the **hypothesis that exposure to warm temperature augments the actions of IGF1 in the growth plate and permanently increases length of the extremities**. This dissertation demonstrates that differences of less than 1.5% are functionally significant measured by a nearly 20% increase in hindlimb weight bearing on heat-treated sides. Heat-enhanced bone elongation is documented in female C57BL/6 mice after 7 days of heat-treatment during the most active period of growth from 3-4 weeks of age. This increase in bone elongation is accompanied by increased chondrocyte proliferation and hypertrophy in the proximal tibial growth plate. Moreover, this study is the first to show that targeted limb-heating impacts local action of IGF1 in growth plate chondrocytes. Results suggest that heat-induced limb length is IGF1 dependent since the growth

effects are attenuated when IGF1 activity is blocked. Administration of a low dose of IGF1 (2.5mg/kg) was found to augment heat enhanced bone elongation and effects were sustained to skeletal maturity (12 weeks of age). These studies help contribute to the ultimate goal of developing a noninvasive method for lengthening bones that may translate in a clinical setting to treat linear growth disorders in children.

CHAPTER I: IN DEPTH REVIEW INTO LONGITUDINAL BONE GROWTH

1.1 POSTNATAL LONGITUDINAL BONE GROWTH THROUGH ENDOCHONDRAL OSSIFICATION

1.1.1 Endochondral Ossification and Growth Plate Morphology

The skeleton develops by means of two different mechanisms: (1) Intramembranous ossification, involving direct differentiation of mesenchyme cells to bone as with the development of the flat bones of the skull and (2) Endochondral ossification, occurring when mesenchyme cells condense and differentiate into cartilage tissue, which then is replaced by bone forming the vertebrae, ribs and limbs (Gilbert, 2014). Endochondral ossification is initiated during fetal life but continues from infancy through adolescence (transitional period from childhood to adulthood). Cartilaginous growth plates found at each end of developing long bones are responsible for longitudinal bone growth (or linear growth). Longitudinal bone growth increases the length of long bones during postnatal development and is mediated by the growth plate. Growth plate cartilage is composed of cells known as chondrocytes that secrete extracellular matrix and are organized into functional zones (Fig. 1).

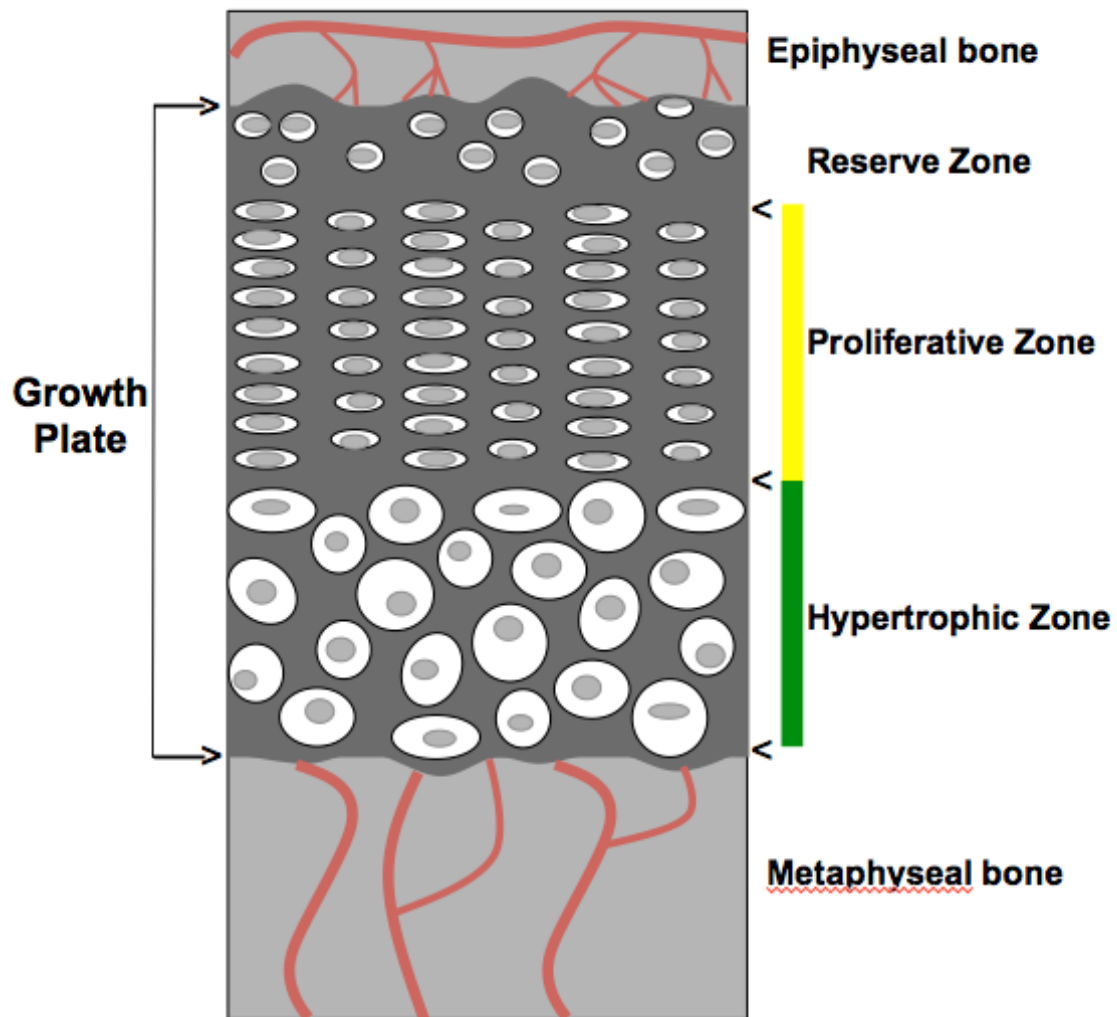


Figure 1. Diagram of a Growth Plate

Illustration represents the different cellular zones of the cartilaginous growth plate (dark gray). Arrows indicate the different zones within the growth plate. The vertical yellow line denotes the proliferative zone (PZ) and the green line denotes the hypertrophic zone (HZ). The PZ is a region of actively dividing chondrocytes stacked and flattened in multicellular columns. The HZ is a region of enlarged chondrocytes. Epiphyseal and metaphyseal bone on each end of the growth plate contain blood vessels (red lines) that supply each region of bone. Illustration based on Mackie, Ahmed, Tatarczuch, Chen, and Mirams (2008).

The cartilaginous growth plate functions as the command center of longitudinal bone growth. Understanding the general morphology of the growth plate is beneficial for appreciating its overall function. The end portion of the long bone is referred to as the epiphysis and the shaft of each long bone is termed the diaphysis. Directly between the epiphysis and the diaphysis is metaphysis, which contains the growth plate. The region adjacent to the epiphysis is the first zone of the growth plate, or the reserve zone (RZ). The RZ consists of round quiescent chondrocytes. The role of the RZ has been debated but is most commonly reported to act as the coordinator for the organization and orientation of the neighboring proliferative zone (PZ) (Abad et al., 2002). It has been suggested that the RZ contains stem-like cells that promote the production of proliferative chondrocytes and that this proliferative capacity decreases with age aiding to the closure of the growth plate associated with skeletal maturity (Abad et al., 2002; Hunziker, 1994b; Raimann, Javanmardi, Egerbacher, & Haeusler, 2017; Schrier et al., 2006). Adjacent to the RZ is the PZ containing rapidly dividing chondrocytes stacked and flattened in multicellular columns. The PZ is a region of actively dividing cells that directs longitudinal growth along the long axis by which the cells line up in their arranged columns.

The proliferating chondrocytes at the base of the columns make the transition from the PZ to the hypertrophic zone (HZ) where chondrocytes behave as terminally differentiated cells that begin to enlarge, secrete extracellular matrix and ultimately undergo physiological death (Kronenberg, 2003; Mackie et al., 2008; Shapiro, Adams, Freeman, & Srinivas, 2005; Ulici, Hoenselaar, Gillespie & Beier, 2008). Hypertrophic chondrocytes induce vascular invasion and recruit osteogenic cells in the process of

endochondral ossification and the replacement of cartilage with bone at the chondro-osseous junction (region of growth cartilage between the growth plate and the newly mineralized bone). A majority of the bone-forming osteoblasts are said to be differentiated from bone marrow stromal cells. However, current research in the mammalian growth plate suggests that not all hypertrophic chondrocytes undergo apoptosis but instead transdifferentiate into osteoblasts during both bone development and repair (Bahney et al., 2014; Enishi et al., 2014; Hu et al., 2017; Zhou et al., 2014). Studies by Bahney et al. (2014) used cartilage grafts to promote bone regeneration through endochondral ossification (analogous to long bone development), and results from lineage tracing experiments showed chondrocytes differentiated into osteoblasts during bone repair. It is suggested that transdifferentiation occurs adjacent to the vasculature at the chondro-osseous junction and that the vasculature may have a signaling role in the transformation of chondrocytes to osteoblasts (Hu et al., 2017). It is not yet known if these chondrocytes undergo the same process of transdifferentiation during development as they do during repair.

1.1.2 Differential Growth of Long Bones

While the anatomical structure of the cartilaginous growth plate is comparable between the developing long bones, the rate at which these growth plates contribute to longitudinal bone growth differs from bone to bone, and from proximal end to distal end. This phenomenon is referred to as differential growth (Digby, 1916; Payton, 1932). The humerus, radius and ulna are the major long bones of the upper limb (excluding the hand and foot), and the lower limb includes the femur and tibia. When comparing

proximal to distal ends of these bones, the faster-growing sites are located at the proximal humerus (shoulder), distal radius and ulna (wrist), and distal femur and proximal tibia (knee) (J. Bisgard & M. Bisgard, 1935; Farnum, 2007; Kember, 1972; Pritchett, 1992; Raimann et al., 2017; Serrat, Lovejoy, & King, 2007; Wilsman, Farnum, Green, Leiferman, & Clayton, 1996a; Wilsman, Farnum, Leiferman, Fry, & Barreto, 1996b; Wilsman, Bernardini, Leiferman, Noonan, & Farnum, 2008). Based on peak growth rates, the most rapid developing growth plate in humans and rodents is at the proximal end of the tibia followed by the distal femur (knee), distal radius (wrist), and proximal humerus (shoulder) (Rolian, 2008). Wilsman et al. (2008) have shown in rats that the proximal tibial growth plate (growth rate of 396 $\mu\text{M}/\text{day}$) is nearly nine times faster than the much slower proximal radial growth plate (growth rate of 47 $\mu\text{M}/\text{day}$).

The main factors contributing to increasing length of long bones and differential growth are the number of columnar cells in the PZ, the rate of proliferation, and the size of expanded cells in the hypertrophic zone (Hunziker, Schenk, & Cruz-Orive, 1987; Hunziker, 1994b; Kember, 1993; Lupu, Terwilliger, Lee, Segre, & Efstratiadis, 2001; Walker & Kember, 1972). Investigators have observed increased numbers of proliferative chondrocytes, increased rates of proliferation, and hypertrophic chondrocyte expansion in the faster-growing sites (Cooper et al., 2013; Farnum, 2007; Hunziker & Schenk, 1989; Kember, 1972; Raimann et al., 2017; Rolian, 2008; Serrat et al., 2007; Wilsman et al., 1996a, 1996b, 2008). Therefore, the cellular components of the growth plate are involved in regulating the process of endochondral bone development and linear growth.

1.1.3 Age Comparison of Mouse and Man

A common model organism in the study of bone growth is the rodent, particularly the house mouse (*Mus musculus*). The murine model is beneficial because the mouse is small in size, cost-effective, easily available, and shares physiological similarities to humans making the mouse the most widely used animal (~59% of total animals used) in biomedical research (Dutta & Sengupta, 2016). However, mice have a shorter lifespan (~24 months) compared to humans (~80 years) (Dutta & Sengupta, 2016). While there may be a momentous difference in lifespan between mice and humans, it allows for accelerated projects when following the mouse throughout stages of development.

Mouse age during different phases of postnatal growth is comparable to human age (Fig. 2). At birth, until approximately 2-3 weeks of age, mice rely completely on their mother for temperature regulation and food. At 3-4 weeks of age, pups will wean and become independent (Dutta & Sengupta, 2016; Latham & Mason, 2004). This phase of natural weaning that is the transition from exclusive nursing to nourishment by other food, is comparable to a 6-month-old infant (Dutta & Sengupta, 2016; Sengupta, 2013; Vail et al., 2015). While longitudinal growth is rapid during early postnatal stages of development, there is a progressive decline in this rate of active growth with approaching maturity. In mice, the accelerated rate of post weaning bone growth is from 3-4 weeks of age, then gradually decelerates from 4-8 weeks of age, and significantly slows between 8-12 weeks of age (Callewaert et al., 2010; Li et al., 2017; Lui, Nilsson, & Baron, 2011) (Fig. 2). In humans, rapid linear growth is observed from infancy to childhood (6 months-3 years), decelerates from childhood through adolescence (3-16

years), and stops at adulthood (18-20 years) (Armstrong, 2007; Dutta & Sengupta, 2016; Sengupta, 2013) (Fig. 2).

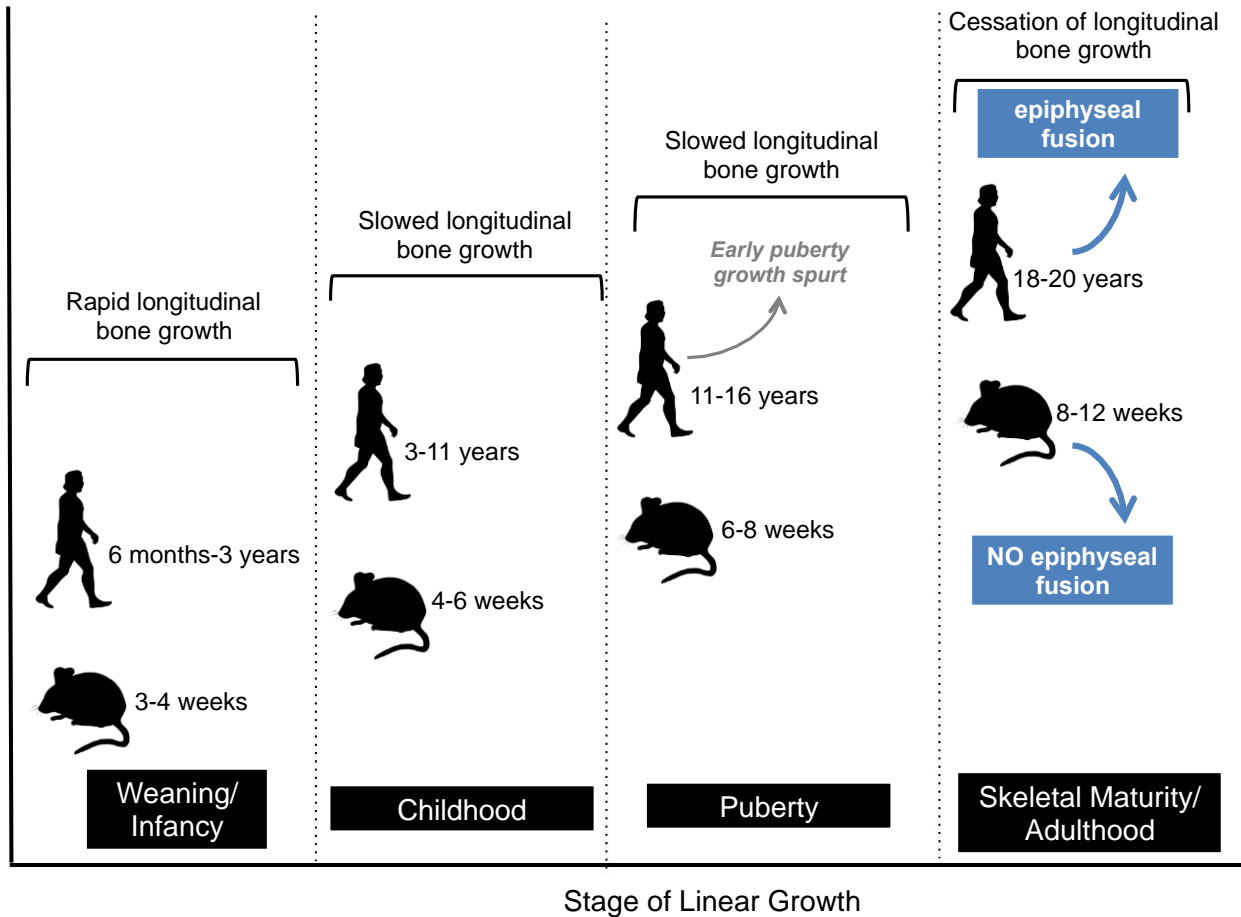


Figure 2. Developmental Stages During Postnatal Linear Bone Growth Compared Between Mouse and Man

Diagram follows the appropriate age ranges of a human with the comparative ages of a mouse during stages of linear growth. Rates of longitudinal bone growth are also noted during each developmental stage. Both human and mouse follow similar trends in linear growth with the exception of epiphyseal closure (indicated by the blue boxes). At the end of puberty, cessation of growth at the human growth plate is accompanied by epiphyseal fusion. No epiphyseal fusion is observed in the mouse. There is also an early pubertal growth spurt specific to humans that interrupts the decline in linear growth (gray). Mouse and human silhouettes provided by GetDrawings.com.

Puberty, when reproduction becomes possible, is reached in mice at 6-8 weeks (Jilka, 2013; Latham & Mason, 2004; Dutta & Sengupta, 2016) and 11-16 years in humans on average (Chirwa, Griffiths, Maleta, & Cameron, 2014; Dutta & Sengupta, 2016; Lee, 1980; Kelly & Diméglio, 2008). Although linear bone growth progressively slows with age, this decline in growth rate is interrupted by an early pubertal growth spurt in humans (Li et al., 2017; Lui et al., 2011; Nilsson & Baron, 2004; Shim, 2015). During this time, increased rates of chondrocyte proliferation and hypertrophy within the growth plate are observed. This growth spurt is one reason why there is concern for childhood sport related physeal injuries, which are most common between 10-16 years of age (Grimmer, Jones, & Williams, 2000; Schwab, 1977) and account for 6-15% of youth fractures (Hunt & Amato, 2003). Disturbances during this period of developing growth cartilage can result in growth deformities (Caine, DiFiori, & Maffaulli, 2006; Mirtz, Chadler, & Eyers, 2011).

Eventually a cessation of growth plate activity occurs as final adult height is reached. The cessation of longitudinal bone growth, also referred to as growth plate senescence, involves decreased rates of chondrocyte proliferation and hypertrophy (Forcinito et al., 2011; Lui et al., 2011; Nilsson & Baron, 2004; Nilsson et al., 2014; Walker & Kember, 1972). There is variation in time of closure between bones, but faster-growing sites such as in the proximal tibia close later (16-18 years of age in a human) than slower growing sites such as in the proximal radius (14-16 years of age in a human) (Schwab, 1977; Zoetis, Tassinari, Bagi, Walthall, & Hurtt, 2003). The process of growth plate senescence varies from species to species (Geiger, Forasiepi, Koyabu, & Sánchez-Villagra, 2014; Kilborn, Trudel, & Uthoff, 2002). In humans, growth plate

cessation at the end of puberty is accompanied by epiphyseal fusion and the formation of a bony union (Geiger et al., 2014; Nilsson & Baron, 2004; Parfitt, 2002). In mice, there is not a complete closure of the growth plate (Dawson, 1925, 1935; Geiger et al., 2014). The lack of complete epiphyseal fusion in mice contributes to complications in forming a direct comparison to humans. However, research has shown that even without complete closure, growth plate senescence still occurs at comparable developmental periods with similar cellular kinetics (Dawson, 1925, 1935; Geiger et al., 2014; Walker & Kember, 1972). Skeletal maturity, not to be confused with sexual maturity, is similar between mice (8-12 weeks of age) (Kilborn et al., 2002; Li et al., 2017; Serrat et al., 2007; Stempel, Fritsch, Pfaller, & Blumer, 2011; Zoetis et al., 2003) and humans (18-20 years of age) (Duren, Seselj, Froehle, Nahhas, & Sherwood, 2013; Dutta & Sengupta, 2016; Schwab, 1977) in regard to the proportion of their lifespan (Kilborn et al., 2002). When skeletal maturity is reached, chondrocyte proliferation, hypertrophy and longitudinal growth essentially stops despite the presence of a previously active growth plate.

1.1.4 Limb Length Discrepancy

An orthopedic condition that is characterized by asymmetric length of lower extremity pairs is referred to as anisomelia, or limb length discrepancy (LLD) (Baker, Liu, Robertson, & Efstratiadis, 1993; Gurney, 2002). LLD usually emerges during childhood but the etiology varies and may be congenital, acquired or idiopathic. Prior to the development of the polio vaccine in the 1960s, the most common cause of LLD in children was poliomyelitis (viral infection causing paralysis) that resulted in leg

shortening (Morscher, 1977; Wilson & Thompson, 1939). While polio has been eliminated from the United States, treatment options are still studied for middle-aged patients suffering from long-term LLD as a result of poliomyelitis developed during their childhood (Kirienko et al., 2011; Sonekatsu, Sonohata, Kitajima, Kawano, & Mawatari, 2018). Aside from paralysis, other acquired causes of LLD include infection, tumors, and trauma (Morscher, 1977; Shapiro, 1982; Wilson & Thompson, 1939). LLDs caused by trauma most commonly involve epiphyseal fractures (shortening on the fractured side) and meta- and diaphyseal fractures (lengthening on the fractured side) (Hansson, Stenström, & Thorngren, 1976; Morscher, 1977; Shapiro, 1982; Togrul, Bayram, Gulsen, Kalaci, & Ozabarlas, 2005; Truesdell, 1921; Wilson & Thompson, 1939; Wray & Goodman, 1961). Regardless of the cause of the LLD, untreated inequalities into adulthood have been associated with painful musculoskeletal disorders (Campbell, Ghaedi, Ghongomu, & Welch, 2018; Gurney, 2002) including lower back pain (Friberg, 1983; Defrin, Ben Benyamin, Aldubi, & Pick, 2005), gait abnormalities (Aiona, Do, Emara, Dorociak, & Pierce, 2015; Kaufman, Miller, & Sutherland, 1996; Khamis & Carmeli, 2017; Mahmood, Huffman, & Harris, 2010; Song, Halliday, & Little, 1997), scoliosis (abnormal curvature of the spine) (Papaioannou, Stokes, & Kenwright, 1982), and osteoarthritis of the hip and knee (Golightly, Tate, Burns, & Gross, 2007a; Golightly et al., 2007b; Harvey et al., 2010; Resende, Kirkwood, Deluzio, Morton, & Fonseca, 2016).

The severity of limb length discrepancy varies depending on the condition, as well as the onset of acquired cases. Limb length inequalities of 2 cm or more involve surgical methods of treatment with intentions of permanently correcting unequal length

of limbs (Gurney, 2002; Stevens, 2016; Vitale et al., 2006; Zhang, Hamamura, Turner, & Yokota, 2010). Limb shortening is recommended for limb length inequalities of 2-5 cm using epiphysiodesis procedures (Stevens, 2016). This method involves shortening the longer limb by either permanently halting growth from a surgically formed bony bridge (Phemister, 1933) or temporarily slowing of growth using guided growth techniques (Pendleton, Stevens, & Hung, 2013; Sabharwal, Nelson, & Sontich, 2015; Stevens, 2016). Limb lengthening is recommended for those with limb length inequalities over 5 cm (Stevens, 2016) and includes methods based off the traditional Ilizarov technique using external fixators (Ilizarov, 1988) or by mechanical bone guidance (Hasler & Krieg, 2012). The aforementioned surgical interventions involve a variation of percutaneous drilling and use of external and internal fixation devices (including a cortical screw surgically placed through the epiphysis, across the growth plate, and into the metaphysis). In addition to the high cost of these invasive procedures, they are also often associated with complications including pain, implant failure, angular deformities and infection (Hasler & Krieg, 2012; Wilson & Thompson, 1939).

For relative comparison, a 2 cm discrepancy is roughly equivalent to a 2.8-2.4% difference using a reference limb length of 72-82.5 cm (total height minus sitting height averaged from mean male and female reference data) corresponding to a 10-16 year old adolescent (Fredricks et al., 2005; McDowell, Fryar, & Ogden, 2009) during the period of sexual maturity/puberty (Fig. 2) when still growing but approaching final height. A 5 cm discrepancy is therefore roughly equivalent to a 6.9-6.1% difference. It is important to note that these percent differences based on total limb length vary through development until final height is reached. At final height (reference limb length of 85 cm

for a young adult), a 2 cm discrepancy is a difference of 2.4%, while a 5 cm discrepancy is a difference of 5.9% (Fredricks et al., 2005; McDowell et al., 2009; Racine, Meadows, Ion, & Serrat, 2018).

The projected limb length discrepancy at the point of maturity varies between congenital cases (based on a fixed limb length inequality) and acquired cases (based on how much limb growth remains) (Kelly & Diméglio, 2008). There have been numerous methods of predicting final limb length including the Green-Anderson method (Anderson, Green, & Messner, 1963), Menelaus method (Menelaus, 1966), Moseley method (Moseley, 1977), and Paley method (Paley, Bhave, Herzenberg, & Bowen, 2000). The predicated final limb length discrepancy varies vastly between these methods (Monier, Aronsson, & Sun, 2015) and thus there is not one method that is more accurate than another. Therefore, determining the most effective timing to start treatment is difficult and can lead to possible over- or under-compensation for the observed unequal limb length. When the correction is not successful, either because of surgical failure or miscalculated predictions of final limb length discrepancy, surgical interventions have to be repeated (Stevens, 2016) and therefore increase the risk of post-surgical complications.

While surgical intervention is typically recommended only for discrepancies of 2 cm or more (Gross, 1978; Gurney 2002; Knutson, 2005), some studies have shown that discrepancies of 0.5-1 cm (0.6-1.2% limb length difference based on young adult height) may impact everyday walking (White, Gilchrist, & Wilk, 2004) leading to problems into adulthood including knee osteoarthritis (Harvey et al., 2010; Resende et al., 2016). Conservative methods of correction are typically recommended for those with these

minor limb length inequalities such as shoe lifts or prosthetics (Campbell et al., 2018; Hasler & Kreig, 2012; Wilson & Thompson, 1939). While inexpensive and less invasive, these methods do not permanently change the length of the bone. An alternative non-invasive method for permanently lengthening limbs would therefore be ideal. A study by Zhang et al. (2010) showed that applying intermittent 0.5 N lateral loads to the knee joints of mice (~8-weeks old) increased femoral (2.3%) and tibial length (3.7%). This increase in limb length is noteworthy because treatment occurred during slower rates of longitudinal bone growth when mice were close to reaching skeletal maturity. Long-term effects of these studies have also not yet been done. Serrat et al. (2015) demonstrated that using once daily targeted limb heating (40°C for 40mins/day) to unilaterally increase femoral (1.3%) and tibial (1.5%) length of growing mice (3-5 weeks of age) is another non-invasive alternative to treating limb length discrepancies. At skeletal maturity (12 weeks of age), femoral (1.0%) and tibial (1.0%) lengths remained significantly increased on the heat-treated sides (Serrat et al., 2015).

1.2 REGULATION OF GROWTH PLATE DURING POSTNATAL LINEAR GROWTH

1.2.1 Endocrine Regulation of Linear Growth

The process of postnatal longitudinal growth is tightly controlled by 1) endocrine actions by molecules, such as hormones, distributed in the blood that act on target cells of the growth plate, and 2) paracrine/autocrine actions by locally produced factors expressed in epiphyseal chondrocytes or surrounding perichondrium. Mutations in genes encoding any of these regulators result in dysfunctional chondrocytes, abnormal longitudinal growth, and skeletal dysplasia including short-limbed dwarfism. By

endocrine action, systemic factors shown to regulate longitudinal growth include growth hormone (GH), insulin-like growth factor 1 (IGF1), thyroid hormone, estrogen, androgen, glucocorticoids, and vitamin D (Börjesson et al., 2010; van der Eerden, Karperien, & Wit, 2003; Lui, Nilsson, & Baron, 2014; Ohlsson et al., 1993; Simpson, Asling, & Evans, 1950; Tryfonidou et al., 2010; Wang, Shao, & Ballock, 2010). For example, while circulating thyroid hormone has been shown to increase longitudinal bone growth indirectly by increasing systemic GH secretion (Ohlsson et al., 1993), it also has been shown to directly interact with the epiphyseal chondrocytes and initiate terminal differentiation (Ohlsson, Nilsson, Isaksson, Bentham, & Lindahl, 1992a; Stevens et al., 2000).

1.2.2 Autocrine/Paracrine Regulation of Linear Growth

In regards to autocrine/paracrine regulation within growth plate cartilage, locally acting factors reported include Indian hedgehog (Ihh), parathyroid hormone-related protein (PTHrP), fibroblast growth factors (FGFs) (including FGF1, -2, -9 and -18), bone morphogenic proteins (BMPs) (including BMP2-7), vascular endothelial growth factor (VEGF), IGF1, and Wnt (van der Eerden et al., 2003; Karimian, Chagin, & Säwendahl, 2012; Kronenberg, 2003; Lui et al., 2014; Maeda, Schipani, Densmore, & Lanske, 2010; Tryfonidou et al., 2010; Wang et al., 2010). Different regional zones of growth plate chondrocytes are regulated by particular factors. For instance, regulation of prehypertrophic chondrocytes (chondrocytes at maturation that no longer proliferate) in the region between the proliferative zone and hypertrophic zone, have been characterized by the expression of signaling molecules responsible for the successful

and timely transition from proliferative to hypertrophic chondrocytes. These include FGF receptors (Lazarus, Hedge, Andrade, Nilsson, & Baron, 2007; Su, Jin, & Chen, 2014), BMPs (Garrison, Yue, Hanson, Baron, & Lui, 2017; Nilsson et al., 2007), and Ihh/PTHrP receptors (Vortkamp et al., 1996).

Often, it has been shown that longitudinal bone growth is controlled by the collaboration of both endocrine and paracrine/autocrine actions when systemic factors interact with locally expressed factors of the growth plate cartilage to promote chondrocyte proliferation and hypertrophy. Among these interactions, estrogen (endocrine) has been shown to regulate expression of IGF1 (autocrine/paracrine) in growth plate chondrocytes (Börjesson et al., 2010). Thus, in addition to the independent influences of systemic and local factors on the growth plate, there are important interactions between regulators to maintain growth. While the impact of some factors (such as IGF1) act predominantly over others, there is no evidence supporting that one is mutually exclusive from the rest in regulating longitudinal bone growth. There is still much to be understood regarding the molecular mechanisms involved in linear growth and further research will lead to a greater depth of comprehension.

1.3 GROWTH HORMONE AND INSULIN-LIKE GROWTH FACTOR REGULATE LINEAR GROWTH

1.3.1 Evolution of the Somatomedin Hypothesis

GH and IGFs have an integral role in maintaining normal growth and development. The original understanding of the means by which GH and IGFs regulate growth was set into motion after experiments conducted in 1957 by Salmon and Daughaday (Salmon & Daughaday, 1957). In the early 1970s, the same group in

addition to other investigators referred to their findings as the somatomedin hypothesis, which described pituitary-gland derived GH to act upon the liver to secrete an intermediate hormone stimulating somatic growth (Daugaday et al., 1972). The intermediates were termed insulin-like growth factor 1 (IGF1) and insulin-like growth factor 2 (IGF2) (also referred to as somatomedin C and A) later in the decade (Rinderknecht & Humbel, 1978a,b). Both factors are important for growth and development and when disrupted display abnormal phenotypes (Table 1).

Table 1. Mouse Models with Disrupted IGF1 Regulation

Model	Phenotype	Citation
<i>Igf1</i> null mice (global IGF1 disruption)	95% mice died prenatally; undetectable levels of IGF1 in serum and tissues; significant decrease in tibial length (70%); abnormal chondrocyte proliferation and differentiation	Baker et al., 1993 Bikle et al., 2001 Powell-Braxton et al., 1993 Wang et al., 2006
<i>Igf2</i> null mice (global IGF2 disruption)	Mice are viable; reduced body growth (60%) at birth; normal postnatal growth	DeChiara, Efstratiadis, & Robertson, 1990 Yakar et al., 1999
LID mice (systemic disruption of liver-derived IGF1)	75% reduction in serum IGF1; no significant change in body length; no significant change in tibial length; slight decrease in femoral length (6%)	Sjögren et al., 1999 Yakar et al., 1999
ALS knockout mice (systemic disruption ternary complexes (IGF1/ALS/IGFBP-3))	65% reduction in serum IGF1; no significant change in body length; slight decrease in femoral length (7.5%)	Ueki et al., 2000
LID+ALSKO mice (systemic disruption of liver-derived IGF1 and ternary complexes (IGF1/ALS/IGFBP-3))	85-90% reduction in serum IGF1; significant reduction in body length (30%); significant decrease in femoral length (20%)	Yakar et al., 2002
(Col2a1)-driven Cre mice (local disruption of chondrocyte-derived IGF1)	40% reduction in chondrocyte IGF1; Significant decrease in postnatal body length; no morphological differences in proliferative and hypertrophic regions	Govoni et al., 2007a
^{Cart} <i>Igf1r</i> ^{-/-} mice (local disruption of cartilage-specific IGF1R)	Mice died shortly after birth	Wang et al., 2011
Tam ^{Cart} <i>Igf1r</i> ^{-/-} mice (local disruption of cartilage-specific IGF1R induced by tamoxifen injections)	Significant decrease in body length (40%); disorganized growth plates associated with reduced chondrocyte proliferation and differentiation	Tahimic, Wang, & Bikle, 2013 Wang et al., 2011 Wu, Yang, & De Luca, 2015

The introduction of the dual effector theory in 1985 disputed the original somatomedin hypothesis and proposed an additional IGF1-independent role of GH (Green, Morikawa, & Nixon, 1985). This revision came with reports of local IGF1 production in nonhepatic tissues, including bone (Tahimic et al., 2013) demonstrating that IGF1 acts as both an endocrine and autocrine/paracrine factor. In the growth plate, investigators found that GH directly stimulated cell differentiation in the RZ of precursor cells, while local IGF1 production mediated clonal expansion of the resulting PZ chondrocytes (Isaksson, Jansson, & Gause, 1982, Isaksson, Eden, & Jansson, 1985; Ohlsson et al., 1992a; Ohlsson, Nilsson, Isaksson, & Lindahl, 1992b; Ohlsson, Bengtsson, Isaksson, Andreassen, & Słotweg 1998; Schlechter, Russell, Greenberg, Spencer, & Nicoll, 1986). Recent research also supports the direct contribution of GH acting on the growth plate independent of IGF1 (Dobie et al., 2015; Wu et al., 2015). The evolution of the somatomedin hypothesis incorporates an adaptation of previous theories to describe a more complex interplay between GH and IGF1, including negative feedback mechanisms where IGF1 inhibits further GH production (Moody et al., 2014). The interaction between IGF1 and GH is commonly referred to as the GH/IGF1 axis (Fig. 3).

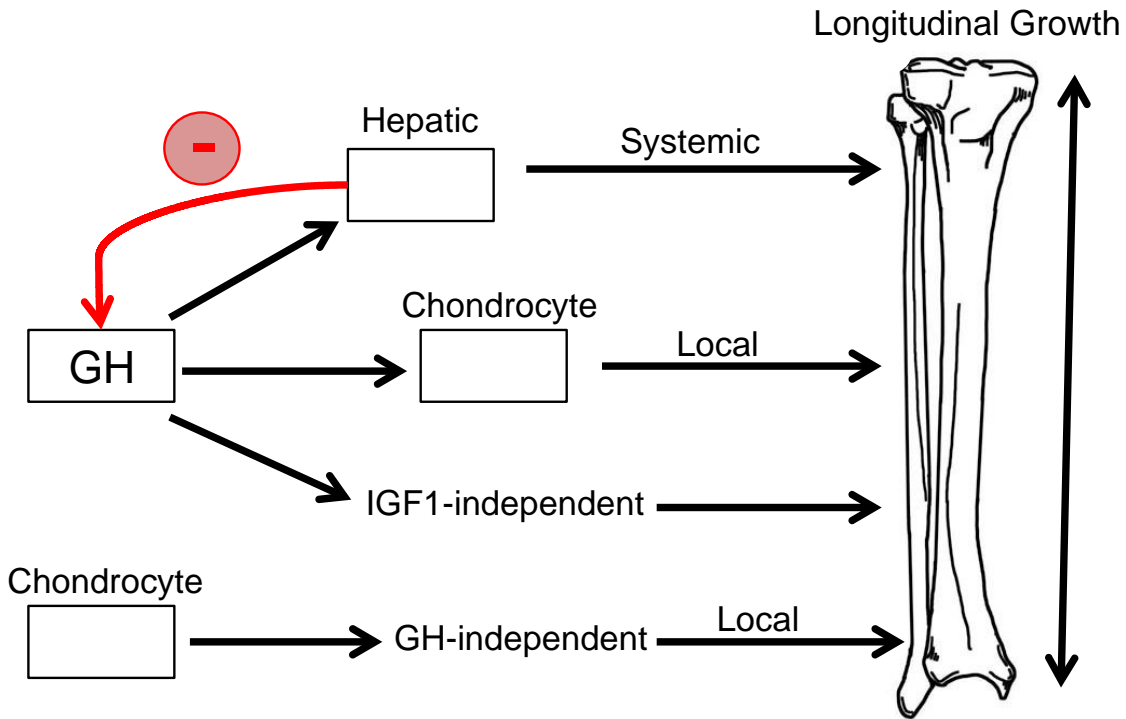


Figure 3. GH/IGF1 Axis in Postnatal Limb Elongation

Flow diagram illustrates the complex interplay between GH and IGF1 in promoting longitudinal bone growth. In addition to stimulating IGF1 production in the liver as originally proposed in the somatomedin hypothesis, GH also stimulates longitudinal growth (1) by promoting local production of IGF1 in growth plate chondrocytes and (2) independent of IGF1 as explained by the dual effector theory. IGF1 also has autocrine/paracrine effects independent of GH promoting longitudinal growth locally in growth plate chondrocytes. The red arrow demonstrates the negative feedback mechanism of IGF1 inhibiting further GH synthesis and release. Tibia illustration provided with permission by Amsel S on Exploring Nature Educational Resources (2018).

1.3.2 IGF Induced Signaling Pathway

IGF binding protein-3 (IGFBP-3) is the major carrier of IGFs. In serum, majority of IGFs (~75%) exist in a ternary complex of one molecule each of IGF1, IGFBP-3, and the acid labile subunit (ALS) (Holman & Baxter, 1996; Yakar et al., 2002). The ternary complex prolongs the half-life of serum IGFs and regulates transport from the circulation to the target tissue (Baxter, 2000; Holman & Baxter, 1996; Le Roith, Bondy, Yakar, Liu, & Butler, 2001). Similar to IGF1, IGF2 binds to IGFBPs (Baxter, 2000; Le Roith et al., 2001). Upon release at the surface of the target tissue, both IGFs are capable of binding to the receptor tyrosine kinase type 1 IGF receptor (IGF1R) (Le Roith et al., 2001) expressed in all regions of the growth plate (Parker et al., 2007; E. Wang, J. Wang, Chin, Zhou, & Bondy, 1995). The activation of the IGF1R leads to a signaling cascade involving the phosphatidylinositide 3-kinase (P13K) and mitogen-activated protein kinase (MAPK) pathways ultimately leading to cell survival and proliferation, which contributes to longitudinal growth rate (Fig. 4). IGF2 is classically described to be essential only during prenatal growth (DeChiara et al., 1990; Lund et al., 1986; Yakar et al., 1999), whereas IGF1 is expressed at low levels during embryonic development and is important for postnatal growth (Baker et al., 1993; Liu, Baker, Perkins, Robertson, & Efstratiadis, 1993; Powell-Braxton et al., 1993). Evidence supports that IGF1 is more critical to postnatal longitudinal bone growth compared to IGF2 because the postnatal phenotype of the *Igf1* null is more severe than the *Igf2* null mice (see Table 1) (Baker et al., 1993; DeChiara et al., 1990; Liu et al., 1993; Yakar et al., 1999).

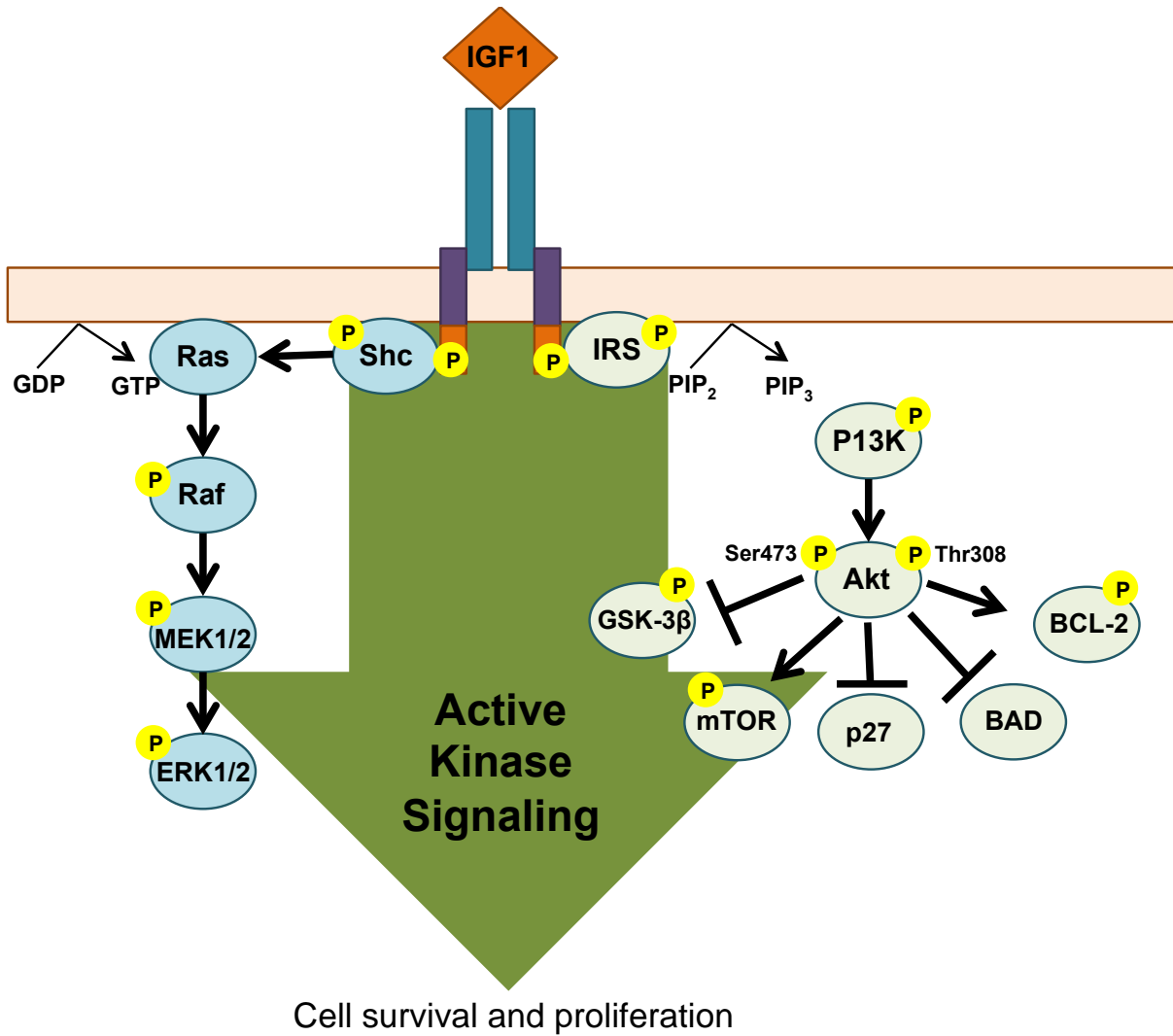


Figure 4. IGF1 Induced Intracellular Signaling Pathway

Model demonstrates how IGF1 functions as a ligand and binds to its receptor (IGF1R) triggering two downstream signaling cascades including the phosphatidylinositol-3 kinase (P13K) and mitogen-activated protein kinase (MAPK) pathways and ultimately leading to cell survival and proliferation. Illustration based on Crudden, Girnita, A, and Girnita, L (2015).

1.3.3 GH and IGF1 Distinct and Overlapping Functions on Linear Growth

One example of a mouse model that demonstrates the importance of the GH/IGF1 axis is the growth hormone receptor knockout (*GHR*^{-/-}) mouse. The *GHR*^{-/-} mouse is a model of human Laron Syndrome, a recessively inherited inactivating mutation(s) in the GHR. The disease is characterized by GH resistance, high serum GH, and low serum IGF1 (Laron, 2015a; List et al., 2011; Sims et al., 2000; Zhou et al., 1997). While at birth these mice are similar in size to their wild-type littermates (suggesting prenatal growth not dependent on GH), the significant size difference becomes apparent during postnatal development (Zhou et al., 1997). *GHR*^{-/-} mice have a 30-40% reduction in body size (List et al., 2011; Sims et al., 2000; Yakar & Isaksson, 2016; Zhou et al., 1997) as well as a 65% reduction in tibial growth rate (Davies et al., 2007; Wang, Zhou, Cheng, Kopchick, & Bondy, 2004) and decreased chondrocyte proliferation and hypertrophy (List et al., 2011). Studies by Lupu et al. (2001) determined that GH and IGF1 have distinct, yet overlapping, functions during mammalian linear growth. When comparing mutant mouse models of *Igf1* mutant mice, *GHR*^{-/-} (lacking GH action), and double-mutants (*Ghr/Igf1*), it was determined that the observed growth retardation of the double *Ghr/Igf1* nullizygotes was more severe than that of either single mutant model (Lupu et al., 2001). With advancements in the field of endocrinology, investigators continue to refine the original somatomedin hypothesis and study how GH and IGF1 interact to regulate linear growth.

1.3.4 GH and IGF1 Treatment of Hormonal Deficiencies

As described, normal longitudinal bone growth requires functional hormonal regulation. Hormonal disorders involving the deficient or excessive production of the important hormones of growth (GH, IGF1, thyroid hormones, glucocorticoids, and sex steroids), can lead to abnormally short or tall stature. Short stature characterized by stunted linear growth may result from GH deficiency (Lupu et al., 2001; Ohlsson et al., 1998; Tritos & Klibanski, 2016), IGF1 deficiency (Liu et al., 1993; Mohan et al., 2003; Powell-Braxton et al., 1993; Wang, Zhou, & Bondy, 1999; Wang et al., 2006; Yakar & Isaksson, 2016), hypothyroidism (Bassett & Williams, 2016), or hypercortisolism (Bello & Garrett, 1999; Silvestrini et al., 2000). Thyroid hormone (T_3) deficiency in children is associated with growth retardation (Rivkees, Bode, & Crawford, 1988) and studies in mice using knockout models have shown that linear growth is impaired in thyroid hormone deficient mice (Basset et al., 2008; Friedrichsen et al., 2003) when levels are normal but the thyroid receptor ($TR\alpha_1$ and $TR\beta$) is mutated (Göthe et al., 1999; Kindblom et al., 2005).

One of the main problems associated with short stature in children is the development of behavioral and emotional problems (van der Eerden et al., 2003; Gordon, Crouthamel, Post, & Richman, 1982; Sandberg, 2000). The most common treatment option for children with stunted linear growth involves frequent subcutaneous injections of recombinant human GH until adult height is reached (Ohlsson et al., 1998; Pfäffle, 2015; Wit & Oostdijk, 2015). In addition to treatment of short stature as a result of hormonal disorders, GH has also been used to treat short stature resulting from chromosomal disorders and genetic syndromes including Turner syndrome (Pfäffle,

2015; Ranke, 1995a, Tritos & Klibanski, 2016; Wit & Oostdijk, 2015), Achondroplasia (Harada et al., 2017), Prader-Willi syndrome (Moix, Gimébez-Palop, & Caixàs, 2018; Pfäffle, 2015), and Noonan syndrome (Noonan & Kappelgaard, 2015; Pfäffle, 2015). Other therapies including oxandrolone (man-made steroid similar to testosterone), estrogens, gonadotropin-releasing hormone (GnRH) and IGF1 have also been used to increase linear bone growth (Wit & Oostdijk, 2015). While GH therapy is more commonly used in clinical settings, IGF1 has also been shown to effectively reverse skeletal growth discrepancies (Azcona et al., 1999; Backeljauw, Kuntze, Frane, Calikoglu, & Chernausek, 2013; Chernausek et al., 2007; Laron & Klinger, 2000; Laron, 2001; Laron & Kauli, 2015b; Lupu et al., 2001; Midyett et al., 2010; Ranke et al., 1995b, 1999; Sims et al., 2000). However, there are more adverse effects associated with IGF1 treatment including hypoglycemia (abnormally low levels of glucose in the bloodstream) (Clemmons, 2004; Guevara-Aguirre et al., 1997; Laron & Klinger, 2000; Lindsey & Mohan, 2016; Ross, Lee, Gut, & Germak, 2015). In patients that already show symptoms of hypoglycemia, such as those with Laron's Syndrome (GH insensitive), IGF1 therapy can intensify these symptoms and can lead to loss of consciousness or seizures (Chernausek et al., 2007; Cohen et al., 2014; Kovacs et al., 1999). Other risks with IGF1 treatment include headaches, intracranial hypertension, growth of the nasopharyngeal lymphoid tissues, hearing loss, and injection site lipohypertrophy (Backeljauw et al., 2013; Chernausek et al., 2007; Midyett et al., 2010; Ranke et al., 1995b). Therefore, it would be favorable to develop a successful drug treatment regimen using a lower dose of IGF1 to avoid the adverse effects of increased systemic levels.

1.4 IGF1 AS A PRIMARY MEDIATOR OF LONGITUDINAL BONE GROWTH

1.4.1 Function of Locally Expressed IGF1

Numerous studies have supported the importance of both GH and IGF1 in mediating linear bone growth; however, IGF1 appears to be the most critical regulator of postnatal growth. In mutant animal models where GH action is impaired (Laron, 2015a; List et al., 2011; Lupu et al., 2001; Sims et al., 2000; Wang et al., 2004; Zhou et al., 1997), animals thrived despite being significantly smaller than the wild-type counterparts. In contrast, in mutant animals where local IGF1 action is impaired, most animals died shortly after birth and those that did survive had severe growth defects (Tahimic et al., 2013; Wang et al., 2011; Wu et al., 2015) supporting the importance of local chondrocyte-produced IGF1. The observed growth defects suggest that while a degree of circulating IGF1 is necessary (Yakar et al., 2002), local action of IGF1 may be more critical for longitudinal bone growth than serum IGF1 (see Table 1).

The role of local IGF1 in the proliferation of chondrocytes in mice and rats has been debated. Investigators have detected the expression of IGF1 in the PZ of the epiphyseal growth plate measured by *in situ* hybridization (Lazowski et al., 1994; Lupu et al., 2001; Nilsson, Carlsson, Isgaard, Isaksson, & Rymo, 1990; Ohlsson et al., 1992a). However, these results were not in agreement with the findings of two different groups from the early to mid-1990s that were both unable to detect IGF1 mRNA in proliferating chondrocytes by *in situ* hybridization methods, and instead found IGF2 mRNA (Shinar, Endo, Halperin, Rodan, & Weinreb, 1993; Wang et al., 1995). Additional investigators also identified the expression of IGF2 in the PZ (Parker et al., 2007; Reinecke, Schmid, Heyberger-Meyer, Hunziker, & Zapf, 2000). In all cases, it was

consistently reported that the level of IGF2 expression in the PZ decreased with age. Overall IGF1 expression levels increase after birth, including those in proliferating chondrocytes (Parker et al., 2007). The absence of IGF1 mRNA in proliferating chondrocytes by Shinar et al. (1993) and Wang et al. (1995) was reported using rodents during the earliest stages of postnatal development. Therefore, it is possible that these rodents had not yet reached the postnatal age by which an increase in IGF1 expression in the PZ can be detected, such as that reported by Parker et al. (2007).

The significance of IGF2 in early postnatal chondrocyte development, secondary to IGF1, has begun to emerge. IGF2 is not included in the GH-IGF1 axis (Humbel, 1990; Pierce, Dickey, Felli, Swanson, & Dickhoff, 2010) but recent studies are now investigating the role of IGF2 in postnatal bone growth after a group discovered that human postnatal growth restriction was associated with nonsense *IGF2* mutations (Begemann et al., 2015). Uchimura et al. (2017) have shown significant reductions in bone length in *IGF2*-null mice at postnatal periods prior to weaning (1-3 weeks of age) and their histological analysis suggests IGF2 has a role in regulating chondrocyte development by controlling the progression from proliferation to hypertrophy. The mechanism and extent by which IGF2 regulates longitudinal bone growth through cartilage development remains unclear and its evaluation will be important in future experiments.

Regardless of its local versus systemic roles, IGF1 is undisputedly a significant factor in epiphyseal cartilage development. Local regulation of IGF1 has been studied in other regions of the growth plate aside from the PZ. Cell kinetic studies using hypophysectomized rats (pituitary gland removed reducing systemic levels of GH and

IGF1) determined that IGF1 regulated all phases of chondrocyte differentiation in the growth plate including the RZ of chondrocyte precursors (Hunziker, Wagner, & Zapf, 1994a). IGF1 expression has also been observed in the HZ of epiphyseal growth plates (Lazowski et al., 1994; Nilsson et al., 1990) and local regulation by IGF1 has been shown to augment chondrocyte hypertrophy (Abbaspour et al., 2008; Mushtaq, Bijman, Ahmed, & Farquharson, 2004; J. Wang et al., 1999; Y. Wang et al., 2006). An observed 35% reduction in HZ height was reported in an *IGF1* null mouse model (Wang et al., 1999). IGF1 has also been shown to induce collagen X production (made in the HZ) (Repudi, Patra, & Sen, 2013; Wang et al., 1999). When local expression of IGF1 was blocked by the binding of Wnt induced secreted protein 3 (WISP3), a protein involved in cell differentiation, IGF1-induced collagen X expression was reduced (Repudi et al., 2013).

1.4.2 IGF1 Antagonists

Mouse models designed to control the expression of IGF1 through genetic manipulation are a useful method for studying IGF1 regulation. Another approach for studying IGF1 action and its role in regulating linear bone growth is by blocking IGF1 action. The major target of an IGF1 antagonist is the IGF1R, which serves as the gateway for IGF1 action (see Fig. 3). When activation of the IGF1R is inhibited, the growth promoting effects of IGF1 are blocked (Fig. 4). Multiple types of antagonists of IGF1 have been studied including small-molecule tyrosine kinase inhibitors (TKIs) and competitive antagonists such as monoclonal antibodies directed against the IGF1R or the use of IGF1 peptide analogs (Table 2). Since hormones and growth factors,

including IGF1, function to promote growth by inducing cell proliferation and survival, hormone antagonists are often investigated as means for treating abnormal cell growth such as carcinogenesis. However, many of these antagonists face scrutiny because of the reports of failure in clinical trials (Guha, 2013). Therefore, investigators are continuing to seek a better understanding of these antagonists using animal models (Moody et al., 2014) and continue to research alternatives for IGF1 antagonists to improve targeted therapies (Guha, 2013).

Apart from clinical studies using IGF1 antagonists as anti-cancer drugs, testing antagonists for their ability to block IGF1 action in various tissues, including bone, should be done. Since many of these drugs are administered systemically, the smaller sized antagonists (<0.9 kDa) are more soluble and better for transport out of the vasculature and into the tissue (Hadacek & Bachmann, 2015; Macielag, 2012). As highlighted in Table 2, IGF1 peptide analogs are effective because of their specificity, small molecular size (0.6-1.2 kDa) and low toxicity (Haylor et al., 2000; Huang, Golden, Tarjan, Madison, & Stern, 2000; Kleinridders, 2016; Pietrkowski, Wernicke, Porcu, Jameson, & Baserga, 1992; Smith et al., 1999). Multiple IGF1 peptide analogs have been used to inhibit cellular proliferation including JB1, JB2 and JB3 (Pietrkowski et al., 1992). Presently, JB1 is the analog commercially available to researchers that competitively binds to IGF1R and blocks downstream IGF1 activity (Brock et al., 2011; Huang et al., 2000; Kleinridders, 2016; Todd, Fraley, Peck, Schwartz, & Etgen, 2007; Wen et al., 2012) (Fig. 5). As with many antagonists, resistance is possible. Haylor et al. (2000) reported a bell-shaped curve with the dose response of JB3 and its successful inhibition of kidney growth in rats. In addition to determining an effective range of

treatment, challenges still arise in eliciting a tissue specific response without affecting other systems dependent on IGF1 for normal growth. Therefore, further investigation into methods of targeting small molecules will be beneficial in optimizing application of IGF1 antagonists.

Table 2. Summary of IGF1 Antagonists in Inhibiting Overall Growth

Antagonist	Advantage	Disadvantage	Citation
Anti-IGF1R antibodies (i.e. ganitumab and α IR3)	Highly specific for the IGF1R	Activates the insulin receptor and promotes unwanted growth; Large molecular weight (145-155kDa); Drug resistance	Huang et al., 2000 Moody et al., 2014
Small-molecule TKIs (i.e. Linsitinib and BMS-754807)	Targets both IGF1R and insulin receptor; Small molecular weight (0.42-0.46kDa)	Less specific; Reported toxicity (i.e. diarrhea and myelosuppression); Drug resistance	Li, Pourpak, & Morris, 2009 Pillai & Ramalingam, 2013 Refolo et al., 2017
IGF1 peptide analogs (i.e. JB1, JB2 and JB3)	Highly specific for the IGF1R; Small molecular weight (0.6-1.2kDa); Low toxicity	Drug resistance	Haylor et al., 2000 Huang et al., 2000 Kleinridders, 2016 Pietrzkowski et al., 1992 Smith et al., 1999

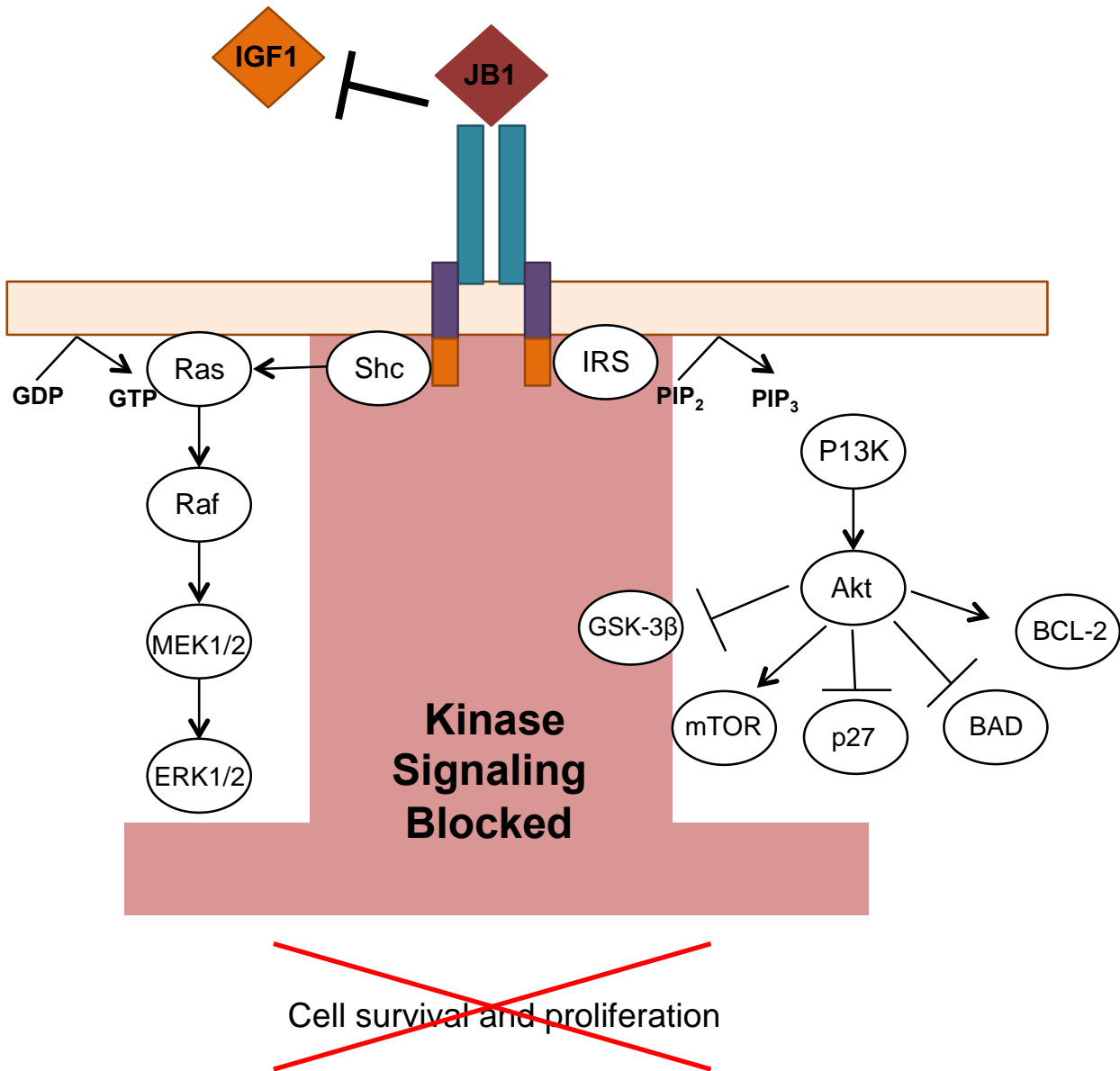


Figure 5. JB1 Blocks IGF1R Signaling

Model demonstrates how IGF1 peptide analog, JB1, competitively binds to the IGF1R. JB1 thus inhibits IGF1 binding preventing IGF1R activation and ultimately blocking kinase signaling that would otherwise lead to cell survival and proliferation (repressed downstream effects indicated by the red "X"). Illustration based on Crudden et al. (2015).

1.5 REGULATION OF LINEAR GROWTH BY TEMPERATURE

1.5.1 Temperature Regulates Linear Growth in Nature

For over 50 years, several environmental factors have been shown to influence bone growth and development. As reviewed by Schell, Gallo, & Ravenscroft (2009), environmental factors include nutrition, altitude, climate and temperature. Temperature has classically been described to influence extremity length as described by Allen's rule that warm-blooded animals living in cold climates display decreased length of extremities and appendages (Allen, 1877). Temperature regulated limb length is thought to be an adaptation to the cold climate by reducing the body mass to surface area ratio (Newman, 1953).

1.5.2 Temperature Regulates Linear Growth in Laboratory Setting

Allen's rule is often still applied to a variety of different species in present day studies. In humans, Allen's rule was demonstrated in a study suggesting that shorter limbs (including those of Neanderthals, a group of archaic humans) are advantageous for survival in cold climates by reducing the metabolic cost of maintaining body temperature (Tilkens, Wall-Scheffler, Weaver, & Steudel-Numbers, 2007). In reptiles, studies have shown that increased incubation temperature (32°C) of embryonic crocodiles led to increased tibial length (Pollard et al., 2017). Serrat (2014b) thoroughly reviewed the impact of temperature on extremity growth in various species. For instance, mice from 3.5-12 weeks of age housed at warm ambient temperature (27°C) displayed longer limbs than cold-reared mice (7°C) (Serrat, Williams, & Farnum, 2010). Overall results of Allen's rule replicated in laboratory settings (mainly in rodents) appear

to be most profound when experimentation occurs during the active period of postnatal growth. Al-Hilli and Wright (1983) studied effects of warm ambient temperature (33°C) on tail growth in young mice (3 weeks of age) and showed heat enhanced tail growth occurred during the first 3-4 weeks of exposure. Serrat (2013) reanalyzed this temperature sensitive period of postnatal growth in young mice (3 weeks of age) and found that the “critical phase” of temperature sensitive growth occurs between 3-5 weeks of age, followed by a later “maintenance phase,” whereby limb length differences are simply maintained.

1.5.3 Unilateral Heating Model Enhances Bone Lengthening

Serrat et al. (2015) later showed that targeted unilateral limb heating (40°C) in growing mice (3-5 weeks of age) increased limb length on heat-treated sides. However, the mechanism of action is unclear. It can be difficult to narrow down a single mechanism responsible for temperature-altered physiology, as there are numerous possibilities, both direct and indirect, and include altered cellular gene expression, vascularization, transport of nutrients and growth factors (Serrat, 2014b), and systemic hormone concentrations. It is likely that multiple mechanisms are involved in temperature-enhanced limb growth. Since the cartilaginous growth plate drives linear bone growth and the observed temperature induced changes in limb length occur concurrently with periods of elevated growth plate activity (3-5 weeks of age in the mouse), it is likely that temperature elicits direct and indirect effects on the growth plate.

1.5.4 Potential Function of IGF1 in Heat-Enhanced Linear Growth

As previously discussed, IGF1 is the main regulator of linear growth since normal skeletal development does not occur without functional IGF1 activity (see Table 1) (Liu et al., 1993; Mohan et al., 2003; Powell-Braxton et al., 1993; Wang et al., 2006). In addition to liver-derived serum IGF1 (endocrine), it has also been suggested by rodent studies that locally expressed IGF1 (autocrine/paracrine) regulates cellular mechanisms of longitudinal bone growth in the growth plate (Isaksson et al., 1982, 1985; Isaksson, Ohlsson, Nilsson, Isgaard, & Lindahl, 1991; Ohlsson et al. 1992a, 1992b, 1998; Schlechter et al., 1986). Therefore, a working hypothesis for heat-enhanced linear growth is that temperature increases activity of IGF1, which increases rates of chondrocyte proliferation and hypertrophy to subsequently enhance limb growth. Heat-enhanced linear growth may occur by: (1) indirectly increasing IGF1 access to the growth plate with temperature-enhanced blood flow (endocrine actions), (2) directly increasing IGF1 activity within the growth plate (autocrine/paracrine actions) with temperature-enhanced expression of regulators, or (3) a combination of both.

While supporting evidence of temperature-enhanced blood flow and vascular transport are discussed in later sections, literature also supports that IGF1 expression increases with higher temperature. A recent study showed that during early development in a population of eels (endoskeleton is entirely made of bone), those reared in warmer temperatures (22°C) compared to colder temperatures (16°C), were significantly longer in length and had increased gene expression of *IGF1* (Politis et al., 2017). Other studies comparing the effect of thermal manipulation on IGF1 expression in skeletal muscles of growing broiler chicks showed increased expression associated

with increased temperature (Al-Zghoul et al., 2016; Halevy, Krispin, Leshem, McMurtry, & Yahav, 2001). In addition to the suggested relationship between temperature and IGF1 expression in developing tissues, temperature has also been shown to weaken the affinity of IGF1 binding to ALS in its ternary complex (ALS-IGF1-IGFBP3) accounting for increased free IGF1 in the circulation (Holman & Baxter, 1996). Further research is required to determine if temperature impacts IGF1 action in bone and cartilage tissue in mammals during development.

1.6 ROLE OF VASCULATURE IN PROMOTING LONGITUDINAL BONE GROWTH

1.6.1 Vascular Supply of the Growth Plate

In addition to local and systemic factors that regulate the well-controlled process of endochondral ossification, vascular systems are also crucial because they transport regulators that are essential for longitudinal bone growth. Therefore, it is important to understand the blood supply of growth plate cartilage. Although bone is a highly vascularized tissue, signaling molecules involved in bone elongation must overcome a challenge that is unique to the growth plate. Cartilage does not have a penetrating blood supply. Systemic factors essential for bone elongation are delivered from surrounding blood vessels (Brodin, 1955; Maes, 2013; Trueta, 1968). These vascular routes include: 1) epiphyseal vessels, 2) metaphyseal vessels, and 3) perichondral vessels (Brookes & Revell, 1998; Brighton, 1978; Spira & Farin, 1967; Wirth et al., 2002). Perichondral vessels arise from a ring vessel found in the encircling fibrochondrosseous structure in the perichondrium known as the groove of Ranvier (Brookes & Revell, 1998; Walzer et al., 2014). The epiphyseal vessels have been reported to provide the means for normal

chondrocyte proliferation, while chondrocyte hypertrophy is dependent on the metaphyseal vessels (Trueta & Amato, 1960; Zoetis et al., 2003). Studies have shown that the epiphyseal vasculature is essential for normal growth plate cartilage development (Maes et al. 2004; Maes, 2013; Trueta, 1968; Williams, Zipfel, Tinsley, & Farnum, 2007). While the viability of chondrocytes may be dependent on epiphyseal vasculature as opposed to metaphyseal vasculature (Trueta, 1968), metaphyseal vessels are essential for providing osteogenic factors that replace cartilage with bone during the process of endochondral ossification.

Studies have recently emerged using novel techniques to investigate the not fully elucidated mechanism of molecular transport into the growth plate through the surrounding vasculature. Multiphoton microscopy (MPM) as described by Zipfel, Williams, & Webb (2003) is an attractive, noninvasive method of *in vivo* fluorescent imaging in living anesthetized animals. Investigators have used MPM imaging as a means of tracking systemic fluorescent tracers through the vasculature into the growth plate (Farnum, Lenox, Zipfel, Horton, & Williams, 2006; Serrat, Williams, & Farnum, 2009; Serrat et al., 2010; Serrat, Efaw, & Williams 2014a; Williams et al., 2007). For biological significance, the size of the fluorescent tracers was selected based on the range of endogenous molecules that diffuse into the growth plate. The comprehension of how signaling molecules enter the growth plate through the surrounding vasculature is helpful in understanding regulation of growth plate chondrocytes. For example, very small amounts of molecules larger than 40kDa enter the growth plate (Serrat et al., 2014a), but molecules less than 10kDa were found to enter the growth plate through all three vascular routes (Farnum et al., 2006). Larger sized molecules (10kDa and

greater) appear to enter the growth plate from the surrounding perichondral vessels (Williams et al., 2007). Transport of molecules into the growth plate is relevant to understanding how larger signaling molecules such as FGFs (FGF2, 18kDa; FGF18, 23kDa), PTHrP (9-23kDa), and BMPs (BMP-2, 26kDa) expressed in the perichondrium regulate growth plate chondrogenesis (Kronenberg, 2003).

1.6.2 Transport of Systemic IGF1 into the Growth Plate

IGF1 is the major circulating hormone of growth. At a molecular weight of 7.6kDa, IGF1 falls within the range of molecules that readily enter the growth plate through the surrounding vasculature (less than 10kDa). Therefore, it is beneficial to study IGF1 transport and improve our understanding of its role in regulating growth plate chondrocytes. In an attempt to develop the means to facilitate this expansion in knowledge, Serrat and Ion (2017) developed a methodology for fluorescently labeling IGF1 in order to track its transport into the growth plate using MPM. They showed that biologically active IGF-488 (IGF1 conjugated with Alexa Fluor 488) entered the growth plate and localized to chondrocytes (Serrat & Ion, 2017). In addition to the general comprehension of growth plate chondrocyte regulation, vascular transport studies also are important in the development of therapies for growth plate disorders. IGF1 is used as a drug to treat impaired growth in growth hormone insensitive children, i.e Laron Syndrome patients (Azcona et al., 1999; Backeljauw et al., 2013; Chernausek et al., 2007; Laron & Klinger, 2000; Laron, 2001, 2015a; Laron & Kauli, 2015b; Lupu et al., 2001; Midyett et al., 2010; Ranke, 1995a; Ranke et al., 1995b, 1999; Sims et al., 2000). It is therefore essential to understand how IGF1 can be modulated to improve effective

treatment. Modulation may include methods for increasing IGF1 activity within the growth plate, or better targeting its delivery to the growth plate.

Environmental factors, such as temperature, can affect vascular systems in bone and affect their growth (Reviewed by Serrat (2014b)). *In vivo* imaging studies using MPM have shown that warm temperature increases molecular uptake into the growth plate (Serrat et al., 2009, 2010, 2014a). Temperature enhanced solute delivery is size-dependent as the transport of smaller molecules (less than 10kDa) is increased by over 150%, while larger molecules (40kDa and larger) are increased by less than 50% (Serrat et al., 2014a).

1.6.3 Chondrocyte Expression of Angiogenic Factors

Angiogenesis (development of new blood vessels) is essential for normal linear bone growth. During endochondral ossification, hypertrophic chondrocytes secrete angiogenic factors that initiate vascular invasion and recruit bone absorbing and forming cells to replace mineralized cartilage with bone. The key regulator of angiogenesis during both prenatal and postnatal growth and development is vascular endothelial growth factor (VEGF). Survival is dependent on functional VEGF during both embryonic (Carmeliet et al., 1996; Ferrara et al., 1996) and early postnatal life (Gerber et al., 1999a). Different VEGF isoforms exist but only VEGF-A is expressed in growth plate cartilage and therefore is the most important for regulating longitudinal bone growth (Emons et al., 2010). There are also additional splice isoforms of VEGF-A that vary between species. Hypertrophic chondrocytes in both human and murine growth plates secrete VEGF (Filipowska, Tomaszewski, Niedźwiedzki Ł, Walocha, Niedźwiedzki T,

2017; Gerber et al., 1999b; Horner et al., 1999; Hunziker, 1994b; Maes et al., 2004; van der Eerden et al., 2003; Zelzer & Olsen, 2005) to promote vascular invasion from the metaphyseal bone throughout postnatal limb elongation. In human growth plates, the most common splice isoforms are VEGF₁₂₁, VEGF₁₆₅ and VEGF₁₈₉ (Emons et al., 2010; Maes et al., 2004). The analogous isoforms in mice are VEGF₁₂₀, VEGF₁₆₄ and VEGF₁₈₈ (Maes et al., 2002, 2004). Interestingly, Maes et al. (2004) discovered that different processes of vascularization require specific isoforms of VEGF-A and that the combined action of VEGF₁₂₀ and VEGF₁₈₈ is required for both epiphyseal and metaphyseal vascularization. Other local factors expressed by hypertrophic chondrocytes that promote angiogenesis include FGFs (Baron et al., 1994; Hung, Yu, Lavine, & Ornitz, 2007; Liu, Lavine, Hung, & Ornitz, 2007) and matrix metalloproteinase 9 (MMP-9) (Engsig et al., 2000; Gerber et al., 1999b; Maes et al., 2002; van der Eerden et al., 2003; Vu et al., 1998). Systemic factors including estrogen (Emons et al., 2010) and IGF1 (Ahmed & Farquharson, 2010; Álvarez-García et al., 2010) have also been shown to induce vascular invasion by stimulation of VEGF in growth plate chondrocytes.

Normal longitudinal bone growth is dependent on VEGF expression in growth plate chondrocytes. Inhibition of VEGF in young mice (24 days old) suppressed blood vessel invasion, lengthened the hypertrophic zone and reduced bone growth, all of which was corrected after anti-VEGF treatment ended (Gerber et al., 1999b). These results are clinically relevant to actively growing children that may require therapeutic intervention using angiogenesis inhibitors to prevent unwanted formation of new blood vessels such as in pediatric cancers. A monoclonal antibody against VEGF, bevacizumab (Avastin®; Genentech, Inc), has been used in adults as a FDA approved

anti-cancer agent (Ferrara, 2004) and is considered a promising treatment option for children (Barone & Rubin, 2013; Han et al., 2016). It is especially important to improve chemotherapy in pediatric patients since children are undergoing an essential stage of bone development requiring growth factors, including IGF1 and VEGF, for bone elongation. Therefore, as with IGF1 antagonists, the development of non-invasive methods for targeting drugs directly to a tissue is beneficial for preserving linear growth in children.

1.7 SCOPE OF CURRENT WORK

The goal of the current studies in this dissertation is to build upon an established method of targeted limb heating as a potential non-invasive alternative to enhance bone lengthening. This study tests the **overall hypothesis that exposure to warm temperature augments the actions of IGF1 in the growth plate and permanently increases length of the extremities**. The central aims of this study are 1) to determine if IGF1 enhances bone elongation in heat-treated extremities and 2) determine the long-term extent of left-right limb length asymmetries and potential vasculature modifications resulting from unilateral heat-treatment.

The application of the model for targeted limb heating (unilateral heating model) and its functional impact is described in Chapter 2. This chapter sets the foundation for following experiments using the unilateral heating model as a means to test the overall hypothesis. As discussed above, the epiphyseal growth plate is the primary site of longitudinal bone growth, and regulated by IGF1 (Börjesson et al., 2010; Lui et al., 2014; Ohlsson et al., 1993; Tryfonidou et al., 2010; van der Eerden, 2003; Wang et al.,

2010). Chapter 3 tests the hypothesis that there will be a unilateral increase in bone length associated with increased chondrocyte proliferation and hypertrophic zone expansion in the growth plate with heat-treatment. Observation of morphological changes in the growth plate is a means to assess heat-enhanced bone elongation. In Chapter 4, a study administering a low dose of IGF1 (2.5 mg/kg, once daily) coupled with targeted limb heating tests the hypothesis that IGF1 administered with heat-treatment will further enhance limb length than with heat alone. To further test the overall hypothesis of this thesis, Chapter 5 describes the outcome of linear growth with heat-treatment when IGF1 activity is blocked. The hypothesis is that with diminished IGF1 activity, heat-enhanced limb length is attenuated. The goal shared by both Chapter 4 and 5 is to demonstrate that unilateral exposure to warm temperature augments actions of IGF1 in the growth plate to enhance bone length.

The long-term impact of targeted limb heating after the end of treatment is elucidated in Chapter 6. This study tests the hypothesis that differential limb length will be maintained throughout skeletal development after treatments have ended. The goal of this chapter was also to demonstrate that persistent limb length differences will be prominent in mice administered IGF1 following heat-treatment. The final chapter of this thesis (Chapter 7) describes a pilot study measuring limb surface temperature following heating and tests the hypothesis that skin temperature of heat-treated limbs will remain elevated for an extended time following treatment. This chapter prefaces future studies into possible mechanisms of the targeted heating-model as it suggests a heat-induced increase in blood flow that accelerates bone lengthening. Together, current studies

within the chapters of this thesis will use the unilateral heating model to test the overall hypothesis (as stated above).

CHAPTER II: FUNCTIONAL IMPACT OF TARGETED LIMB HEATING IN MICE

2.1 INTRODUCTION

Both congenital and acquired bone elongation disorders arise during early stages of development. Without childhood medical intervention, problems associated with these disorders can persist into adulthood and often are accompanied by painful health conditions. Limb length discrepancy (LLD) of the lower limbs is characterized by the asymmetric length of the lower extremities and can result from trauma or disease (Morscher, 1977; Shapiro, 1982; Wilson & Thompson, 1939). Untreated LLD can lead to chronic and painful musculoskeletal disabilities (Campbell et al., 2018; Gurney, 2002). While the options for intervention vary based on the severity of the discrepancy, research has addressed possible treatment options that typically involve more permanent, invasive procedures (Gurney, 2002; Hasler & Krieg, 2012; Niedzielski, Flont, Domżański, Lipczyk, & Malecki, 2016; Pendleton et al., 2013; Sabharwal et al., 2015; Stevens, 2016). Traditionally, intervention is recommended for what has been considered an important functional discrepancy of 2 cm or more (Gross, 1978; Gurney 2002; Knutson, 2005). However, studies within the last two decades have shown that a left-right asymmetry in limb length of less than 2 cm (0.5-1 cm) is functionally significant (Harvey et al., 2010; Resende et al., 2016; White et al., 2004). Smaller left-right asymmetries involve more conservative methods for correction such as shoe lifts or prosthetics (Campbell et al., 2018; Golightly et al., 2007a; Hasler & Krieg, 2012; Wilson & Thompson, 1939), but these methods do not permanently change the length of the bone. It is important to explore alternative, noninvasive methods for correcting LLD,

including even small discrepancies, during critical stages of postnatal longitudinal bone growth.

A promising noninvasive alternative involves using targeted heat (40°C) to increase bone length on one side of the body (Serrat et al., 2015). After two weeks of localized unilateral heating, Serrat et al. (2015) demonstrated increases in tibial elongation rate (>12%), femoral length (1.3%) and tibial length (1.5%). The ultimate goal of these studies is to use heat-based therapy to correct a range of bone growth impairments such as LLD in children. However, one fundamental question is whether these heat-induced limb length differences are functionally significant.

One functional outcome of LLD includes gait disturbances (Aiona et al., 2015; Kaufman et al., 1996; Khamis & Carmeli, 2017; Mahmood et al., 2010; Song et al., 1997) resulting from a pelvic tilt toward the shorter side (Kerr, Grant, & MacBain, 1943; Rush & Steiner, 1946). Therefore, this study aimed to determine if the small discrepancies after one week of daily intermittent targeted limb-heating result in changes in weight bearing. Longitudinal x-ray imaging and weight bearing distribution analyses were used to test **the hypothesis that heat-induced limb length asymmetry has a functional impact on weight bearing in mouse hindlimbs.**

2.2 MATERIAL AND METHODS

2.2.1 Animals and Experimental Design

All procedures were approved by the Institutional Animal Care and Use Committee of Marshall University (Protocol 558). Female C57BL/6 (N=12) mice were obtained from Hilltop Lab Animals, Inc. (Scottsdale, PA, USA) at 21 days weaning age.

Previous studies have shown that heat-enhanced bone elongation occurs in both male and female mice with unilateral heat-treatment (Serrat et al., 2015). These studies focused only on female mice since there were no reported differences between the sexes and because other related studies in our laboratory required females. Mice were singly housed at 21°C in standard plastic caging, exposed to a 12 hour light/dark cycle and provided with food and water ad libitum.

Mice post-weaning were treated with 40 minutes of daily unilateral heat (40°C) for 7 days beginning when mice were 3-weeks old following methods described by Serrat et al. (2015). This period of postnatal growth was chosen because it has previously been shown as a period of rapid, temperature sensitive growth (Serrat, 2013). Relative to human development, this pre-pubertal age range is comparable to the period between toddler age and elementary school (as shown in Fig. 2). Mice were anesthetized under 1.5% isoflurane and positioned right lateral recumbent on a 40°C gel heating pad each day (Fig. 6). Heat-treatment was deliberately scheduled to begin at the same time each day at the beginning of the light cycle (~7 a.m.) when growth plate height and growth rate are maximal (Noonan et al., 2004; Stevenson, Hunziker, Hermann, & Schenk, 1990). For each day of treatment, placement of each individual mouse was rotated along the anesthesia manifold to account for any positioning effects (the end positions for example are closer to the edge of the gel heating pad and closer/further from the source of isoflurane). Limbs on the heat-treated side were fitted in custom made insulating booties to warrant uniform heat distribution. Foam separators were placed between the limbs as a thermal shield preventing heat transfer to the non-heated limb (30°C). Ear and hindlimb temperatures were taken throughout heating and

core temperature and respirations were recorded as means of physiological monitoring. The procedural room temperature remained at 19°C throughout the duration of treatment.

ISOFLURANE

1.5%

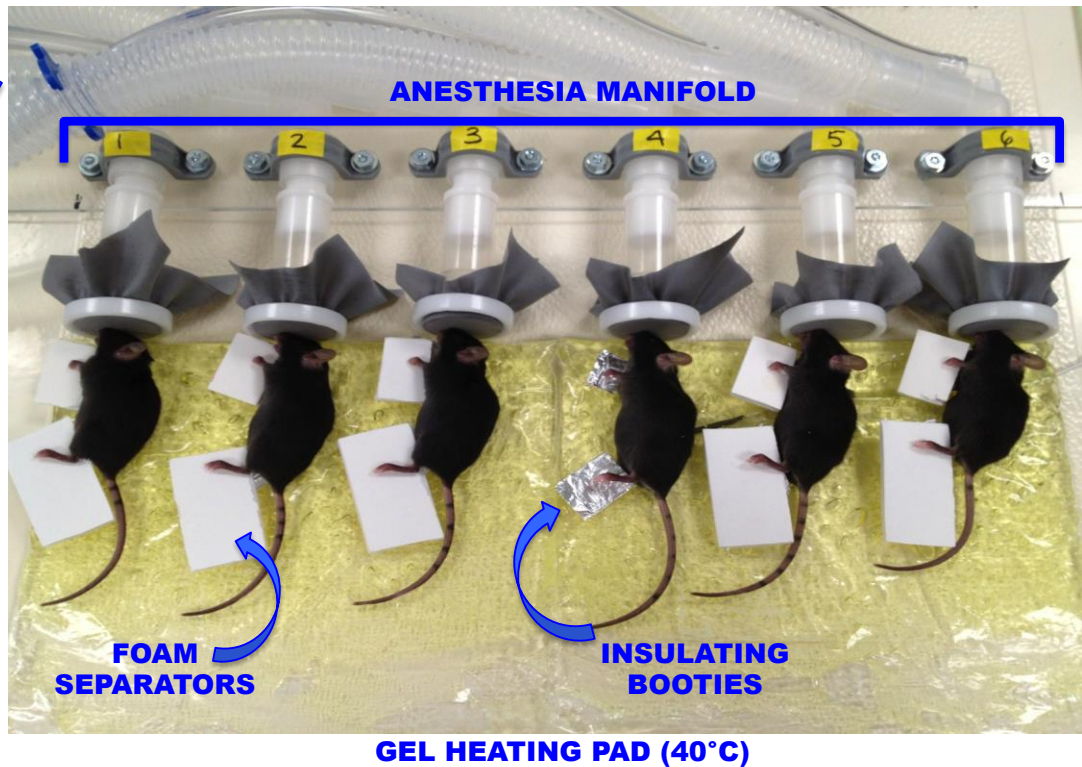


Figure 6. Diagram of the Unilateral Heating Method

Labeled photograph shows the unilateral heating method during the 40 minutes of treatment (40°C). Temperature of heating pad topped with custom gel packs (colored yellow) is manually controlled by a thermostat (not shown in image) and maintained at 40°C. Mice are positioned right lateral recumbent along the anesthesia manifold and anesthetized with 1.5% isoflurane. Isoflurane flows through the plastic tubing controlled for each individual mouse. Limbs on the heat-treated side are fitted in custom made insulating booties. Foam separators are placed between the limbs (temporarily removed from position 4 to reveal the insulating booties underneath).

2.2.2 Tibial Radiographs

Radiographs were collected from mice (N=6) at the start (3 weeks of age) and end (4 weeks of age) of the limb-heating experiments using an IVIS Lumina XRMS live animal imaging system (Perkin Elmer, Waltham, MA, USA). Mice were anesthetized individually under 1.5% isoflurane and positioned in ventral recumbency on a heated platform. Each mouse was secured to the platform with adhesive tape with its hindlimbs extended and taped down following published methods to ensure reproducible limb positioning and a true projection of the tibia (Fig. 7) (Hughes & Tanner, 1970). High-resolution x-ray images were taken following methods described in the literature (McManus & Grill, 2011) using modified settings (animal energy, 35 Kv 100 μ A, filtered x-rays) at 5 cm X 5 cm field of view with f/stop set at 4 and subject height at 1.5 cm. The mouse was then returned to its individual cage and observed during anesthesia recovery (1-2 minutes). Methodology adapted from Racine et al. (2018).

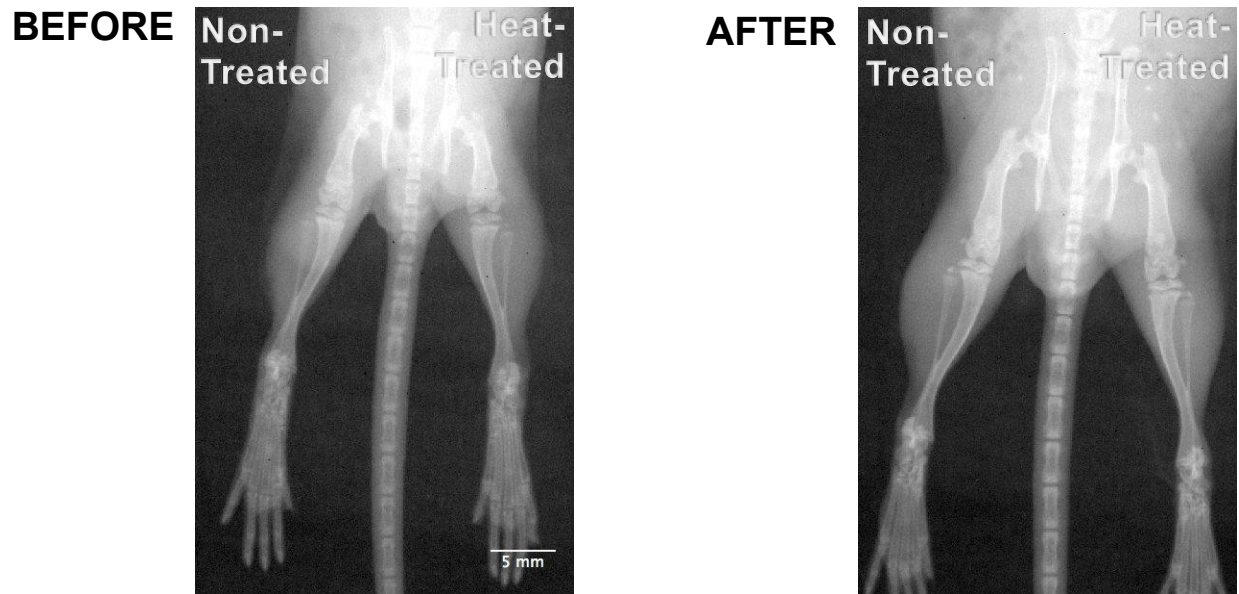


Figure 7. Radiographs Collected Before and After Unilateral Heat-Treatment

Digital radiographs (29 X 45mm area) of the same mouse taken with an IVIS Lumina XRMS live animal imaging system before (3-weeks of age) and after (4-weeks of age) heating. Individual mouse represents one of the experimental group (N=6) used to measure tibial length before and after targeted limb heating.

2.2.3 Hindlimb Weight Bearing

Starting and ending weight-bearing data were collected from mice (N=12) following x-ray procedures (~2 hours after anesthesia recovery). Weight bearing was measured using an incapitance meter (Stoelting Company, Wood Dale, IL, USA), a device for measuring weight distribution of the two hindlimbs of a small rodent or bird. The incapitance meter records hindlimb weight bearing of each side of the mouse. The mouse is placed in an angled plexiglass chamber positioned in a rearing posture so that each hindlimb is placed over a separate force plate. Prior to collection, mice were acclimated (2-5 minutes) to the chamber following published methods (TenBroek, Yunker, Nies, & Bendele, 2016). Measurements were collected during 3-second intervals and mean weight distribution was calculated during that period, thus accounting for possible shifts in weight from one side to another during testing. A total of 3-5 recordings were taken per mouse at each time point and mean weight distribution from each hindlimb was used in data analyses. Methodology adapted from Racine et al. (2018).

2.2.4 Tissue Collection

All experimental mice (N=12) were euthanized for tissue collection 1 day after the last day of heat-treatment when final x-ray and weight bearing analyses were performed at the 4 weeks of postnatal age endpoint. Long bones (femora) from each side were dissected, cleaned, dried, and scanned on a flatbed scanner. It has previously been found that the intact femur can be dissected and cleaned most consistently for reliable bone length data. Proximal tibiae from each hindlimb were dissected, cleaned and

bisected. One unfixed half was arranged on a glass slide and cover-slipped with glycerol in PBS prepared for tibial elongation rate analysis. Methodology adapted from Racine et al. (2018).

2.2.5 Tibial Elongation Rate Analysis and Long Bone Measurements

A single intraperitoneal injection of oxytetracycline (OTC) (7.5 mg/kg, Norbrook 200 mg/mL) was administered to mice at the experimental start, 8 days prior to euthanization and tissue collection. OTC is a calcium chelator that integrates into mineralizing tissue and leaves a band of fluorescence that can be visualized using a UV filter. Fluorescence was visualized in unfixed slab sections of tibiae using Ocular Image Acquisition Software (version 1.05.211) under 2.5X magnification with a Leica DM2500 epifluorescence microscope (Leica Microsystems, Wetzlar, Germany) coupled with a QImaging Retiga R6 6.0 megapixel monochrome camera (Surrey, BC, Canada) and using a UV filter. Tibial elongation rate ($\mu\text{M}/\text{day}$) was quantified by measuring the distance between the metaphyseal chondro-osseous junction, where calcification begins, and the proximal edge of the OTC band in metaphyseal bone, where the fluorescent label is visualized after the 8-day period of growth.

Images of scanned femora were calibrated in ImageJ (version 1.48, National Institutes of Health, USA) using a metric ruler and measurements were taken by drawing a line between proximal and distal landmarks on the articular ends. Femoral length was measured as the distance between the proximal-most point on the greater trochanter and the distal-most point on the medial condyle. These methods of quantifying tibial elongation rate and limb length have been described as reliable

techniques in past experiments (Lee et al., 2016; Rolian, 2008; Serrat et al., 2015; Wilsman et al., 2008).

Tibial length was measured from digital x-rays at the start and end of the study (Fig. 7). Radiographs were calibrated in ImageJ using a razor blade for scale. The tibia was selected for analysis because its landmarks could be most consistently identified in both left and right hindlimbs of the same animal over time. Tibial length was measured as the distance from the middle of the proximal articular surface to the distal-most projection of the medial malleolus. Methodology adapted from Racine et al. (2018).

2.2.6 Statistical Analysis and Sample Size

Statistical analyses were performed using SPSS 25.0 software (IBM Corporation, Armonk, NY) with $p < 0.05$ as accepted significance. Non-treated and heat-treated side comparisons for femoral length, tibial length, and tibial elongation rate were made using one-tailed paired t-tests. Linear regression, with asymmetry in tibial elongation rate as the regressor and weight bearing as the dependent variable, was used to assess the relationship between weight bearing of hindlimbs and tibial elongation rate. Data were reported as mean \pm standard deviation (SD) in tabular format and as mean \pm standard error (SE) in graphical format. Study included a total of N=12 mice to account for potential loss of samples and missing cases were excluded from statistical analysis on an analysis-by-analysis basis. Sample sizes for measurements that are documented as *less than the size of the experimental sample* set was a result of either sample loss due to damage during dissection, poor acclimation to the incapacitance meter, and/or improper limb position in the x-ray imager (Racine et al., 2018).

2.3 RESULTS

2.3.1 Unilateral Heating Parameters

After 7 days of unilateral heating, mice gained an average of 5 g between the start and the end of the study, consistent with the weight gain of age-matched non-treated control mice (Serrat et al., 2015). The core temperature averaged 36°C during heat-treatment, which is analogous to the core temperature of a healthy C57BL/6 mouse (Gordon, 2012, 2017). While anesthetized the average surface temperature of non-treated hindlimbs was 30°C and the heat-treated hindlimbs were 40°C. The average time to anesthesia recovery after limb heating was 1 minute.

2.3.2 Bone Length and Tibial Elongation Rate

At the beginning of the study, prior to unilateral heating, there were no significant left-right differences in tibial length (paired $t=0.65$, $p=0.55$) measured on x-rays (Fig. 7, Table 3). At the experimental end when mice were 4 weeks of age following 7 days of targeted limb heating, tibial length (paired $t=11.5$, $p<0.001$) measured on x-rays increased by 0.9% on heat-treated sides (Fig. 7, Table 3) and femoral length (paired $t=7.7$, $p<0.001$) measured from the digital scans increased by 1.4% on the heat-treated side (Fig. 8A). Tibial elongation rate measured by OTC labeling averaged $160\pm 14\mu\text{M}/\text{day}$ on the non-treated side and $170\pm 13\mu\text{M}/\text{day}$ on the heat-treated side with an increase of 6.5% on the heat-treated side over the 8-day labeling period (Fig. 8B).

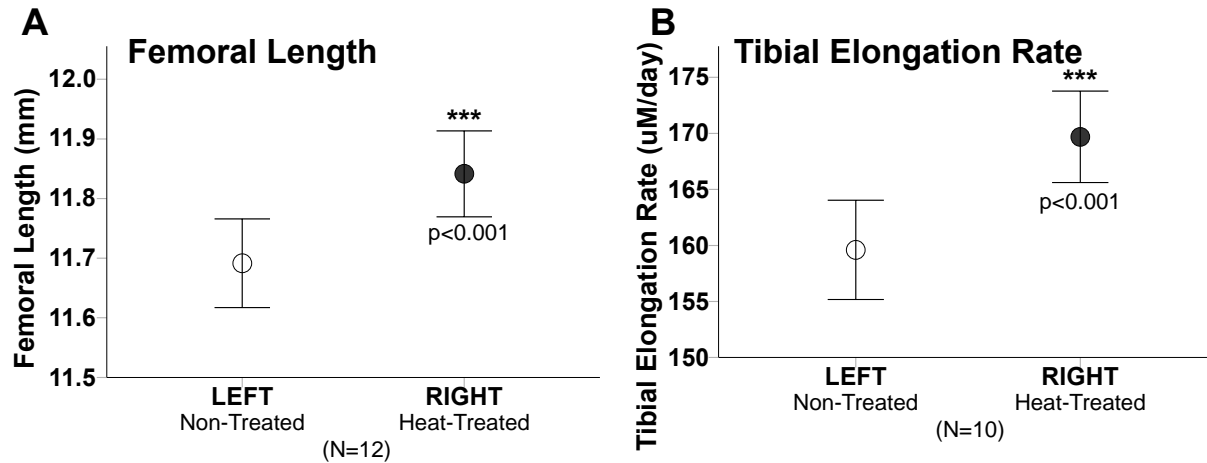


Figure 8. Extremities are Lengthened on the Heat-Treated Side

(A) Error bar plot comparing femoral length of non-treated and heat-treated limbs, show femoral length increased on the heat-treated side by 1.4% after 7 days of heating. (B) Tibial elongation rate increased on the heat-treated side by 6.5%. Mean ± 1 standard error plotted. *** $p < 0.001$, significance in left-right comparisons.

Table 3. Comparison of Hindlimb Weight Bearing and Tibial Length Measured by X-Rays.

Parameter		Non-Treated (30°C)	Heat-Treated (40°C)	Percent Increase	N
Tibial Length (mm)					
measured from x-rays	Before	12.93 (0.27)	12.94 (0.26) ^{ns}	0.1	6
	After	14.19 (0.14)	14.32 (0.12) ^{***}	0.9	5
Hindlimb Weight Bearing (g)					
measured using incapitance meter	Before	3.36 (0.38)	3.23 (0.25) ^{ns}	-2.9	7
	After	5.44 (0.58)	6.51 (0.80) ^{***}	19.6	8

Values are mean (standard deviation). Sample size (N) is number of left-right pairs. Significantly larger on heat-treated side by one-tailed paired t-test: * $p < 0.05$; ** $p < 0.01$; *** $p < 0.001$; ns, non-significant.

2.3.3 Hindlimb Weight Bearing

As with starting tibial length, there were no significant left-right differences in hindlimb weight bearing (paired $t=0.94$, $p=0.38$) at the start of the study (Table 3). Although not statistically significant, hindlimb bearing was about 3% greater on the intended non-treated side prior to unilateral heating. After 7 days of targeted limb heating, hindlimb weight bearing (paired $t=11.9$, $p<0.001$) was nearly 20% greater on the heat-treated side (Table 3). There was also a significant positive linear relationship between the increase in weight bearing and increase in tibial elongation rate ($R^2=0.82$, $p<0.01$) on the heat-treated side (Fig. 9).

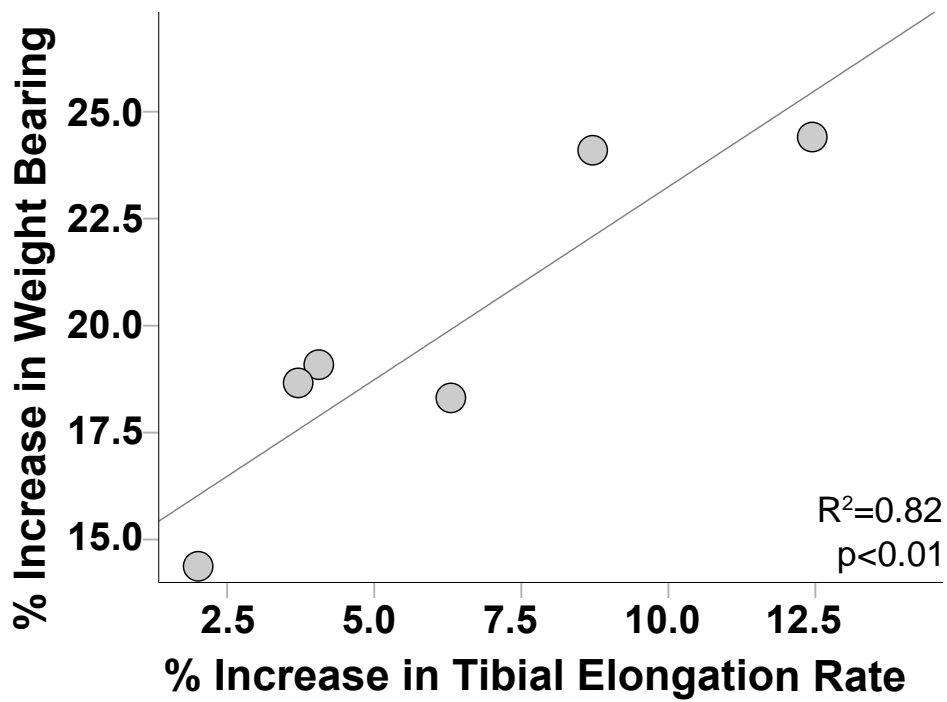


Figure 9. Increase in Weight Bearing and Tibial Elongation Rate are Correlated After 7 Days of Unilateral Heat-Treatment

Scatter plot of individual mice shows a significant positive linear relationship between the increase in weight bearing and increase in tibial elongation rate after 7 days of targeted limb heating ($y = 14.23 + 0.9x$).

2.4 DISCUSSION

The goal of this study was to determine if the heat-induced differences in limb length are functionally significant as assessed by changes in hindlimb weight bearing. Our data support the hypothesis that heat-induced limb length asymmetry has a functional impact on weight bearing in mouse hindlimbs.

After 7 days of targeted limb heating, there was a nearly 1% increase in tibial length on the heat-treated side determined by measurements from x-ray images of live anesthetized mice (Table 3). This increase in tibial length is comparable to the 1.4% increase in femoral length measured by postmortem femoral scans (Fig. 8). While the femoral length increase was slightly greater, this may be due to a larger sample size, or because the dried femoral landmarks were more distinct than those of the tibia in the radiographs. The femur was not measured in radiographs because its proximal and distal ends were more prone to distortion. Endpoint tibial length measured from whole tibia postmortem was also not accomplished since tibiae were reserved for tibial elongation rate analyses.

The heat-enhanced bone length and tibial elongation rate measured after 7 days of heating was associated with a nearly 20% increase in hindlimb weight bearing on the heat-treated side (Table 3). This increase in hindlimb weight bearing positively correlates to tibial elongation rate indicating that gait asymmetry increases along with bone elongation (Fig. 9). The positive correlation between hindlimb weight bearing and tibial elongation rate is consistent with similar findings in human studies (Kaufman et al., 1996; Khamis & Carmeli, 2017). One limitation to this study was the difficulty to obtain longitudinal weight bearing data (before and after measurements from the same mouse)

using the incapacitance meter since data could only be used when the mice were calm, immobile, and properly positioned within the plexiglass chamber. Using a dynamic gait analysis would be beneficial because it would enable the collection of data in unrestrained mice in their natural posture. An additional study to further support the functional significance of heat-induced limb length asymmetry may include a balance beam test with mice. Assessment of motor coordination and balance response to heat-treatment would be relevant since poor balance is associated with human limb length discrepancies (Azizan et al., 2018; Bonnet, Cherraf, Szaffarczyk, & Rougier, 2014).

Radiography and weight bearing analyses were useful methods for acquiring before and after bone length and hindlimb weight bearing measurements from the same mouse. Measurements collected at the start of the experiment are useful for evaluating the functional importance of targeted limb heating because they demonstrate the natural differences in both bone length and weight bearing prior to experimental manipulation. In humans, many individuals have a degree of normal left-right asymmetry in the lengths of their lower limbs (Green & Anderson, 1955; Knutson, 2005). Serrat et al. (2015) showed that there was no inherent side asymmetry in non-treated control animals. The current study further supported that left-right asymmetry is heat-induced and not a natural variation by comparing the before and after measurements of both tibial length and weight bearing.

2.5 CONCLUSION

In conclusion, even small discrepancies in limb length (nearly 1% to 1.4%) have a functional impact on hindlimb weight distribution (nearly 20%) in young mice. These

results suggest that heat-based therapies should continue to be pursued as a non-invasive alternative to surgical correction of limb length discrepancy. Chapter 6 tests the hypothesis that heat-induced limb length asymmetry is maintained to skeletal maturity (12 weeks of age). However, future studies will determine if left-right limb length asymmetry in skeletally mature mice has a functional impact on weight bearing. This would be translatable to the orthopedic problems described to accompany LLD and gait disturbances in adulthood. The functional significance of the heat-induced difference in limb length sets the foundation to further experimentation using the unilateral heating model to gain a better understanding of heat-enhanced limb growth.

CHAPTER III: CHONDROCYTE PROLIFERATION AND HYPERTROPHY IN TIBIAL GROWTH PLATES INCREASES AFTER 7 DAYS OF TARGETED LIMB HEATING

3.1 INTRODUCTION

During longitudinal bone growth via endochondral ossification, cartilaginous growth plates undergo a process of proliferation, expansion and apoptosis. Bone growth rate is largely dependent on the dynamics of cartilage growth. It is therefore likely that heat enhanced bone elongation involves modifications to growth plate cartilage. Others have determined the main contributing factors to longitudinal growth include: the amount of columnar cells in the proliferative zone of the growth plate, the rate of proliferation, and the size of expanded cells in the hypertrophic zone (Cooper et al., 2013; Farnum, 2007; Hunziker et al., 1987; Hunziker & Schenk, 1989; Hunziker, 1994b; Kember, 1993; Rolian, 2008; Walker & Kember, 1972; Wilsman et al., 1996a, 1996b, 2008).

The growth period from 3-5 weeks of age in mice post weaning is the most rapid, temperature sensitive period of longitudinal bone growth (Al-Hilli & Wright, 1983; Callewaert et al., 2010; Li et al., 2017; Serrat, King, & Lovejoy, 2008). Temperature as a therapeutic intervention therefore should be most effective during this stage of early postnatal linear growth in mice. Treatment with 40°C unilateral heat for 40 minutes/day over a period of 14 days in mice starting at 3 weeks of age resulted in extremity lengthening and enhanced tibial elongation rate in both male and female mice (Serrat et al., 2015). This phase of growth is an ideal period to focus therapeutics for optimum limb lengthening results.

The objective of this study was to determine how localized heating impacts bone growth at the site of the cartilage growth plate after one and two weeks of limb heating. The one week duration of heating was selected in addition to two weeks since the mice have the largest gain in body mass from 3-4 weeks of age as shown by growth curves provided by Hilltop Lab Animals, Inc (“Growth Chart C57BL/6,” 2018) and The Jackson Laboratory (“Body Weight Information for C57BL/6J,” 2018). This study tested **the hypothesis that increased bone length in heat-treated limbs will be associated with increased chondrocyte proliferation and hypertrophic zone expansion compared to the non-treated contralateral limbs.**

3.2 MATERIAL AND METHODS

3.2.1 Animals and Experimental Design

All procedures were approved by the Institutional Animal Care and Use Committee of Marshall University (Protocol 558). Female C57BL/6 (N=24) mice were obtained from Hilltop Lab Animals, Inc. (Scottsdale, PA, USA) at 21 (N=18) or 28 (N=6) days weaning age. Mice were singly housed at 20°C in standard plastic caging, exposed to a 12 hour light/dark cycle and provided with food and water ad libitum.

As indicated by the unilateral heating methods schematic (Fig. 10) mice post-weaning were treated with daily unilateral heat (40°C). Unilateral heat-treatment for 7 days began when mice were 3 weeks (N=6) and 4 weeks old (N=6), and treatment for 14 days started when mice were 3 weeks old (N=6). The procedural room temperature remained at 19°C while mice were anesthetized under 1.5% isoflurane and positioned right lateral recumbent on a 40°C heating pad each day for 40 minutes.

Mice were weighed and given subcutaneous injections of a saline solution (3:1, 1xPBS:dH₂O) at a volume of 0.01mL/g daily at the beginning of the light cycle. Mice were injected with saline because they serve as a control group to compare with their weight-matched littermates injected with drug treatments discussed in Chapters 4 and 5. Previous studies in our laboratory have shown that there are no significant differences in heat-treatment outcome variables between non-injected and saline-injected mice (unpublished data). Localized heating occurred one hour following injections.

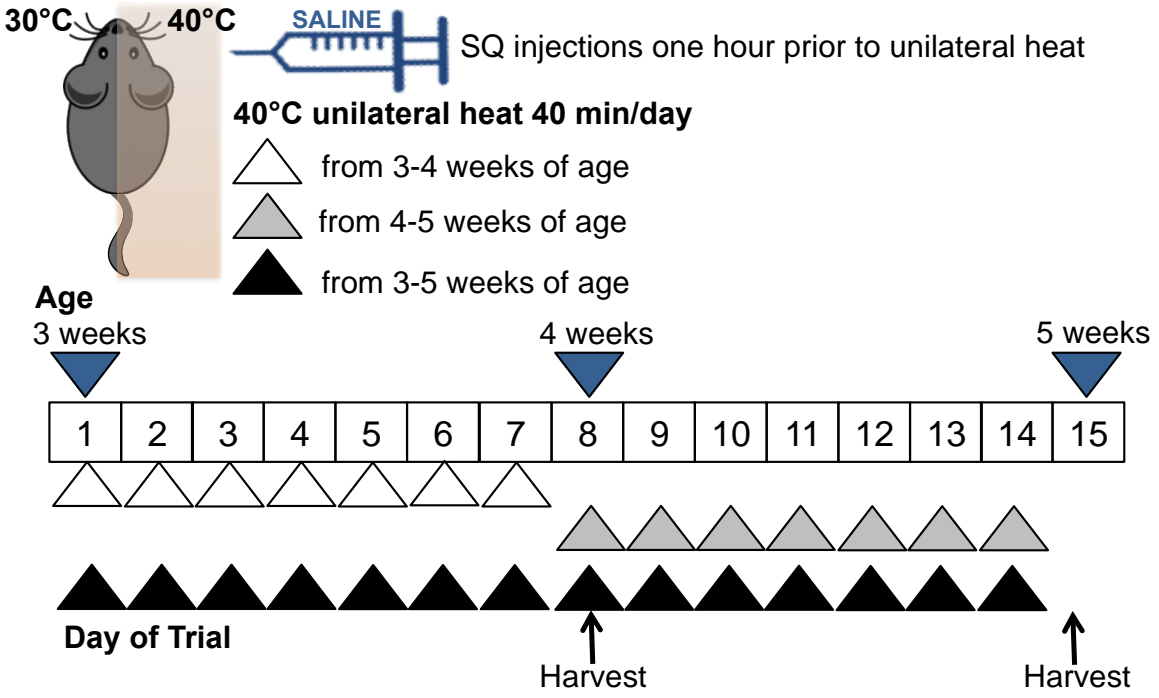


Figure 10. Unilateral Heating Schematic
 Mice were injected subcutaneously (SQ) with saline one hour prior to treatment of 40°C unilateral heat for 40 minutes daily for: (1) 7 days from 3-4 weeks of age, (2) 7 days from 4-5 weeks of age or (3) 14 days from 3-5 weeks of age. Euthanasia and tissue collection occurred 1 day after the last day of heat-treatment. Mouse illustration based on "mouse clip art black and white" from clipartstockphotos.com.

3.2.2 Tissue Collection

All experimental mice (N=24) were euthanized for tissue collection 1 day after the last day of heat-treatment. Mice that were subjected to unilateral heating from 3-4 weeks of postnatal age (N=6) were euthanized at the 4 weeks of age endpoint and those treated from 3-5 weeks of postnatal age (N=18) were euthanized at the 5 weeks of age endpoint (Fig. 10). It is important to note that although tissues were collected from mice treated for 7 days from 4-5 weeks of age, only weight gain comparisons are made from these mice in this study since mice from 3-4 weeks of age grew more rapidly in comparison. Therefore, mice treated for 7 days from 3-4 weeks of age were preferable for analysis.

Long bones (femora and humeri) from each side were dissected, cleaned, dried, and scanned on a flatbed scanner. Proximal tibiae from each hindlimb were dissected, cleaned and bisected. One unfixed half was arranged on a glass slide and cover-slipped with glycerol in PBS prepared for tibial elongation rate analysis. The other tibial half was fixed in 10% neutral buffered formalin for 24 hours, decalcified in 19% EDTA (pH 7.4) for 1 week, rinsed in PBS, dehydrated in a series of ethanol, cleared in xylene, and embedded in paraffin. Sagittal sections 6 μ M thick were cut with a microtome (Leica RM2125) and mounted on Diamond™ White Glass slides (Globe Scientific) for histological analysis.

3.2.3 Tibial Elongation Rate Analysis and Long Bone Measurements

A single intraperitoneal injection of oxytetracycline (OTC) (7.5 mg/kg, Norbrook 200 mg/mL) was administered to mice 7 days prior to euthanization and tissue

collection. Fluorescence was visualized in unfixed slab sections of tibiae using the UV filter on a fluorescence stereoscope. Measurements collected from scans of femora, and quantification of tibial elongation rate, were done as described in Chapter 2 (Material and Methods 2.2.5). Images of scanned humeri were also calibrated and measured in ImageJ, but humeral length was measured as the distance between the proximal- and distal-most articular ends.

3.2.4 Growth Plate Morphometry

Serial sections of proximal tibiae were deparaffinized in xylene, rehydrated in a graded series of ethanol, and incubated in Weigert's hematoxylin for 6 minutes prior to Safranin-O (0.1%, Sigma)/ fast green (0.01%, Fisher) staining. Stained sections were dehydrated in graded series of ethanol and xylenes and cover slipped with DPX (Sigma). Sections were then imaged using Ocular Image Acquisition Software (version 1.05.211) under 20X magnification with a Leica DM2500 optical microscope (Leica Microsystems, Wetzlar, Germany) fitted with a QImaging Retiga R6 color camera (QImaging Corporation).

The heights of individual growth plate zones (reserve, proliferative and hypertrophic) were measured from calibrated images in ImageJ. Measurements were taken at five different points across the width of the growth plate and the mean was calculated to represent the height for each zone. Total growth plate height was determined by the sum of the individual zones. Each individual zone was then normalized to the total growth plate height to allow comparisons among ages. It is

important to note that tibiae from mice (N=6) treated for two weeks (N=12) were not used for histological analysis due to sample loss during tissue processing.

3.2.5 Immunohistochemistry

Serial sections of proximal tibiae from mice treated from 3-4 weeks of age were stained using a rabbit polyclonal antibody against PCNA (Santa Cruz, sc-7907) at a dilution of 1:200 (Table 4). Serial sections of proximal tibiae from mice treated 3-5 weeks of age were stained using a monoclonal rabbit antibody against PCNA (Cell Signalling, #13110) at a dilution of 1:200 after the previously used antibody against PCNA was discontinued. In both cases, antigen unmasking was accomplished by incubating slides at 40°C with a pre-warmed sodium citrate buffer (pH 3.5) for 30 minutes followed by a rinse cycle and another incubation at 40°C in a 1:100 dilution of chondroitinase ABC (Sigma, C2905) for 10 minutes. Endogenous peroxidase activity was quenched with 3% hydrogen peroxide (H₂O₂) at room temperature (21°C) for 10 minutes followed by a 1-hour incubation in normal blocking serum. Incubation with the primary antibody occurred in the humidified chamber at room temperature overnight. The avidin-biotin complex (ABC) horseradish peroxidase method was then used to detect positive immunostaining either with the ImmunoCruz rabbit ABC staining system (Santa Cruz Biotechnology, sc-2018) or the VECTASTAIN Elite ABC-HRP kit (Vector, Rabbit IgG, PK-6101). Both methods used DAB as the chromagen (Vector, SK-4100) and all were counterstained with 0.1% methyl green (Sigma), dehydrated and cover slipped with DPX before allowing to dry overnight prior to imaging.

Stained sections were imaged using the Leica DM2500 optical microscope as previously described above. Chondrocytes within the proliferative zone of the proximal tibial growth plate visualized as dark brown nuclei were manually counted as positively stained cells for PCNA. Chondrocytes were counted in a 130 μ M wide sample area (two per section). This size was chosen because it consistently contained an area of the growth plate encompassing all zones of chondrocytes to allow comparisons among samples. The percent of positively stained cells was quantified by dividing the number of counted positive cells by the total number of chondrocytes within the proliferative zone.

Table 4. List of Primary Antibodies and Secondary Antibody Kits Used in the Study

Length of Heat-Treatment	1° Ab / 2° Ab Detection Kit	Company	Catalog No.	Dilution
7 days (3-4 weeks of age)	PCNA	Santa Cruz	sc-7907	1:200
	IGF1R	Santa Cruz	sc-712	1:200
	Phospho-IGF1R	abcam	ab39396	1:100
	ImmunoCruz ABC	Santa Cruz	sc-2018	as instructed
14 days (3-5 weeks of age)	PCNA	Cell Signalling	#13110	1:200
	IGF1R	abcam	ab131476	1:100
	Phospho-IGF1R	abcam	ab39398	1:100
	Vectastain Elite ABC	Vector Laboratories	PK-6101	as instructed

3.2.6 Statistical Analysis and Sample Size

Statistical analyses were performed using SPSS 25.0 software (IBM Corporation, Armonk, NY) with $p < 0.05$ as accepted significance. Non-treated and heat-treated side comparisons for humeral length, femoral length, tibial elongation rate, growth plate zone heights and percent cells positive for PCNA expression were made using one-tailed paired t-tests. Multiple comparisons made between durations of heat-treatment were made using a one-way ANOVA with the Tukey post hoc test. Data were reported as mean \pm standard deviation (SD) in tabular format and as mean \pm standard error (SE) in graphical format.

Sample sizes for measurements that are documented as *less than the size of the experimental sample set* was a result of either sample loss during dissection or sample processing. Since left-right comparisons are made, if one side is damaged during dissection, sample preparation, tissue processing, sectioning or staining, the entire left-right pair is lost. Samples and missing cases were excluded from statistical analysis on an analysis-by-analysis basis.

3.3 RESULTS

3.3.1 Unilateral Heating Parameters

Mice treated for 7 days from 3-4 weeks of age gained 4.7 ± 0.7 g, and mice treated for 7 days from 4-5 weeks of age gained 1.6 ± 1.0 g in mass (Fig. 11). Thus, the largest growth spurt of experimental mice occurred from 3-4 weeks of age. This growth spurt is as shown by Hilltop Lab Animals, Inc (“Growth Chart C57BL/6,” 2018) and The Jackson Laboratory (“Body Weight Information for C57BL/6J,” 2018). Change in mass

significantly differed between each experimental group as determined by multiple comparison analysis using one-way ANOVA and Tukey post hoc test ($F(2,21)=53.3$, $p<0.01$). Therefore, the mice treated for 7 days from 3-4 weeks of age were selected for analysis instead of the slower growing mice from 4-5 weeks of age.

Mice treated for 14 days from 3-5 weeks of age gained 6.0 ± 0.9 g in mass (Fig. 11). This total gain is nearly equivalent to the sum of the mass gained after 7 days of heating from mice 3-4 weeks and 4-5 weeks of age. The core temperature averaged 36°C during all extents of unilateral heating, consistent with the other limb heating studies in the previous chapter and those to follow. While anesthetized the average surface temperature of non-treated hindlimbs was 30°C and the heat-treated hindlimbs were 40°C for all durations of unilateral heating.

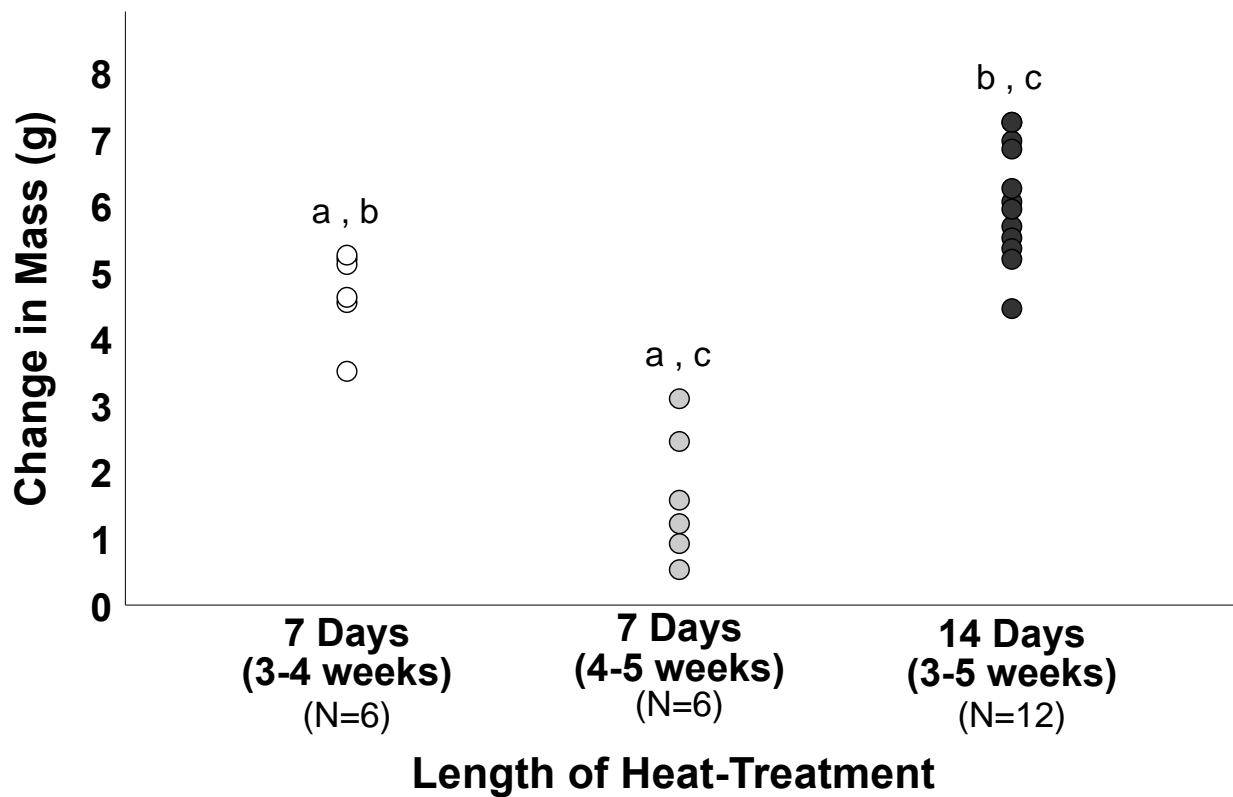


Figure 11. Majority of Body Mass Gained During 14 Days of Unilateral Heat-Treatment Occurs During the First 7 Days

Scatter plots show the change in mass of individual mice treated for (1) 7 days from 3-4 weeks of age (open circles), (2) 7 days from 4-5 weeks of age (gray circles) and (3) 14 days from 3-5 weeks of age (dark gray circles). Significance ($p < 0.05$) in the mean change in mass between heat-treatment durations is denoted as: ^a, 3-4 weeks and 4-5 weeks of age; ^b, 3-4 weeks and 3-5 weeks of age; ^c, 4-5 weeks and 3-5 weeks of age.

3.3.2 Bone Length and Tibial Elongation Rate

At experimental end, mice treated for 14 days from 3-5 weeks of age had an increase in femoral length (paired $t=10.1$, $p<0.001$) of 1.1% on the heat-treated side (Fig. 12A; Table 5). Humeral length did not differ (paired $t=1.0$, $p=0.34$) (Table 5). Mice treated for 7 days from 3-4 weeks of age, femoral length (paired $t=4.4$, $p<0.01$) increased by 1.7% (Fig. 12A, Table 5). Humeral length did not differ (paired $t=0.74$, $p=0.50$) (Table 5). Multiple comparisons by one-way ANOVA with Tukey post hoc tests showed no significant differences in heat-enhanced femoral length between durations of treatment ($F(1,14)=2.7$, ns, $p=0.12$).

Mice treated for 14 days had a tibial elongation rate of $110\pm 11\mu\text{M}/\text{day}$ on the non-treated side and $121\pm 11\mu\text{M}/\text{day}$ on the heat-treated side with an increase on the heat-treated side (paired $t=7.8$, $p<0.001$) of nearly 11% (Fig. 12B; Table 5). Mice treated for 7 days of treatment had a tibial elongation rate of $157\pm 11\mu\text{M}/\text{day}$ on the non-treated side and $169\pm 13\mu\text{M}/\text{day}$ on the heated side with an increase on the heat-treated side (paired $t=4.6$, $p<0.01$) of nearly 8% (Fig. 12B; Table 5). Multiple comparison analysis by one-way ANOVA determined no significant differences in heat-enhanced tibial elongation rate between durations of treatment ($F(2,17)=4.74$, $p<0.05$).

Table 5. Comparison of Non-Treated and Heat-Treated Sides of Saline-Injected Experimental Mice Bone Parameters.

Parameter	Length of Heat-Treatment	Non-Treated (30°C)	Heat-Treated (40°C)	Percent Increase	N
Humeral Length (mm)	7 days (3-4 weeks)	9.27 (0.14)	9.23 (0.20) ^{ns}	-0.4	6
	14 days (3-5 weeks)	10.14 (0.11)	10.15 (0.13) ^{ns}	0.1 ^{ns}	9
Femoral Length (mm)	7 days (3-4 weeks)	10.44 (0.19)	10.62 (0.26) ^{**}	1.7	6
	14 days (3-5 weeks)	12.86 (0.18)	13.00 (0.17) ^{***}	1.1 ^{ns}	9
Tibial Elongation Rate (µM/day)	7 days (3-4 weeks)	156.88 (11.24)	168.94 (12.85) ^{**}	7.7	5
	14 days (3-5 weeks)	109.57 (11.18)	121.22 (10.70) ^{***}	10.8 ^{ns}	8

Values are mean (standard deviation). Length of heat-treatment is in days (age of mice during treatment). Sample size (N) is number of left-right pairs. Significantly larger on heat-treated side by one-tailed paired *t*-test: ***p*<0.01; ****p*<0.001; ns, not significant. Significant differences in percent increase between durations of heat-treatment by one-way ANOVA: ns, not significant.

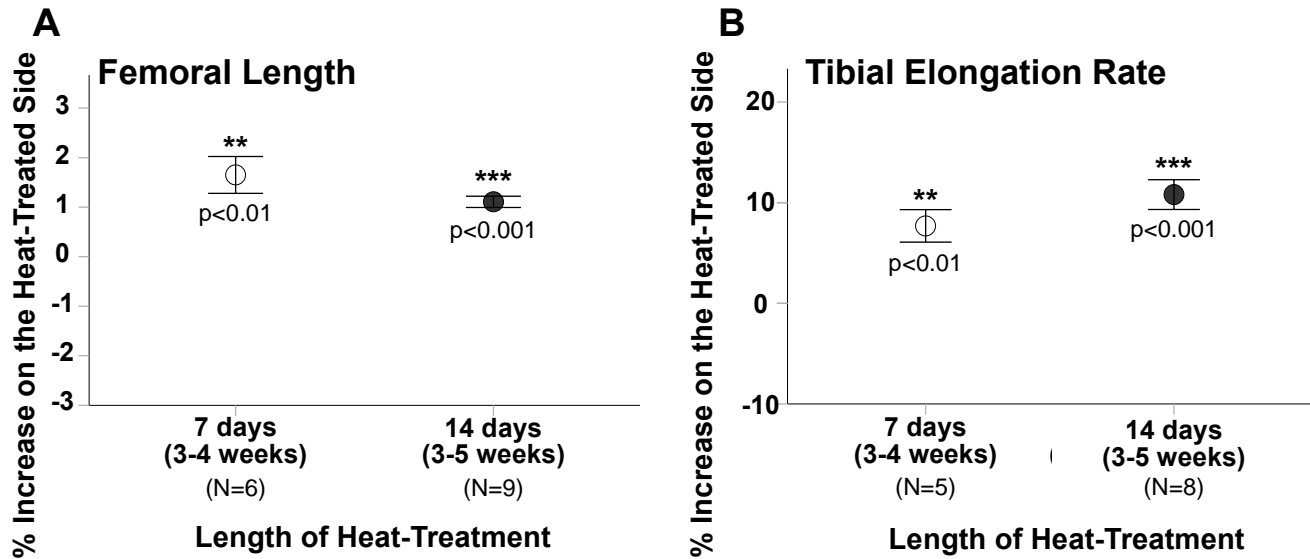


Figure 12. Extremities are Lengthened on the Heat-Treated Side

(A) Error bar plots show percent change in heat-treated limb compared to non-treated limb. Femoral length increased on the heat-treated side by 1.7% and 1.1% for mice treated for 7 days (3-4 weeks of age) and 14 days (3-5 weeks of age) respectively. (B) Tibial elongation rate increased on the heat-treated side by 7.7% and 10.8% after 7 days of heating and 14 days of heating respectively. Mean \pm 1 standard error plotted. **p<0.01; ***p<0.001, significance in left-right comparisons.

3.3.3 Growth Plate Morphometry

Normalized proliferative zone (PZ) height was reduced by 9.0% on the heat-treated sides of mice treated for 7 days from 3-4 weeks of age (paired $t=10.2$, $p<0.001$), and 7.3% on the heat-treated sides of mice treated for 14 days from 3-5 weeks of age (paired $t=3.5$, $p<0.05$) (Fig. 13A, C; Table 6). The normalized hypertrophic zone (HZ) height increased by 8.6% on the heat-treated sides of mice treated for 7 days (paired $t=9.0$, $p<0.001$) and 8.8% on the heat-treated sides of mice treated for 14 days (paired $t=4.2$, $p<0.05$) (Fig. 13B, C; Table 6). There were no significant changes in reserve zone height (zone of quiescent chondrocytes) at any duration of heat-treatment (paired $t=0.0$ and 0.6 ; $p=1.00$ and 0.59 respective to as reported above). Multiple comparison analysis by one-way ANOVA determined no significant differences in heat-enhanced PZ height ($F(2,14)=0.84$, ns, $p=0.46$) and HZ height ($F(2,14)=0.94$, ns, $p=0.42$) between durations of heat-treatment.

Table 6. Comparison of Growth Plate Morphometry between Non-Treated and Heat-Treated Sides of Saline-Injected Experimental Mice.

Parameter	Length of Heat-Treatment	Non-Treated (30C)	Heat-Treated (40C)	Percent Increase	N
Reserve Zone Height (Normalized)	7 days (3-4 weeks)	0.104 (0.015)	0.104 (0.011) ^{ns}	0.9	5
	14 days (3-5 weeks)	0.118 (0.008)	0.114 (0.015) ^{ns}	-0.4 ^{ns}	5
Proliferative Zone Height (Normalized)	7 days (3-4 weeks)	0.450 (0.023)	0.412 (0.019) ^{**}	-9.0	5
	14 days (3-5 weeks)	0.466 (0.039)	0.430 (0.027) [*]	-7.3 ^{ns}	5
Hypertrophic Zone Height (Normalized)	7 days (3-4 weeks)	0.448 (0.026)	0.484 (0.025) ^{**}	8.6	5
	14 days (3-5 weeks)	0.420 (0.032)	0.454 (0.021) [*]	8.8 ^{ns}	5

Values are mean (standard deviation). Length of heat-treatment is in days (age of mice during treatment). Sample size (N) is number of left-right pairs. Significantly larger on heat-treated side by one-tailed paired t-test: * $p < 0.05$; ** $p < 0.01$; *** $p < 0.001$; ns, non-significant. Significant differences in percent increase between durations of heat-treatment by one-way ANOVA: ns, not significant.

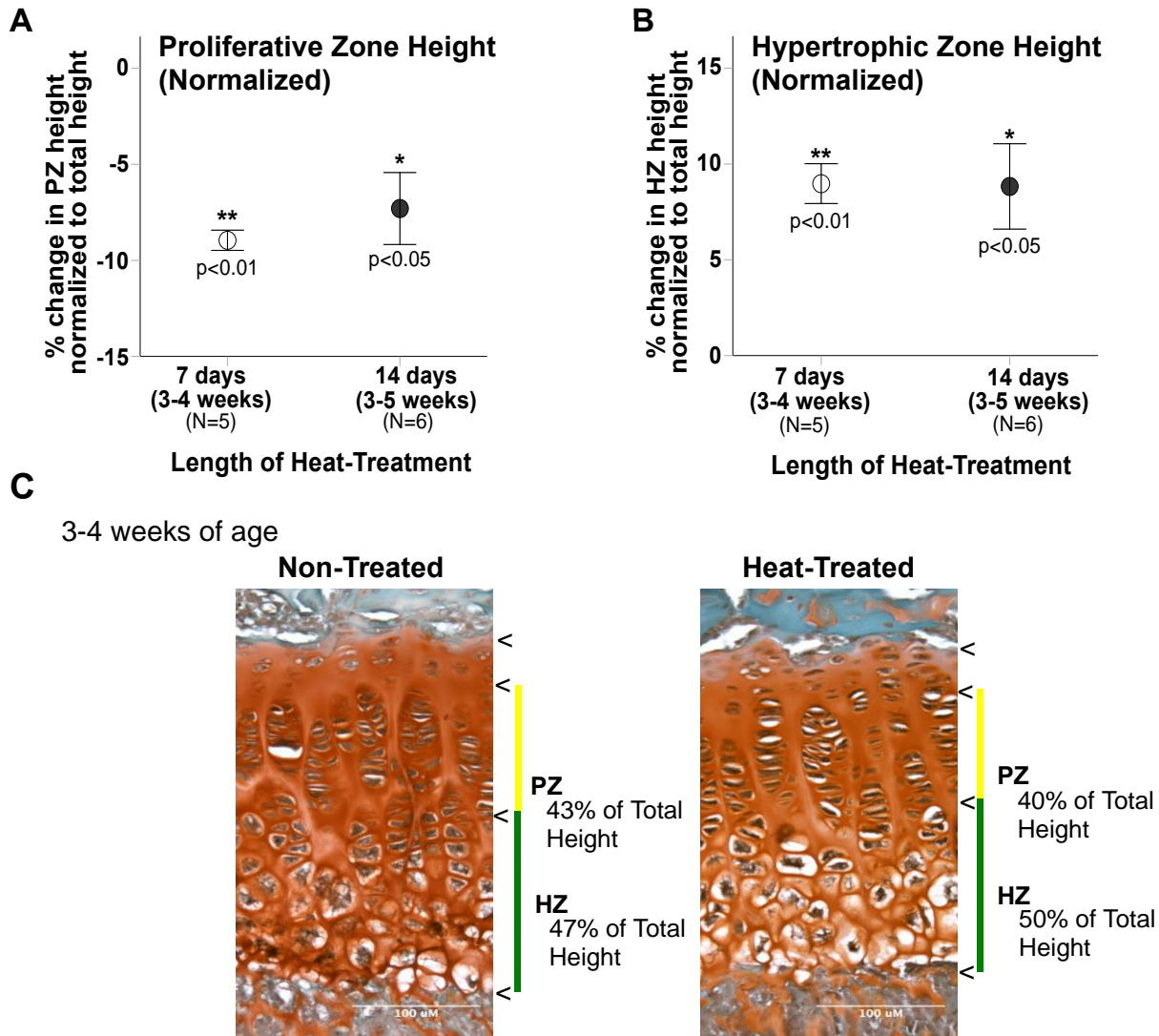


Figure 13. When Normalized to Total Proximal Tibial Growth Plate Height, PZ is Reduced on the Heat-Treated Side and HZ is Enlarged

(A) Error bar plot shows percent change in heat-treated limb compared to non-treated limb. Normalized proliferative zone (PZ) height is reduced on the heat-treated side by 9.0% in mice treated for 7 days from 3-4 weeks of age and 7.3% in mice treated for 14 days from 3-5 weeks of age. (B) Normalized hypertrophic zone (HZ) height is enlarged by 8.6% in mice treated for 7 days from 3-4 weeks of age and 8.8% in mice treated for 14 days from 3-5 weeks of age. (C) Non-treated and heat-treated tibial growth plates from the same mouse treated from 3-4 weeks of age, stained with Safranin-O/fast green to distinguish cartilage (red) from bone (green/blue). Arrows indicate the different zones within the growth plate. The vertical yellow line denotes the PZ while the green line denotes the HZ. Mean \pm 1 standard error plotted.

3.3.4 PCNA Expression

PCNA expression in chondrocytes of the PZ was increased on the heat-treated side of mice treated for both 7 days (3-4 weeks of age) and 14 days (3-5 weeks of age) (Fig. 14). Expression of PCNA increased by 8.6% on the heat-treated side of mice treated for 7 days from 3-4 weeks of age (paired $t=2.7$, $p<0.05$) and 16.7% on the heat-treated side when mice were treated for 7 days from 3-5 weeks of age (paired $t=2.9$, $p<0.05$) (Fig. 14A). Multiple comparisons by one-way ANOVA determined no significant differences between durations of treatment ($F(2,16)=2.16$, ns, $p=0.15$).

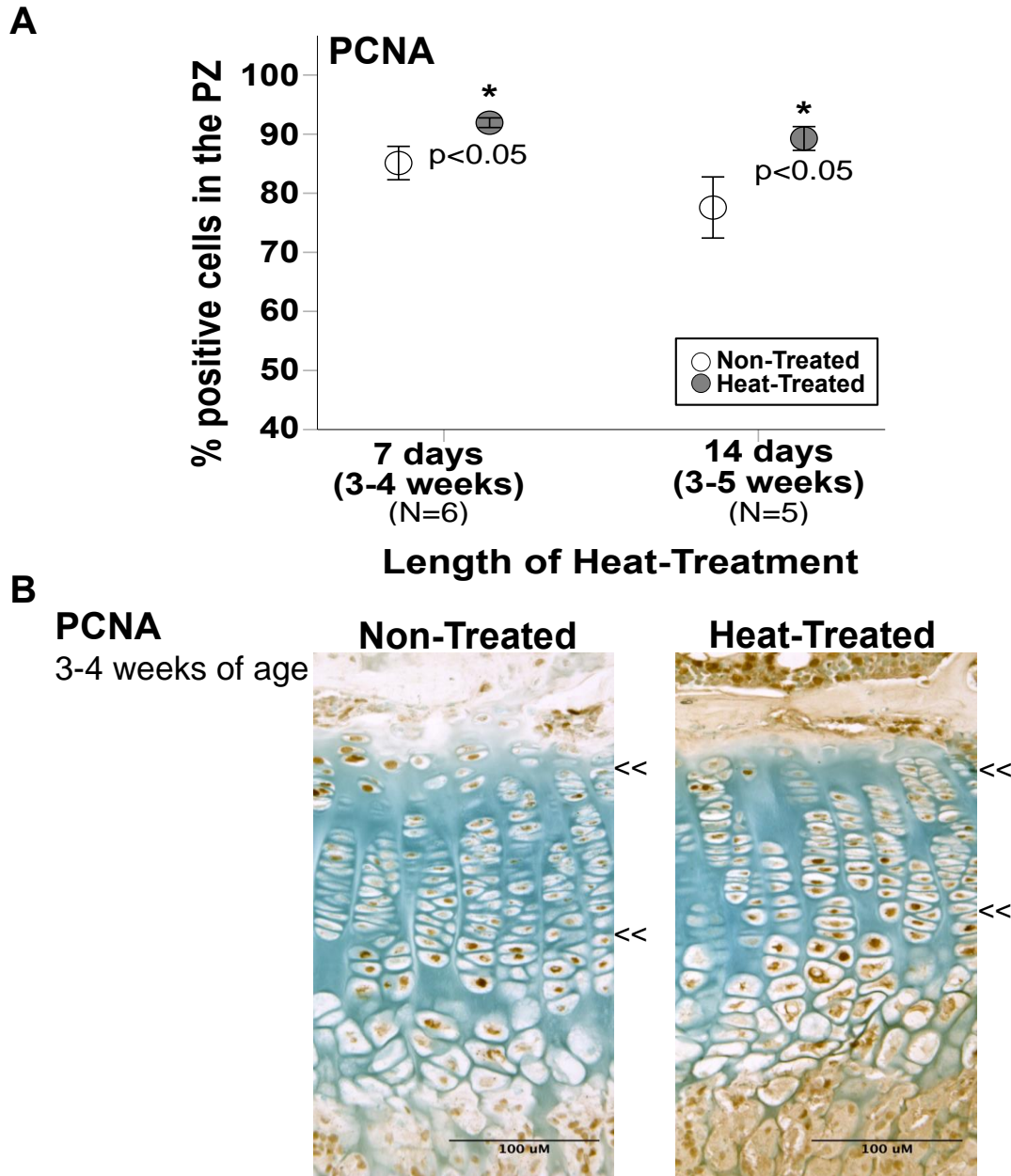


Figure 14. Expression of PCNA, Marker for Cell Proliferation, Increased with Heat-Treatment in the PZ of the Proximal Tibial Growth Plate

(A) Error bar plot shows percent of chondrocytes positive for PCNA expression on non-treated (open circles) and heat-treated (gray circles) sides. PCNA expression increased by 8.6% on the heat-treated sides of mice treated for 7 days from 3-4 weeks of age and increased by 16.7% on the heat-treated sides of mice treated for 14 days from 3-5 weeks of age. (B) Immunoreactivity of PCNA in non-treated and heat-treated proximal tibial growth plates from the same mouse treated from 3-4 weeks of age. Positive staining, shown by dark brown nuclei, within the PZ of the growth plate (region between the double arrows) increases on the heat-treated side by >10%. Mean \pm 1 standard error plotted. * $p < 0.05$, significance in left-right comparisons.

3.4 DISCUSSION

The goal of this study was to determine how unilateral heating enhances longitudinal bone growth at the cellular level. Femoral length (1.7%) and tibial elongation rate (7.7%) increased on the heat-treated sides of mice treated for 7 days from 3-4 weeks of age (Fig. 12, Table 5). Chondrocyte proliferation (8.6%) and size of the hypertrophic zone (8.6%) also increased in these mice (Fig. 13B, 12; Table 6). After 14 days of treatment, femoral length (1.1%) and tibial elongation rate (10.8%) increased on the heat-treated sides of mice treated 3-5 weeks of age (Fig. 12, Table 5). Chondrocyte proliferation (16.7%) and size of the hypertrophic zone (8.8%) also increased in these mice (Fig. 13B, 12; Table 6).

The data supported the hypothesis that there will be a unilateral increase in bone length associated with increased chondrocyte proliferation and hypertrophic zone expansion in the growth plate with heat-treatment. Humeral length did not differ between non-treated and heat-treated sides (Table 5), consistent with previous studies from our laboratory. The likely explanation is the similarity of humeral skin temperature to body core temperature accounting for a marginal temperature differential during treatment (Serrat et al., 2015). Results from Chapter 2 (mice were treated from 3-4 weeks of age) suggest that one week of unilateral heat-treatment can effectively increase bone length (Fig. 8, Table 3). In this study, two separate age groups (3-4 weeks and 4-5 weeks of age) were chosen for one week of unilateral heat-treatment. Mice from 3-4 weeks of age gained more mass after 7 days of treatment than the mice treated from 4-5 weeks (Fig. 11). The growth spurt that occurred when mice were

treated from 3-4 weeks of age supported the rationale for choosing that age group for data analysis.

Although the impact of temperature on postnatal longitudinal bone growth has been documented (Serrat, 2014b), there had been a gap in our understanding of the kinetics of the growth plate cartilage with heating. This study demonstrated that longitudinal bone growth is accompanied by increased proliferation and hypertrophic zone expansion. Increased proliferation may be due to either an increase in chondrocyte number (not measured in this study), or rate of proliferation (Kember, 1993; Rolian, 2008). Here we measured proliferation as (PCNA) expression within the proliferative zone of the growth plate. PCNA immunohistochemistry was chosen over other methods for analyzing cell proliferation such as bromodeoxyuridine (BrdU), because PCNA is a less invasive technique and both methods have shown similar results (Wildemann et al., 2003).

PCNA expression increased on the heat-treated sides at all durations of heat-treatment, but trends indicate that proliferation was increased to a larger extent with two weeks of treatment (Fig. 14). While PCNA expression was exclusively measured in the proliferative zone of the growth plate, there was observed positive staining in the hypertrophic zone as well. Other studies have also reported positive staining of PCNA in the hypertrophic zone of rabbit growth plates (Enishi et al., 2014) and suggest hypertrophic chondrocytes (more commonly described to undergo programmed cell death) survive, proliferate and transdifferentiate into bone forming cells (Bahney et al., 2014; Enishi et al., 2014; Hu et al., 2017; Zhou et al., 2014).

In addition to hypertrophic zone height, the height of the reserve and proliferative zones were also analyzed (Table 6). Reserve zone height was unaffected as expected since chondrocytes in this zone are quiescent and do not participate in bone growth. Minor differences in total height of the growth plate were seen on heat-treated sides (data not shown), which is similar to what was observed in a study comparing control- (21°C) and warm-housed (27°C) mice (Serrat, 2014b).

Interestingly, the height of the proliferative zone decreased on heat-treated sides after 7 days (9.0%) and 14 days (7.3%) of unilateral heating (Fig 13A; Table 6). A cause for the reduced proliferative zone height after heat-treatment may be explained by the mechanical properties of proliferating chondrocytes. Periods of rapid bone growth are often accompanied by increased matrix synthesis exerting pressure on the chondrocytes causing them to flatten (Prein et al., 2016; Walker & Kember, 1972). Compressed columns of chondrocytes may also be a consequence of the expanding hypertrophic zone. Therefore, a shortened proliferative zone height does not necessarily reflect decreased proliferation, but a more compressed region of cells. However, to show the cells are compressed would involve comparing numbers of chondrocytes in the proliferative zone between growth plates of non-treated and heat-treated limbs (not done in this study). Another possibility for a shortened proliferative zone height may be due to heat-induced changes to Indian hedgehog (Ihh)/parathyroid hormone-related protein (PTHrP) negative feedback mechanisms that control the transition from proliferative, to hypertrophic chondrocytes. Downregulation of Ihh/PTHrP (maintains chondrocyte proliferation, and delays chondrocyte hypertrophy) would promote cell differentiation and leads to faster turnover to hypertrophic chondrocytes (van der

Eerden et al., 2003; Kronenberg, 2003; Wang et al., 2011). As an example, IGF1 has an important role in downregulating PTHrP to promote chondrocyte differentiation (Wang et al., 2011).

Limitations of this study include the sample size for heat-treatment. While power analysis indicates 6 animals to be a sufficient effect size, it can be difficult to attain this number because of the laborious nature of the experiments. Our studies focus on left-right differences after unilateral heat-treatment, and thus consistent collection of samples from both sides of the animal is necessary. If one side is damaged during dissection, sample preparation, tissue processing, sectioning or staining, the entire left-right pair is lost. Left-right comparisons also limit the ability to collect the same samples for a variety of analyses. For example, since both left and right femora are needed to make left-right length comparisons, they cannot also be used for histological analysis. The rationale for selecting the proximal tibia for growth rate and histological analysis is because the proximal tibia contributes most to tibial lengthening compared to the distal end (as discussed in Chapter 1, Section 1.1.2) (J. Bisgard & M. Bisgard, 1935; Farnum, 2007; Kember, 1972; Pritchett, 1992; Raimann et al., 2017; Rolian, 2008; Serrat et al., 2007; Wilsman et al., 1996a, 1996b, 2008). The growth plate of the proximal tibia also has been shown to have a higher rate of cell division and hypertrophy compared to sites of other long bones including that of the distal femur (Rolian, 2008).

3.5 CONCLUSION

In conclusion, evidence supports the hypothesis that there will be a unilateral increase in bone length associated with increased chondrocyte proliferation and

hypertrophic zone expansion in the growth plate with heat-treatment. The hypothesis was supported by results from mice treated for 7 days (3-4 weeks of age) and 14 days (3-5 weeks of age). This study demonstrated that investigating morphological changes in the growth plate is a means to assess heat-enhanced bone elongation. Future studies will determine how targeted limb heating affects the activity of insulin-like growth factor I (IGF1), the major growth factor that regulates longitudinal bone growth. Improving and understanding the methods for using targeted limb heating to enhance bone elongation is important for developing a noninvasive alternative for treatment of limb lengthening disorders in children.

CHAPTER IV: SUBCUTANEOUS INJECTIONS OF LOW DOSE IGF1 IN CONJUNCTION WITH TARGETED LIMB HEATING CAN AUGMENT HEAT-ENHANCED BONE GROWTH

4.1 INTRODUCTION

The GH/IGF1 axis has been extensively studied and is often described as the major control system of postnatal growth and development (Le Roith et al., 2001; Woodall, Breier, O'Sullivan, & Gluckman, 1991) particularly of skeletal growth (Isgaard, Nilsson, Lindahl, Jansson, & Isaksson, 1986; Hunziker et al., 1994a; Lindsey & Mohan, 2016; Lupu et al., 2001; Mohan et al., 2003; Oberbauer & Peng, 1995; Yakar & Isaksson, 2016; Wu et al., 2015). This anabolic axis involves the dependent and independent relationship between GH and IGF1 and their associated factors in regulating linear growth in both an endocrine and paracrine/autocrine manner. Severe growth retardation observed in double *Ghr/Igf1* mutant mice supports that both GH and IGF1 are essential for linear growth (Lupu et al., 2001). However, IGF1 is a critical part of this axis because there is greater linear growth defects without the action of IGF1 (Baker et al., 1993; Bikle et al., 2001; Liu et al., 1993; Mohan et al., 2003; Powell-Braxton et al., 1993; Wang et al., 2006) compared to when GH action is impaired (Kasukawa, Baylink, Guo, & Mohan, 2003; Mohan et al., 2003). It has been reported that 83% of postnatal growth is dependent on the GH/IGF1 system and 69% of that dependent on IGF1 (Ciarmatori, Kiepe, Haarmann, Huegel, & Tönshoff, 2007). While studies have shown that postnatal growth can occur absent circulating levels of IGF1 (Fan et al., 2009; Sjögren et al., 1999; Ueki et al., 2000; Yakar et al., 1999, 2002; Yakar & Isaksson, 2016), disruptions in local IGF1 impair longitudinal bone growth (Govoni et

al., 2007a,b; Sheng, Zhou, Bonewald, Baylink, & Lau, 2013; Wang et al., 2011; Yakar, Courthland, & Clemmons, 2010; Yakar & Isaksson, 2016).

Administration of GH and IGF1 has been used for treatment of stunted linear growth. GH therapy is more commonly used in clinical settings to treat short stature (Ohlsson et al., 1998; Pfäffle, 2015; Wit & Oostdijk, 2015) such as those resulting from GH deficiency or other chromosomal and genetic syndromes (Harada et al., 2017; Moix et al., 2018; Noonan & Kappelgaard, 2015; Pfäffle, 2015; Ranke, 1995a, Tritos & Klibanski, 2016; Wit & Oostdijk, 2015). IGF1 is not as commonly used because of the adverse effects associated with increased serum IGF1 (such as hypoglycemia) during treatment (Clemmons, 2004; Guevara-Aguirre et al., 1997; Laron & Klinger, 2000; Lindsey & Mohan, 2016; Ross et al., 2015). However, long-term treatment with IGF1 has been shown to effectively reverse skeletal growth discrepancies (Azcona et al., 1999; Backeljauw et al., 2013; Chernausek et al., 2007; Laron & Klinger, 2000; Laron, 2001; Laron & Kauli, 2015b; Lupu et al., 2001; Midyett et al., 2010; Ranke et al., 1995b, 1999; Sims et al., 2000).

It is clear that IGF1 has an essential role in longitudinal growth. Without the action of IGF1, if survived past birth, there is a reported 70% reduction in body size and 40% reduction in linear bone growth (Liu et al., 1993; Mohan et al., 2003; Powell-Braxton et al., 1993; J. Wang et al., 1999; Y. Wang et al., 2006; Yakar & Isaksson, 2016). Studies have used IGF1 to enhance linear growth in various animal models. It has been shown that IGF1 administered through local administration directly into the growth plate has significantly increased bone length (Isgaard et al., 1986). Since targeted heat can increase vascular supply to the growth plate (Chapter 1, Section

1.6.2), the goal of this study was to use unilateral limb heating as a method to target a low dose of IGF1 administered subcutaneously once daily to the growth plate on the heat-treated side. This study tests **the hypothesis that IGF1 administration with heat-treatment will further enhance limb length than with heat alone**. Published studies are still ongoing to optimize IGF1 therapy in children without complications (Hansen-Pupp et al., 2017). Using limb heating to target once daily, low doses of IGF1 only to sites of longitudinal bone growth would improve current IGF-based therapies for children by enhancing limb elongation without the negative side effects.

4.2 MATERIAL AND METHODS

4.2.1 Animals and Experimental Design

All procedures were approved by the Institutional Animal Care and Use Committee of Marshall University (Protocol 558). Female C57BL/6 (N=32) mice were obtained from Hilltop Lab Animals, Inc. (Scottsdale, PA, USA) at 21 (N=12) and 28 (N=24) days weaning age. Mice were singly housed at 21°C in standard plastic caging, exposed to a 12 hour light/dark cycle and provided with food and water ad libitum.

As described in the previous chapters and as indicated by the unilateral heating methods schematic (Fig. 15), mice were subjected to same procedural conditions. Mice were treated for 7 days from 3-4 weeks of age and for 14 days 3-5 weeks of age. Mice were weighed each day and given subcutaneous injections of IGF1 (2.5mg/kg; Peptrotech). IGF1 injections were administered daily at the start of the light cycle one hour prior to heat-treatment for 7 days (N=6) and 14 days (N=12). IGF1 has been administered subcutaneously anywhere from once daily, to continuously, in other animal

studies at a dosage range of 2-6 mg/kg (Ding, List, Bower, & Kopchick, 2011; Lynch, Cuffe, Plant, & Gregorevic, 2001; Sims et al., 2000; Woodall et al., 1991). Therefore, the selected dose of 2.5 mg/kg administered once daily is considered low in comparison. While IGF1-injected twice a day may be more effective at promoting overall growth, this study aimed to target a small dose of IGF1 unilaterally using warm temperature without subsequent systemic effects. The timing of injections was also deliberate because peak IGF1 in circulation is approximately one hour after subcutaneous injections (Woodall et al., 1991) and study intended to time the peak of IGF1 with heat-treatment. Left-right comparisons in IGF1-injected mice were made to the saline-injected control mice treated for 7 days from 3-4 weeks of age (N=6) and 14 days from 3-5 weeks of age (N=12) as discussed in Chapter 3.

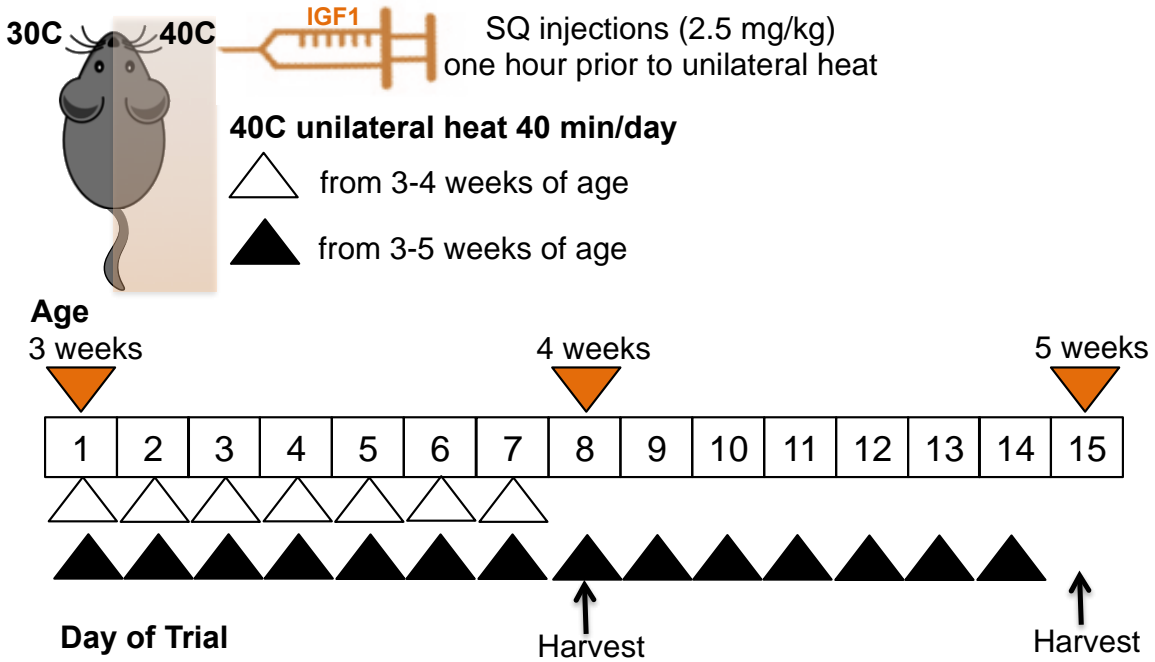


Figure 15. Unilateral Heating Schematic

Mice were injected subcutaneously (SQ) with IGF1 (2.5mg/kg) one hour prior to treatment of 40°C unilateral heat for 40 minutes daily for 7 days from 3-4 weeks of age or 14 days from 3-5 weeks of age. Euthanasia and tissue collection occurred 1 day after the last day of heat-treatment. Mouse illustration based on “mouse clip art black and white” from clipartstockphotos.com.

4.2.2 Tissue Collection and Sample Analysis

Long bones (femora and humeri) were collected and measured as described in Chapter 3 (Sections 3.2.2 and 3.2.3). Proximal tibial halves from each hindlimb were collected (Section 3.2.2) for tibial elongation rate analysis (Section 3.2.3) and growth plate morphometry (Sections 3.2.4) following methods described in Chapter 3.

4.2.3 Immunohistochemistry

Serial sections of proximal tibiae from mice subjected to 7 days (N=12, 6 per saline control and IGF1) and 14 days (N=12, 6 per saline control and IGF1) of unilateral heating were stained using rabbit polyclonal antibodies against PCNA following methods as described in Chapter 3 (Section 3.2.5). Rabbit polyclonal antibodies against IGF1R and phospho-IGF1R (phospho-Y1161) were also used to assess IGF1 activity in the PZ of growth plates following the same methods. Analysis focused on the proliferative zone (PZ) specifically as the site of actively proliferating chondrocytes to determine the heat-enhanced effect in conjunction with IGF1 administration.

4.2.4 Statistical Analysis and Sample Size

Statistical analyses were performed using SPSS 25.0 software (IBM Corporation, Armonk, NY) with $p < 0.05$ as accepted significance. Non-treated and heat-treated side comparisons for humeral length, femoral length, tibial elongation rate, growth plate zone heights, and percent cells positive for protein expression were made using one-tailed paired *t*-tests. Multiple comparisons made between saline controls and

IGF1-injected mice were made using a one-way ANOVA. Data were reported as mean \pm standard deviation (SD) in tabular format and as mean \pm standard error (SE) in graphical format.

Sample sizes for measurements that are documented as *less than the size of the experimental sample set* was a result of either sample loss during dissection or sample processing. Since left-right comparisons are made, if one side is damaged during dissection, sample preparation, tissue processing, sectioning or staining, the entire left-right pair is lost. Samples and missing cases were excluded from statistical analysis on an analysis-by-analysis basis.

4.3 RESULTS

4.3.1 Unilateral Heating Parameters

IGF1-injected mice treated for 7 days from 3-4 weeks of age gained 5.1 ± 0.5 g while saline control mice (established in Chapter 3) gained 4.7 ± 0.7 g (Fig. 16A). IGF1-injected mice treated for 14 days from 3-5 weeks of age gained 6.4 ± 0.8 g while saline control mice (also established in Chapter 3) gained 6.0 ± 0.9 g (Fig. 16B). There was no significant difference in the amount of mass gained between saline and IGF1-injected mice after 7 days ($F(1,11)=1.4$, ns, $p=0.27$) or 14 days ($F(1,23)=0.9$, ns, $p=0.35$) of limb heating. The core temperature averaged 36°C during all extents of unilateral heating. During the duration mice were anesthetized, the average surface temperature of non-treated hindlimbs was 30°C and the heat-treated hindlimbs were 40°C , consistent with parameters during the daily limb heating reported in previous chapters. At the end of each daily heat-treatment (40mins), the average time for saline control mice to recover

from anesthesia after 7 days and 14 days of heating was 1.6 ± 0.33 mins and 1.5 ± 0.37 mins respectively. The average time for IGF1-injected mice to recover from anesthesia was 3.3 ± 0.79 mins and 3.0 ± 0.80 mins, which was significantly longer than the saline controls after both 7 days ($F(1,11)=22.35$, $p<0.001$) and 14 days ($F(1,23)=31.5$, $p<0.001$) of unilateral heating.

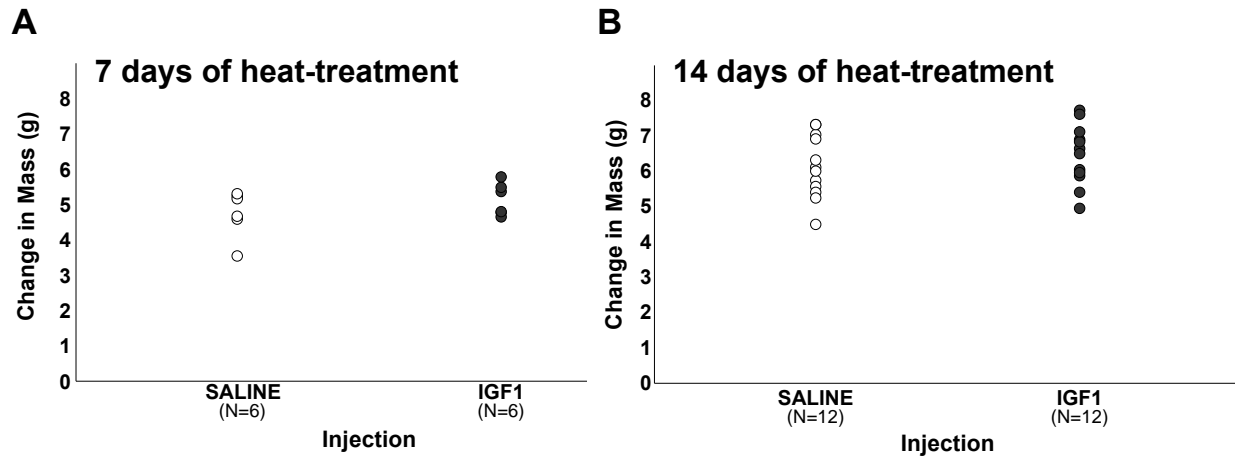


Figure 16. Overall Change in Mass was not Impacted by IGF1 Injections at Either Length of Heat-Treatment

(A) Scatter plots show the change in mass of individual mice after 7 days of heat-treatment from 3-4 weeks of age. Saline control mice (open circles) gained an average of 4.7g and IGF1-injected mice (gray circles) gained an average of 5.1g. (B) Scatter plots show the change in mass of individual mice after 14 days of heat-treatment from 3-5 weeks of age. Saline control mice gained 6.0g and IGF1-injected mice gained 6.4g. Significance ($p < 0.05$) is the mean change in mass between injections. One-way ANOVA indicated no significant difference in overall gain in mass between saline control and IGF1-injected mice with either length of heat-treatment.

4.3.2 Length of Long Bones and Tibial Elongation Rate

Femoral length of IGF1-injected mice treated for 7 days increased on the heat-treated sides by 1.7% (paired $t=3.8$, $p<0.05$) (Fig. 17A(a), Table 7). Femoral length of IGF1-injected mice treated for 14 days increased by 1.9% (paired $t=7.6$, $p<0.001$) on the heat-treated sides (Fig. 17B(a); Table 7). Compared to saline controls (Chapter 3; Fig. 12A, Table 5), the heat-induced increase in femoral length of IGF1-injected mice (1.7%) treated for 7 days was equivalent to that of the controls. However, femoral length of IGF1-injected mice (1.9%) treated for 14 days was significantly greater ($F(1,20)=6.3$, $p<0.05$) than that of the saline controls (1.1%) as determined by one-way ANOVA.

Humeral length did not differ between non-treated and heat-treated sides in saline control mice as shown in Chapter 3 (Table 5). Humeral length of IGF1-injected mice treated for 7 days also did not differ (paired $t=1.4$, ns, $p=0.23$). However, there was a slight 0.7% increase in humeral length on the heat-treated side of IGF1-injected mice treated for 14 days (paired $t=3.6$, $p<0.05$), which was significantly greater ($F(1,20)=6.5$, $p<0.05$) than saline mice as determined by one-way ANOVA.

Tibial elongation rate of IGF1-injected mice treated for 7 days increased on the heat-treated side by 7.3% (paired $t=2.9$, $p<0.05$) (Fig. 17A(b), Table 7). Tibial elongation rate of IGF1-injected mice treated for 14 days increased by 18.7% (paired $t=7.2$, $p<0.001$) on the heat-treated side (Fig. 17B(b), Table 7). Compared to saline controls (Chapter 3; Fig. 12B, Table 5), the heat-induced increase in tibial elongation rate of IGF1-injected mice (7.3%) treated for 7 days was not greater than the controls (7.7%) as determined by one-way ANOVA ($F(1,9)=0.02$, ns, $p=0.89$). However, tibial elongation rate of IGF1-injected mice (18.7%) treated for 14 days was significantly greater

($F(1,18)=5.3$, $p<0.05$) than that of the saline controls (10.8%) as determined by one-way ANOVA. Together, left-right comparisons of femoral and humeral length, as well as tibial elongation rate, indicate that injections of low dose IGF1 further enhances heat induced limb elongation only after mice are treated for 14 days from 3-5 weeks of age.

Table 7. Comparison of Non-Treated and Heat-Treated Sides of IGF1-Injected Experimental Mice Bone Parameters.

Parameter	Length of Heat-Treatment	Non-Treated (30C)	Heat-Treated (40C)	Percent Increase	N
Humeral Length (mm)	7 days (3-4 weeks)	9.31 (0.23)	9.27 (0.19) ^{ns}	-0.4	6
	14 days (3-5 weeks)	10.29 (0.15)	10.36 (0.16) ^{***}	0.7	12
Femoral Length (mm)	7 days (3-4 weeks)	10.51 (0.20)	10.68 (0.28) [*]	1.7	6
	14 days (3-5 weeks)	12.86 (0.18)	13.10 (0.22) ^{***}	1.9	12
Tibial Elongation Rate ($\mu\text{M}/\text{day}$)	7 days (3-4 weeks)	157.51 (6.16)	168.85 (8.93) [*]	7.3	5
	14 days (3-5 weeks)	103.38 (9.43)	122.32 (11.61) ^{***}	18.7	11

Values are mean (standard deviation). Sample size (N) is number of left-right pairs. Significantly larger on heat-treated side by one-tailed paired t-test: * $p < 0.05$; *** $p < 0.001$; ns, non-significant.

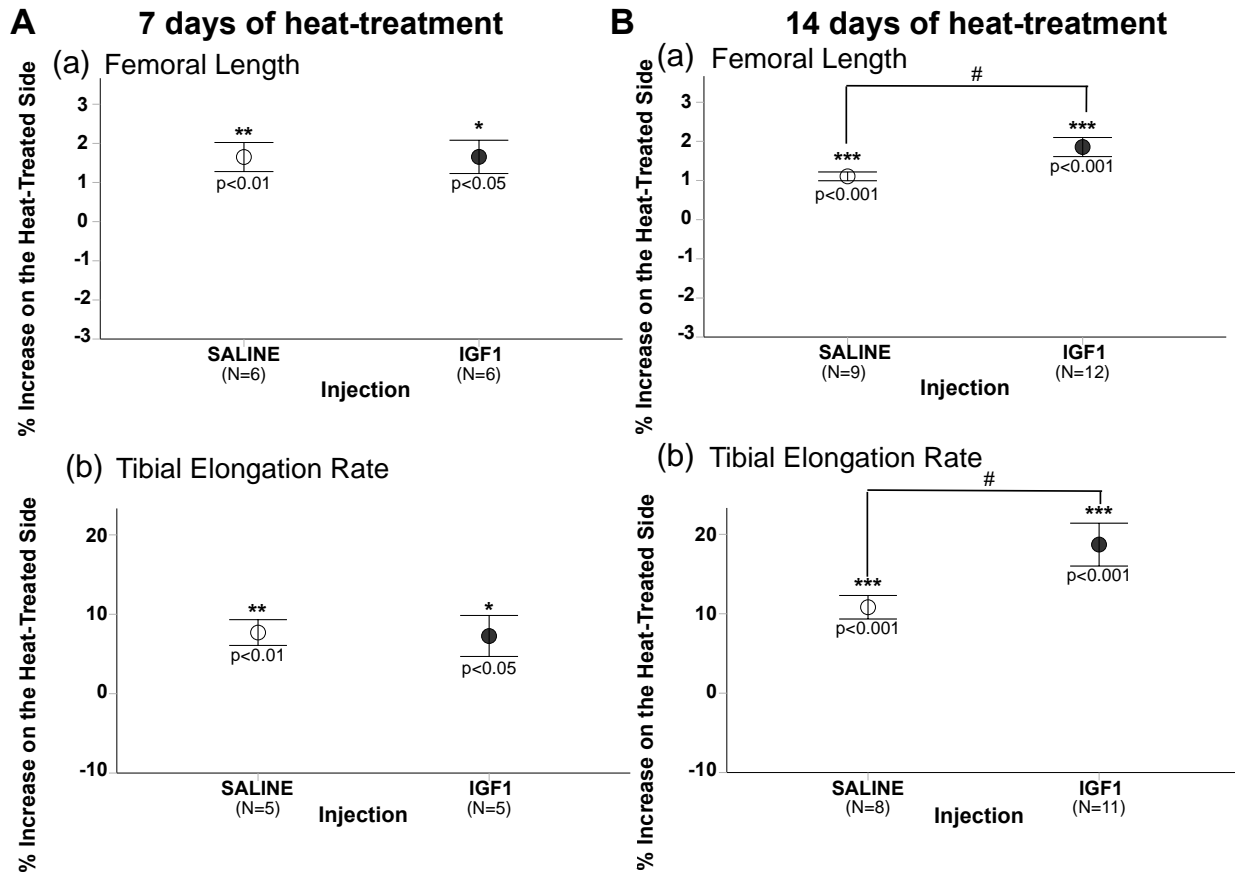


Figure 17. Extremities are Lengthened on the Heat-Treated Sides when Injected with Saline and IGF1

(A) Error bar plots compare saline- and IGF1-injected mice treated for 7 days (3-4 weeks of age) and shows percent change in heat-treated limb compared to non-treated limb. (a) Femoral length increased by 1.7% on the heat-treated sides of both saline and IGF1-injected mice (b) Tibial elongation rate increased by 7.7% and 7.3% on the heat-treated sides of saline and IGF1-injected mice. (B) Error bar plots compare saline- and IGF1-injected mice treated for 14 days (3-5 weeks of age). (a) Femoral length increased by 1.1% and 1.9% on the heat-treated side of saline and IGF1-injected mice. (b) Tibial elongation rate increased by 10.8% and 18.7% on the heat-treated side of saline and IGF1-injected mice. Mean \pm 1 standard error plotted. * $p < 0.05$; ** $p < 0.01$; *** $p < 0.001$, significance in left-right comparisons; # $p < 0.05$ comparing % change in saline control and IGF1-injected mice.

4.3.3 Growth Plate Morphometry

The height of the PZ normalized to total growth plate height was significantly reduced by 9.0% on the heat-treated sides of saline control mice (Chapter 3; Fig. 13A, C; Table 6) and by 5.9% on the heat-treated sides of IGF1-injected mice (paired $t=2.6$, ns, $p=0.059$) treated for 7 days (Fig. 18A(a), Table 8). The height of the PZ was reduced by 7.3% on the heat-treated sides of saline mice (Chapter 3; Fig. 13A, C; Table 6) and by 7.8% on heat-treated sides of IGF1-injected mice (paired $t=3.7$, $p<0.05$) treated for 14 days (Fig. 18B(a), Table 8).

The height of the hypertrophic zone (HZ) normalized to the total growth plate height was significantly enlarged by 8.6% on the heat-treated sides of saline control mice (Chapter 3; Fig. 13B, C; Table 6) and by 5.3% on the heat-treated sides of IGF1-injected mice (paired $t=5.1$, $p<0.01$) treated for 7 days (Fig. 18A(b), Table 8). The expansion in the HZ height observed in IGF1-injected mice (5.3%) was significantly less than that of the controls (8.6%) as determined by one-way ANOVA ($F(1,9)=7.8$, $p<0.05$). The height of the HZ expanded by 8.8% on the heat-treated sides of saline mice (Chapter 3; Fig. 13B, C; Table 6) and by 9.4% of IGF1-injected mice (paired $t=4.4$, $p<0.05$) treated for 14 days (Fig. 18B(b), Table 8). Overall, PZ and HZ height was comparable between saline and IGF1-injected mice. However, the left-right differences in zonal height were greater in saline mice treated for 7 days.

Table 8. Comparison of Growth Plate Morphometry Between Non-Treated and Heat-Treated Sides of IGF1-Injected Experimental Mice.

Parameter	Length of Heat-Treatment	Non-Treated (30C)	Heat-Treated (40C)	Percent Increase	N
Resting Zone Height (Normalized)	7 days (3-4 weeks)	0.104 (0.019)	0.106 (0.011) ^{ns}	5.7	5
	14 days (3-5 weeks)	0.138 (0.011)	0.134 (0.011) ^{ns}	-1.0	5
Proliferative Zone Height (Normalized)	7 days (3-4 weeks)	0.450 (0.029)	0.422 (0.028) ^{ns}	-5.9	5
	14 days (3-5 weeks)	0.460 (0.010)	0.426 (0.023) [*]	-7.8	5
Hypertrophic Zone Height (Normalized)	7 days (3-4 weeks)	0.448 (0.023)	0.474 (0.031) ^{**}	5.3	5
	14 days (3-5 weeks)	0.404 (0.022)	0.442 (0.031) [*]	9.4	5

Values are mean (standard deviation). Sample size (N) is number of left-right pairs. Significantly larger on heat-treated side by one-tailed paired t-test: *p< 0.05; **p<0.01; ***p<0.001; ns, non-significant.

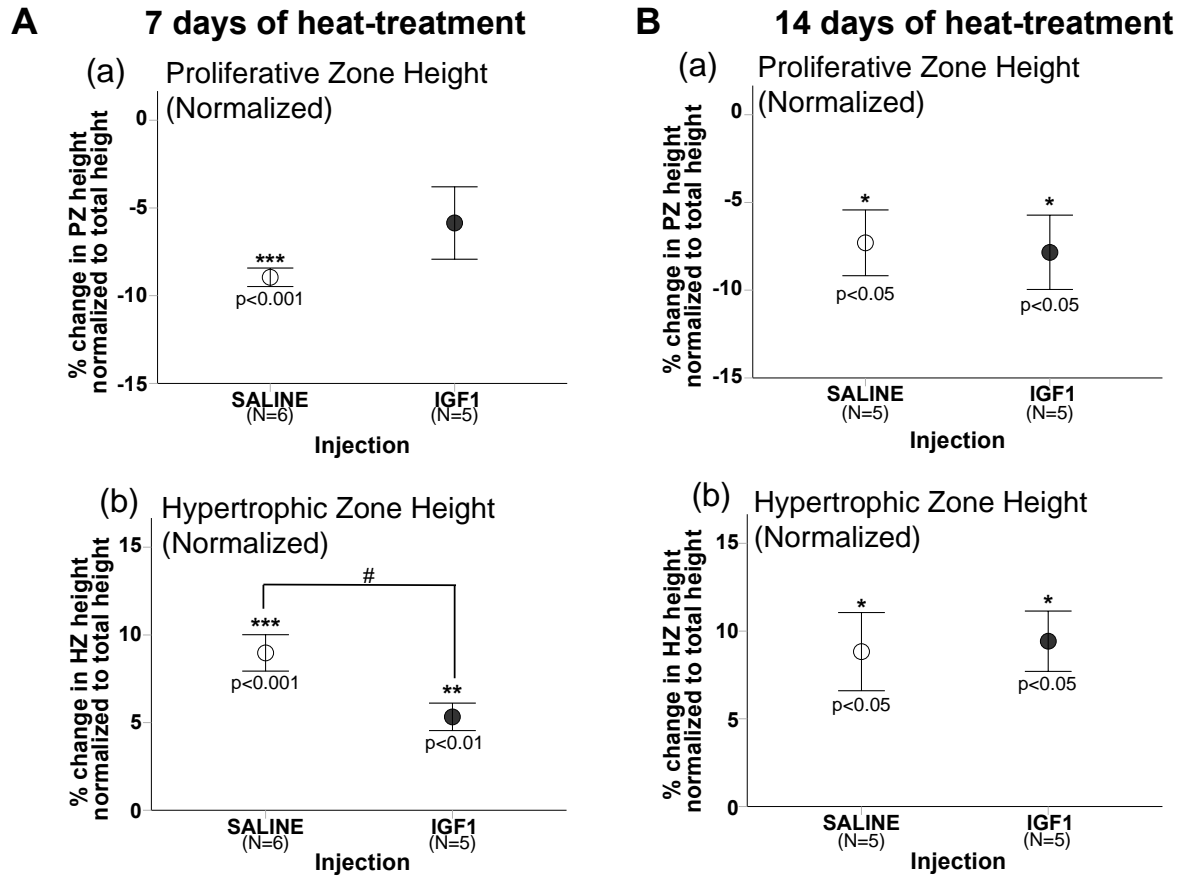


Figure 18. Proximal Tibial Growth Plate Morphometry After Administration of Low Dose IGF1 with Targeted Heating

(A) Error bar plots compare growth plate (GP) morphometry of mice treated for 7 days and shows percent change in heat-treated limb compared to non-treated limb. (a) Proliferative zone (PZ) height decreased by 9.0% and 5.9% on heat-treated sides of saline control and IGF1-injected mice respectively. (b) Hypertrophic zone (HZ) height increased by 8.6% and 5.3% in saline and IGF1-injected mice. (B) Error bar plots compare GP morphometry of mice after 14 days of treatment. (a) PZ height decreased by 7.3% and 7.8% in saline and IGF1-injected mice (b) HZ height increased by 8.8% and 9.4% in saline and IGF1-injected mice. Mean \pm 1 standard error plotted. * $p < 0.05$; ** $p < 0.01$; *** $p < 0.001$, significance in left-right comparisons; # $p < 0.05$ comparing % change in IGF1-injected mice with saline controls.

4.3.4 PCNA Expression

In saline control mice treated for 7 days, the percent of chondrocytes positive for PCNA in the PZ was $85.1 \pm 6.9\%$ on the non-treated sides, and $91.9 \pm 2.0\%$ on the heat-treated sides for an 8.6% increase in expression (Chapter 3; Fig. 14). Chondrocytes in the PZ of IGF1-injected mice were positive for a lesser $79.3 \pm 4.6\%$ on non-treated sides and $83.3 \pm 4.4\%$ on the heat-treated sides for a 5.0% increase in PCNA expression (paired $t=3.5$, $p<0.05$) on the heat-treated side (Fig. 19A). In saline mice treated for 14 days, chondrocytes were positive for PCNA in $77.6 \pm 11.5\%$ and $89.3 \pm 4.5\%$ on the non-treated and heat-treated sides respectively for an increase of 16.7% (Chapter 3; Fig. 14). Chondrocytes in the PZ of IGF1-injected mice were positive for $84.9 \pm 4.5\%$ and $93.2 \pm 3.9\%$ PCNA on the non-treated and heat-treated sides respectively for an increase of 9.9% (paired $t=5.1$, $p<0.01$) on the heat-treated side (Fig. 19B). There were no significant differences in the heat-induced increase in PCNA expression between saline and IGF1-injected mice treated for 7 day days ($F(1,10)=0.7$, ns, $p=0.43$) and 14 days ($F(1,9)=1.0$, ns, $p=0.34$).

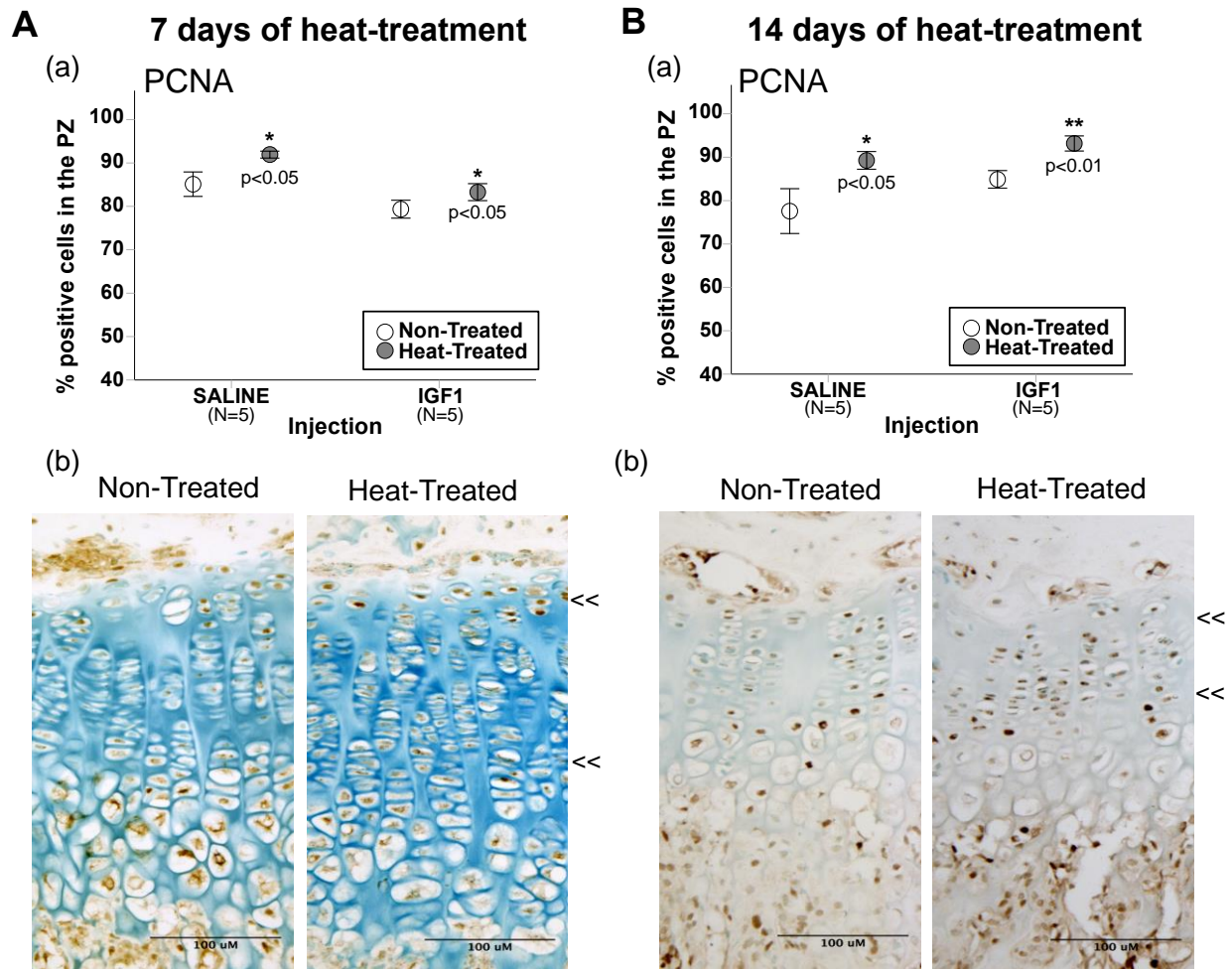


Figure 19. Expression of PCNA in the PZ of Proximal Tibial Growth Plates After Administration of Low Dose IGF1 with Targeted Heating

(A) PCNA expression in mice treated for 7 days (a) Error bar plots show percent of chondrocytes positive for PCNA expression on non-treated (open circles) and heat-treated (gray circles) sides. PCNA expression increased by 8.6% and 5.0% on the heat-treated sides of saline and IGF1-injected mice respectively. (b) Left-right comparison of proximal tibial growth plates from an IGF1-injected mouse immunostained for PCNA. A larger quantity of PCNA staining was counted on heat-treated sides. Positive staining is shown by dark brown nuclei within the PZ of the growth plate (region between the double arrows). (B) PCNA expression in mice treated for 14 days (a) Error bar plot shows a 16.7% and 9.9% increase in saline and IGF1-injected mice. (b) Left-right comparison of proximal tibial growth plate from an IGF1-injected mouse immunostained for PCNA. There was more PCNA staining on heat-treated sides.

4.3.5 IGF1R and pIGF1R Expression in Proliferating Chondrocytes

IGF1R expression in the PZ of mice treated for 7 days increased by 14.5% (paired $t=3.2$, $p<0.05$) and 7.7% (paired $t=2.39$, ns, $p=0.076$) on the heat-treated sides of saline control and IGF1-injected mice respectively (Fig. 20A(a), Table 9). This increase of IGF1R expression on the heat-treated sides of IGF1-injected mice was 2-fold less compared to the saline mice ($F(2,15)=26.6$, $p<0.001$). Activation of the IGF1R, assessed by pIGF1R expression in the PZ, increased by 7.7% (paired $t=5.3$, $p<0.01$) and 28.2% (paired $t=3.5$, $p<0.05$) on the heat-treated sides of saline and IGF1-injected mice respectively (Fig. 20A(b), Table 9). This increase of pIGF1R expression on the heat-treated sides of IGF1-injected mice was over 3-fold more compared to the saline ($F(2,15)=16.8$, $p<0.001$). Therefore, even though IGF1-injected mice had less of a heat-induced increase in IGF1R expression, there was a greater increase in activation of these receptors compared to saline controls.

IGF1R expression in the PZ of mice treated for 14 days increased by 37.6% (paired $t=6.1$, $p<0.01$) and 30.8% (paired $t=3.5$, $p<0.05$) on the heat-treated side of saline and IGF1-injected mice respectively (Fig. 20B(a), Table 9). Differences were comparable between saline and IGF1-injected mice ($F(1,7)=0.16$, ns, $p=0.70$). Expression of pIGF1R increased by 23.9% (paired $t=5.2$, $p<0.01$) and 25.4% (paired $t=6.3$, $p<0.01$) on the heat-treated sides of saline and IGF1-injected mice respectively (Fig. 20B(b), Table 9). Differences were comparable between the injection groups ($F(1,7)=0.03$, ns, $p=0.86$).

Table 9. Comparison of Non-Treated and Heat-Treated Expression of Markers for IGF1 Activation in Proliferative Zone of Tibial Growth Plates in Saline and IGF1-Injected Mice.

Length of Heat-Treatment	Antibody in Proliferative Zone	Treatment	Non-Treated (30C)	Heat-Treated (40C)	Percent Increase	N	
7 days (3-4 weeks)	IGF1R expression	Saline	69.68 (6.36)	79.52 (7.61)*	14.5	5	
		IGF1	72.10 (11.87)	75.70 (11.63) ^{ns}	7.7 [#]	5	
	pIGF1R expression	Saline	84.85 (10.36)	90.97 (7.90)**	7.7	6	
		IGF1	62.44 (8.74)	78.72 (4.09)*	28.2 [#]	5	
	14 days (3-5 weeks)	IGF1R expression	Saline	37.98 (11.24)	51.03 (11.44)**	37.6	4
			IGF1	47.40 (22.22)	57.93 (17.43)*	30.8 ^{ns}	4
pIGF1R expression		Saline	59.28 (9.40)	72.48 (4.84)*	23.9	4	
		IGF1	47.70 (4.13)	59.85 (6.94)**	25.4 ^{ns}	4	

Values are mean (standard deviation). Sample size (N) is number of left-right pairs. Significantly larger on heat-treated side by one-tailed paired t-test: *p< 0.05; **p<0.01; ns, non-significant. Significant differences in percent increase between saline controls and IGF1-injected mice by one-way ANOVA: [#]p<0.05; ns, non-significant.

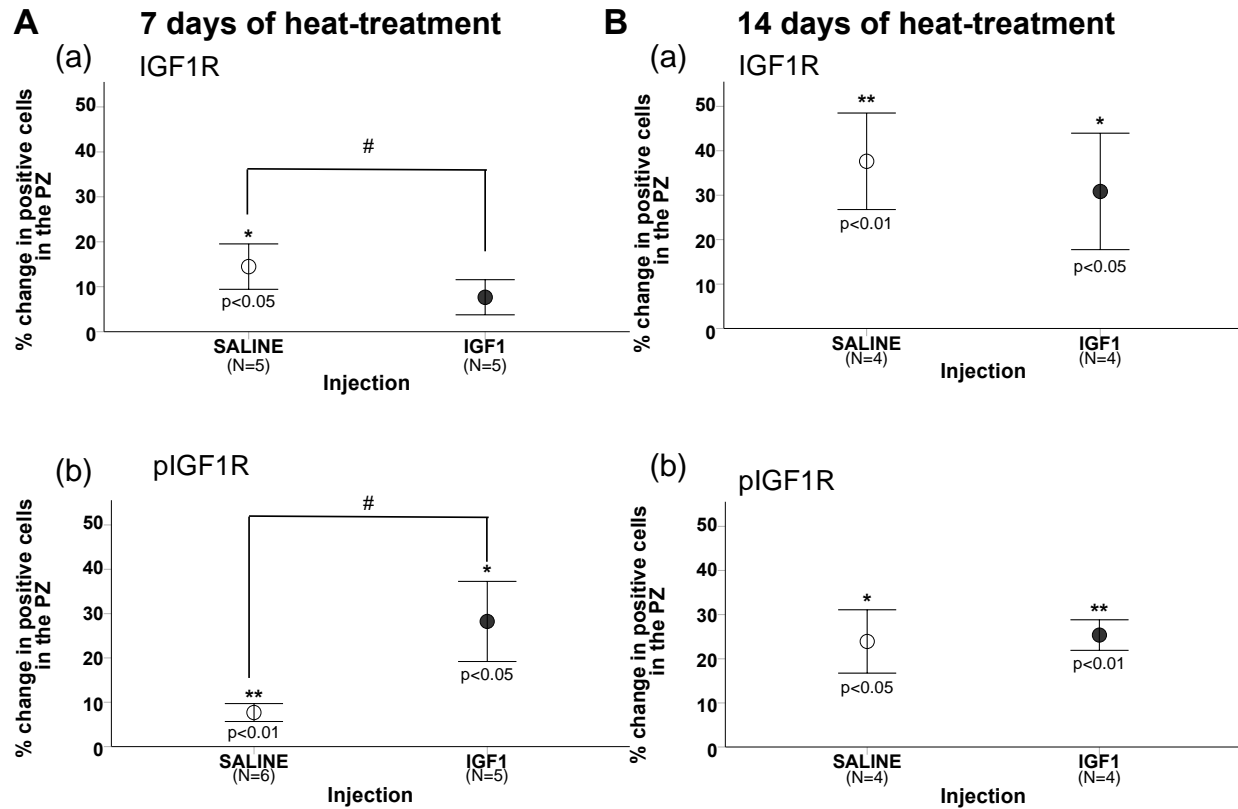


Figure 20. Heat-Induced Effect on IGF1 Activity in the PZ of the Tibial Growth Plate with IGF1 Administration

(A) Expression in saline control and IGF1-injected mice with 7 days of unilateral heating. (a) Error bar plot shows percent change in heat-treated limb compared to non-treated limb. IGF1R expression increased by 14.5% and 7.7% in the PZ on the heat-treated side of saline and IGF1-injected mice. (b) pIGF1R expression in the PZ increased by 7.7% and 28.2% of saline and IGF1-injected mice. (B) Expression in saline and IGF1-injected mice with 14 days of heating. (a) IGF1R expression in the PZ increased by 37.6% and 30.5% in saline and IGF1-injected mice. (b) pIGF1R expression in the PZ increased by 23.9% and 25.4% in saline and IGF1-injected mice. Mean \pm 1 standard error plotted. * $p < 0.05$; ** $p < 0.01$; ns, significance in left-right comparisons; # $p < 0.05$ comparing % change in IGF1-injected mice with saline controls.

4.4 DISCUSSION

Previous chapters have established that in a group of saline control mice, targeted limb heating can enhance longitudinal growth on the heat-treated sides after both 7 days (shown in Chapters 2 and 3) and 14 days of heating (Chapter 3). Heat-enhanced limb elongation was shown with unilateral increases in femoral length, tibial elongation rate, chondrocyte proliferation and hypertrophic expansion in proximal tibial growth plates. The goal of this study was to determine if targeted limb heating in conjunction with the administration of a low dose of the growth-promoting drug IGF1 would further enhance bone elongation without impacting overall physiology. Results of the current study show that there was an additional heat-enhanced increase in femoral length and tibial elongation rate in IGF1-injected mice. There was also a greater rate of proliferation and hypertrophic zone expansion on heat-treated sides compared to saline controls. Data supported the hypothesis that IGF1 administration with heat-treatment will further enhance limb length than with heat alone.

Both saline and IGF1-injected mice had similar recorded core temperatures and surface limb temperatures. While mice have been shown to demonstrate weight gain with increased serum levels of IGF1 (D'Ercole, 1993; Mathews et al., 1988; Woodall et al., 1991; Yakar & Isaksson, 2016), overall gain in mass did not differ between saline and IGF1-injected mice (Fig. 16). Livers collected and weighed from both saline and IGF1-injected mice (data not shown) also were comparable between saline and IGF1-injected mice treated for 7 days ($p=0.49$) and 14 days ($p=0.68$). Similar liver mass between saline and IGF1-injected mice was not unexpected, as the stimulatory effect of GH on the liver has been shown to be independent of IGF1 (Blutke et al., 2014).

Comparable weights between treatment groups further supported the rationale to use a low dose of IGF1.

An interesting observation during the unilateral heating regimen was the differential anesthesia recovery time between the saline controls and IGF1 mice. The mice injected with IGF1 took on average twice as long to wake up from the anesthesia than the saline controls which was observed throughout the duration of both the 7 days and 14 days of heating. Anesthesia recovery is a concern for patients with pituitary disease (Menon, Murphy, & Lindley, 2011) including those with acromegaly (excess GH, normal to high IGF1). Acromegaly presents a variety of challenges for general anesthesia including prolonged awakening associated with obstructed airways (Chung & Mokhlesi, 2014) common in these patients (Menon et al., 2011). While recovery time with IGF1 has not been previously reported in the literature, other drugs including caffeine (Fong et al., 2017; Wang, Fong, Mason, Fox, & Xie, 2014) have been shown to accelerate recovery from anesthesia by facilitating neurotransmitter release. Since IGF1 has been shown to cross the blood-brain barrier (Pan & Kastin, 2000; Yan et al., 2011), it is likely prolonged anesthesia recovery as an outcome of IGF1 administration could be explained by IGF1 regulation in the brain. Since other tissues, including the brain, were not examined in this study the cause of extended recover time with IGF1 remains unknown. However, this finding aided to support if IGF1 administration was successful throughout the duration of heat-treatment.

While not intended to be an indicator of effective IGF1 treatment, comparing wake up times was a useful method throughout experimentation. These observations were not supported by other means of confirming successful IGF1 administration, such

as measuring levels of IGF1 or glucose in the blood following injections. Assays for serum IGF1 require a considerable volume of blood that could not be collected daily since mice are very small in size and to collect a sufficient volume of blood would require animal sacrifice. A smaller volume of blood is needed to measure serum glucose and lower levels of glucose would be indicative of increased serum IGF1 (Clemmons, 2004). However, to obtain even a small amount of blood from experimental mice would cause a degree of stress to the animals, potentially interfering with the results of heat-treatment. Since low levels of glucose, or hypoglycemia, is associated with increased levels of IGF1, mice were monitored during the first couple days of treatment. While uncommon, there were cases when mice required glucose injections (15% glucose solution, 0.01mL per gram body weight) when demonstrating adverse signs of IGF1 administration following heat-treatment (nonappearance of anesthesia recovery and labored breathing). Hypoglycemia was another physiological response indicative to increased levels of IGF1.

Outcome variables showed that with 7 days of unilateral heating, there was almost a 2% increase in femoral length in both saline control and IGF1-injected mice (Fig. 17A(a), Table 7). After 14 days of heating, femoral length increased by just over 1% on the heat-treated sides of saline controls but femora were almost 2% longer on the heat-treated sides of IGF1-injected mice (Fig. 17B(a), Table 7). Tibial elongation rate after 7 days of heating was also comparable between saline control and IGF1 mice with a heat-induced increase of over 7% (Fig. 17A(b), Table 7). After 14 days of heating the increase in tibial elongation rate on the heat-treated side was almost 19% with IGF1 administration, 2.5-fold greater than the over 7% increase observed in saline controls

(Fig. 17B(b), Table 7). While both femoral length and tibial elongation rate significantly increased with targeted limb heating, further enhancement with IGF1 was only apparent with 14 days of heating.

In Chapter 3, longitudinal growth was assessed on the cellular level by amount of proliferation and hypertrophy in proximal tibial growth plates. Increased femoral length and tibial elongation rate were accompanied by increased PCNA expression in proliferating chondrocytes and expanded heights of the hypertrophic zone. In this study, when mice were administered IGF1, there was a significant 5.0% and 9.9% increase in PCNA expression on the heat-treated sides after 7 days and 14 days of heating respectively (Fig. 19). These increased levels of expression were not significantly greater than that of saline controls. However, trends in overall PCNA expression suggest an increased rate in proliferation when IGF1-injected mice were treated for 14 days. Longitudinal bone growth gradually slows with age and can be associated with a decline in proliferation and hypertrophic zone height (Forcinito et al., 2011; Lui et al., 2011; Nilsson & Baron, 2004; Nilsson et al. 2014; Walker & Kember, 1972). While comparisons were not made between treatment durations in this study, marginal differences can be seen. Overall PCNA expression in the PZ decreased in saline mice treated for 14 days from 3-5 weeks of age (older) compared to expression in mice treated for 7 days from 3-4 weeks of age (younger) (Fig. 19). However, overall PCNA expression increased in IGF1-injected mice treated for 14 days compared to 7 days which indicates that although the left-right comparisons in PCNA expression levels were similar between saline and IGF1-injected mice at both durations, there was a higher rate of proliferation when IGF1-injected mice were treated for 14 days. However, since

observations are made from trends in overall PCNA expression (not between non-treated and heat-treated sides), further analysis is required to determine if the increased rates in proliferation in IGF1-injected mice are results of targeted limb heating.

Hypertrophic zone expansion was significantly increased by 5% and 9% on the heat-treated sides of IGF1-injected mice after 7 days and 14 days of unilateral heat-treatment respectively (Fig. 18A(b), B(b); Table 8). Again, while there was still a heat-induced increase in expansion, the increase was not beyond that of saline controls. The increase in hypertrophic height in IGF1-injected mice was a significant 3% less than the saline mice after 7 days of heating, and comparable after 14 days of heating. Similar to the trends observed when comparing heat-treatment duration of expression of PCNA, IGF1-injected mice after 14 days of treatment displayed a greater difference in height of the hypertrophic zone compared to those treated for 7 days (Fig. 18).

Multiple explanations are possible to rationalize why extremity lengthening is similar between saline control and IGF1-injected mice with 7 days of heating, yet IGF1 further increases lengthening with 14 of heating. All possibilities require further investigation before determining the contributing factor(s). In normal physiological conditions, IGF1 levels decline after birth then increase during the early rapid stages of postnatal growth (Daughaday, Parker, Borowsky, Trivedi, & Kapadia, 1982; Gluckman & Butler, 1983; Hansen-Pupp et al., 2011), eventually dropping throughout childhood until adolescence. If levels of IGF1 are elevated during the rapid 3-4 week period of growth, then additional IGF1 in the system may not further heat-enhanced growth.

IGF-binding proteins (IGFBPs) regulate the bioavailability of IGF1 in the serum. Studies have shown that mouse models created to lower IGF1s affinity for IGFBPs have

increased bioavailability of IGF1 to tissues resulting in increased body length (Elis et al., 2011). If the low dose of injected IGF1 is bound to IGFBPs, there may not be a enough IGF1 available to the growth plates of long bones to further enhance limb elongation with heat-treatment. In addition, temperature has been shown to weaken the affinity of IGF1 binding to ALS in its ternary complex (ALS-IGF1-IGFBP3) accounting for increased free IGF1 in the circulation (Holman & Baxter, 1996). A longer duration of heat-treatment may be necessary to increase IGF1 bioavailability. Using a similar mouse model allowing us to investigate the effects of IGF1 independent of IGFBPs would be effective to determining if the binding proteins are the limiting factor.

Past studies have also shown that the genetic background of the mouse model may contribute to variation in skeletal growth observed with increased serum IGF1 (Yakar & Isaksson, 2016). It is possible that increased serum IGF1 has minimal effects on enhancing linear growth in C57BL/6 mice from 3-4 weeks of age as another possible explanation of the similarity observed between saline control and IGF1-injected mice with 7 days of heating. An extensive study would need to be conducted to quantify linear growth with increased serum IGF1 in various mouse models.

IGF1 activity was assessed by measuring expression of IGF1R and pIGF1R in the growth plate. IGF1R expression in the PZ on heat-treated sides of IGF1-injected mice treated for 7 days (7.7%) was not significant and was significantly less than the heat-induced increase in IGF1R expression in saline mice (14.5%). As rationalized above, if IGF1 serum levels are further elevated from 3-4 weeks of age, there may be a higher degree of receptor internalization (Chow, Condorelli, & Smith, 1998; Girnita, Worrall, Takahashi, Seregard, & Girnita, 2014) as a result of an increased amount of

IGF1 binding and activating the available receptors. Despite the similarity of IGF1R expression in non-treated and heat-treated sides with IGF1 administration, there was a significant increase in pIGF1R expression (28.2%) on the heat-treated sides, which was 20% greater than what was measured in saline controls (7.7%)(Fig. 20A, Table 9). Both saline and IGF1-injected mice treated for 14 days had a significant increase in IGF1R and pIGF1R expression on heat-treated sides but there was no difference between the injection groups (Fig. 20B, Table 9). Therefore, it is possible that the outcome of increased IGF1 signaling from 3-4 weeks of age is observed by the increased bone elongation measured in heat-treated limbs from mice treated from 3-5 weeks of age. Overall, results suggest that *IGF1 activity was augmented with heat-treatment*, and with additional IGF1 administered in conjunction with unilateral limb heating IGF1 activity is further increased when mice were treated for 7 days. Increased IGF1 activity after 7 days of treatment also indicates that despite the IGF1-driven increase shown in femoral length and tibial elongation rate of mice treated for 14 days (Fig. 17B, Table 7), there was a higher degree of IGF1 signaling detected in the PZ of mice treated for 7 days (Fig. 20A, Table 9). Further investigation is required to better understand the complicated IGF1 signaling cascade involved in growth plate chondrocytes in response to additional IGF1 with targeted limb heating.

One shortcoming of this study is examining IGF1 activity within the limited scope of growth plate chondrocytes. Studies have shown that with an increase in IGF1 activity in osteoblasts via the Col1a1_(3.6) promoter, there was increased femoral length (Brennan-Speranza, Rizzoli, Kream, Rosen, & Ammann, 2011; Jiang et al., 2006). While not examined in this study, IGF1 receptors are expressed in osteoblasts

responsible for bone formation in the process of bone remodeling. With prolonged heat-treatment, IGF1 may increase osteoblast activity to enhance longitudinal bone growth independent of activity within the growth plate. Since osteoblasts also contribute to radial growth, examining bone density would indicate if heat-treatment augments IGF1 activity in osteoblasts with IGF1 injections.

4.5 CONCLUSION

In conclusion, IGF1 activity is augmented with heat-treatment and low dose IGF1-administration in conjunction with targeted limb heating can further enhance bone elongation. IGF1-injected mice treated for 14 days had an additional heat-enhanced increase in femoral length and tibial elongation rate compared to saline control mice (heat alone). There was also more proliferation and an increased hypertrophic zone height on heat-treated sides with IGF1 administration following 14 days of heating despite the comparable left-right differential to saline mice. A heat-enhanced increase in IGF1 activity was shown during both 7 days and 14 days of heating but was more pronounced from mice heated for 7 days during the rapid period of growth. Further studies are needed to better understand IGF1 signaling at the level of growth plate cartilage when IGF1 administration is coupled to targeting limb heating. Chapter 5 will test whether heat-enhanced limb length results in the absence of IGF1.

CHAPTER V: IGF1 IS ESSENTIAL FOR HEAT-ENHANCED BONE ELONGATION

5.1 INTRODUCTION

As discussed in Chapter 1, there are a vast number of possible mechanisms, both indirect and direct, by which localized heat enhances longitudinal growth. Although multiple prospects create various avenues of study, this study focuses on a possible direct effect of temperature on local regulation at the cellular level in the growth plate of long bones. The process of chondrocyte proliferation and hypertrophy in the growth plate is regulated by various contributing factors, none of which are mutually exclusive. Many have reviewed local regulation of the growth plate during postnatal longitudinal growth (Kronenberg, 2003; Lui et al., 2014; Mackie et al., 2008; van der Eerden et al., 2003). Each functional zone of chondrocytes has a degree of local regulation by numerous factors that play a role in maintaining efficient endochondral ossification. For instance, Indian hedgehog (Ihh), parathyroid hormone-related protein (PTHrP), bone morphogenic proteins (BMPs), fibroblast growth factors (FGFs), and insulin-like growth factor-1 (IGF1) among others are expressed throughout distinctive regions of the growth plate and interact to regulate the rate of proliferation and hypertrophy. When these factors are inhibited, disturbances of longitudinal bone growth occur leading to conditions such as short stature (Grunwald & De Luca, 2015; Lee et al., 2016; LuValle & Beier, 2000; Maeda et al., 2010; Wang et al., 2004; Woods, Camacho-Hubner, Savage, & Clark, 1996).

IGF1 produced by epiphyseal chondrocytes has been reported to regulate all regions of growth plate cartilage (Tahimic et al., 2013; Ulici et al., 2008; J. Wang et al., 1999; Y. Wang et al., 2006) despite the conflicting findings on its role in chondrocyte

proliferation (Govoni et al., 2007a; Parker et al., 2007; Reinecke et al., 2000; Shinar et al., 1993; Wang et al., 1995). Increased chondrocyte proliferation and hypertrophy have also been shown following direct treatment with IGF1 as a resulting growth response (Abbaspour et al., 2008; Mushtaq et al., 2004). IGF1 activity in the growth plate whether locally or systemically derived, has a significant role in regulating longitudinal bone growth.

IGF1 is a putative target of study in the process of heat-enhanced limb elongation because of its essential role in longitudinal bone growth. Potential methods for studying the action of IGF1 in the growth plate include (1) the administration of IGF1 blocking drugs such as IGF1 peptide analogues that specifically inhibit the downstream action of the IGF1 receptor (IGF1R) (Pietrzkowski et al., 1992; Smith et al., 1999) and (2) knockout mouse models with the absent or low levels of IGF1 (Yakar et al., 2010; Yakar & Isaksson, 2016). This study uses both. Experiments here utilize a small peptide analog of IGF1 known as JB1 that competitively binds to the receptor and blocks downstream IGF1 activity (Chapter 1, Fig. 5) (Brock et al., 2011; Huang et al., 2000; Kleinridders, 2016; Todd et al., 2007; Wen et al., 2012). This study also includes limited data using the growth hormone receptor knockout mouse (*GHR*^{-/-}) recognized for having low levels of IGF1 and 30-40% reduction in body size (List et al., 2011; Sims et al., 2000; Yakar & Isaksson, 2016; Zhou et al., 1997). This chapter tests **the hypothesis that with diminished IGF1 activity, heat-enhanced limb length is attenuated.**

5.2 MATERIAL AND METHODS

5.2.1 Animals and Experimental Design

All procedures were approved by the Institutional Animal Care and Use Committee of Marshall University (Protocol 558). Female C57BL/6 (N=12) mice were obtained from Hilltop Lab Animals, Inc. (Scottsdale, PA, USA) at 21 days weaning age. Mice were singly housed at 21°C in standard plastic caging, exposed to a 12 hour light/dark cycle and provided with food and water ad libitum.

As described in Chapter 2, and as indicated by the unilateral heating methods schematic (Fig. 21), mice were subjected to the same procedural conditions. Mice (N=6) were weighed each day and given subcutaneous injections of an IGF1 peptide analog (JB1, Sigma) that blocks downstream activity of IGF1. Injections of the IGF1 blocking drug JB1 (2.5 mg/kg) were administered daily at the start of the light cycle one hour prior to heat-treatment. The rationale for the dose and time period of JB1 administration was to be consistent with IGF1 drug treatment experiments described in Chapter 4. Dose was accepted following pilot trials that mimicked experimental conditions and tested the physiological response of the mice to the drug treatment. Saline-injected control (N=6) mice described in Chapter 3 served as the controls.

An additional group of female (N=5) growth hormone receptor (GHR) knockout (*GHR*^{-/-}) mice on a C57BL/6 background was obtained from the Kopchick laboratory at Ohio University (Athens, OH, USA) at 21 days weaning age. *GHR*^{-/-} mice model hereditary dwarfism in humans known as Laron Syndrome characterized by short stature, low serum IGF1, and GH resistance (Laron, 2015a; Laron & Kauli, 2015b; List et al., 2011; Sims et al., 2000; Zhou et al., 1997). These mice were housed under

similar conditions previously described. *GHR*^{-/-} mice were not drug injected and were treated with unilateral heat (40°C for 40 mins/day) for 14 days. Although *GHR*^{-/-} mice were not injected with saline, previous studies have shown that there are no significant differences between non-injected and saline-injected mice (unpublished data).

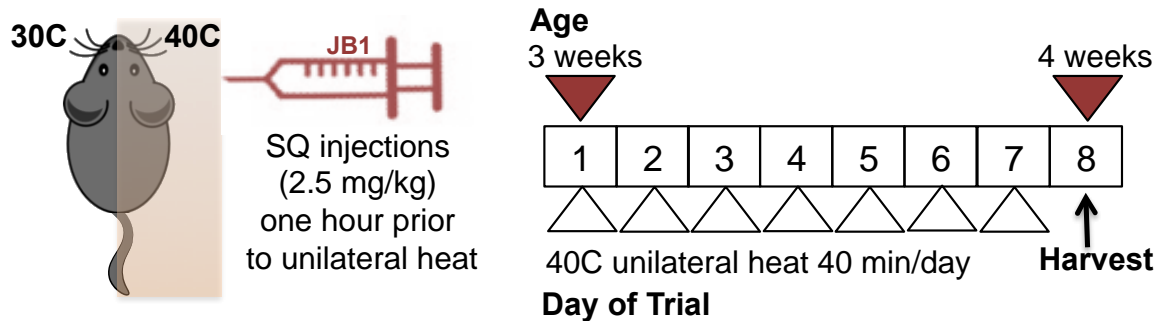


Figure 21. Unilateral Heating Schematic

Mice were injected subcutaneously (SQ) with IGF1 blocking drug (JB1, 2.5 mg/kg) one hour prior to treatment of 40°C unilateral heat for 40 minutes daily from 3-4 weeks of age. Euthanasia and tissue collection occurred 1 day after the last day of heat-treatment. Mouse illustration based on “mouse clip art black and white” from clipartstockphotos.com.

5.2.2 Tissue Collection and Sample Analysis

Long bones (femora and humeri) were collected and measured as described in Chapter 3 (Sections 3.2.2 and 3.2.3). Proximal tibial halves from each hindlimb were collected (Section 3.2.2) for tibial elongation rate analysis (Section 3.2.3) and growth plate morphometry (Sections 3.2.4) following methods described in Chapter 3.

5.2.3 Immunohistochemistry

Serial sections of proximal tibiae from mice subjected to 7 days (N=12, 6 per saline control and JB1) of unilateral heating were stained using rabbit polyclonal antibodies against IGF1R, phospho-IGF1R (phospho-Y1161) and PCNA (as described in Table 4) and rabbit polyclonal antibodies against pAkt, Thr308 (1:200, Santa Cruz, sc-16646) following methods as described in Chapter 3 (Section 3.2.5). Analysis focused on the proliferative zone (PZ) and the hypertrophic zone (HZ). PCNA was used as a marker for rate of proliferation (PZ only) and IGF1R, pIGF1R and pAkt were evaluated as markers of IGF1 activity (PZ and HZ). While an important part of the study, bisected tibiae were not collected from the *GHR*^{-/-} mice following techniques necessary for immunohistochemistry analysis. Therefore, expression levels of PCNA, IGF1R, pIGF1R, and pAkt could, unfortunately, not be done in the *GHR*^{-/-} model.

5.2.4 Statistical Analysis

Statistical analyses were performed using SPSS 25.0 software (IBM Corporation, Armonk, NY) with $p < 0.05$ as accepted significance and comparisons as described in Chapter 4 (Section 4.2.4).

5.3 RESULTS

5.3.1 Unilateral Heating Parameters

There was no significant difference in the amount of mass gained between controls and JB1-injected mice as determined by multiple comparison analysis using one-way ANOVA ($F(1,11)=1.1$, ns, $p=0.311$). JB1-injected mice treated for 7 days from 3-4 weeks of age gained 4.3 ± 0.5 g while saline control mice (established in Chapter 3) gained 4.7 ± 0.7 g (Fig. 22). Therefore, the JB1-inject mice exhibited normal body growth. The core temperature averaged 36°C . While mice were anesthetized, the average surface temperature of non-treated hindlimbs was 30°C and the heat-treated hindlimbs were 40°C .

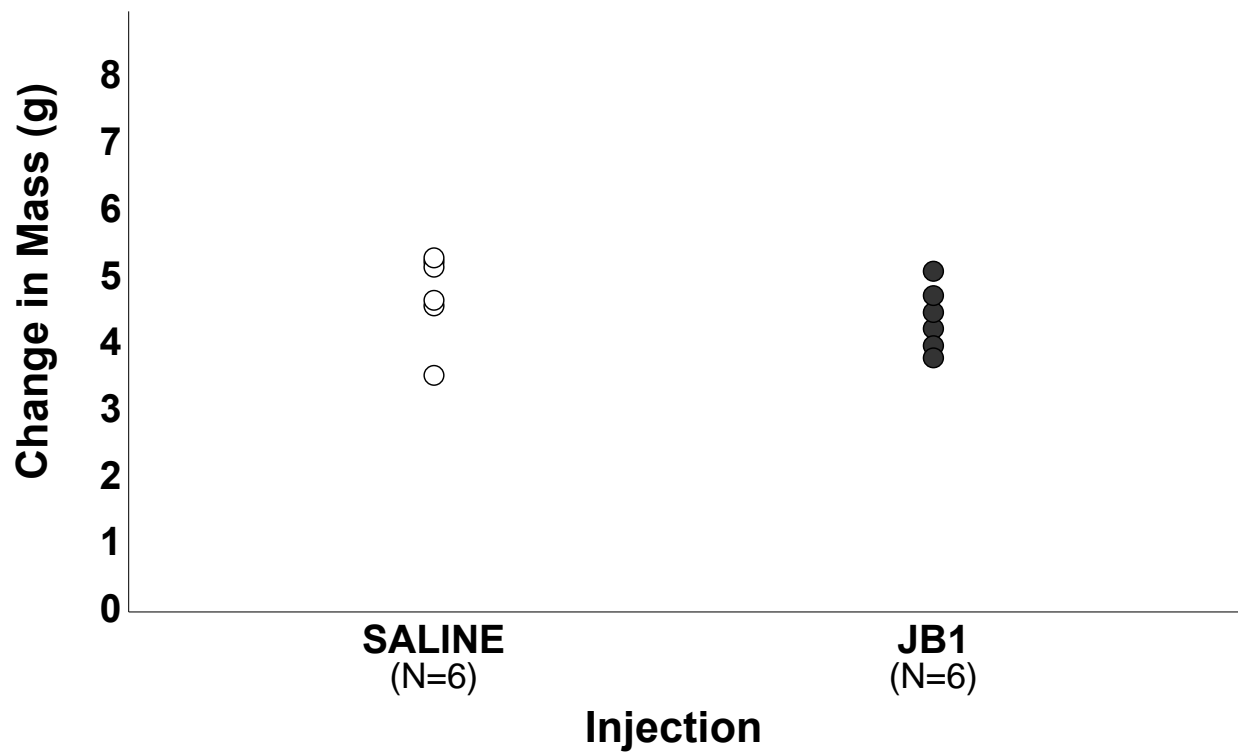


Figure 22. Total Body Mass Gained in Mice Treated for 7 days from 3-4 weeks of Age did not Differ Between Saline Controls and JB1-Injected Mice
 Scatter plots show the change in mass of individual saline mice (open circles) and JB1 mice (dark gray circles). One-way ANOVA revealed no significant differences in overall mass gain between saline and JB1 mice.

5.3.2 Length of Long Bones and Tibial Elongation Rate

Femoral length was comparable on the non-treated sides of saline (10.44 mm) and JB-1 injected mice (10.46 mm) (Table 10). However, femoral length (paired $t=0.3$, ns, $p=0.81$) of JB1-injected mice did not differ between non-treated and heat-treated sides (Fig. 23A; Table 10) while saline mice had a significant 1.7% increase on heat-treated sides (Chapter 3; Fig. 12A, Table 5). This heat-induced increase in femoral length was significantly greater ($F(1,11)=6.2$, $p<0.05$) than the JB1-injected mice. Humeral length was not different between sides for saline (Chapter 3; Table 5) or JB1-injected mice (paired $t=0.1$, ns, $p=0.91$).

Tibial elongation rate was also comparable on the non-treated sides of saline mice (156.88 $\mu\text{M}/\text{day}$) and JB1-injected mice (153.31 $\mu\text{M}/\text{day}$) (Table 10). However, tibial elongation rate of JB1-injected mice decreased by nearly 3% (paired $t=1.9$, ns, $p=0.13$) on the heat-treated side (Fig. 23B, Table 10), while saline mice had a significant increase of nearly 8% on the heat-treated side (Chapter 3; Fig. 12B, Table 5). This observed decrease was significantly less ($F(1,9)=24.8$, $p<0.001$) from the increase in tibial elongation rate in saline mice. The potential of limb heating to target JB1 to the heat-treated side was supported by data since unilateral differences in both femoral length and tibial elongation rate between saline and JB1-injected mice were seen on the heat-treated sides while the non-treated sides were similar between groups. Therefore, these results along with the observed normal body growth (Fig. 22) indicate that JB1 blocked IGF1 locally in the growth plate on heat-treated sides.

Table 10. Comparison of Non-Treated and Heat-Treated Bone Parameters of 4-Week Old Saline- and JB1-Injected Mice Following 7 Days of Heat-Treatment.

Parameter	Treatment	Non-Treated (30C)	Heat-Treated (40C)	Percent Increase	N
Humeral Length (mm)	Saline	9.27 (0.14)	9.23 (0.20) ^{ns}	-0.4	6
	JB1	9.09 (0.27)	9.10 (0.23) ^{ns}	0.1 ^{ns}	6
Femoral Length (mm)	Saline	10.44 (0.19)	10.62 (0.26)**	1.7	6
	JB1	10.46 (0.27)	10.48 (0.33) ^{ns}	0.1 [#]	6
Tibial Elongation Rate (μ M/day)	Saline	156.88 (11.24)	168.94 (12.85)**	7.7	5
	JB1	153.31 (25.72)	148.96 (22.13) ^{ns}	-2.6 [#]	5

Values are mean (standard deviation). JB1 emphasized as an IGF1 blocking drug in red. Sample size (N) is number of left-right pairs. Significantly larger on heat-treated side by one-tailed paired t-test: **p<0.01; ns, non-significant. Significant differences in percent increase between saline controls and JB1-injected mice by one-way ANOVA: #p<0.05; ns, non-significant.

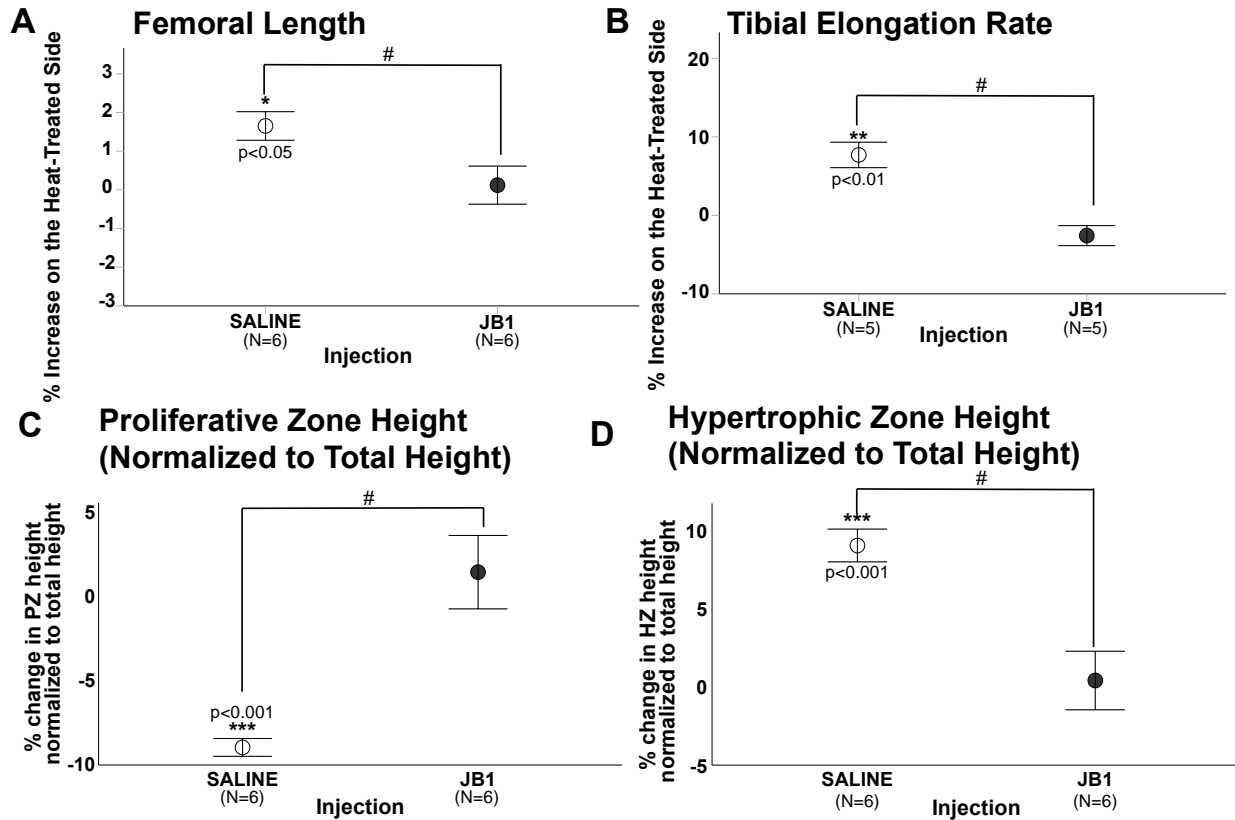


Figure 23. Heat-Enhanced Growth Effects are Attenuated When IGF1 is Blocked

(A) Error bar plots shows percent change in heat-treated limb compared to non-treated limb. Femoral length increased by 1.7% on the heat-treated side of saline control mice and no increase when IGF1 is blocked in mice injected with JB1. (B) Tibial elongation rate increased by 7.7% on the heat-treated side in saline mice and decreased by 2.6% in JB1-injected mice. (C) The PZ of proximal tibial growth plates in saline mice decreased by 9.0% on the heat-treated side but increased by 1.4% in JB1-injected mice. (D) The HZ of proximal tibial growth plates increased by 9.0% on the heat-treated side of saline mice but had a minimal increase of 0.4% in JB1 mice. Mean \pm 1 standard error plotted. * $p < 0.05$; ** $p < 0.01$; *** $p < 0.001$, significance in left-right comparisons; # $p < 0.05$ comparing % change in JB1-injected mice with saline controls.

5.3.3 Growth Plate Morphometry

The height of the PZ normalized to total growth plate height was significantly reduced by 9.0% on the heat-treated sides of saline mice (Chapter 3; Fig. 13A, C; Table 6). JB1-injected mice displayed a 1.4% increase in PZ height (paired $t=0.4$, ns, $p=0.68$) on the heat-treated side (Fig. 23C). The height of the HZ normalized to the total growth plate height was significantly enlarged by 8.6% on the heat-treated sides of saline mice (Chapter 3; Fig. 12B, C; Table 6). JB1-injected mice had a minimal decrease of 0.4% in HZ height (paired $t=0.0$, ns, $p=1.0$) on the heat-treated side (Fig. 23D). The decrease in height of the PZ ($F(1,10)=17.9$, $p<0.01$) and HZ ($F(1,10)=14.4$, $p<0.01$) on heat-treated sides was significantly less when IGF1 is blocked than the increased heights reported in saline mice as determined by one-way ANOVA. Overall, blocking IGF1 activity in tibial growth plates attenuated the localized heat effect on growth plate morphometry.

5.3.4 PCNA Expression

PCNA expression (paired $t=2.0$, ns, $p=0.12$) decreased by 12.1% on the heat-treated sides of JB1-injected mice (Fig. 24, Table 11). PCNA expression was significantly less ($F(1,10)=10.6$, $p<0.01$) than the 8.8% increase in expression on the heat-treated sides of saline control mice (Chapter 3; Fig. 14). Results indicate decreased proliferation in tibial growth plates with localized heating when IGF1 is blocked. However, while overall expression of PCNA was less in JB1-injected mice, chondrocytes still demonstrated a level of proliferation suggesting mechanisms regulated proliferation in the PZ independent of IGF1.

Table 11. Comparison of Non-Treated and Heat-Treated Expression of PCNA in Proliferative Zone of Tibial Growth Plates in Saline and JB1-Injected Mice.

Antibody in Proliferative Zone	Treatment	Non-Treated (30C)	Heat-Treated (40C)	Percent Increase	N
PCNA expression	Saline	85.10 (6.90)	91.93 (1.98)*	8.6	6
	JB1	71.08 (19.04)	62.20 (17.52) ^{ns}	-12.1 [#]	5

Values are mean (standard deviation). JB1 emphasized as an IGF1 blocking drug in red. Sample size (N) is number of left-right pairs. Significantly larger on heat-treated side by one-tailed paired t-test: *p< 0.05; ns, non-significant. Significant differences in percent increase between saline controls and JB1-injected mice by one-way ANOVA: [#]p<0.05.

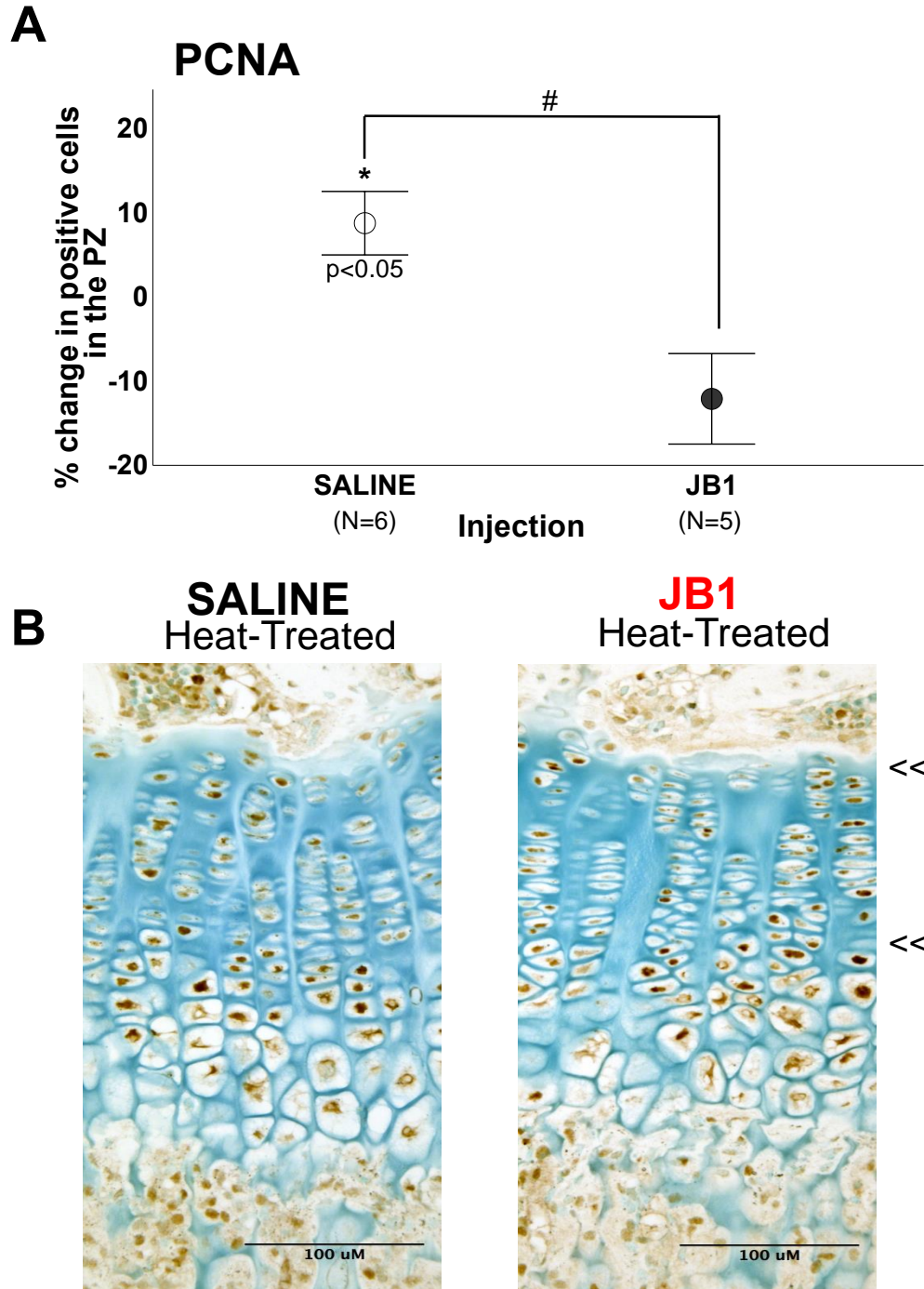


Figure 24. Expression of PCNA in the PZ of Proximal Tibial Growth Plates Decreased when IGF1 is Blocked (Continued on the following page)

Figure 24. (A) Error bar plots shows percent change in heat-treated limb compared to non-treated limb. PCNA expression increased by 8.6% on the heat-treated side of saline mice, and decreased by 12.1% in JB1-injected mice. (B) Comparison of heat-treated proximal tibial growth plates from a saline and JB1-injected mouse immunostained for PCNA. A larger quantity of PCNA staining was counted in saline mice compared to JB1-injected mice. Positive staining is shown by dark brown nuclei within the proliferative zone of the growth plate (region between the double arrows). Mean \pm 1 standard error plotted. * $p < 0.05$ significance in left-right comparisons; # $p < 0.05$ comparing % change in JB1-injected mice with saline controls.

5.3.5 IGF1R, pIGF1R and pAkt Expression

IGF1R expression in the PZ (paired $t=5.0$, $p<0.01$) of tibial growth plates decreased by 28.0% on the heat-treated side of JB1-injected mice. This decrease was significantly less ($F(1,10)=39.4$, $p<0.001$) than the 14.5% increase in IGF1R expression (paired $t=3.2$, $p<0.05$) on the heat-treated side of saline control mice (Fig. 25A, 26A(a); Table 12). Expression of activated IGF1R (pIGF1R) in the proliferative zone (paired $t=3.2$, $p<0.05$) of tibial growth plates decreased by 23.6% on the heat-treated side of JB1-injected mice. This decrease was significantly less ($F(1,10)=24.0$, $p<0.001$) than the 7.7% increase in pIGF1R expression (paired $t=5.3$, $p<0.01$) on the heat-treated side of saline mice (Fig. 25B, 26B(a); Table 12). The phosphatidylinositol-3 (PI-3) kinase pathway is one of several signaling pathways activated by IGF1-IGF1R interaction (the other is the mitogen-activated protein kinase (MAPK) pathway (Chapter 1, Fig. 4). Downstream activation of IGF1R was therefore investigated by measuring phosphorylated Akt (pAkt) expression as one of the key signaling molecules of the PI-3 kinase pathway in the tibial growth plate (Choukair, Hugel, Sander, Uhlmann, & Tonshoff, 2014). Expression of pAkt decreased by 2.1% in the proliferative zone (paired $t=0.2$, ns, $p=0.87$) of tibial growth plates on the heat-treated side of JB1-injected mice. This decrease was significantly less ($F(1,10)=6.4$, $p<0.05$) than the 22.8% increase in pAkt expression (paired $t=4.4$, $p<0.01$) on the heat-treated side of saline control mice (Fig. 25C, Table 12). These data indicate that in the PZ, IGF1 activity is increased with heat-treatment (as reported in Chapter 4), and when IGF1 is blocked, there is a localized decrease in IGF1 activation.

IGF1R expression in the HZ (paired $t=2.7$, $p<0.05$) of tibial growth plates decreased by 19.2% on the heat-treated side of JB1-injected mice. This decrease was significantly less ($F(1,10)=11.0$, $p<0.01$) than the 10.4% increase in IGF1R expression (paired $t=2.1$, ns, $p=0.11$) on the heat-treated side of saline mice (Fig. 25A, 26A(b); Table 13). Expression of pIGF1R in the HZ (paired $t=1.7$, ns, $p=0.17$) of tibial growth plates decreased by 10.1% on the heat-treated side of JB1-injected mice. This decrease was significantly less ($F(1,10)=9.0$, $p<0.05$) than the 10.2% increase in pIGF1R expression (paired $t=3.4$, $p<0.05$) on the heat-treated side of saline mice (Fig. 25B, 26B(b); Table 13). Expression of pAkt decreased by 22.4% in the HZ (paired $t=4.1$, $p<0.05$) of tibial growth plates on the heat-treated sides of JB1-injected mice. This decrease was significantly less ($F(1,10)=8.0$, $p<0.05$) than the 13.5% increase in pAkt expression on the heat-treated side of saline mice (paired $t=1.7$, ns, $p=0.15$) (Fig. 25C, Table 13). These data indicate that in the HZ, there is increased IGF1 activity because when IGF1 is blocked, there is a localized decrease in markers of IGF1 activation.

Table 12. Comparison of Non-Treated and Heat-Treated Expression of Markers for IGF1 Activation in Proliferative Zone of Tibial Growth Plates in Saline and JB1-Injected Mice.

Antibody in Proliferative Zone	Treatment	Non-Treated (30C)	Heat-Treated (40C)	Percent Increase	N
IGF1R expression	Saline	69.68 (6.36)	79.52 (7.61)*	14.5	5
	JB1	68.83 (18.80)	50.25 (18.71)**	-28.0#	6
pIGF1R expression	Saline	84.85 (10.36)	90.97 (7.90)**	7.7	6
	JB1	72.80 (15.38)	53.88 (4.75)*	-23.6#	5
pAkt expression	Saline	55.21 (15.05)	66.23 (12.52)**	22.8	6
	JB1	37.62 (19.87)	38.14 (22.27) ^{ns}	-2.1#	5

Values are mean (standard deviation). JB1 emphasized as an IGF1 blocking drug in red. Sample size (N) is number of left-right pairs. Significantly larger on heat-treated side by one-tailed paired t-test: *p< 0.05; **p<0.01; ns, non-significant. Significant differences in percent increase between saline controls and JB1-injected mice by one-way ANOVA: #p<0.05.

Table 13. Comparison of Non-Treated and Heat-Treated Expression of Markers for IGF1 Activation in Hypertrophic Zone of Tibial Growth Plates in Saline and JB1-Injected Mice.

Antibody in Hypertrophic Zone	Treatment	Non-Treated (30C)	Heat-Treated (40C)	Percent Increase	N
IGF1R expression	Saline	74.22 (9.94)	81.08 (2.95) ^{ns}	10.4	5
	JB1	74.95 (15.10)	59.57 (13.78) [*]	-19.2 [#]	6
pIGF1R expression	Saline	82.13 (7.39)	90.07 (4.23) [*]	10.2	6
	JB1	76.14 (12.74)	67.42 (10.13) ^{ns}	-10.1 [#]	5
pAkt expression	Saline	49.91 (14.15)	56.66 (17.93) ^{ns}	13.5	6
	JB1	57.12 (25.83)	48.46 (29.78) [*]	-22.4 [#]	5

Values are mean (standard deviation). JB1 emphasized as an IGF1 blocking drug in red. Sample size (N) is number of left-right pairs. Significantly larger on heat-treated side by one-tailed paired t-test: *p< 0.05; ns, non-significant. Significant differences in percent increase between saline controls and JB1-injected mice by one-way ANOVA: #p<0.05.

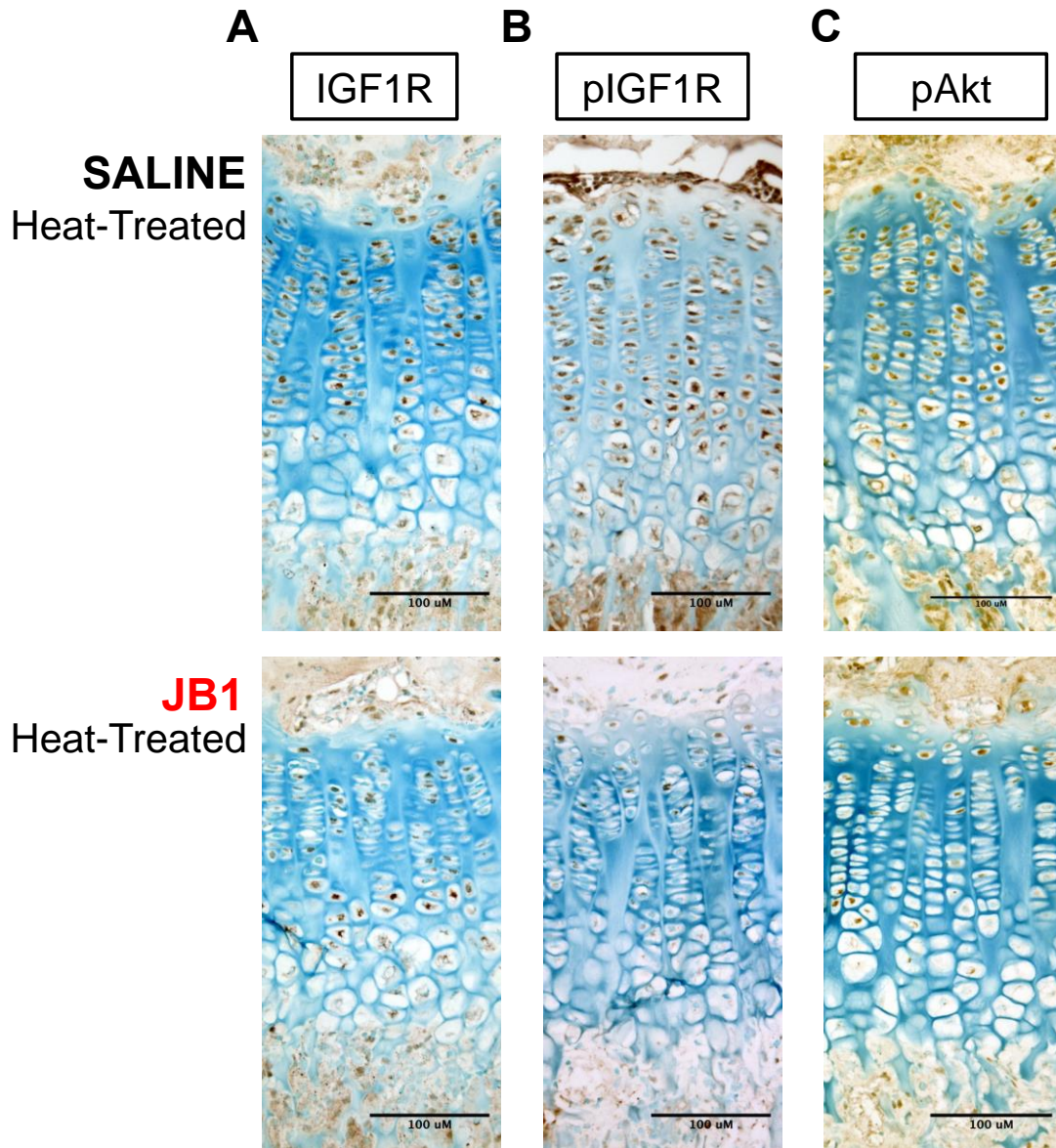


Figure 25. Expression of Markers of IGF1 Activation Decreases in Heat-Treated Proximal Tibial Growth Plates when IGF1 is Inhibited

Comparison of heat-treated proximal tibial growth plates from a saline control and JB1-injected mouse immunostained for (A) IGF1R (B) pIGF1R and (C) pAkt. A larger quantity of positive staining, shown by dark brown nuclei, was counted in saline mice compared to JB1 mice.

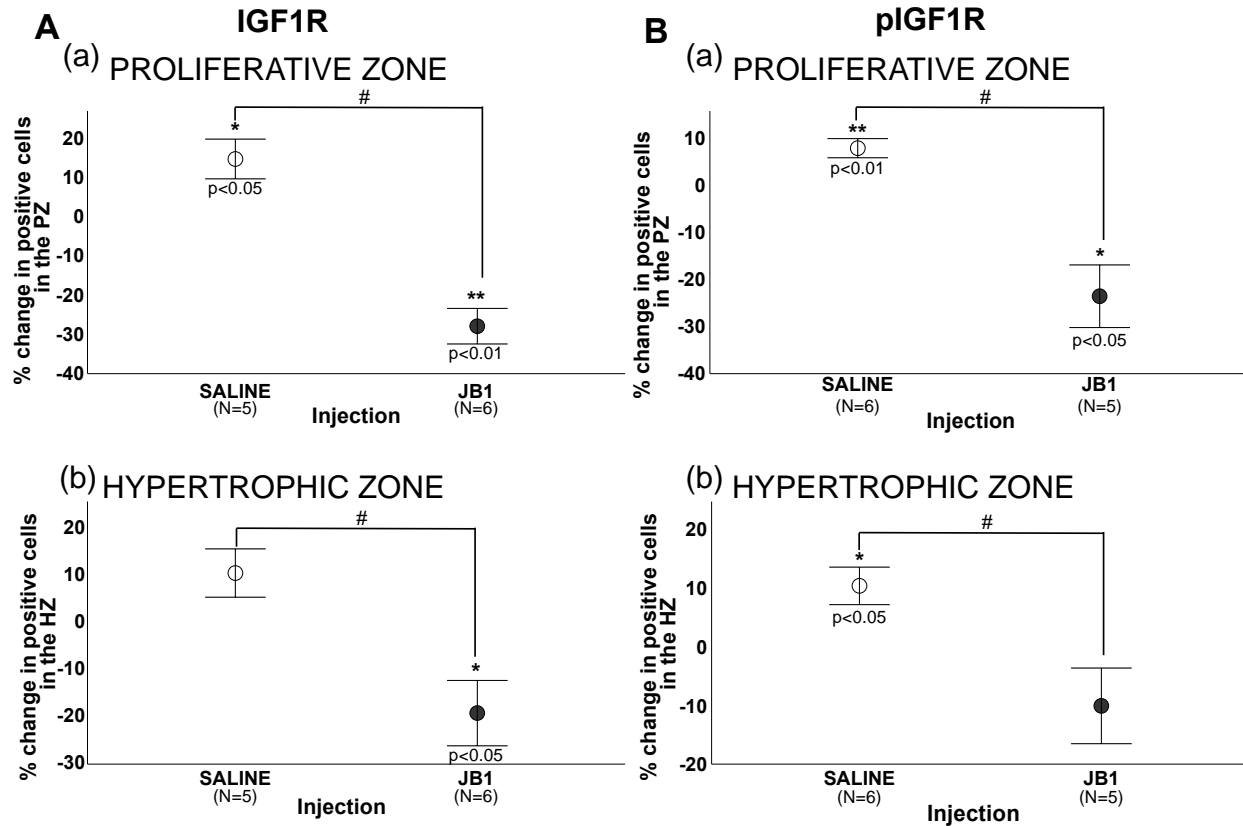


Figure 26. Heat-Induced Effect on IGF1 Activity in the Tibial Growth Plate is Evident in the PZ and HZ

(A) IGF1R expression in saline and JB1-injected mice. (a) Error bar plot shows percent change in heat-treated limb compared to non-treated limb. IGF1R expression in the PZ increased by 14.5% and decreased by 28% on heat-treated sides of saline and JB1-injected mice. (b) IGF1R expression in the HZ increased by 10.4% and decreased by 19.2% in saline and JB1-injected mice. (B) pIGF1R expression in saline and JB1-injected mice. (a) pIGF1R expression in the PZ increased by 7.7% and decreased by 23.6% in saline and JB1-injected mice. (b) pIGF1R expression in the HZ increased by 10.2% and decreased by 10.1% in saline and JB1-injected mice. Mean \pm 1 standard error plotted. * $p < 0.05$; ** $p < 0.01$, significance in left-right comparisons; # $p < 0.05$ comparing % change in JB1-injected mice with saline controls.

5.3.6 *GHR*^{-/-} Growth Parameters

When levels of circulating IGF1 are low, femoral length (paired $t=0.17$, ns, $p=0.88$) and tibial elongation rate (paired $t=0.3$, ns, $p=0.80$) did not differ on the heat-treated sides of 5 week old *GHR*^{-/-} mice treated for 14 days (Fig. 27, Table 14). In wild-type mice, femoral length and tibial elongation rate increased by 1.1% and 10.8% respectively as seen in Chapter 3 (Table 5). The heat-induced increase in femoral length ($F(1,12)=29.2$, $p<0.001$) and tibial elongation rate ($F(1,12)=13.1$, $p<0.01$) was significantly greater from the equivalent left-right pairs measured in *GHR*^{-/-} mice. Humeral length (paired $t=0.2$, ns, $p=0.87$) did not differ as seen in wild-type mice.

Table 14. Comparison of Non-Treated and Heat-Treated Bone Parameters of 5-Week Old Wild-Type and *GHR*^{-/-} Mice.

Parameter	Genotype	Non-Treated (30C)	Heat-Treated (40C)	Percent Increase	N
Humeral Length (mm)	Wild-type	10.14 (0.11)	10.15 (0.13) ^{ns}	0.1	9
	<i>GHR</i> ^{-/-}	7.51 (0.04)	7.51 (0.04) ^{ns}	0.0 ^{ns}	5
Femoral Length (mm)	Wild-type	12.86 (0.18)	13.00 (0.17) ^{***}	1.1	9
	<i>GHR</i> ^{-/-}	9.32 (0.08)	9.32 (0.09) ^{ns}	0.0 [#]	4
Tibial Elongation Rate (μM/day)	Wild-type	109.57 (11.18)	121.22 (10.70) ^{***}	10.8	8
	<i>GHR</i> ^{-/-}	53.98 (12.59)	54.36 (12.23) ^{ns}	0.9 [#]	5

Values are mean (standard deviation). JB1 emphasized as an IGF1 blocking drug in red. Sample size (N) is number of left-right pairs. Significantly larger on heat-treated side by one-tailed paired t-test: ***p<0.001; ns, non-significant. Significant differences in percent increase between saline controls and JB1-injected mice by one-way ANOVA: #p<0.05; ns, non-significant.

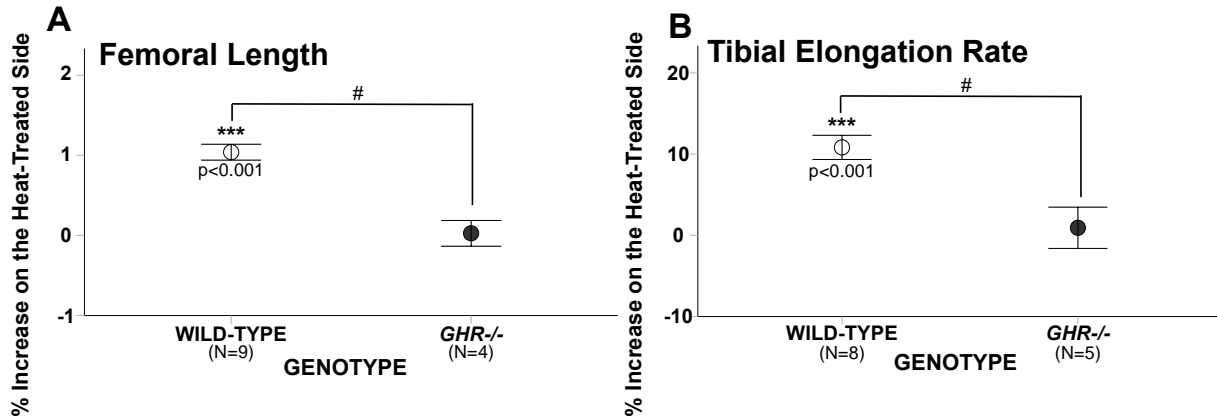


Figure 27. Extremities of Growth-Hormone Receptor Knockout (*GHR*^{-/-}) Mice are not Lengthened with Unilateral Heat-Treatment

(A) Error bar plots shows percent change in heat-treated limb compared to non-treated limb. Femoral length increased by 1.1% on the heat-treated sides of wild-type mice treated for 14 days from 3-5 weeks of age. Femoral length did not change with treatment in *GHR*^{-/-} mice. (B) Tibial elongation rate increased by 10.8% on the heat-treated sides of wild-type mice, and *GHR*^{-/-} mice had a minimal increase of 0.9% with heat-treatment. Mean \pm 1 standard error plotted. *** $p < 0.001$, significance in left-right comparisons; # $p < 0.05$ comparing % change in wild-type and *GHR*^{-/-} mice

5.4 DISCUSSION

The goal of this study was to determine if the heat-enhanced bone elongation observed after targeted limb heating is IGF1 dependent. The heat-treatment effect on bone elongation is attenuated in growing mouse models exhibiting both locally blocked IGF1 and low IGF1. Femoral length and tibial elongation rate was shown to increase by over 1% and 7% respectively in heat-treated limbs of saline control mice after either 7 or 14 days of unilateral heating. In JB1-injected (blocked IGF1) and *GHR*^{-/-} (low levels of IGF1) mice, both femoral length and tibial elongation rate did not differ between the heat-treated and non-treated contralateral sides. Our data supported the hypothesis that with diminished IGF1 activity, heat-enhanced limb length is attenuated.

Although we were not able to perform immunostaining on *GHR*^{-/-} mice the results using our model and JB1 as an antagonist of IGF1 activity demonstrated that heat-enhanced chondrocyte proliferation and hypertrophy in proximal tibial growth plates was attenuated when IGF1 is blocked. Chondrocyte proliferation and hypertrophy are common indicators of longitudinal growth as discussed in Chapter 3. There is a positive relationship between rate of chondrocyte proliferation, size of chondrocyte enlargement, and linear bone growth rate (Cooper et al., 2013; Hunziker, 1994b; Kember, 1993; Rolian, 2008; Wilsman et al., 2008). According to the findings of this study, the proliferative and hypertrophic zones of growth plates on non-injected sides of saline control mice each made up 45% of the total growth plate height (the remaining 10% being the reserve zone). On the heat-treated side, there was a shift in zonal height as the proliferative zone made up 41% of total growth plate height (Fig. 23C) while the hypertrophic zone of chondrocytes took up 48% of total height (Fig. 23D). This observed

shift in zones was absent in mice injected with the IGF1 blocking drug as the proliferative and hypertrophic zone height made up 42% and 47% of total height respectively on both non-treated and heat-treated sides. When evaluating proliferation in the growth plate, expression of PCNA increased by 8.6% on the heat-treated side of saline control mice but decreased by 12.1% when IGF1 was blocked (although not statistically significant) (Fig. 24, Table 11). Results demonstrated that an increased rate of proliferation with heat-treatment is dependent, in part, on IGF1 activity in the proliferative zone of the growth plate.

To test for activation of IGF1 signaling, immunohistochemistry methods detected expression of specific markers for IGF1 activity in tibial growth plates including IGF1R, pIGF1R (activated receptor) and pAkt (downstream IGF1 activation). Measured expression levels of these markers (as done in Chapter 4) suggest in this study that the heat-enhanced increase in IGF1 activity is attenuated when IGF1 is blocked. On heat-treated sides of the saline control mice, there was an increase in IGF1R, pIGF1R and pAkt expression while levels decreased when IGF1 was blocked in JB1-injected mice (Fig. 25, 26; Tables 12,13). Measured expression of signaling molecules as a result of IGF1 activated receptors including pIGF1R and downstream pAkt increased on the heat-treated sides of saline control mice by over 7%. Expression of pIGF1R and pAkt decreased by over 10% and 2% respectively on the heat-treated sides when the antagonist blocked IGF1 from binding to the receptor. This decrease in expression was observed in both the proliferative and hypertrophic zones of the growth plate as expected since IGF1 has been shown to increase cellular proliferation and differentiation both *in vitro* and *in vivo* (Abbaspour et al., 2008; Choukair et al., 2014;

Ciarmatori et al., 2007; Tahimic et al., 2013; Yakar & Isaksson, 2016). However, down regulation of pAkt was more substantial in the hypertrophic zone (22.4% decrease) compared to the proliferative zone (2.1% decrease). One plausible explanation for these results could be rationalized by findings from Ciarmatori et al. (2007) and Kiepe, Ciarmatori, Hoeflich, Wolf, & Tönshoff (2006) in growth plates of both cell lines and whole animals demonstrating that IGF1-driven proliferation is regulated by both the PI-3 kinase and MAPK pathways, while the hypertrophic zone is regulated by only the PI-3 kinase pathway (Ciarmatori et al., 2007; Kiepe et al., 2006). Regulation pathways could be compared in our model by analyzing expression levels of pAkt and important downstream signaling molecules from the MAPK pathway such as ERK.

A surprising finding from this study was the significant decrease in IGF1R expression in both the proliferative zone (28% decrease) and the hypertrophic zone (19% decrease) from growth plates after treatment with the antagonist (Fig. 26A; Tables 12,13). It was expected that with targeted limb heating IGF1R expression would either remain unchanged or increase in mice administered the IGF1 blocking drug since binding of IGF1 to its receptor enhances activation and initiates internalization and recycling of IGF1R (Chow et al., 1998; Yin, Guan, Liao, & Wei, 2009). Cell culture studies modeling the growth plate have shown that other antagonists of IGF1 signaling have reduced chondrocyte proliferation without impacting expression of IGF1R (Choukair et al., 2014). While literature does not support our findings, it is possible that the down regulation of IGF1R is a unique characteristic of IGF1 peptide analog JB1. The obscure ligand-independent mechanisms of IGF1R internalization may be a

potential mechanism of JB1-bound IGF1R down regulation (Morcavallo, Stefanello, Iozzo, Belfiore, & Morrione, 2014; Reilly, Mizukoshi, & Maher, 2004).

Numerous studies have investigated the use of kinase inhibitors as a method for IGF1 inhibition in various tissues (Li et al., 2009; Pillai & Ramalingam, 2013; Refolo et al., 2017). However, blocking IGF1 activity by peptide analogs has been considered a more specific method for inhibiting cellular proliferation (Brock et al., 2011; Huang et al., 2000; Kleinriders, 2016; Pietrzowski et al., 1992; Todd et al., 2007; Smith et al., 1999; Wen et al., 2012). Besides their high specificity, IGF1 peptide analogues also have low molecular weights and low toxicity (Pietrzowski et al., 1992). Monoclonal antibodies, such as α IR3, also have high specificity against IGF1R comparable to the peptide analogues, but are over 100-fold larger in size (Huang et al., 2000). Small molecular size is important for this study because the targeted growth plate is avascular and solute transport occurs by means of surrounding vasculature (Brodin, 1955). In vivo imaging studies have shown that molecules under 10kDa enter the growth plate from all directions of surrounding vasculature, while molecules over 40kDa cannot enter to a significant degree (Farnum et al., 2006). Aside from being commercially available, JB1 was chosen for this study at only 1.2kDa and therefore falls well in the range of molecules capable of vascular transport into the cartilage growth plate. The small size of JB1 may also explain why heat-induced decrease in expression levels of IGF1 signaling proteins were more prominent than the increase in expression seen in the heat-treated saline control mice. It is possible that the smaller size of JB1 (1.2kDa) allows for increased transport into the growth plate relative to IGF1 (7.6kDa).

The use of localized heat-treatment, as explained in Chapter 2, has been established as an effective method for enhancing limb elongation in growing mice (Serrat et al., 2015). Research into the mechanism of action is important in the hopes of translating our findings to develop a noninvasive alternative for treatment of bone elongation disorders in children. The ultimate goal would be to target localized heat to the site of the growth plate and increase limb elongation without impacting overall growth. In this study, there were no significant differences in change of body mass between saline controls and JB1-injected mice over the duration of heat-treatment and did not impact overall growth. The similarity observed between the non-treated sides of saline controls and JB1-injected mice is another indication that the effect of blocking IGF1 was limited to the heat-treated side.

Limitations to this study include the small sample size of the *GHR*^{-/-} mice. Unilateral heating experiments were carried out previous to establishing a consistent methodology as published (Serrat et al., 2015), and as described in the chapters of this dissertation. Also, since expression levels of PCNA, IGF1R, pIGF1R, and pAkt were not measured in the *GHR*^{-/-} model, future studies will be essential to assay these important variables. Expanding upon the findings in the *GHR*^{-/-} mouse model, future studies may be designed to understand the impact of heat-treatment on the GH-IGF1 axis at the level of the epiphyseal growth plate. While the current study focused on local IGF1 activity in the growth plate, GH and related signaling molecules have yet to be studied in targeted limb heating experiments. GH has both direct and indirect control on the growth plate and has been shown to directly stimulate chondrogenesis and induce local IGF1 activity (Isaksson et al., 1982, 1985; Ohlsson, 1992b, 1998; Schlechter et al.,

1986). In hope of translating the limb-heating model to treat children with bone lengthening disorders, including those with irregular GH-IGF1 regulation, it is important to determine if mild heat impacts GH in regulating longitudinal growth. Since the molecular size of GH (22 kDa) exceeds that of IGF1 (7.6 kDa) and the threshold of heat-enhanced vascular delivery (10 kDa) to the growth plate (Serrat et al., 2014a), the effects of heating would be expected to be at the level of local GH regulation. It is also expected that if targeted limb heating increases GH activity, it would not be independent of IGF1 since results from this study showed that when IGF1 activity was inhibited, and GH regulation was normal, the heat-enhanced growth effect was attenuated.

5.5 CONCLUSION

In conclusion, with diminished IGF1 activity, heat-enhanced limb length is attenuated. Bone lengthening effects of temperature in hindlimbs of growing mice, such as increased femoral length and tibial elongation rate, were absent in *GHR*^{-/-} mice (low levels of IGF1), and in JB1-injected mice (IGF1 was locally blocked). When IGF1 activity is blocked, the heat-induced increase in proliferation and height of hypertrophic zone is also attenuated. The variation between saline and JB1-injected mice in left-right differences of bone length, growth plate morphometry and IGF1 signaling despite both exhibiting normal body growth indicates that JB1 locally blocked IGF1 activity on heat-treated sides. Together these results support the hypothesis that in the absence of IGF1 activity, targeted limb heating cannot effectively increase bone elongation in growing mice. Chapter 6 will test whether heat-enhanced limb length can be maintained after treatment has ended into skeletal maturity.

CHAPTER VI: DIFFERENTIAL LIMB LENGTH IS MAINTAINED THROUGHOUT SKELETAL DEVELOPMENT AFTER END OF TREATMENT

6.1 INTRODUCTION

During the post-natal development, functional growth plate cartilage augments bone elongation with a rapid period of growth during early life then undergoes a gradual decline in growth velocity and eventually ceases during adolescence. This process has been termed as growth plate senescence (Lui et al., 2011). Although the murine growth plate does not completely close and form a bony union as it does in humans, both reach a period of growth culmination over a similar time frame and by comparable cellular kinetics (Dawson, 1925, 1935; Geiger et al., 2014; Walker & Kember, 1972). Once skeletal maturity is reached, the growth plate ceases to contribute to linear growth. In mice, skeletal maturity is reached by 12 weeks of age (Kilborn et al., 2002; Li et al., 2017; Serrat et al., 2007; Stempel et al., 2011; Zoetis et al., 2003), while humans are considered skeletally mature at puberty between 13-18 years of age (Kelly & Diméglio, 2008).

Current treatment for bone elongation disorders including the invasive surgical procedures to correct limb length discrepancies, and the drug regimens for GH and IGF1 occur before skeletal maturity. Often, there is only a partially effective outcome after both surgical procedures (Gurney, 2002; Hasler & Krieg, 2012) and drug regimen therapy (Backeljauw et al., 2013; Laron, 2001; Ranke et al., 1995b; Wu et al., 2013). A goal of many therapies for bone elongation disorders is to maintain corrections past skeletal maturity to avoid resulting problems in adulthood. In children, while treatment is

most effective during early childhood when growth is most rapid (Kelly & Diméglio, 2008), therapy continues until growth ceases at the end of puberty.

The concept of using localized heat as a noninvasive alternative to surgical treatment for bone elongation disorders in children has thus far been supported by data demonstrating that targeted limb heating can effectively lengthen extremities during rapid periods of growth. However, in hopes of translating the results of this study into developing a noninvasive method for lengthening bones as a therapy for children, it is important to determine if the heat-enhanced bone elongation can be maintained throughout skeletal development. Studies have shown that femoral and tibial lengths remain almost 1% longer on the heat-treated sides of 12-week-old mice (Serrat et al., 2015). The objective of this project was to understand the ability for unilaterally lengthened extremities to remain longer until skeletal maturity following both a 7 day and 14 day unilateral heating regimen in conjunction with low dose IGF1 administration. It is **hypothesized that differential limb length will be maintained throughout skeletal development after treatments have ended**. It is also expected based on findings from Chapter 4, that persistent limb length differences will be prominent in IGF1-injected mice.

6.2 MATERIAL AND METHODS

6.2.1 Animals and Experimental Design

All procedures were approved by the Institutional Animal Care and Use Committee of Marshall University (Protocol 558). Female C57BL/6 (N=31) mice were obtained from Hilltop Lab Animals, Inc. (Scottsdale, PA, USA) at 21 and 28 days weaning

age. Mice were singly housed at 21°C in standard plastic caging, exposed to a 12 hour light/dark cycle and provided with food and water ad libitum.

As described in the previous chapters and as indicated by the unilateral heating methods schematic (Fig. 28), mice post-weaning were treated with daily unilateral heat (40°C) under the same procedural conditions. Mice were treated for 7 days from 3-4 weeks of age and for 14 days from 3-5 weeks of age. Subcutaneous injections of either saline solution (3:1, 1xPBS:dH₂O) at a volume of 0.01mL/g, or IGF1 (2.5mg/kg; Peptrotech), were administered to mice daily at the start of the light cycle one hour prior to heat-treatment for 7 days and 14 days (N=6 per group). These experimental groups have not yet been described in previous chapters as tissue collection occurred later in development. A group of non-heated, non-injected 3-week-old mice (N=7) were also kept under equivalent housing conditions as non-treated controls. Daily mass was recorded during the duration of limb heating, and then weekly mass was measured until euthanization.

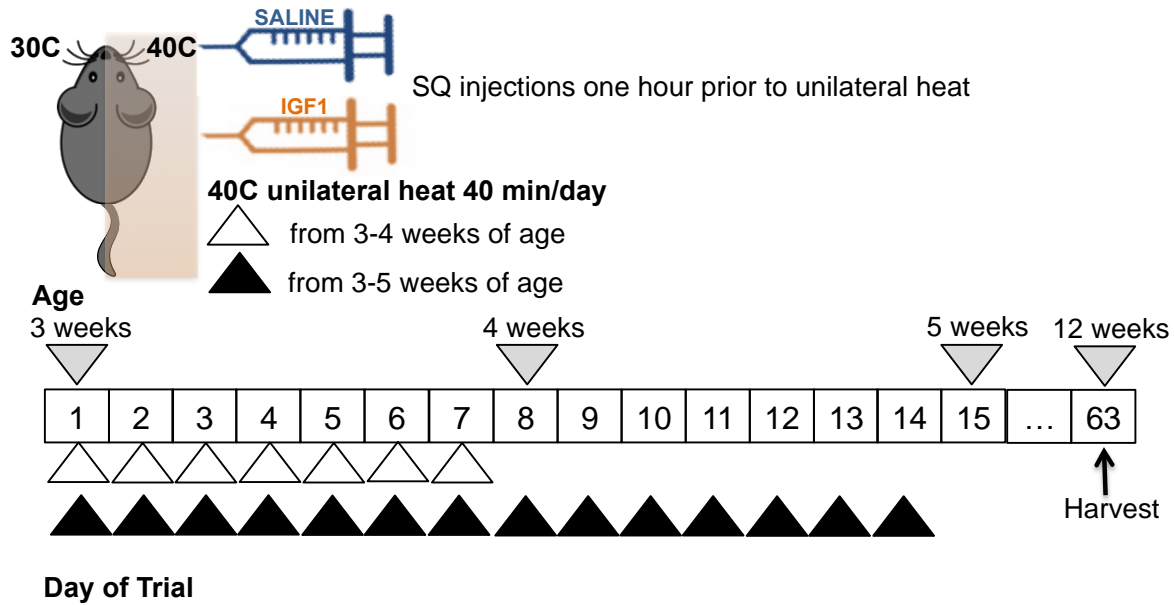


Figure 28. Unilateral Heating Schematic

Mice were injected subcutaneously (SQ) with either saline or IGF1 (2.5mg/kg) one hour prior to treatment of 40°C unilateral heat for 40 minutes daily for 7 days from 3-4 weeks of age and 14 days from 3-5 weeks of age. Euthanasia and tissue collection occurred at 12 weeks of age when mice were skeletally mature. Mouse illustration based on “mouse clip art black and white” from clipartstockphotos.com.

6.2.2 Tissue Collection and Long Bone Measurements

Long bones (femora and humeri) were collected and measured as described in Chapter 3 (Sections 3.2.2 and 3.2.3) but all experimental mice (N=31) were euthanized for tissue collection at 12-weeks of age at skeletal maturity. In this study tibiae were collected for long bone measurements since no histology was done. Non-treated controls (N=7) were also euthanized at the same endpoint to evaluate natural limb length differences at skeletal maturity.

6.2.3 Statistical Analysis

Statistical analyses were performed using SPSS 25.0 software (IBM Corporation, Armonk, NY) with $p < 0.05$ as accepted significance and comparisons as described in Chapter 4 (Section 4.2.4).

6.3 RESULTS

6.3.1 Unilateral Heating Parameters

At the start of 7 day unilateral heating, a group of 3-week-old female mice (N=17) were partitioned out into the corresponding non-treated controls (N=5) and heat-treated saline (N=6) and IGF1-injected mice (N=6). At the experimental start, all mice were comparable in mass ($F(2,16)=2.7$, ns, $p < 0.12$), weighing an average of 9.0g (Fig. 29A, Table 15). At skeletal maturity, mice were also comparable in mass ($F(2,18)=2.3$, ns, $p=0.14$), weighing an average of 23.0g. The overall gain in mass was therefore 14.0g with no significant differences between non-treated controls, saline mice treated for 7 days, or IGF1-injected mice treated for 7 days, as determined by multiple comparison

analysis using one-way ANOVA (Table 15). At the start of 14 days unilateral heating, another group of 3-week-old female mice (N=12) were separated into heat-treated saline (N=6) and IGF1-injected mice (N=6). At the experimental start, all mice were comparable in mass ($F(1,11)=0.1$, ns, $p=0.83$), weighing an average of 10.0g (Fig. 29A, Table 15). At skeletal maturity, mice were also similar in mass ($F(1,11)=2.5$, ns, $p=0.14$), weighing an average of 22.5g. Although IGF1-injected mice (23.1g) overall gained about 1.0g more than the saline controls (22.2g), this was not statistically significant ($F(1,11)=2.0$, ns, $p=0.19$). Therefore, with either 7 days or 14 days of limb heating, mass remained comparable between groups from the start at 3 weeks of age until skeletal maturity at 12 weeks of age (Table 15).

The core temperature averaged 36°C during unilateral heating. While mice were anesthetized, the average surface temperature of non-treated hindlimbs was 30°C and the heat-treated hindlimbs were 40°C. These recorded temperatures were consistent with parameters during the daily limb heating reported in previous chapters. As reported in Chapter 4, the recovery time from anesthesia was longer in IGF1-injected mice compared to saline controls in this study. At the end of each daily heat-treatment (40mins), the average time for saline mice to recover from anesthesia after 7 days and 14 days of heating was 1.4 ± 0.23 mins and 1.1 ± 0.04 mins respectively. The average time for IGF1-injected mice to recover from anesthesia was 2.6 ± 0.50 mins and 2.7 ± 0.40 mins, which was significantly *longer* than the saline controls after both 7 days ($F(1,11)=33.2$, $p<0.001$) and 14 days ($F(1,11)=101.9$, $p<0.001$) of unilateral heating.

Table 15. Comparison of Mass Between Heat-Treatment Groups at the Start of Treatment and at Skeletal Maturity

Length of Heat-Treatment	Injection	Mass at Start (g) 3-weeks old	Mass at End (g) 12-weeks old	Change in Mass (g)	N
None	None	8.6 (0.8)	22.7 (1.0)	14.0 (0.9)	5
7 days	Saline	9.3 (0.4)	23.6 (1.1)	14.3 (1.2)	6
	IGF1	9.2 (0.3)	22.4 (0.8)	13.2 (1.0)	6
14 days	Saline	10.1 (0.7)	22.2 (0.9)	12.2 (1.3)	6
	IGF1	10.0 (0.4)	23.1 (0.9)	13.1 (0.9)	6

Values are mean (standard deviation). Sample size (N) is number of mice weighed.

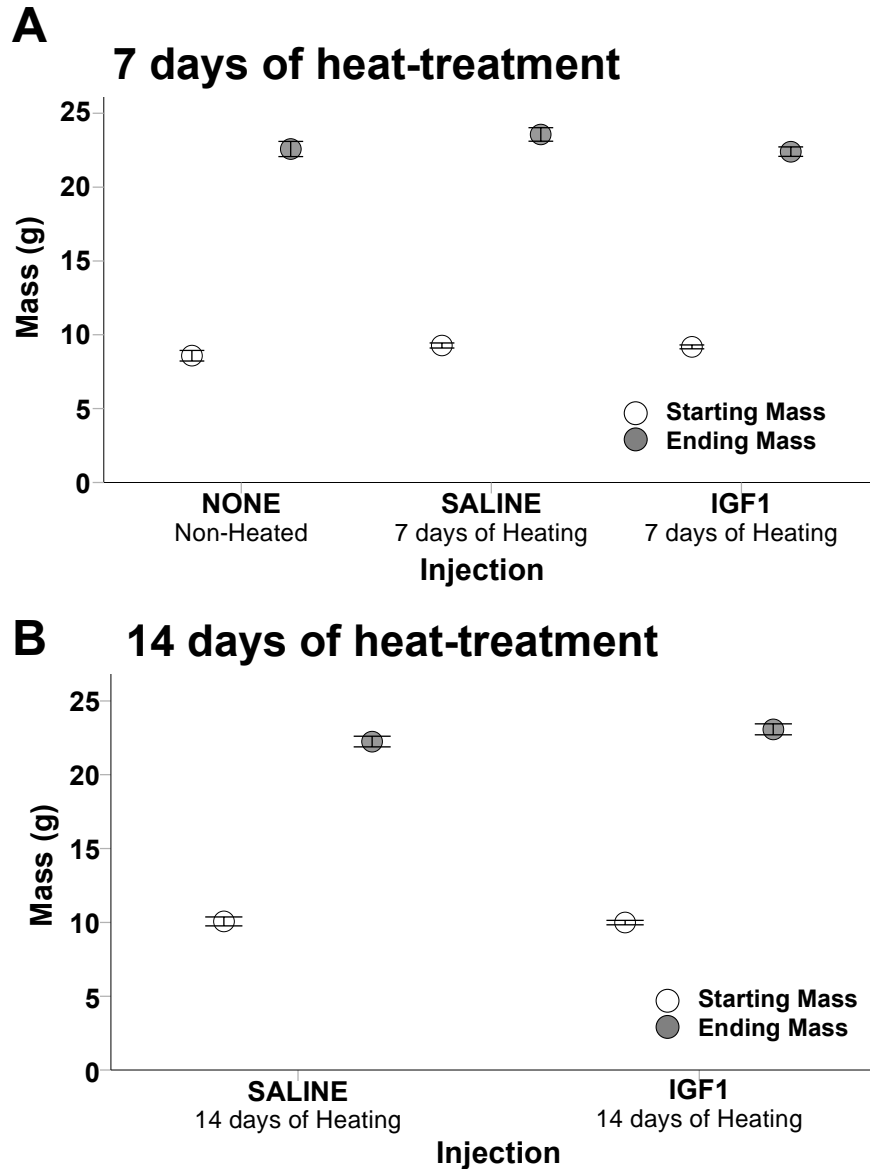


Figure 29. Mass did not Differ Between Non-Treated Controls, Heat-Treated Saline Control Mice, and Heat-Treated IGF1-Injected Mice at Either Duration of Limb Heating

(A) Error bar plots comparing starting (open circles) (at 3 weeks of age) and ending mass (gray circles) (at 12 weeks of age) of starting and ending mass from mice separated for 7 days of heating. (B) Comparison of starting and ending mass from mice separated for 14 days of heating. Mean \pm 1 standard error plotted.

6.3.2 Length of Long Bones Following 7 days of Heating

In non-treated control mice (N=7) humeral (paired $t=1.5$, ns, $p=0.19$), femoral (paired $t=0.2$, ns, $p=0.84$) and tibial length (paired $t=0.95$, ns, $p=0.41$) did not differ between left-right non-heated sides at skeletal maturity when mice were 12 weeks old (Fig. 30). Following 7 days of limb heating, there was no difference in humeral length at skeletal maturity in saline (paired $t=0.21$, ns, $p=0.84$) and IGF1-injected mice (paired $t=0.42$, ns, $p=0.69$) (Table 16). Femoral length was increased by 0.5% (paired $t=2.1$, ns, $p=0.09$) and 1.0% (paired $t=5.8$, $p<0.01$) on the heat-treated sides of saline and IGF1-injected mice respectively (Fig. 30A(a), Table 16). Tibial length was increased by 0.5% (paired $t=3.7$, $p<0.05$) and 0.4% (paired $t=2.5$, ns, $p=0.06$) on the heat-treated sides of saline and IGF1-injected mice respectively (Fig. 30A(b), Table 16). No significant differences in humeral ($p=0.91$), femoral ($p=0.16$) and tibial length ($p=0.96$) were determined between saline controls and IGF1-injected mice.

Table 16. Comparison of Non-Treated and Heat-Treated Sides of Experimental Mice Bone Parameters Following 7 Days of Limb Heating.

Parameter	Injection	Non-Treated (30C)	Heat-Treated (40C)	Percent Increase	N
Humeral Length (mm)	Saline	11.89 (0.16)	11.89 (0.17) ^{ns}	0.0	6
	IGF1	11.84 (0.16)	11.82 (0.12) ^{ns}	-0.1 ^{ns}	6
Femoral Length (mm)	Saline	15.46 (0.30)	15.53 (0.25) ^{ns}	0.5	6
	IGF1	15.21 (0.18)	15.36 (0.18) ^{**}	1.0 ^{ns}	6
Tibial Length (mm)	Saline	17.55 (0.37)	17.63(0.33) [*]	0.5	5
	IGF1	17.38 (0.20)	17.45 (0.17) ^{ns}	0.4 ^{ns}	6

Values are mean (standard deviation). Sample size (N) is number of left-right pairs. Significantly larger on heat-treated side by one-tailed paired t-test: *p< 0.05; **p<0.01; ns, non-significant. Significant differences in percent increase between saline controls and IGF1-injected mice by one-way ANOVA: ns, non-significant.

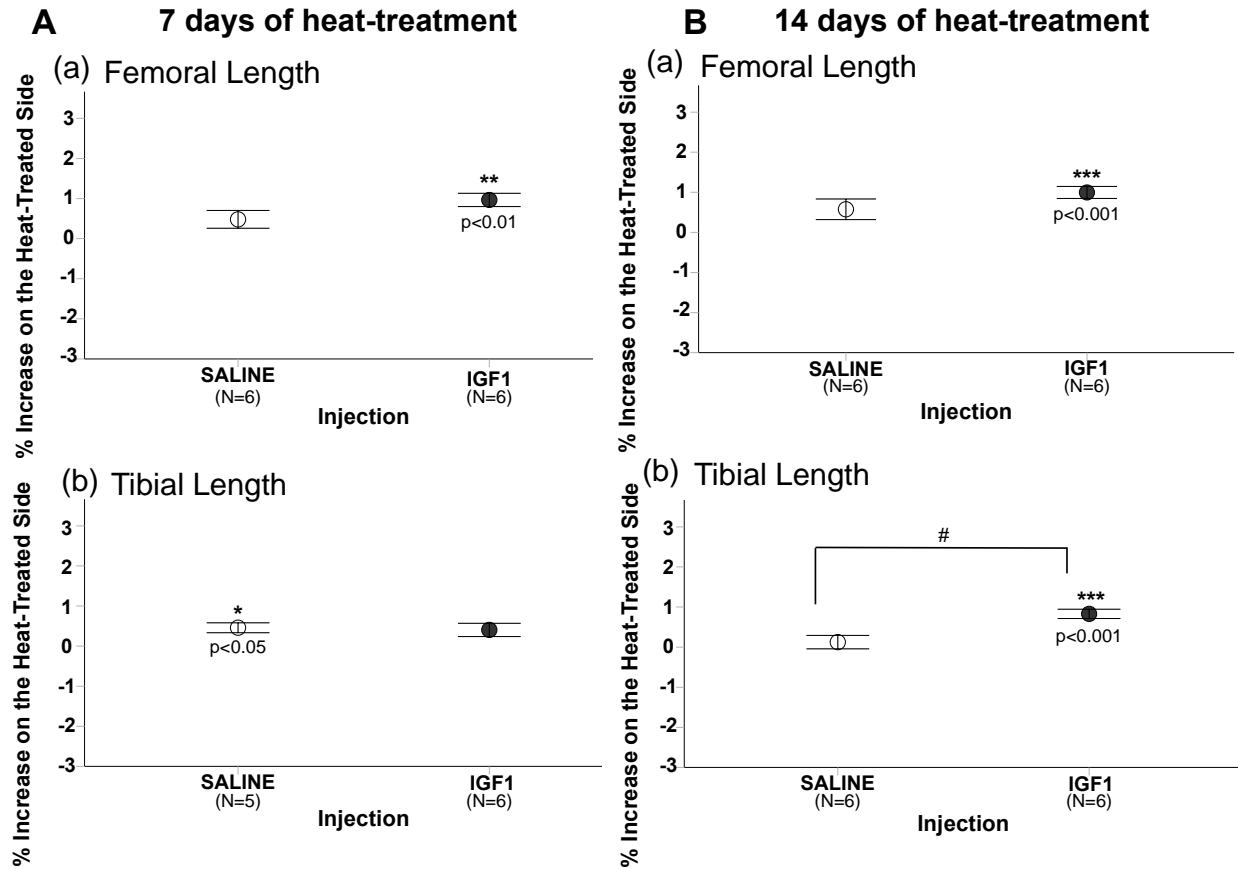


Figure 30. Extremities Remained Longer on the Heat-Treated Sides at Skeletal Maturity when Limb Heating was Coupled with IGF1 Administration

(A) Error bar plots show percent change in heat-treated limb compared to non-treated limb compare in saline and IGF1-injected mice treated for 7 days. (a) Femoral length was 0.5% and 1.0% longer on the heat-treated sides of saline and IGF1-injected mice (b) Tibial length was 0.5% and 0.4% longer on the heat-treated sides of saline and IGF1-injected mice. (B) Error bar plots compare % increase in bone length in saline and IGF1-injected mice treated for 14 days. (a) Femoral length was 0.6% and 1.0% longer on the heat-treated sides of saline and IGF1-injected mice (b) Tibial length was 0.1% and 0.8% longer on heat-treated sides of saline and IGF1-injected mice. Mean \pm 1 standard error plotted. *p< 0.05; **p<0.01; ***p<0.001, significance in left-right comparisons; #p<0.05 comparing % change in IGF1-injected mice with saline controls.

6.3.3 Length of Long Bones Following 14 Days of Heating

Following 14 days of limb heating, there was no difference in humeral length at skeletal maturity in saline (paired $t=0.95$, ns, $p=0.39$) and IGF1-injected mice (paired $t=0.06$, ns, $p=0.95$) (Table 17). Femoral length was increased by 0.6% (paired $t=2.3$, ns, $p=0.07$) and 1.0% (paired $t=6.7$, $p<0.001$) on the heat-treated sides of saline and IGF1-injected mice respectively (Fig. 30B(a), Table 17). The increase in femoral length on heat-treated sides was comparable ($F(1,11)=2.0$, ns, $p=0.19$) between saline and IGF1-injected mice. Tibial length increased by 0.1% (paired $t=0.74$, ns, $p=0.49$) and 0.8% (paired $t=7.3$, $p<0.001$) on the heat-treated sides of saline and IGF1-injected mice respectively (Fig. 30B(b), Table 17). No significant differences in humeral ($p=0.89$) and femoral ($p=0.28$) lengths were determined between saline and IGF1-injected mice, but the increase in tibial length on heat-treated sides of IGF1-injected mice was greater than saline ($p<0.01$). Overall, results demonstrate that a degree of heat-enhanced bone length is maintained into skeletal maturity when limb heating is coupled with administration of IGF1 and particularly following 14 days of unilateral heat-treatment.

Table 17. Comparison of Non-Treated and Heat-Treated Sides of Experimental Mice Bone Parameters Following 14 days of Limb Heating.

Parameter	Injection	Non-Treated (30C)	Heat-Treated (40C)	Percent Increase	N
Humeral Length (mm)	Saline	11.73 (0.15)	11.74 (0.13) ^{ns}	0.1	6
	IGF1	11.90 (0.20)	11.90 (0.16) ^{ns}	0.0 ^{ns}	6
Femoral Length (mm)	Saline	15.30 (0.08)	15.39 (0.15) ^{ns}	0.6	6
	IGF1	15.41 (0.14)	15.56 (0.14) ^{***}	1.0 ^{ns}	6
Tibial Length (mm)	Saline	17.42 (0.17)	17.44 (0.18) ^{ns}	0.1	6
	IGF1	17.49 (0.33)	17.63 (0.32) ^{***}	0.8 [#]	6

Values are mean (standard deviation). Sample size (N) is number of left-right pairs. Significantly larger on heat-treated side by one-tailed paired t-test: *p< 0.05; **p<0.01; ***p<0.001; ns, non-significant. Significant differences in percent increase between saline controls and IGF1-injected mice by one-way ANOVA: #p<0.05; ns, non-significant.

6.4 DISCUSSION

In this study, differences in long bone length were examined in skeletally mature mice (12 weeks of age) to determine if the resulting heat-enhanced limb lengthening in young mice (3-4 and 3-5 weeks of age) reported in previous chapters is sustained until adulthood. IGF1 therapy has been shown to effectively increase skeletal growth and when administered in conjunction with 14 days of unilateral heating augments heat-enhanced limb elongation (Chapter 4). Therefore, this study examined the long-term impact of IGF1 administration in conjunction with limb heating.

As reported in Chapter 4, immediately following treatment end points, femoral lengths of saline mice treated for 7 days and 14 days were 1.7% and 1.1% longer on heat-treated sides respectively. Femoral length of IGF1-injected mice treated for 7 days and 14 days was 1.7% and 1.9% longer on heat-treated sides respectively. This study reports significant increases in femoral length of IGF1-injected mice after 7 days (1.0%) and 14 days (1.0%) of treatment, but less than significant increases in femoral length on heat-treated sides of saline mice after 7 days (0.5%) and 14 days (0.6%) of treatment (Fig. 30A(a), B(a); Tables 16, 17). Femoral length compared between sides of non-treated mice was equivalent. Data supported the hypothesis that differential limb length was maintained throughout skeletal development after treatments have ended, and more so when heating was coupled with IGF1 administration.

These results are not analogous to those reported by Serrat et al. (2015) in another study comparing persistent left-right increases in femoral length at skeletal maturity following 14 days of treatment. Serrat et al. (2015) reported a significant 1.0% increase in femoral length in non-injected 12-week-old mice treated for 14 days.

Discrepancy between studies may be explained by variations in methodology. It can be speculated whether or not an augmented limb length differential at skeletal maturity would have also been seen if that study were done in conjunction with IGF1 administration. It was also reported by Serrat et al. (2015) that femoral length was 1.3% longer on heat-treated sides of mice treated for 14 days. Importantly, both studies show that despite the significant increase in femoral length maintained into adulthood, length differential was not sustained by the same extent at skeletal maturity as immediately following treatment. The diminished differential in limb length at skeletal maturity may be explained by similar mechanisms to those regulating the phenomenon of “catch-up” growth. Typically, catch-up growth is explained as recovery in linear growth from growth-inhibiting conditions (Lui et al., 2011; Reich et al., 2008). During catch-up growth, growth plates increase activity. Further investigation would be needed to determine if the heat-enhanced linear growth accelerates the onset of growth plate senescence and the non-treated side thus partially “catches-up” to the heat-treated side.

Since the growth plate at skeletal maturity no longer contributes to longitudinal growth, tibial growth plates were not collected for growth rate and histological analysis as in previous studies described thus far. Therefore, the tibia served as an additional long bone for comparison of length. Tibial length was 0.5% and 0.1% on the heat-treated sides of saline control mice after 7 days and 14 days of heating respectively (Fig. 30A(b), B(b); Tables 16, 17). The IGF1-injected mice had an increase of 0.4% and 0.8% in tibial length on the heat-treated sides following 7 days and 14 days of heating respectively. Based on tibial length, the IGF1-injected mice maintained a more

substantial differential in length compared to saline controls, but only with 14 days of heating. Similar to what was observed in femoral length, the non-treated control left-right tibial length was nearly equivalent. One limitation in this study is the possible discrepancy in tibiae measurements from inconsistent disarticulation and cleaning of bones from mice after the 7-day heat-treatment. Multiple personnel were responsible for the process of obtaining clean tibiae for measurement and collecting whole tibiae for long bone measurements was not as practiced and concise as those done for femora and humeri. However, the same individual consistently collected all tibiae from the 14-day experiments.

6.5 CONCLUSION

In conclusion, heat-enhanced limb length is maintained throughout skeletal development after treatments have ended, and more so when heating was coupled with IGF1 administration. Since other studies have shown that heat-alone can maintain limb length differential, repeated studies are recommended to increase sample size and gain a better understanding of the potential of limb length differences to be maintained into adulthood. Nevertheless, in this study, IGF1 has a role in permanently sustaining heat-enhanced bone growth. Future studies will investigate if heat-treatment elicits permanent changes to the growth plate allowing for maintenance of the limb length differential, such as permanent increases in vascular supply. It is important to determine the full potential of unilateral heat-treatment in maintaining limb length differential in order to translate these methods to treatment in children with bone growth disorders

with the prospective of producing permanent changes to be upheld throughout adolescence.

CHAPTER VII: THERMAL IMAGING REVEALS TEMPERATURE RETENTION IN HINDLIMBS OF MICE AFTER TARGETED INTERMITTENT LIMB HEATING

7.1 INTRODUCTION

The relationship between the vascular system (blood and vessels) and the epiphyseal growth plate is a complicated one. While bone is a highly vascularized tissue, growth plate cartilage is avascular and requires indirect vascular routes to supply nutrients and hormones that are essential for longitudinal bone growth (Brodin, 1955; Maes, 2013; Trueta, 1968). Temperature regulates vasculature (Serrat, 2014b). Heat increases blood flow in the limbs (Barcroft & Edholm, 1943; Chiesa, Trangmar, & González-Alonso, 2016) and exposure to warm temperature has also been shown to increase transport into the growth plate (Serrat et al., 2009, 2010, 2014a). Therefore, it is plausible that the heat-enhanced linear bone growth is enabled by changes in vasculature.

Infrared thermal imaging is a technique that has been used to measure surface limb temperature in both clinical and veterinary applications (Inagaki, Ohno, Histome, Tanaka, & Takeshita, 1992; Jones, 1998; Soerensen & Pedersen, 2015; Turner, 2001) as well as in experimental settings (Dezechache, Wilke, Richi, Neumann, & Zuberbühler, 2017; McGreevy, Warren-Smith, Guisard, 2012; Tattersall & Milson, 2003; Tattersall, 2016). Tattersall and Milson (2003) captured infrared thermal images of golden-mantled ground squirrels to demonstrate a shift in blood flow to the periphery associated with cooling in hypoxic conditions. The advantage to using thermal imaging is methodology entails minimal stress to unanesthetized animals as a non-contact approach of acquiring skin temperature. Studies have shown that blood flow positively

correlates with skin temperature (Carter et al., 2014; Senay, Prokop, Cronau, & Hertzman, 1963; Song, Chelstrom, Levitt, Haumschild, 1989; Turner, 2001). Therefore, thermal imaging can be used to measure heat retention at the surface of the limb as an indicator of the extent of increased blood flow. If targeted limb heating results in an increase in blood flow as expected, it is **hypothesized that skin temperature of heat-treated limbs will remain elevated for an extended time following treatment.**

7.2 MATERIAL AND METHODS

7.2.1 Infrared Thermal Imaging

As an extensive pilot study (IACUC approved) to determine the period of time in which limb temperature remains elevated on the heat-treated side after each daily regimen, female C57BL/6 (N=12) mice were obtained (Fig. 31). Experimental mice were treated with daily unilateral heat (40°C) under the same procedural conditions as described in previous chapters. Mice were treated for 7 days from 3-4 weeks of age (N=6) and 14 days from 3-5 weeks of age (N=6). No injections were administered. Infrared thermal images were captured at 320 X 240 resolution using a FLIR E8 infrared camera (sensitivity <0.06C in temperature range of -20 to 250°C). Images were captured 1 hour prior to limb heating and then 1, 4 and 8 hours post-heating. Imaging times were chosen based on a pilot study conducted prior to experiments that determined the optimal imaging settings. During the 7-day and 14-day heating regimen, 5 separate days (over a total of 14 days of treatment) were chosen for imaging. Temperatures recorded over the 5 days (N=6 mice per day) were pooled at each time

point (N=5 recordings per time point) for a total of N=30 temperature recordings per time point.

When each mouse was removed from the cage for imaging, the sleeping position was noted (if possible) to account for any positioning impact on surface temperature. Imaging intervals were chosen to avoid excessive imaging that negatively impacted daily gain in body mass. Mice were positioned consistently on a 4 inch cylindrical piece of polyethylene foam mounted to a mouse cage lid on a customized imaging cart. The camera was placed in a tailor-made stand at a 67.5° angle. Surface temperatures of the heat-treated (right) and non-treated (left) hindlimbs were obtained from calibrated images using the FLIR tools 2.1 software. Mean surface temperature was averaged from three different points along the distal end of each limb approximately above the tibia.

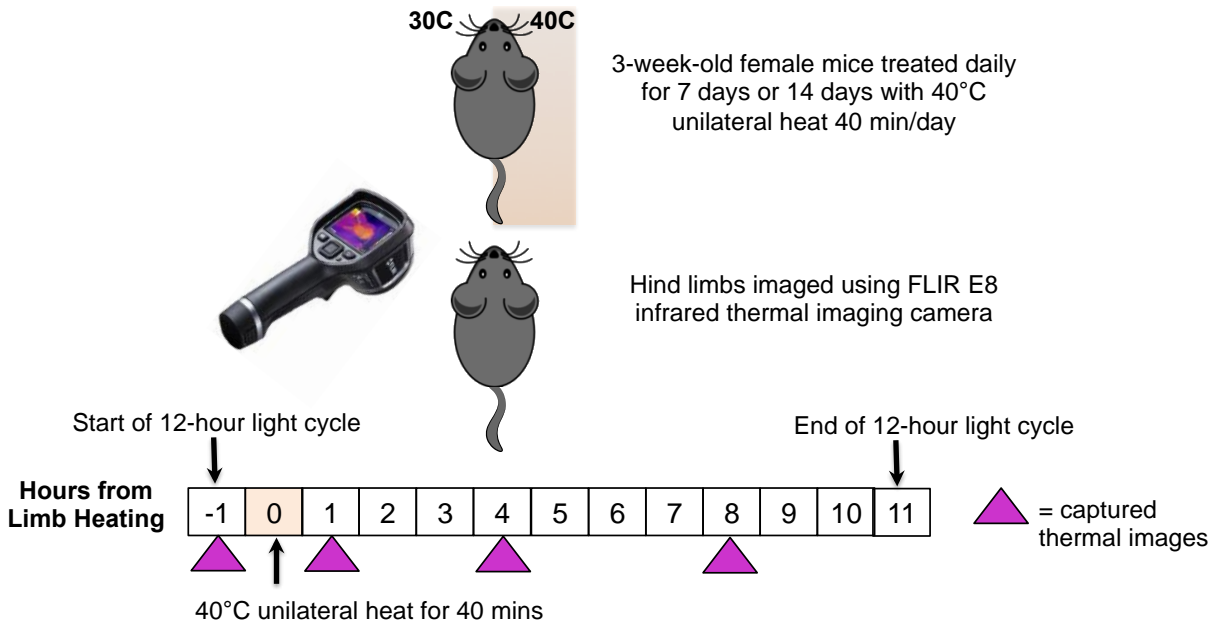


Figure 31. Infrared Thermal Imaging Schematic

Mice were treated with 40°C unilateral heat for 40 minutes daily for 7 days from 3-4 weeks of age or 14 days from 3-5 weeks of age. Thermal images of hind limbs were captured using a FLIR E8 infrared thermal imaging camera (2008 © FLIR® Systems, Inc) 1 hour prior to, and 1 hour, 4 hours, and 8 hours post-heating. Euthanasia and tissue collection occurred 1 day after the last day of heat-treatment. Mouse illustration based on “mouse clip art black and white” from clipartstockphotos.com.

7.2.2 Statistical Analysis and Sample Size

Statistical analyses were performed using SPSS 25.0 software (IBM Corporation, Armonk, NY) with $p < 0.05$ as accepted significance. Non-treated and heat-treated side comparisons for surface temperatures were done using one-tailed paired t-tests. The one-way ANOVA with a Tukey post hoc test was used to determine significant differences between multiple treatment days that infrared thermal images were captured throughout the duration of limb heating. Data were reported as mean \pm standard deviation (SD) in tabular format and as mean \pm standard error (SE) in graphical format. Sample sizes for measurements that are documented as less than the size of the experimental sample set were a result of failure to confidently obtain surface temperatures from thermal images such as when the limbs were properly positioned.

7.3 RESULTS

7.3.1 Temperature Retention in Hindlimbs Post-Heating

Hindlimb surface temperature of female mice (N=6) was assessed using infrared thermal imaging recorded over 5 days throughout the duration of limb heating. Data were pooled at each time point (1hr prior to heating, and 1hr, 4hrs and 8hrs post-heating) since no significant differences were observed between the multiple treatment days that infrared thermal images were captured ($F(1,29)=0.20$, ns, $p=0.94$). Surface limb temperature was $31.1 \pm 0.2^\circ\text{C}$ on the non-treated side (left) and $30.8 \pm 0.2^\circ\text{C}$ on the intended heat-treated side (right), 1hr prior to treatment (Fig. 32A). The 0.8% difference in temperature was not significant between contralateral sides (paired $t=1.6$, ns, $p=0.13$). Surface limb temperature was $30.3 \pm 0.9^\circ\text{C}$ and $30.4 \pm 0.9^\circ\text{C}$ on the non-treated

and heat-treated sides respectively, 1hr following treatment (Fig. 32A). The 0.4% difference in limb temperature was not significant between contralateral sides (paired $t=0.7$, ns, $p=0.51$). Surface limb temperature was $31.1\pm0.7^{\circ}\text{C}$ and $31.5\pm0.8^{\circ}\text{C}$ on the non-treated and heat-treated sides respectively, 4hrs following treatment (Fig. 32A, B). The 1.2% increase in limb temperature on the heat-treated side was significantly warmer than the non-treated side (paired $t=2.3$, $p<0.05$). Surface limb temperature was $31.1\pm0.9^{\circ}\text{C}$ and $30.9\pm0.7^{\circ}\text{C}$ on the non-treated and heat-treated sides respectively, 8hrs following treatment (Fig. 32A). The 0.4% difference in limb temperature was not significant between contralateral sides (paired $t=0.8$, ns, $p=0.40$). Therefore, limb temperature remained elevated on the heated side up to 4 hours after treatment.

If apparent at the onset of imaging, the sleeping position of the mouse was noted to compare if the hindlimb surface temperature reflected the huddled position of the mouse during sleep. Since mice have been shown to demonstrate a degree of handedness (Biddle, Coffaro, Ziehr, & Eales, 1993), if they also displayed sleep position preference (left versus right side sleeping) that may account for the measured limb temperature differentials. However, while some positions were not obvious, the positions that were observed did not relate to measured surface limb temperature of individual mice. Therefore, sleeping position seemed to be independent of hindlimb temperature.

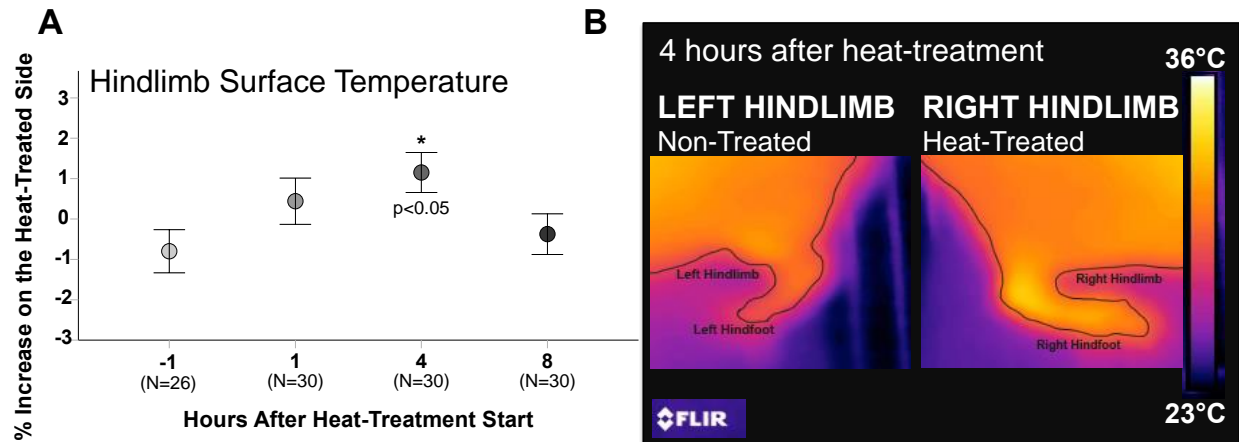


Figure 32. Thermal Imaging Shows Hindlimb Surface Temperature Remains Elevated up to 4 Hours Post-Heating

(A) Error bar plot shows the difference in limb temperature between non-treated and heat-treated limbs at each time point (N=30, N=6 left-right limb temperatures pooled over N=5 days of heating). The heat-treated side was -0.8%, 0.4%, 1.2% and -0.4% warmer than the contralateral non-treated sides. (B) Captured infrared thermal images 4 hours post-heating of non-treated (left) and heat-treated (right) hindlimbs. Image analyzed in FLIR tools using the iron color pallet to distinguish thermal profiles between 23°C and 36°C. Warmer temperatures as seen by the lighter color profile, are observed on the heat-treated side.

7.4 DISCUSSION

Warm temperature increases blood flow in limbs (Barcroft & Edholm, 1943; Chiesa et al., 2016) and measured skin temperature is positively correlated to blood flow (Carter et al., 2014; Senay et al., 1963; Song et al., 1989; Turner, 2001). Thermal imaging data revealed that temperature remained elevated (1.2% increase) on the heated side up to 4 hours post-heating. Therefore, data support the hypothesis that skin temperature of heat-treated limbs will remain elevated for an extended time following treatment. Results indicate that targeted limb heating caused an increase of blood flow in the limbs that is sustained up to 4 hrs after treatment ends. It is possible that this retention in limb temperature is due to a heat-enhanced increase in blood flow that facilitates bone lengthening.

Temperatures were nearly equivalent (0.4% difference) 1 hr following treatment suggesting a systemic post-anesthesia thermoregulatory response. By 8 hrs post-heating, limb temperatures were again similar (0.4% difference) reflecting increased activity as mice approached the dark cycle. Another possible explanation for these results are exemplified in a study by Song et al. (1989) measuring blood flow in heated human forearms (40°C for 60 mins). They found that blood flow momentarily declined before increasing for several minutes and then rapidly declining corresponding with changes in volume and speed of red blood cells (Song et al., 1989). Comparable, this study demonstrated a similar trend in changes in skin temperature but over a period of hours instead of minutes. This time differential may be due to whole limb warming versus only a localized portion of the limb, as well as a much smaller animal (mouse) compared to humans.

One important question at the start of this pilot study was whether or not heat retention was additive with consecutive days of heat-treatment. After collection of temperatures at various time points during different treatment days, no differences were seen in the mean hindlimb temperature at each time point. While hindlimb surface temperature remained elevated up to 4 hours after treatment, it was independent on the day of heating. Comparable temperatures recorded between the days of treatment indicated that temperature retention does not increase with additional days of heating, and heat-enhanced temperature effects occur within the first 4 hours post-heating.

Results in this study suggest heat-enhanced linear growth is enabled by changes in vasculature since blood flow positively correlates with skin temperature (Carter et al., 2014; Senay et al., 1963; Song et al., 1989; Turner, 2001). However, the means by which heat-induced changes in vasculature occur remain unknown. In addition to the transport and delivery of essential nutrients and hormones, the vascular system also has a role in the delivery of heat (Scholander, 1955; Serrat et al., 2008; Serrat, 2014b). Therefore, vasculature has the potential to facilitate limb growth through the delivery of warm blood to the growth plate and modulate temperature-sensitive genes and pathways.

During endochondral ossification, hypertrophic chondrocytes secrete angiogenic factors that initiate vascular invasion and recruitment of bone absorbing and forming cells that replace mineralized cartilage with bone (van der Eerden et al., 2003; Filipowska et al., 2017; Gerber et al., 1999b; Horner et al., 1999; Hunziker, 1994b; Maes et al., 2004; Zelzer & Olsen, 2005). The key regulator involved in this process of endochondral ossification is vascular endothelial growth factor (VEGF) (Emons et al., 2010; Gerber et al., 1999b). Other factors expressed in the growth plate, such as IGF1

(Ahmed & Farquharson, 2010; Álvarez-García et al., 2010), have also been shown to stimulate VEGF and induce vascular invasion.

One method for assessing heat-induced changes in vasculature at the site of the growth plate is to study expression of angiogenic factors (VEGF and CD31) in hypertrophic chondrocytes with heat-treatment. A preliminary study collected (non-quantitated) images of the proximal tibial growth plate from mice treated for 7 days from 3-4 weeks of age dual stained with fluorescent antibodies against VEGF (magenta) and CD31 (yellow) (Fig. 31). Expression of angiogenic markers (CD31 and VEGF) appeared to increase in the hypertrophic zone on heat-treated sides. However, a method for standardizing and quantifying these images is necessary to determine significance.

Another methodology for studying vascular changes at the growth plate is by multiphoton microscopy (MPM). MPM is a novel method of *in vivo* live animal imaging (Zipfel et al., 2003) and can be used to fluorescently label and track transport of small molecules into the growth plate (Serrat & Ion, 2017). Serrat et al. (2009, 2010, 2014a) have already shown that temperature increases solute uptake into the growth plate. By fluorescently labeling specific regulators or linear growth (such as IGF1 and VEGF), this method could be used in future studies to determine if targeted limb heating increases vascular transport of these molecules to the growth plate to promote heat-enhanced limb elongation. Although vasculature stands out as a key player in facilitating the heat-enhanced limb growth response, it is also possible that heat may modulate temperature-sensitive genes and pathways through more direct mechanisms as an alternate to, or in addition to, vascular transport.

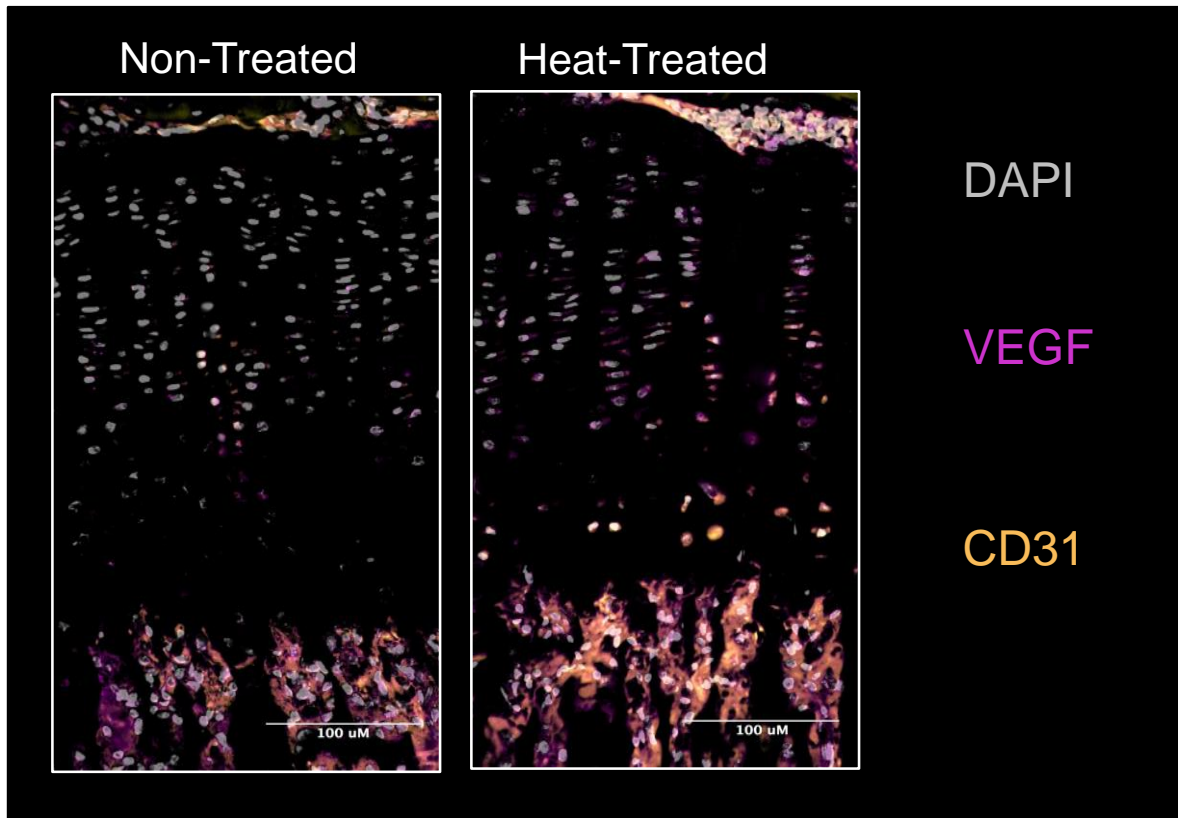


Figure 33. Expression of VEGF and CD31 Appeared to Increase in the Growth Plate on the Heat-Treated Sides

Left-right comparison of proximal tibial growth plate from mice treated for 7 days from 3-4 weeks of age. A greater trend in positive immunofluorescent staining for VEGF (magenta) and CD31 (yellow) was observed on the heat-treated sides. Sections were stained using immunohistochemistry methods and primary antibodies were detected by double immunofluorescence (IF). Mouse monoclonal antibody against VEGF (1:50, ThermoFisher Scientific, MA1-16629) and rabbit polyclonal antibody against CD31 (1:50, abcam, ab28364) were detected by the VectaFluor Duet double labeling kit (Vector Laboratories, DK-8818) using Dylight® 488 anti-rabbit IgG and Dylight® 594 anti-mouse IgG. Since using a mouse primary antibody on mouse tissue, the Vector M.O.M. kit (Vector Laboratories, MP-2400) was used to eliminate high background staining. Imaged using the Leica DM2500 optical microscope and filters blue (DAPI), green (CD31) and red (VEGF) to detect fluorescence. Exposure was adjusted uniformly for both CD31 and VEGF, but DAPI was taken at a lower exposure (a great deal brighter in comparison). The same section of sample was taken at 20X for each filter for consistency when images were merged in ImageJ.

7.5 CONCLUSION

While results from this extensive preliminary study support our hypothesis that skin temperature of heat-treated limbs will remain elevated for an extended time following treatment, future studies are necessary to further validate the connection between increased blood flow and linear growth. These studies will be important for determining if the duration of elevated skin temperature is associated with an increased blood supply to the growth plate. The results from this chapter preface future studies into possible mechanisms of the targeted heating-model, as it suggests a heat-induced increase in blood flow that accelerates bone lengthening.

CHAPTER VIII: CONCLUDING REMARKS AND FUTURE DIRECTIONS

Bone elongation disorders, whether congenital or acquired in origin, can lead to painful musculoskeletal disabilities in adulthood (Gurney, 2002). Intervention is recommended for children during critical stages of postnatal longitudinal bone growth. Existing treatment options to correct left-right asymmetry in limb length involve invasive surgery and/or drug regimens, which are often only partially effective (Gurney, 2002; Hasler & Krieg, 2012; Niedzielski et al., 2016; Pendleton et al., 2013; Sabharwal et al., 2015; Stevens, 2016). Therefore, it is important to find alternative, less invasive treatment options for bone lengthening. Previous studies in weanling mice demonstrated that after 14 days of targeted limb heating (40°C) on one side of the body, femoral length (1.3%) and tibial elongation rate (>12%) increased on heat-treated sides (Serrat et al., 2015). The goal of this dissertation was to build upon an established method using targeted limb heating as a potential non-invasive alternative to enhance bone lengthening.

The epiphyseal growth plate is the main site of longitudinal growth and the main regulator of local cartilage growth is IGF1. Therefore, investigation focused on the effects of temperature on chondrocyte morphology and IGF1 action in the growth plate. It was **hypothesized that exposure to warm temperature augments the actions of IGF1 in the growth plate and permanently increases length of the extremities.** The central aims of the study were 1) determine if IGF1 enhances bone elongation in heat-treated extremities and 2) determine potential vasculature modifications and long-term extent of left-right limb length asymmetries resulting from unilateral heat-treatment.

The application of the model for targeted limb heating (unilateral heating model) and its functional impact is described in Chapter 2. X-ray and weight bearing data indicated that even small discrepancies in limb length (nearly 1%) have a functional impact on hindlimb weight distribution (nearly 20%) in young mice. These findings set the foundation for following experiments using the unilateral heating model as a means to test the overall hypothesis. The impact of heat-treatment on the cellular level of the growth plate had previously been unexplored. Others have determined that the main contributing factors to longitudinal growth include the rate of chondrocyte proliferation and hypertrophy (Cooper et al., 2013; Farnum, 2007, Hunziker et al., 1987; Hunziker & Schenk, 1989; Hunziker, 1994b; Kember, 1993; Rolian, 2008; Walker & Kember, 1972; Wilsman et al., 1996a,b, 2008). It was expected that targeted limb heating would be accompanied by an increase in bone elongation, chondrocyte proliferation (assessed by PNCA expression in proliferative zone), hypertrophic zone height, and expression of IGF1 signaling (IGF1R, pIGF1R, pAkt) in growth plate chondrocytes. Mice treated for 7 days from 3-4 weeks of age (determined in Chapter 2 and 3 to be an efficient age range for heat-induced bone elongation), femoral length (1.7%), tibial elongation rate (7.7%), hypertrophic zone height (8.6%) and chondrocyte proliferation (8.6%) increased on heat-treated sides of saline-injected controls (Chapter 3). There was also an increase in IGF1R (14.5%) and pIGF1R (7.7%) expression in the proliferative zone demonstrating heat-enhanced IGF1 activity in the growth plate (Chapter 5). Left-right limb length asymmetry, along with enhanced growth plate kinetics was also observed in mice administered a low dose of IGF1 (2.5 mg/kg, once daily) in conjunction with targeted limb heating. However, advanced bone elongation compared to heat alone (saline-

injected controls) was only observed when IGF1 was administered with 14 days of heat-treatment (Chapter 4).

There was no heat-induced increase in the parameters assessing linear bone growth when IGF1 activity was blocked in JB1 injected mice and levels were low in *GHR*^{-/-} mice (Chapter 5). The overall gain in mass, one physiological outcome subjective to changes in IGF1, did not differ between groups suggesting targeted limb heating affects local regulation of IGF1 in growth plate chondrocytes. Future studies may re-examine the potential differences between male and female mice that may be observed with heat-enhanced IGF1 activity in the growth plate. While previous studies showed no differences in heat-enhanced bone elongation between sexes (Serrat et al., 2015) these mice were not administered IGF1.

In the preliminary investigation of heat-induced changes in vascular supply, skin temperature was measured by infrared thermal imaging. Limb surface temperatures were recorded prior to, and at various times following, unilateral heat-treatment. It was concluded that limb surface temperature remained elevated (1.2%) on the heat-treated sides up to 4 hrs post treatment (Chapter 7) but this heat-retention was not accumulative after consecutive days of heating. These results suggest that the retention in skin temperature may be due to an increase in blood flow that normalizes after 4 hours of heat-treatment. To verify if there is a true correlation between the observed retention in limb temperature and increased blood flow, experiments to quantify blood flow (such as the Doppler method) would need to be conducted in conjunction with thermal imaging. *In vivo* multiphoton microscopy would also be useful to quantify if

increased blood flow correlates to increased delivery of growth enhancing molecules to the growth plate.

An additional study to determine heat-enhanced changes to vascular supply observed angiogenic factors (VEGF and CD31) in hypertrophic chondrocytes by immunohistochemistry (IHC) analysis. Images seem to indicate an increase in VEGF and CD31 expression in hypertrophic chondrocytes signifying a heat-induced increase in angiogenesis in the growth plate (Chapter 7). Future studies will be necessary to quantify expression levels and to determine if increased expression of angiogenic markers is a result of heat-induced increases in transport of signaling molecules, or a result of temperature-sensitive genes and pathways (either directly or by indirect delivery of warm-blood through the vasculature).

Long-term effects of heat-treatment were also assessed by the heat-induced left-right asymmetries in limb length sustained at skeletal maturity (12 weeks of age) (Chapter 6). Femoral length was increased on heat-treated sides of saline (0.5%) and IGF1-injected (1.0%) after 7 days of unilateral heat-treatment. Heat-treated femora were also increased in saline (0.6%) and IGF-injected (1.0%) mice after 14 days of heating. While femoral length differential was observed at skeletal maturity at both durations of treatment, these differences were only statistically significant in mice administered IGF1 during heat-treatment. Tibial length increase on heat-treated sides (0.8%) was also maintained in IGF1-injected mice at the 12 week of age endpoint, but only following 14 days of treatment. Further studies will need to be done to understand how IGF1 administration in conjunction with heating elicits a more permanent limb lengthening effect compared to saline control mice. Next steps of this study will also be to collect x-

ray images and weight bearing data (as described in Chapter 2) at skeletal maturity to provide translation relevance.

The purpose of this study was to build upon the established method using targeted limb heating. The findings reviewed in the chapters of this dissertation have achieved this by determining that heat-enhanced growth is dependent on IGF1 and its local regulation of growing cartilage, which may involve changes to vasculature supply. While aware that other factors play a role in regulating longitudinal bone growth, IGF1 was the focus of these studies since it has been shown to be essential for normal linear growth. Throughout this dissertation the role of IGF1, GH and VEGF have been described in detail to regulate longitudinal bone growth in the growth plate (Fig. 34). Both endocrine (GH and IGF1) and autocrine/paracrine (IGF1 and VEGF) actions of these factors have shown to be important in regulating linear growth. However future studies will be needed to determine how heat-treatment affects GH and VEGF, as well as other factors that regulate chondrocytes of the growth plate, including the Ihh/PThrP feedback loop (not demonstrated in Fig. 34).

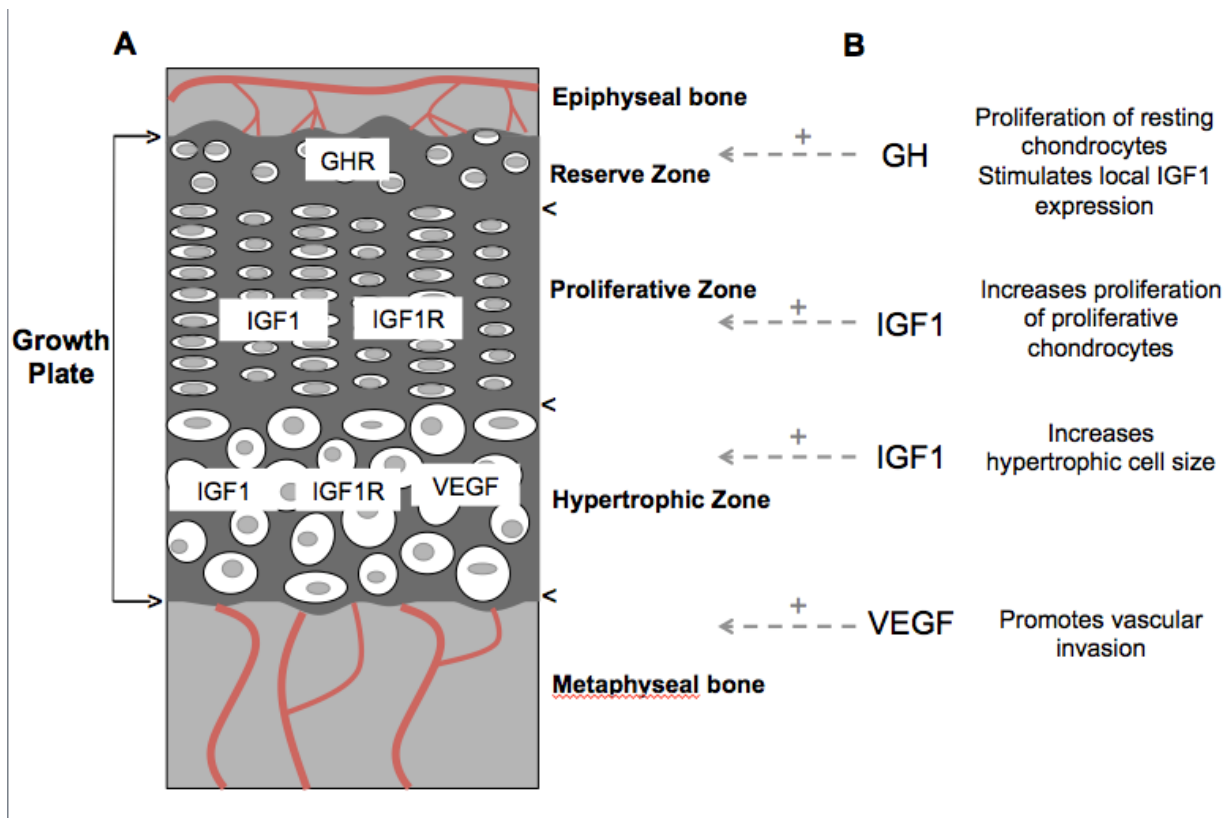


Figure 34. Diagram Summarizes the Action of Important Factors in the Different Zones of the Growth Plate

(A) Demonstrates regions of the growth plate in which growth hormone receptor (GHR), insulin-like growth factor 1 receptor (IGF1R), IGF1 and VEGF are expressed. (B) Indicates the effects of GH, IGF1 and VEGF on growth plate chondrocytes. Illustration focuses on main factors discussed in this dissertation and excludes other endocrine and autocrine/paracrine factors that also regulate the growth plate. Illustration based on Mackie et al. (2008).

Filling gaps in these studies mentioned above would be beneficial for expanding upon the unilateral limb-heating model in the mouse. However, further studies using a larger animal model will be fundamental to advancing toward the ultimate goal of translating these methods clinically to humans in the hopes to develop an alternative, non-invasive treatment to enhance linear growth in children with bone lengthening disorders. The next step would be to use the targeted limb heating approach using larger animal models to work towards answering questions such as: how does 40°C heat-treatment translate into a larger animal? Is 40-minutes long enough to warm the entire limb and elicit lengthening effects (considering the threshold of heat-tolerance in larger animals)? What is the optimal period of postnatal growth in larger animals for heat-treatment (such as the comparable toddler to elementary school age in humans)? What device can be used to administer localized heat (such as a heating cuff)? This device would help control for uniform heating as an alternative to warming the entire side of the body done in mice. Continuing these studies using the targeted heating model may lead to new approaches to increase bone lengthening in children with linear growth disorders that would otherwise cause painful, chronic musculoskeletal conditions in adulthood. Summaries of the concluding remarks (Table 18) and future directions (Table 19), for this dissertation are found on the following pages.

Table 18. Summary of Concluding Remarks.

Concluding Remarks
<ul style="list-style-type: none">• Current treatment options for bone elongation disorders involve invasive surgery and/or drug regimens that are often only partially effective and can lead to painful musculoskeletal disabilities in adulthood• Targeted limb heating is a potential non-invasive alternative to enhance bone lengthening and shows that even small discrepancies in limb length (nearly 1%) have a functional impact on hindlimb weight distribution (nearly 20%) in mice• Heat-enhanced limb elongation is accompanied by increased chondrocyte proliferation, increased hypertrophic zone height, and increased IGF1 activity (increased pIGF1R expression) in the proliferative zone of proximal tibiae growth plates• Administration of low-dose IGF1 (2.5 mg/kg) in conjunction with targeted limb heating further enhances bone elongation and is maintained throughout skeletal development• With diminished IGF1 activity, heat-enhanced limb length is attenuated• Skin temperature of heat-treated limbs remains elevated up to 4 hours following treatment suggesting an increase in blood flow• <u>Exposure to warm temperature augments the actions of IGF1 in the growth plate and permanently increases length of extremities of young mice</u>

Table 19. Summary of Future Directions.

Future Directions
<ul style="list-style-type: none">• Study other factors that may be involved with heat-enhanced bone elongation (such as Growth Hormone or Ihh/PTHrP)• Determine how IGF1 activity increases with heat-treatment in the growth plate, including potential heat-enhanced changes to vascular supply• Measure weight bearing in skeletally mature mice following targeted limb heating to determine the long-term functional impact of treatment• Determine if there is a difference in the heat-enhanced IGF1 activity if male mice were used in the study• Repeat studies using a larger animal model for uniform heating of limbs versus entire side of body and closer to translating methods to humans

REFERENCES

Abad, V., Meyers, J.L., Weise, M., Gafni, R.I., Barnes, K.M., Nilsson, O., et al. (2002). The role of the resting zone in growth plate chondrogenesis. *Endocrinology*, *143*(5), 1851-1857. doi: 10.1210/endo.143.5.8776

Abbaspour, A., Takata, S., Matsui, Y., Katoh, S., Takahashi, M., & Yasui, N. (2008). Continuous infusion of insulin-like growth factor-I into the epiphysis of the tibia. *International Orthopaedics*, *32*(3), 395-402. doi: 10.1007/s00264-007-0336-7

Ahmed, S.F., & Farquharson, C. (2010). The effect of GH and IGF1 on linear growth and skeletal development and their modulation by SOCS proteins. *Journal of Endocrinology*, *206*(3), 249-59. doi: 10.1677/JOE-10-0045

Aiona, M., Do, K.P., Emara, K., Dorociak, R., & Pierce, R. (2015). Gait patterns in children with limb length discrepancy. *Journal of Pediatric Orthopaedics*, *35*(3), 280-284. doi: 10.1097/BPO.0000000000000262

Al-Hilli, F., & Wright, E.A. (1983). The effects of changes in the environmental temperature on the growth of tail bones in the mouse. *British Journal of Experimental Pathology*, *64*(1), 34-42.

Allen, J.A. (1877). The influence of physical conditions in the genesis of species. *Radical Review*, *1*, 108-140.

Álvarez-García, Ó., García-López, E., Loredó, V., Gil-Peña, H., Rodríguez-Suárez, J., Ordóñez, F.Á., et al. (2010). Rapamycin induces growth retardation by disrupting angiogenesis in the growth plate. *Kidney International*, *78*(6), 561-568. doi: 10.1038/ki.2010.173

Al-Zghoul, M.B., Al-Natour, M.Q., Dalab, A.S., Alturki, O.I., Althnaian, T., Al-ramadan S.Y., et al. (2016). Thermal manipulation mid-term broiler chicken embryogenesis: effect on muscle growth factors and muscle marker genes. *Revista Brasileira de Ciência Avícola*, *18*(4), 607-618. doi: 10.1590/1806-9061-2016-0260

Amsel, S. (2018). Tibia and fibula (calf) bony features coloring page [Online image]. Retrieved from <http://www.exploringnature.org/db/view/Tibia-and-Fibula-Calf-Bony-Features-Coloring-Page>

Anderson, M., Green, W.T., & Messner, M.B. (1963). Growth and predictions of growth in the lower extremities. *The Journal of Bone & Joint Surgery*, *45-A*, 1-14.

Armstrong, T. (2007). *The human odyssey: Navigating the twelve stages of life*. Sterling Publishing Company.

- Azcona, C., Preece, M.A., Rose, S.J., Fraser, N., Rappaport, R., Ranke, M.B., et al. (1999). Growth response to rhIGF-1 80 microg/kg twice daily in children with growth hormone insensitivity syndrome: relationship to severity of clinical phenotype. *Clinical Endocrinology (Oxford)*, 51(6), 787-792. doi: 10.1046/j.1365-2265.1999.00887.x
- Azizan, N.A., Basaruddin, K.S., Salleh, A.F., Sulaiman, A.R., Safar, M.J.A., & Rusli, W.M.R. (2018). Leg length discrepancy: dynamic balance response during gait. *Journal of Healthcare Engineering*, 2018, 7815451. doi: 10.1155/2018/7815451
- Backeljauw, P.F., Kuntze, J., Frane, J., Calikoglu, A.S., & Chernausek, S.D. (2013). Adult and near-adult height in patients with severe insulin-like growth factor-1 deficiency after long-term therapy with recombinant human insulin-like growth factor-1. *Hormone Research Paediatrics*, 80(1), 47-56. doi: 10.1159/000351958
- Bahney, C.S., Hu, D.P., Taylor, A.J., Ferro, F., Britz, H.M., Hallgrímsson, B., et al. (2014). Stem cell-derived endochondral cartilage stimulates bone healing by tissue transformation. *Journal of Bone and Mineral Research*, 29(5), 1269-1282. doi: 10.1002/jbmr.2148
- Baker, J., Liu, J.P., Robertson, E.J., & Efstratiadis, A. (1993). Role of insulin-like growth factors in embryonic and postnatal growth. *Cell*, 75, 73-82.
- Barcroft, H., & Edholm, O.G. (1943). The effect of temperature on blood flow and deep temperature in the human forearm. *Journal of Physiology*, 102, 5-20.
- Baron, J., Klein, K.O., Yanovski, J.A., Novosad, J.A., Bacher, J.D., Bolander, M.E., et al. (1994). Induction of growth plate cartilage ossification by basic fibroblast growth factor. *Endocrinology*, 135(6), 2790-2793.
- Barone, A., & Rubin, J.B. (2013). Opportunities and challenges for successful use of bevacizumab in pediatrics. *Frontiers in Oncology*, 3, 92. doi: 10.3389/fonc.2013.00092
- Bassett, J.H., Williams, A.J., Murphy, E., Boyde, A., Howell, P.G.T, Swinhow, R., et al. (2008). A lack of thyroid hormones rather than excess thyrotropin causes abnormal skeletal development in hypothyroidism. *Molecular Endocrinology*, 22(2), 501-512. doi: 10.1210/me.2007-0221
- Bassett, J.H.D., & Williams, G.R. (2016). Role of thyroid hormone in skeletal development and bone maintenance. *Endocrine Reviews*, 37(2), 135-187. doi: 10.1210/er.2015-1106
- Baxter, R.C. (2000). Insulin-like growth factor (IGF)-binding proteins: interactions with IGFs and intrinsic bioactivities. *American Journal of Physiology-Endocrinology and Metabolism*, 278(6), E967-976. doi: 10.1152/ajpendo.2000.278.6.E967

Begemann, M., Zirn, B., Santen, G., Wirthegen, E., Soellner, L., Büttel, H.M., et al. (2015). Paternally inherited IGF2 mutation and growth restriction. *New England Journal of Medicine*, 373, 349-356. doi: 10.1056/NEJMoa1415227

Bello, C.E., & Garrett, S.D. (1999). Therapeutic issues in oral glucocorticoid use. *Lippincott's Primary Care Practice*, 3, 333-341.

Biddle, F.G., Coffaro, C.M., Ziehr, J.E., & Eales, B.A. (1993). Genetic variation in paw preference (handedness) in the mouse. *Genome*, 36, 935-943. doi: 10.1139/g93-123

Bikle, D., Majumdar, S., Laib, A., Powell-Braxton, L., Rosen, C., Beamer, W., et al. (2001). The skeletal structure of insulin-like growth factor I-deficient mice. *Journal of Bone and Mineral Research*, 16(12), 2320-2329. doi: 10.1359/jbmr.2001.16.12.2320

Bisgard, J.D., & Bisgard, M.E. (1935). Longitudinal growth of long bones. *Archives of Surgery*, 31, 568-578. doi: 10.1001/archsurg.1935.01180160064005

Blutke, A., Schneider, M.R., Renner-Müller, I., Herbach, N., Wanke, R., & Wolf, E. (2014). Genetic dissection of IGF1-dependent and -independent effects of permanent GH excess on postnatal growth and organ pathology of mice. *Molecular and Cellular Endocrinology*, 394(1-2), 88-98. doi: 10.1016/j.mce.2014.07.002

Body weight information for C57BL/6J (000664). (2018). Retrieved from The Jackson Laboratory website, <https://www.jax.org/jax-mice-and-services/strain-data-sheet-pages/body-weight-chart-000664>

Bonnet, C.T., Cherraf, S., Szaffarczyk, S., & Rougier, P.R. (2014). The contribution of body weight distribution and center of pressure location in the control of mediolateral stance. *Journal of Biomechanics*, 47(7), 1603-1608. doi: 10.1016/j.jbiomech.2014.03.005

Börjesson, A.E., Lagerquist, M.K., Liu, C., Shao, R., Windahl, S.H., Karisson, C., et al. (2010). The role of estrogen receptor α in growth plate cartilage for longitudinal bone growth. *Journal of Bone and Mineral Research*, 25(12), 2690-2700. doi: 10.1002/jbmr.156

Brennan-Speranza, T.C., Rizzoli, R., Kream, B.E., Rosen, C., & Ammann, P. (2011). Selective osteoblast overexpression of IGF-1 in mice prevents low protein-induced deterioration of bone strength and material level properties. *Bone*, 49, 1073-1079. Doi: 10.1016/j.bone.2011.07.039

Brighton, C.T. (1978). Structure and function of the growth plate. *Clinical Orthopaedics and Related Research*, (136), 22-32. doi: 10.1097/00003086-197810000-00003

- Brock, R.S., Gebrekristos, B.H., Kuniyoshi, K.M., Modanlou, H.D., Falcao, M.C., & Beharry, K.D. (2011). Biomolecular effects of Jb1 (an IGF-1 peptide analog) in a rat model of oxygen-induced retinopathy. *Pediatric Research*, 69(2), 135-141. doi: 10.1203/PDR.0b013e318204e6fa
- Brodin, H. (1955). Longitudinal bone growth and nutrition of the epiphyseal cartilages and the local blood supply: an experimental study in the rabbit. *Acta Orthopaedica Scandinavica*, 26(Suppl 20), 3-92. doi: 10.3109/ort.1955.26.suppl-20.01
- Brookes, M., & Revell, W.J. (1998). Growth Cartilages. In *Supply of Bone: Scientific Aspects* (pp. 152-176). Springer, London.
- Caine, D., DiFiori, J., & Maffaulli, N. (2006). Physeal injuries in children's and youth sports: reasons for concern. *British Journal of Sports Medicine*, 40(9), 749-760. doi: 10.1136/bjism.2005.017822
- Callewaert, F., Venken, K., Kopchick, J.J., Tocasio, A., van Lenthe, G.H., Boonen, S., et al. (2010). Sexual dimorphism in cortical bone size and strength but no density is determined by independent and time-specific actions of sex steroid and IGF-1; evidence from pubertal mouse models. *Journal of Bone and Mineral Research*, 25(3), 617-626. doi: 10.1359/jbmr.090828
- Campbell, T.M., Ghaedi, B.B., Ghongomu, T., & Welch, V. (2018). Shoe lifts for leg length discrepancy in adults with common painful musculoskeletal conditions: a systematic review of the literature. *Archives of Physical Medicine and Rehabilitation*, 99(5), 981-993.e2. doi: 10.1016/j.apmr.2017.10.027
- Carmeliet, P., Ferreira, V., Breier, G., Pollefeyt, S., Kieckens, L., Gertsenstein, M., et al. (1996). Abnormal blood vessel development and lethality in embryos lacking a single VEGF allele. *Nature*, 380(6573), 435-439. doi: 10.1038/380435a0
- Carter, H.H., Spence, A.L., Atkinson, C.L., Pugh, C.J., Cable, N.T., Thijssen, D.H., et al. (2014). Distinct effects of blood flow and temperature on cutaneous microvascular adaption. *Medicine and Science in Sports and Exercise*, 46(11), 2113-2121. doi: 10.1249/MSS.0000000000000349
- Chernausek, S.D., Backeljauw, P.F., Frane, J., Kuntze, J., Underwood, L.E., & GH Insensitivity Syndrome Collaborative Group. (2007). Long-term treatment with recombinant insulin-like growth factor (IGF)-I in children with severe IGF-1 deficiency due to growth hormone insensitivity. *The Journal of Clinical Endocrinology & Metabolism*, 92(3), 902-910. doi: 10.1210/jc.2006-1610
- Chiesa, S.T., Trangmar, S.J., & González-Alonso, J. (2016). Temperature and blood flow distribution in the human leg during passive heat stress. *Journal of Applied Physiology*, 120(9), 1047-1058. doi: 10.1152/jappphysiol.00965.2015

Chirwa, E.D., Griffiths, P.L., Maleta, S.A., & Cameron, N. (2014). Multi-level modeling of longitudinal child growth data from Birth-to-Twenty Cohort: a comparison of growth models. *Annals of Human Biology*, 41(2):168-179. doi: 10.3109/03014460.2013.839742

Choukair, D., Hügel, U., Sander, A., Uhlmann, L., & Tönshoff, B. (2014). Inhibition of IGF-1-related intracellular signaling pathways by proinflammatory cytokines in growth plate chondrocytes. *Pediatric Research*, 76(3), 245-251. doi: 10.1038/pr.2014.84

Chow, J.C., Condorelli, G., & Smith, R.J. (1998). Insulin-like growth factor-I receptor internalization regulates signaling via the Shc/Mitogen-activated protein kinase pathway, but not the insulin receptor substrate-1 pathway. *Journal of Biological Chemistry*, 273(8), 4672-4680. doi: 10.1074/jbc.273.8.4672

Chung, F., & Mokhlesi, B. (2014). Postoperative complications associated with obstructive sleep apnea: time to wake up. *Anesthesia & Analgesia*, 118(2), 251-253. doi: 10.1213/ANE.0000000000000067

Ciarmatori, S., Kiepe, D., Haarmann, A., Huegel, U., & Tönshoff, B. (2007). Signaling mechanisms leading to regulation of proliferation and differentiation of the mesenchymal chondrogenic cell line RCJ3.1C5.18 in response to IGF-1. *Journal of Molecular Endocrinology*, 38(4), 493-508. doi: 10.1677/jme.1.02179

Clemmons, D.R. (2004). Role of insulin-like growth factor in maintaining normal glucose homeostasis. *Hormone Research in Paediatrics*, 62(1), 77-82. doi: 10.1159/000080763

Cohen, J., Blethen, S., Kuntze, J., Smith, S.L., Lomax, K.G., & Mathew, P.M. (2014). Managing the child with severe primary Insulin-like growth factor-1 deficiency (IGFD): IGFD diagnosis and management. *Drugs in R&D*, 14(1), 25-29. doi: 10.1007/s40268-014-0039-7

Cooper, K.L., Oh, S., Sung, Y., Dasari, R.R., Kirschner, M.W., & Tabin, C.J. (2013). Multiple phases of chondrocyte enlargement underlie differences in skeletal proportions. *Nature*, 495(7441), 375-378. doi: 10.1038/nature11940

Crudden, C., Girnita, A., & Girnita, L. (2015). Targeting the IGF-1R: the tale of the tortoise and the hare. *Frontiers in Endocrinology*, 6, 64. doi: 10.3389/fendo.2015.00064

D'Ercole, A.J. (1993). Expression of insulin-like growth factor I in transgenic mice. *Annals of the New York Academy of Sciences*, 692(1), 149-160. doi: 10.1111/j.1749-6632.1993.tb26213.x

Daughaday, W.H., Hall, K., Raben, M.S., Salmon, W.D., Van den Brande, J.L., & Van Wyk, J.J. (1972). Somatomedin: proposed designation for sulphation factor. *Nature*, 235(5333), 107. doi: 10.1038/235107a0

- Daughaday, W.H., Parker, K.A., Borowsky, S., Trivedi, B., & Kapadia, M. (1982). Measurement of somatomedin-related peptides in fetal, neonatal, and maternal rat serum by insulin-like growth factor (IGF) I radioimmunoassay, IGF-II radioreceptor assay (RRA), and multiplication-stimulating activity RRA after acid-ethanol extraction. *Endocrinology*, *110*(2), 575-581. doi: 10.1210/endo-110-2-575
- Davies, J.S., Gevers, E.F., Stevenson, A.E., Coschigano, K.T., El-Kasti, M.M., Bull, M.J., et al. (2007). Adiposity profile in the dwarf rat: an unusually lean model of profound growth hormone deficiency. *American Journal Physiology-Endocrinology and Metabolism*, *292*(5), E1483-E1494. doi: 10.1152/ajpendo.00417.2006
- Dawson, A.B. (1925). The age order of epiphyseal union in the long bones of the albino rat. *The Anatomical Record*, *31*(1), 1-17. doi: 10.1002/ar.1090310102
- Dawson, A.B. (1935). The influence of hereditary dwarfism on the differential skeleton of the mouse. *The Anatomical Record*, *61*(4), 485-493. doi: 10.1002/ar.1090610410
- DeChiara, T.M., Efstratiadis, A., & Robertson, E.J. (1990). A growth-deficiency phenotype in heterozygous mice carrying an insulin-like growth factor II gene disrupted by targeting. *Nature*, *345*(6270), 78-80. doi: 10.1038/345078a0
- Defrin, R., Ben Benyamin, S., Aldubi, R.D., & Pick, C.G. (2005). Conservative correction of leg-length discrepancies of 10mm or less for the relief of chronic low back pain. *Archives of Physical Medicine and Rehabilitation*, *86*(11), 2075-2080. doi: 10.1016/j.apmr.2005.06.012
- Dezechache, G., Wilke, C., Richi, N., Neumann, C., & Zuberbühler, K. (2017). Skin temperature and reproductive condition in wild female chimpanzees. *PeerJ*, *5*, e4116. doi: 10.7717/peerj.4116
- Digby, K.H. (1916). The measurement of the diaphyseal growth in proximal and distal directions. *Journal of Anatomy and Physiology*, *50*(Pt 2), 187-188.
- Ding, J., List, E.O., Bower, B.D., & Kopchick, J.J. (2011). Differential effects of growth hormone versus insulin-like growth factor-I on the mouse plasma proteome. *Endocrinology*, *152*(10), 3791-3801. doi: 10.1210/en.2011-1217
- Dobie, R., Ahmed, S.F., Staines, K.A., Pass, C., Jasim, S., Macrae, V.E., et al. (2015). Increased linear bone growth by GH in the absence of SOCS2 is independent of IGF-1. *Journal of Cellular Physiology*, *230*(11), 2796-2806. doi: 10.1002/jcp.25006
- Duren, D.L., Seselj, M., Froehle, A.W., Nahhas, R.W., & Sherwood, R.J. (2013). Skeletal growth and the changing genetic landscape during childhood and adulthood. *American Journal of Physical Anthropology*, *150*(1), 48-57. doi: 10.1002/ajpa.22183

Dutta, S., & Sengupta, P. (2016). Men and mice: relating their ages. *Life Sciences*, 152, 244-248. doi: 10.1016/j.lfs.2015.10.025

Elis, S., Wu, Y., Courtland, H.W., Cannata, D., Sun, H., Beth-On, M., et al. (2011). Unbound (bioavailable) IGF1 enhances somatic growth. *Disease Models & Mechanisms*, 4, 649-658. Doi: 10.1242/dmm.006775

Emons, J., Chagin, A.S., Malmlöf, T., Lekman, M., Tivesten, A., Ohlsson, C., et al. (2010). Expression of vascular endothelial growth factor in the growth plate is stimulated by estradiol and increases during pubertal development. *Journal of Endocrinology*, 205(1), 61-68. doi: 10.1677/JOE-09-0337

Engsig, M.T., Chen, Q.J., Vu, T.H., Pedersen, A.C., Therkidsen, B., Lund, L.R., et al. (2000). Matrix metalloproteinase 9 and vascular endothelial growth factor are essential for osteoclast recruitment into developing long bones. *The Journal of Cell Biology*, 151(4), 879-89. doi: 10.1083/jcb.151.4.879

Enishi, T., Yukata, K., Takahashi, M., Sato, R., Sairyo, K., & Yasui, N. (2014). Hypertrophic chondrocytes in the rabbit growth plate can proliferate and differentiate into osteogenic cells when capillary invasion is interposed by a membrane filter. *PLoS ONE*, 9(8), e104638. doi: 10.1371/journal.pone.0104638

Fan, Y., Menon, R.K., Cohen, P., Hwang, D., Clemens, T., DiGirolamo, D.J., et al. (2009). Liver-specific deletion of the growth hormone receptor reveals essential role of growth hormone signaling in hepatic lipid metabolism. *Journal of Biological Chemistry*, 284(30), 19937-19944. doi: 10.1074/jbc.M109.014308

Farnum, C.E., Lenox, M., Zipfel, W., Horton, W., & Williams, R. (2006). In vivo delivery of fluoresceinated dextrans to the murine growth plate: imaging of three vascular routes by multiphoton microscopy. *The Anatomical Record Part A: Discoveries in Molecular, Cellular, and Evolutionary Biology*, 288(1), 91-103. doi: 10.1002/ar.a.20272

Farnum, C.E. (2007). Postnatal growth of fins and limbs through endochondral ossification. In Hall, BK (Ed.), *Fins into Limbs: Evolution, Development, and Transformation* (pp. 118-151). University of Chicago Press.

Ferrara, N., Carver-Moore, K., Chen, H., Dowd, M., Lu, L., O'Shea, K.S., et al. (1996). Heterozygous embryonic lethality induced by targeted inactivation of the VEGF gene. *Nature*, 380(6573), 439-442. doi: 10.1038/380439a0

Ferrara, N. (2004). Vascular endothelial growth factor as a target for anticancer therapy. *The Oncologist*, 9(Suppl 1), 2-10. doi: 10.1634/theoncologist.9-suppl_1-2

Filipowska, J., Tomaszewski, K.A., Niedźwiedzki, Ł., Walocha, J.A., & Niedźwiedzki, T. (2017). The role of vasculature in bone development, regeneration and proper systemic functioning. *Angiogenesis*, 20(3), 291-302. doi: 10.1007/s10456-017-9541-1

- Fong, R., Khokhar, S., Chowdhury, A.N., Wong, J.H., Fox, A.P., & Xie, Z. (2017). Caffeine accelerates recovery from general anesthesia via multiple pathways. *Journal of Neuropathology*, 118(3), 1591-1597. doi: 10.1152/jn.00393.2017
- Forcinito, P., Andrade, A.C., Finkelstein, G.P., Baron, J., Nilsson, O., & Lui, J.C. (2011). Growth-inhibiting conditions slow growth plate senescence. *Journal of Endocrinology*, 208(1), 59-67. doi: 10.1677/JOE-10-0302
- Fredricks, A.M., van Buuren, S., van Heel, W.J., Dijkman-Neerincx, R.H., Verioove-Vanhorick, S.P., & Wit, J.M. (2005). Nationwide age references for sitting height, leg length, and sitting height/height ratio, and their diagnostic value for disproportionate growth disorders. *Archives of Disease in Childhood*, 90(8), 807-812. doi: 10.1136/adc.2004.050799
- Friberg, O.R.A. (1983). Clinical symptoms and biomechanics of lumbar spine and hip joint in leg length inequality. *Spine*, 8(6), 643-651.
- Friedrichsen, S., Christ, S., Heuer, H., Schäfer, M.K., Mansouri, A., Bauer, K., et al. (2003). Regulation of iodothyronine deiodinases in the Pax8^{-/-} mouse model of congenital hypothyroidism. *Endocrinology*, 144(3), 777-784. doi: 10.1210/en.2002-220715
- Garrison, P., Yue, S., Hanson, J., Baron, J., & Lui, J.C. (2017). Spatial regulation of bone morphogenetic proteins (BMPs) in postnatal articular and growth plate cartilage. *PLoS ONE*, 12(5), e0176752. doi: 10.1371/journal.pone.0176752
- Geiger, M., Forasiepi, A.M., Koyabu, D., & Sánchez-Villagra, M.R. (2014). Heterochrony and post-natal growth in mammals- an examination of growth plate limbs. *Journal of Evolutionary Biology*, 27(1), 98-115. doi: 10.1111/jeb.12279
- Gerber, H.P., Hillan, K.J., Ryan, A.M., Kowalski, J., Keller, G.A., Rangell, L., et al. (1999a). VEGF is required for growth and survival in neonatal mice. *Development*, 126(6), 1149-1159.
- Gerber, H.P., Vu, T.H., Ryan, A.M., Kowalski, J., Werb, Z., & Ferrara, N. (1999b). VEGF couples hypertrophic cartilage remodeling, ossification and angiogenesis during endochondral bone formation. *Nature Medicine*, 5(6), 623-628. doi: 10.1038/9467
- Gilbert, S.F. (2014). Development of the tetrapod limb. *Developmental Biology* (pp. 489-516). Sunderland (MA): Sinauer Associates, Inc.
- Girrita, L., Worrall, C., Takahashi, S.I., Seregard, S., & Girrita, A. (2014). Something old, something new and something borrowed: emerging paradigm of insulin-like growth factor type 1 receptor (IGF-1R) signaling regulation. *Cellular and Molecular Life Sciences*, 71(13), 2403-2427. doi: 10.1007/s00018-013-1514-y

Gluckman, P.D., & Butler, J.H. (1983). Parturition-related changes in insulin-like growth factors-I and -II in the perinatal lamb. *Journal of Endocrinology*, *99*(2), 223-232. doi: 10.1677/joe.0.0990223

Golightly, Y.M., Allen, K.D., Renner, J.B., Helmick, C.G., Salazar, A., & Jordan, J.M. (2007b). Relationship of limb length inequality with radiographic knee and hip osteoarthritis. *Osteoarthritis and Cartilage*, *15*(7), 824-829. doi: 10.1016/j.joca.2007.01.009

Golightly, Y.M., Tate, J.J., Burns, C.B., & Gross, M.T. (2007a). Changes in pain and disability secondary to shoe lift intervention in subjects with limb length inequality and chronic low back pain: a preliminary report. *Journal of Orthopaedic & Sports Physical Therapy*, *37*(7), 380-388. doi: 10.2519/jospt.2007.2429

Gordon, C.J. (2012). The mouse: an “average” homeotherm. *Journal of Thermal Biology*, *37*(4), 286-290. doi: 10.1016/j.jtherbio.2011.06.008

Gordon, C.J. (2017). The mouse thermoregulatory system: its impact on translating biomedical data to humans. *Physiology & Behavior*, *179*, 55-66. doi: 10.1016/j.physbeh.2017.05.026

Gordon, M., Crouthamel, C., Post, E.M., & Richman, R.A. (1982). Psychosocial aspects of constitutional short stature: social competence, behavior problems, self-esteem, and family functioning. *The Journal of Pediatrics*; *101*(3), 477-480. doi: 10.1016/S0022-3476(82)80093-0

Göthe, S., Wang, Z., Ng, L., Kindblom, J.M., Barros, A.C., Ohlsson, C., et al. (1999). Mice devoid of all known thyroid hormone receptors are viable but exhibit disorders of the pituitary-thyroid axis, growth, and bone maturation. *Genes & Development*, *13*(10), 1329-1341. doi: 10.1101/gad.13.10.1329

Govoni, K.E., Lee, S.K., Chung, Y.S., Behringer, R.R., Wergedal, J.E., Baylink, D.J., et al. (2007a). Disruption of insulin-like growth factor-1 expression in type IIa1 collagen-expressing cells reduces bone length and width in mice. *Physiological Genomics*, *30*(3), 354-362. doi: 10.1152/physiolgenomics.00022.2007

Govoni, K.E., Wergedal, J.E., Florin, L., Angel, P., Baylink, D.J., & Mohan, S. (2007b). Conditional deletion of insulin-like growth factor-I in collagen type 1 α 2-expressing cells results in postnatal lethality and a dramatic reduction in bone accretion. *Endocrinology*, *148*(12), 5706-5715. doi: 10.1210/en.2007-0608

Green, H., Morikawa, M., & Nixon, T. (1985). A dual effector theory of growth-hormone action. *Differentiation*, *29*(3), 195-198. doi: 10.1111/j.1432-0436.1985.tb00316.x

Green, W.T., & Anderson, M. (1955). The problem of unequal leg length. *Pediatric Clinics of North America*, *2*(4), 1137-1155. doi: 10.1016/S0031-3955(16)30303-0

- Grimmer, K.A., Jones, D., & Williams, J. (2000). Prevalence of adolescent injury from recreational exercise: an Australian perspective. *Journal of Adolescent Health, 27*(4), 266-272. doi: 10.1016/S1054-139X(00)00120-8
- Gross, R.H. (1978). Leg length discrepancy: how much is too much? *Orthopedics, 1*(4), 307-310.
- Growth chart C57BL/6 C57BL/H1a®CVF®*. (2018). Retrieved from Hilltop Lab Animals, Inc website, <http://www.hilltoplabs.com/public/c57growth.html>
- Grunwald, T., & De Luca, F. (2015). Role of fibroblast growth factor 21 (FGF21) in the regulation of statural growth. *Current Pediatric Reviews, 11*(2), 98-105. doi: 10.2174/1573396311666150702105152
- Guevara-Aguirre, J., Rosenbloom, A.L., Vasconez, O., Martinez, V., Gargosky, S.E., Allen, L., et al. (1997). Two-year treatment of growth hormone (GH) receptor deficiency with recombinant insulin-like growth factor I in 22 children: comparison of two dosage levels and to GH-treated GH deficiency. *Journal of Clinical Endocrinology & Metabolism, 82*(2), 629-633. doi: 10.1210/jc.82.2.629
- Guha, M. (2013). Anticancer IGF1R classes take more knocks. *Nature Reviews Drug Discovery, 12*(4), 250. doi: 10.1038/nrd3992
- Gurney, B. (2002). Leg length discrepancy. *Gait & Posture, 15*(2), 195-206. doi: 10.1016/S0966-6362(01)00148-5
- Hadacek, F., & Bachmann, G. (2015). Low-molecular-weight metabolite systems chemistry. *Frontiers in Environmental Science, 3*, 12. doi: 10.3389/fenvs.2015.00012
- Halevy, O., Krispin, A., Leshem, Y., McMurtry, J.P., & Yahav, S. (2001). Early-age heat exposure affects skeletal muscle satellite cell proliferation and differentiation in chicks. *American Journal of Physiology-Regulatory, Integrative and Comparative Physiology, 281*(1), R302-309. doi: 10.1152/ajpregu.2001.281.1.R302
- Han, K., Peyret, T., Quartino, A., Gosselin, N.H., Gururangan, S., Casanova, M., et al. (2016). Bevacizumab dosing strategy in paediatric cancer patients based on population pharmacokinetic analysis with external validation. *British Journal of Clinical Pharmacology, 81*(1), 148-160. doi: 10.1111/bcp.12778
- Hansen-Pupp, I., Hellström, A., Hamdani, M., Tocoian, A., Kreher, N.C., Ley, D., et al. (2017). Continuous longitudinal infusion of rhIGF-1/rhIGFBP-3 in extremely preterm infant: evaluation of feasibility in a phase II study. *Growth Hormone & IGF Research, 36*, 44-51. doi: 10.1016/j.ghir.2017.08.004

Hansen-Pupp, I., Hövel, H., Hellström, A., Hellström-Westas, L., Löfqvist, C., Larsson, E.M., et al. (2011). Postnatal decrease in circulating insulin-like growth factor-I and low brain volumes in very preterm infants. *The Journal of Clinical Endocrinology & Metabolism*, 96(4), 1129-1135. doi: 10.1210/jc.2010-2440

Hansson, L.I., Stenström, A., & Thorngren, K.G. (1976). Effect of fracture on longitudinal bone growth in rats. *Acta Orthopaedica Scandinavica*, 47(6), 600-606. doi: 10.3109/17453677608988745

Harada, D., Namba, N., Hanioka, Y., Ueyama, K., Sakamoto, N., Nakano, Y., et al. (2017). Final adult height in long-term growth hormone-treated achondroplasia patients. *European Journal of Pediatrics*, 176(7), 873-879. doi: 10.1007/s00431-017-2923-y

Harvey, W.F., Yang, M., Cooke, T.D., Segal, N.A., Lane, N., Lewis, C.E., et al. (2010). Association of leg-length inequality with knee osteoarthritis: a cohort study. *Annals of Internal Medicine*, 152(5), 287-295. doi: 10.7326/0003-4819-152-5-201003020-00006

Hasler, C.C., & Krieg, A.H. (2012). Current concepts of leg lengthening. *Journal of Children's Orthopaedics*, 6(2), 89-104. doi: 10.1007/s11832-012-0391-5

Haylor, J., Hickling, H., Eter, E.E., Moir, A., Oldroyd, S., Hardisty, C., et al. (2000). JB3, an IGF-I Receptor Antagonist, Inhibits Early Renal Growth in Diabetic and Uninephrectomized Rats. *Journal of the American Society of Nephrology*, 11(11), 2027-2035.

Holman, S.R., & Baxter, R.C. (1996). Insulin-like growth factor binding protein-3: factors affecting binary and ternary complex formation. *Growth Regulation*, 6(1), 42-47.

Horner, A., Bishop, N.J., Bord, S., Beeton, C., Kelsall, A.W., Coleman, N., et al. (1999). Immunolocalisation of vascular endothelial growth factor (VEGF) in human neonatal growth plate cartilage. *Journal of Anatomy*, 194(4), 519-524. doi: 10.1046/j.1469-7580.1999.19440519.x

Hu, D.P., Ferro, F., Yang, F., Taylor, A.J., Chang, W., Miciau, T., et al. (2017). Cartilage to bone transformation during fracture healing is coordinated by the invading vasculature and induction of the core pluripotency genes. *Development*, 144(2), 221-234. doi: 10.1242/dev.130807

Huang, B.K., Golden, L.A., Tarjan, G., Madison, L.D., & Stern, P.H. (2000). Insulin-like growth factor I production is essential for anabolic effects of thyroid hormone in osteoblasts. *Journal of Bone and Mineral Research*, 15(2), 188-197. doi: 10.1359/jbmr.2000.15.2.188

Hughes, P.C. & Tanner, J.M. (1970). The assessment of skeletal maturity in the growing rat. *Journal of Anatomy*, 106(Pt 2), 371-402.

- Humbel, R.E. (1990). Insulin-like growth factors I and II. *European Journal of Biochemistry*, 190(3), 445-462. doi: 10.1111/j.1432-1033.1990.tb15595.x
- Hung, I.H., Yu, K., Lavine, K.J., & Ornitz, D.M. (2007). FGF9 regulates early hypertrophic chondrocyte differentiation and skeletal vascularization in the developing stylopod. *Development Biology*, 307(2), 300-313. doi: 10.1016/j.ydbio.2007.04.048
- Hunt, T.N., & Amato, H.K. (2003). Epiphyseal-plate fracture in an adolescent athlete. *Athletic Therapy Today*, 8(34), 34-36. doi: 10.1123/att.8.1.34
- Hunziker, E.B., Schenk, R.K., & Cruz-Orive, L.M. (1987). Quantitation of chondrocyte performance in growth-plate cartilage during longitudinal bone growth. *The Journal Bone and Joint Surgery*. American Volume, 69(2), 162-173.
- Hunziker, E.B., & Schenk, R.K. (1989). Physiological mechanisms adopted by chondrocytes in regulating longitudinal bone growth in rats. *The Journal of Physiology*, 414(1), 55-71. doi: 10.1113/jphysiol.1989.sp017676
- Hunziker, E.B., Wagner, J., & Zapf, J. (1994a). Differential effects of insulin-like growth factor I and growth hormone on developmental stages of rat growth plate chondrocytes in vivo. *Journal of Clinical Investigation*, 93(3), 1078-1086. doi: 10.1172/JCI117058
- Hunziker, E.B. (1994b). Mechanism of longitudinal bone growth and its regulation by growth plate chondrocytes. *Microscopy Research and Technique*, 28(6), 505-519. doi: 10.1002/jemt.1070280606
- Ilizarov, G.A. (1988). The principles of the Ilizarov method. *Bulletin of the Hospital for Joint Diseases Orthopaedic Institute*, 48(1), 1-11.
- Inagaki, M., Ohno, K., Histome, I., Tanaka, Y., Takeshita, K. (1992). Relative hypoxia of the extremities in Fabry disease. *Brain and Development*, 14(5), 328-33. doi: 10.1016/S0387-7604(12)80153-7
- Isaksson, O.G., Jansson, J.O., & Gause, I.A. (1982). Growth hormone stimulates longitudinal bone growth directly. *Science*, 216(4551), 1237-1239. doi: 10.1126/science.7079756
- Isaksson, O.G.P., Ohlsson, C., Nilsson, A., Isgaard, J., & Lindahl, A. (1991). Regulation of cartilage growth by growth hormone and insulin-like growth factor I. *Pediatric Nephrology*, 5(4), 451-453. doi: 10.1007/BF01453680
- Isaksson, O.G.P., Eden, S., & Jansson, J.O. (1985). Mode of action of pituitary growth hormone on target cells. *Annual Review of Physiology*, 47(1), 483-499. doi: 10.1146/annurev.ph.47.030185.002411

- Isgaard, J., Nilsson, A., Lindahl, A., Jansson, J.O., & Isaksson, O.G. (1986). Effects of local administration of GH and IGF-1 on longitudinal bone growth in rats. *American Journal of Physiology-Endocrinology and Metabolism*, 250(4), E367-372. doi: 10.1152/ajpendo.1986.250.4.E367
- Jiang, J., Lichtler, A.C., Gronowicz, G.A., Adams, D.J., Clark, S.H., Rosen, C.J., et al. 2006. Transgenic mice with osteoblast-targeted insulin-like growth factor I show increased bone remodeling. *Bone* 39(3), 494-504. doi: 10.1016/j.bone.2006.02.068
- Jilka, R.L. (2013). The relevance of mouse models for investigating age-related bone loss in humans. *The Journals of Gerontology Series A: Biological Sciences and Medical Sciences*, 68(10), 1209-1217. doi: 10.1093/gerona/glt046
- Jones, B.F. (1998). A reappraisal of the use of infrared thermal image analysis in medicine. *IEEE Transactions on Medical Imaging*, 17(6), 1019-1027. doi: 10.1109/42.746635
- Karimian, E., Chagin, A.S., & Säwendahl, L. (2012). Genetic regulation of the growth plate. *Frontiers in Endocrinology (Lausanne)*, 2, 113. doi: 10.3389/fendo.2011.00113
- Kasukawa, Y., Baylink, D.J., Guo, R., & Mohan, S. (2003). Evidence that sensitivity to growth hormone (GH) is growth period and tissue type dependent: studies in GH-deficient lit/lit mice. *Endocrinology*, 144(9), 3950-3957. doi: 10.1210/en.2002-0123
- Kaufman, K.R., Miller, L.S., & Sutherland, D.H. (1996). Gait asymmetry in patients with limb-length inequality. *Journal of Pediatric Orthopaedics*, 16(2), 144-150.
- Kelly, P.M., & Diméglio, A. (2008). Lower-limb growth: how predictable are predictions? *Journal of Children's Orthopaedics*, 2(6), 407-415.
- Kember, N.F. (1972). Comparative patterns of cell division in epiphyseal cartilage plates in the rat. *Journal of Anatomy*, 111(1), 137-142.
- Kember, N.F. (1993). Cell kinetics and the control of bone growth. *Acta Paediatrica*, 82(Suppl 392), 61-65. doi: 10.1111/j.1651-2227.1993.tb12932.x
- Kerr, H.E., Grant, J.H., & MacBain, R.N. (1943). Some observations on the anatomical short leg in a series of patients presenting themselves for treatment of low-back pain. *The Journal of the American Osteopathic Association*, 42(10), 437-440.
- Khamis, S. & Carmeli, E. (2017). Relationship and significance of gait deviations associated with limb length discrepancy: A systematic review. *Gait & Posture*, 57, 115-123. doi: 10.1016/j.gaitpost.2017.05.028

- Kiepe, D., Ciarmatori, S., Hoeflich, A., Wolf, E., & Tönshoff, B. (2006). IGF-1 stimulates cell proliferation and induces IGFBP-3 and IGFBP-5 gene expression in cultured growth plate chondrocytes via distinct signaling pathways. *Endocrinology*, *146*(7), 3096-3104. doi: 10.1210/en.2005-0324
- Kilborn, S.H., Trudel, G., & Uthoff, H. (2002). Review of growth plate closure compared with age at sexual maturity and lifespan in laboratory animals. *Journal of the American Association for Laboratory Animal Science*, *41*(5), 21-26.
- Kindblom, J.M., Gevers, E.F., Skrtic, S.M., Lindberg, M.K., Göthe, S., Törnell, J., et al. (2005). Increased adipogenesis in bone marrow but decreased bone mineral density in mice devoid of thyroid hormone receptors. *Bone*, *36*(4), 607-616. doi: 10.1016/j.bone.2005.01.017
- Kirienko, A., Peccati, A., Abdellatif, I., Elbatrawy, Y., Mostaf, Z.M., & Necci, V. (2011). Correction of poliomyelitis foot deformities with Ilizarov method. *Strategies in Trauma and Limb Reconstruction*, *6*(3), 107-120. doi: 10.1007/s11751-011-0111-6
- Kleinridders, A. (2016). Deciphering brain insulin receptor and insulin-like growth factor 1 receptor signaling. *Journal of Neuroendocrinology*, *28*(11), 1-13. doi: 10.1111/jne.12433
- Knutson, G.A. (2005). Anatomic and functional leg-length inequality: a review and recommendation for clinical decision-making. Part I, anatomic leg-length inequality: prevalence, magnitude, effects and clinical significance. *Chiropractic & Osteopathy*, *13*, 11. doi: 10.1186/1746-1340-13-11
- Kovacs, G.T., Worgall, S., Schwabach, P., Steichele, I., Mehls, O., & Rosivall, L. (1999). Hypoglycemic effects of insulin-like growth factor-1 in experimental uremia: can concomitant growth hormone administration prevent this effect. *Hormone Research in Paediatrics*, *51*(4), 193-200. doi: 10.1159/000023357
- Kronenberg, H.M. (2003). Developmental regulation of the growth plate. *Nature*, *423*(6937), 332-336. doi: 10.1038/nature01657.
- Laron, Z., & Kauli, R. (2015b). Fifty seven years of follow-up of Israeli cohort of Laron Syndrome patients-From discovery to treatment. *Growth Hormone & IGF Research*, *28*, 53-56. doi: 10.1016/j.ghir.2015.08.004
- Laron, Z., & Klinger, B. (2000). Comparison of the growth-promoting effects of insulin-like growth factor I and growth hormone in the early years of life. *Acta Paediatrica*, *89*(1), 38-41. doi: 10.1111/j.1651-2227.2000.tb01184.x
- Laron, Z. (2001). Insulin-like growth factor 1 (IGF-1): a growth hormone. *Molecular Pathology*, *54*(5), 311-316. doi: 10.1136/mp.54.5.311

- Laron, Z. (2015a). Lessons from 50 years of study of Laron syndrome. *Endocrine Practice*, 21(12), 1395-1402. doi: 10.4158/EP15939.RA
- Latham, N., & Mason, G. (2004). From house mouse to mouse house: the behavioral biology of free-living *Mus musculus* and its implications in the laboratory. *Applied Animal Behavior Science*, 86(3), 261-289. doi: 10.1016/j.applanim.2004.02.006
- Lazarus, J.E., Hegde, A., Andrade, A.C., Nilsson, O., & Baron, J. (2007). Fibroblast growth factor expression in the postnatal growth plate. *Bone* 40(3), 577-586. doi: 10.1016/j.bone.2006.10.013
- Lazowski, D.A., Fraher, L.J., Hodzman, A., Steer, B., Modrowski, D., & Han, V.K. (1994). Regional variation of insulin-like growth factor-I gene expression in mature rat bone and cartilage. *Bone* 15(5), 563-576. doi: 10.1016/j.bone.2006.10.013
- Lee, D., Kim, Y.S., Song, J., Kim, H.S., Lee, J.H., Guo, H., et al. (2016). Effects of *Phlomis umbrosa* root on longitudinal bone growth rate in adolescent female rats. *Molecules*, 21(4), 461. doi: 10.3390/molecules21040461
- Lee, P.A. 1980. Normal ages of pubertal events among American males and females. *Journal of Adolescent Health Care*, 1(1), 26-29. doi: 10.1016/S0197-0070(80)80005-2
- Le Roith D., Bondy, C., Yakar, S., Liu, J.L., & Butler, A. (2001). The somatomedin hypothesis: 2001. *Endocrine Reviews*, 22(1), 53-74. doi: 10.1210/edrv.22.1.0419
- Li, C., Chai, Y., Wang, L., Gao, B., Chen, H., Gao, P., et al. (2017). Programmed cell senescence in skeleton during late puberty. *Nature Communications*, 8(1), 1312. doi: 10.1038/s41467-017-01509-0
- Li, R., Pourpak, A., & Morris, S.W. (2009). Inhibition of the insulin-like growth factor-1 receptor (IGF1R) tyrosine kinase as a novel cancer therapy approach. *Journal of Medicinal Chemistry*, 52(16), 4981-5004. doi: 10.1021/jm9002395
- Lindsey, R.C., & Mohan, S. (2016). Skeletal effects of growth hormone and insulin-like growth factor-I therapy. *Molecular and Cellular Endocrinology*, 432, 44-55. doi: 10.1016/j.mce.2015.09.017
- List, E.O., Sackmann-Sala, L., Berryman, D.E., Funk, K., Kelder, B., Gosney, E.S., et al. (2011). Endocrine parameters and phenotypes of the growth hormone receptor gene disrupted (GHR^{-/-}) mouse. *Endocrine Reviews*, 32(3), 356-586. doi: 10.1210/er.2010-0009
- Liu, J.P., Baker, J., Perkins, A.S., Robertson, E.J., & Efstratiadis, A. (1993). Mice carrying null mutations of the genes encoding insulin-like growth factor I (Igf-1) and type 1 IGF receptor (Igf1r). *Cell*, 75(1), 59-72. doi: 10.1016/S0092-8674(05)80084-4

- Liu, Z., Lavine, K.J., Hung, I.H., & Ornitz, D.M. (2007). FGF18 is required for early chondrocyte proliferation, hypertrophy and vascular invasion of the growth plate. *Developmental Biology*, 302(1), 80-91. doi: 10.1016/j.ydbio.2006.08.071
- Lui, J.C., Nilsson, O., & Baron, J. (2011). Growth plate senescence and catch-up growth. *Endocrine Development*, 21, 23-29. doi: 10.1159/000328117
- Lui, J.C., Nilsson, O., & Baron, J. (2014). Recent research on the growth plate: Recent insights into the regulation of the growth plate. *Journal of Molecular Endocrinology*, 53(1), T1-9. doi: 10.1530/JME-14-0022
- Lund, P.K., Moats-Staats, B.M., Hynes, M.A., Simmons, J.G., Jansen, M., D'Ercole, A.J., et al. (1986). Somatomedin-C/insulin-like growth factor-I and insulin-like growth factor-II mRNAs in rat fetal and adult tissues. *Journal of Biological Chemistry*, 261(31), 14539-14544.
- Lupu, F., Terwilliger, J.D., Lee, K., Segre, G.V., & Efstratiadis, A. (2001). Roles of growth hormone and insulin-like growth factor 1 in mouse postnatal growth. *Developmental Biology*, 229(1), 141-162. doi: 10.1006/dbio.2000.9975
- LuValle, P., & Beier, F. (2000). Cell cycle control in growth plate chondrocytes. *Frontiers in Bioscience*, 1(5), D493-503.
- Lynch, G.S., Cuffe, S.A., Plant, D.R., & Gregorevic, P. (2001). IGF-I treatment improves the functional properties of fast- and slow-twitch skeletal muscles from dystrophic mice. *Neuromuscular Disorders*, 11(3), 260-268. doi: 10.1016/S0960-8966(00)00192-9
- Macielag, M.J. (2012). Chemical properties of antimicrobials and their uniqueness. In *Antibiotic Discovery and Development* (pp. 793-820). Springer, Boston, MA.
- Mackie, E.J., Ahmed, Y.A., Tatarczuch, L., Chen, K.S., & Mirams, M. (2008). Endochondral ossification: How cartilage is converted into bone in the developing skeleton. *The International Journal of Biochemistry & Cell Biology*, 40(1), 46-62. doi: 10.1016/j.biocel.2007.06.009
- Maeda, Y., Schipani, E., Densmore, M.J., & Lanske, B. (2010). Partial rescue of postnatal growth plate abnormalities in *Ihh* mutants by expression of constitutively active PTH/PTHrP receptor. *Bone*, 46(2), 472. doi: 10.1016/j.bone.2009.09.009
- Maes, C., Carmeliet, P., Moermans, K., Stockmans, I., Smets, N., Collen, D., et al. (2002). Impaired angiogenesis and endochondral bone formation in mice lacking the vascular endothelial growth factor isoforms VEGF₁₆₄ and VEGF₁₈₈. *Mechanisms of Development*, 111(1-2), 61-73. doi: 10.1016/S0925-4773(01)00601-3

- Maes, C., Stockmans, I., Moermans, K., Van Looveren, R., Smets, N., Carmeliet, P., et al. (2004). Soluble VEGF isoforms are essential for establishing epiphyseal vascularization and regulating chondrocyte development and survival. *The Journal of Clinical Investigation*, 113(2), 188-199. doi: 10.1172/JCI19383
- Maes, C. (2013). Role and regulation of vascularization processes in endochondral bones. *Calcified Tissue International*, 92(4): 307-323. doi: 10.1007/s00223-012-9689-z
- Mahmood, S., Huffman, L.K., & Harris, J.G. (2010). Limb-length discrepancy as a cause of plantar fasciitis. *Journal of the American Podiatric Medical Association*, 100(6), 452-455. doi: 10.7547/1000452
- Mathews, L.S., Hammer, R.E., Behringer, R.R., D'Ercole, A.J., Bell, G.I., Brinster, R.L., et al. (1988). Growth enhancement of transgenic mice expressing human insulin-like growth factor I. *Endocrinology*, 123(6), 2827-2833. doi: 10.1210/endo-123-6-2827
- McDowell, M.A., Fryar, C.D., & Ogden, C.L. (2009). Anthropometric reference data for children and adults: United States, 1988-1994. *Vital and Health Statistics*, 11(249), 1-68.
- McGreevy, P., Warren-Smith, A., & Guisard, Y. (2012). The effect of double bridles and jaw-clamping crank nosebands on temperature of eyes and facial skin of horses. *Journal of Veterinary Behavior*, 7(3), 142-148. doi: 10.1016/j.jveb.2011.08.001
- McManus, M.M., & Grill, R.J. (2011). Longitudinal evaluation of mouse hind limb bone loss after spinal cord injury using novel, in vivo, methodology. *Journal of Visualized Experiments*, (58), 3246. doi: 10.3791/3246
- Menelaus, M.B. (1966). Correction of leg length discrepancy by epiphyseal arrest. *The Journal of Bone and Joint Surgery. British Volume*, 48(2), 336-339.
- Menon, R., Murphy, P.G., & Lindley, A.M. (2011). Anaesthesia and pituitary disease. *Continuing Education in Anesthesia Critical Care & Pain*, 11(4), 133-137. doi: 10.1093/bjaceaccp/mkr014
- Midyett, L.K., Rogol, A.D., Van Meter, Q.L., Frane, J., Bright, G.M., & MS301 Study Group. (2010). Recombinant insulin-like growth factor (IGF)-1 treatment in short children with low IGF-1 levels: first-year results from a randomized clinical trial. *The Journal of Clinical Endocrinology & Metabolism*, 95(2), 611-619. doi: 10.1210/jc.2009-0570
- Mirtz, T.A., Chadler, J.P., & Eysers, C.M. (2011). The effects of physical activity on the epiphyseal growth plates: a review of literature on normal physiology and clinical implications. *Journal of Clinical Medicine Research*, 3(1), 1-7. doi: 10.4021/jocmr477w

- Mohan, S., Richman, C., Guo, R., Amaar, Y., Donahue, L.R., Wergedal, J., et al. (2003). Insulin-like growth factor regulates peak bone mineral density in mice by both growth hormone-dependent and -independent mechanisms. *Endocrinology*, *144*(3), 929-936. doi: 10.1210/en.2002-220948
- Moix, E.G., Gimébez-Palop, O., & Caixàs, A. (2018). Treatment with growth hormone in the prader-willi syndrome. *Endocrinologia, diabetes y nutricion*, *65*(4), 229-236. doi: 10.1016/j.endien.2018.01.004
- Monier, B.C., Aronsson, D.D., & Sun, M. (2015). Percutaneous epiphysiodesis using transphyseal screws for limb-length discrepancies: high variability among growth predictor models. *Journal of Children's Orthopaedics*, *9*(5), 403-410. doi: 10.1007/s11832-015-0687-3
- Moody, G., Beltra, P.J., Mitchell, P., Cajulis, E., Chung, Y.A., Hwang, D., et al. (2014). IGF1R blockade with ganitumab results in systemic effects on the GH-IGF axis in mice. *Journal of Endocrinology*, *221*(1), 145-155. doi: 10.1530/JOE-13-0306
- Morcavallo, A., Stefanello, M., Iozzo, R.V., Belfiore, A., & Morrione, A. (2014). Ligand-mediated endocytosis and trafficking of the insulin-like growth factor receptor I and insulin receptor modulate receptor function. *Frontiers in Endocrinology*, *5*, 220. doi: 10.3389/fendo.2014.00220
- Morscher, E. (1977). Etiology and pathophysiology of leg length discrepancies. In *Progress in Orthopaedic Surgery 1* (pp. 9-19). doi: 10.1007/978-3-642-66549-3_2
- Moseley, C.F. (1977). A straight-line graph for leg-length discrepancies. *The Journal of Bone & Joint Surgery*, *59*(2), 174-179.
- Mushtaq, T., Bijman, P., Ahmed, S.F., & Farquharson, C. (2004). Insulin-like growth factor-I augments chondrocyte hypertrophy and reverses glucocorticoid-mediated growth retardation in fetal mice metatarsal cultures. *Endocrinology*, *145*(5), 2478-2486. doi: 10.1210/en.2003-1435
- Newman, M.T. (1953). The application of ecological rules to the racial anthropology of the aboriginal New World. *American Anthropologist*, *55*(3), 311-327. doi: 10.1525/aa.1953.55.3.02a00020
- Niedzielski, K., Flont, P., Domżański, M., Lipczyk, Z., & Malecki, K. (2016). Lower limb equalization with, percutaneous epiphysiodesis of the knee joint area. *Acta Orthopaedica Belgica*, *82*(4), 843-849.
- Nilsson, A., Carlsson, B., Isgaard, J., Isaksson, O.G., & Rymo, L., (1990). Regulation of GH of insulin-like growth factor-I mRNA expression in rat epiphyseal growth plate as studied with in-situ hybridization. *Journal of Endocrinology*, *125*(1), 67-74. doi: 10.1677/joe.0.1250067

- Nilsson, O., & Baron, J. (2004). Fundamental limits on longitudinal bone growth: growth plate senescence and epiphyseal fusion. *Trends in Endocrinology & Metabolism*, 15(8), 370-374. doi: 10.1016/j.tem.2004.08.004
- Nilsson, O., Parker, E.A., Hegde, A., Chau, M., Barnes, K.M., & Baron, J. (2007). Gradients in bone morphogenetic protein-related gene expression across the growth plate. *Journal of Endocrinology*, 193(1), 75-84. doi: 10.1677/joe.1.07099
- Nilsson, O., Weise, M., Landman, E.B.M., Meyers, J.L., Barnes, K.M., & Baron, J. (2014). Evidence that estrogen hastens epiphyseal fusion and cessation of longitudinal bone growth by irreversibly depleting the number of resting zone progenitor cells in female rabbits. *Endocrinology*, 155(8), 2892-2899. doi: 10.1210/en.2013-2175
- Noonan, K.J., Farnum, C.E., Leiferman, E.M., Lampl, M., Markel, M.D., & Wilsman, N.J. (2004). Growing pains: are they due to increased growth during recumbency as documented in a lamb model? *Journal of Pediatric Orthopaedics*, 24(6), 726-731.
- Noonan, J.A., & Kappelgaard, A.M. (2015). The efficacy and safety of growth hormone therapy in children with noonan syndrome: a review of the evidence. *Hormone Research in Paediatrics*, 83(3), 157-166. doi: 10.1159/000369012
- Oberbauer, A.M., & Peng, R. (1995). Growth hormone and IGF-1 stimulate cell function in distinct zones of the rat epiphyseal growth plate. *Connective Tissue Research*, 31(3), 189-195. doi: 10.3109/03008209509010810
- Ohlsson, C., Bengtsson, B.A., Isaksson, O.G., Andreassen, T.T., & Słotweg, M.C. (1998). Growth hormone and bone. *Endocrine Reviews*, 19(1), 55-79. doi: 10.1210/er.19.1.55
- Ohlsson, C., Isgaard, J., Törnelli, J., Nilsson, A., Isaksson, O.G.P., & Lindahl, A. (1993). Endocrine regulation of longitudinal bone growth. *Acta Paediatrica*, 82(s392), 33-40. doi: 10.1111/j.1651-2227.1993.tb12925.x
- Ohlsson, C., Nilsson, A., Isaksson, O., Bentham, J., & Lindahl, A. (1992a). Effects of triiodothyronine and insulin-like growth factor-I (IGF-I) on alkaline phosphatase activity, [3H]thymidine incorporation and IGF-I receptor mRNA in cultured rat epiphyseal chondrocytes. *Journal of Endocrinology*, 135(1), 115-23.
- Ohlsson, C., Nilsson, A., Isaksson, O., & Lindahl, A. (1992b). Growth hormone induces multiplication of the slowly cycling germinal cells of the rat tibial growth plate. *Proceedings of the National Academy of Sciences*, 89(2), 9826-9830. doi: 10.1073/pnas.89.20.9826
- Paley, D., Bhave, A., Herzenberg, J.E., & Bowen, J.R. (2000). Multiplier method for predicting limb-length discrepancy. *The Journal of Bone and Joint Surgery-American Volume*, 82(10), 1432-1446. doi: 10.2106/00004623-200010000-00010

- Pan, W., & Kastin, K. (2000). Interactions of IGF-1 with the blood-brain barrier in vivo and in situ. *Neuroendocrinology*, *72*(3), 171-178. doi: 10.1159/000054584
- Papaoannou, T., Stokes, I., & Kenwright, J. (1982). Scoliosis associated with limb-length inequality. *The Journal of Bone & Joint Surgery*, *64*(1), 59-62. doi: 10.2106/00004623-198264010-00009
- Parfitt, A.M. (2002). Misconceptions (1): Epiphyseal fusion causes cessation of growth. *Bone*, *30*(2), 337-339. doi: 10.1016/S8756-3282(01)00668-8
- Parker, E.A., Hegde, A., Buckley, M., Barnes, K.M., Baron, J., & Nilsson, O. (2007). Spatial and temporal regulation of GH-IGF-related gene expression in growth plate cartilage. *Journal of Endocrinology*, *194*(1), 31-40. doi: 10.1677/JOE-07-0012
- Payton, C.G. (1932). The growth in length of the long bones in the madder-fed pig. *Journal of Anatomy*, *66*, 414-425.
- Pendleton, A.M., Stevens, P.M., & Hung, M. (2013). Guided growth for the treatment of moderate leg-length discrepancy. *Orthopedics*, *36*(5), e575-80. doi: 10.3928/01477447-20130426-18
- Pfäffle, R. (2015). Hormone replacement therapy in children: the use of growth hormone and IGF-I. *Best Practice & Research Clinical Endocrinology & Metabolism*, *29*(3), 339-352. doi: 10.1016/j.beem.2015.04.009
- Phemister, D.B. (1933). Operative arrestment of longitudinal growth of bone in the treatment of deformities. *The Journal of Bone & Joint Surgery*, *15*, 1-15.
- Pierce, A.L., Dickey, J.T., Felli, L., Swanson, P., & Dickhoff, W.W. (2010). Metabolic hormones regulate basal and growth hormone-dependent igf2 mRNA level in primary cultured coho salmon hepatocytes: effects of insulin, glucagon, dexamethasone, and triiodothyronine. *Journal of Endocrinology*, *204*(3), 331-339. doi: 10.1677/JOE-09-0338
- Pietrzkowski, Z., Wernicke, D., Porcu, P., Jameson, B.A., & Baserga, R. (1992). Inhibition of cellular proliferation by peptide analogues of insulin-like growth factor 1. *Cancer Research*, *52*(23), 6447-6451.
- Pillai, R.N., & Ramalingam, S.S. (2013). Inhibition of insulin-like growth factor receptor: end of a targeted therapy. *Translational Lung Cancer Research*, *2*(1), 14-22. doi: 10.3978/j.issn.2218-6751.2012.11.05
- Politis, S.N., Mazurais, D., Servili, A., Zambonion-Infante, J.L., Miest, J.J., Sørensen, S.R., et al. (2017). Temperature effects on gene expression and morphological development of European eel, *Anguilla Anguilla* larvae. *PLoS One*, *12*(8), e0182726. doi: 10.1371/journal.pone.0182726

Pollard, A.S., Charlton, B.G., Hutchinson, J.R., Gustafsson, T., McGonnell, I.M., Timmons, J.A., et al. (2017). Limb proportions show developmental plasticity in response to embryo movement. *Scientific Reports*, 7(1), 41926. doi: 10.1038/srep41926

Powell-Braxton, L., Hollingshead, P., Warburton, C., Dowd, M., Pitts-Meek, S., Dalton, et al. (1993). IGF-I is required for normal embryonic growth in mice. *Genes & Development*, 7(12b), 2609-2617. doi: 10.1101/gad.7.12b.2609

Prein, C., Warmbold, N., Farkas, Z., Schieker, M., Aszodi, A., Clausen-Schaumann, H. (2016). Structural and mechanical properties of the proliferative zone of the developing murine growth plate cartilage assessed by atomic force microscopy. *Matrix Biology*, 50, 1-15. doi: 10.1016/j.matbio.2015.10.001

Pritchett, J.W. (1992). Longitudinal growth and growth-plate activity in the lower extremity. *Clinical Orthopaedics and Related Research*, (275), 274-279.

Racine, H.L., Meadows, C.M., Ion, G., & Serrat, M.A. (2018). Heat-induced limb length asymmetry has functional impact on weight bearing in mouse hindlimbs. *Frontiers in Endocrinology*, 9, 289. doi: 10.3389/fendo.2018.00289

Raimann, A., Javanmardi, A., Egerbacher, M., & Haeusler, G. (2017). A journey through growth plates: tracking differences in morphology and regulation between the spine and the long bones in a pig model. *The Spine Journal*, 17(11), 1674-1684. doi: 10.1016/j.spinee.2017.06.001

Ranke, M.B., Savage, M.O., Chatelain, P.G., Preece, M.A., Rosenfeld, R.G., Blum, W.F., et al. (1995b). Insulin-like growth factor I improves height in growth hormone insensitivity: two years' results. *Hormone Research*, 44(6), 253-264. doi: 10.1159/000184637

Ranke, M.B., Savage, M.O., Chatelain, P.G., Preece, M.A., Rosenfeld, R.G., & Wilton, P. (1999). Long-term treatment of growth hormone insensitivity syndrome with IGF-1. Results of the European Multicentre Study. The Working Group on Growth Hormone Insensitivity Syndromes. *Hormone Research in Paediatrics*, 51(3), 128-134. doi: 10.1159/000023345

Ranke, M.B. (1995a). Growth hormone therapy in Turner syndrome. *Hormone Research*, 44(3), 35-41. doi: 10.1159/000184672

Refolo, M.G., D'Alessandro, R., Lippolis, C., Carella, N., Cavallini, A., Messa, C., et al. (2017). IGF-1R tyrosine kinase inhibitors and Vitamin K1 enhance the antitumor effects of Regorafenib in HCC cell lines. *Oncotarget*, 8(61), 103465-103476. doi: 10.18632/oncotarget.21403

- Reich, A., Sharir, A., Zelzer, E., Hacker, L., Monsonego-Ornan, E., & Shahar, R. (2008). The effect of weight loading and subsequent release from loading on the postnatal skeleton. *Bone*, *43*(4), 766-774. doi: 10.1016/j.bone.2008.06.004
- Reilly, J.F., Mizukoshi, E., & Maher, P.A. (2004). Ligand dependent and independent internalization and nuclear translocation of fibroblast growth factor (FGF) receptor 1. *DNA and Cell Biology*, *23*(9), 538-548. doi: 10.1089/dna.2004.23.538
- Reinecke, M., Schmid, A.C., Heyberger-Meyer, B., Hunziker, E.B., & Zapf, J. (2000). Effect of growth hormone and insulin-like growth factor I (IGF-I) on the expression of IGF-I messenger ribonucleic acid and peptide in rat tibial growth plate and articular chondrocytes in vivo. *Endocrinology*, *141*(8), 2847-2853. doi: 10.1210/endo.141.8.7624
- Repudi, S.R., Patra, M., & Sen, M. (2013). WISP3-IGF1 interaction regulates chondrocyte hypertrophy. *Journal of Cell Science*, *126*(7), 1650-1658. doi: 10.1242/jcs.119859
- Resende, R.A., Kirkwood, K.N., Deluzio, K.J., Morton, A.M., & Fonseca, S.T. (2016). Mild leg length discrepancy affects lower limbs, pelvis and trunk biomechanics of individuals with knee osteoarthritis during gait. *Clinical Biomechanics*, *38*, 1-7. doi: 10.1016/j.clinbiomech.2016.08.001
- Rinderknecht, E., & Humbel, R.E. (1978a). The amino acid sequence of human insulin-like growth factor I and its structural homology with proinsulin. *The Journal of Biological Chemistry*, *253*, 2769-2776.
- Rinderknecht, E., & Humbel, R.E. (1978b). Primary structure of human insulin-like growth factor II. *FEBS Letters*, *89*(2), 283-286. doi: 10.1016/0014-5793(78)80237-3
- Rivkees, S., Bode, H.H., & Crawford, J.D. (1988). Long-term growth in juvenile acquired hypothyroidism: the failure to achieve normal adult stature. *The New England Journal of Medicine*, *318*(10), 599-602. doi: 10.1056/NEJM198803103181003
- Rolian, C. (2008). Developmental basis of limb length in rodents: evidence for multiple divisions of labor in mechanisms of endochondral bone growth. *Evolution & Development*, *10*(1), 15-28. doi: 10.1111/j.1525-142X.2008.00211.x
- Ross, J.L., Lee, P.A., Gut, R., & Germak, J. (2015). Attaining genetic height potential: Analysis of height outcomes from the ANSWER Program in children treated with growth hormone over 5 years. *Growth Hormone & IGF Research*, *25*(6), 286-293. doi: 10.1016/j.ghir.2015.08.006
- Rush, W.A., & Steiner, H.A. (1946). A study of lower extremity length inequality. *The American Journal of Roentgenology Radium Therapy and Nuclear Medicine*, *56*(5), 616-623.

Sabharwal, S., Nelson, S.C., & Sontich, J.K. (2015). What's new is limb lengthening and deformity correction. *The Journal of Bone & Joint Surgery*, 97(16), 1375-1384.

Salmon, W.D., & Daughaday, W.H. (1957). A hormonally controlled serum factor which stimulates sulfate incorporation by cartilage in vitro. *Journal of Laboratory and Clinical Medicine*, 49, 825-836.

Sandberg, D.E. (2000). Should short children who are not deficient in growth hormone be treated. *Western Journal of Medicine*, 172(3), 186-189. doi: 10.1136/ewjm.172.3.186

Schell, L.M., Gallo, M.V., & Ravenscroft, J. (2009). Environmental influences on human growth and development: historical review and case study of contemporary influences. *Annals of Human Biology*, 36(5), 459-477. doi: 10.1080/03014460903067159

Schlechter, N.L., Russell, S.M., Greenberg, S., Spencer, E.M., & Nicoll, C.S. (1986). A direct growth effect of growth hormone in rat hindlimb shown by arterial infusion. *American Journal of Physiology-Endocrinology and Metabolism*, 250(3), E231-235. doi: 10.1152/ajpendo.1986.250.3.E231

Scholander, P.F. (1955). Evolution of climatic adaption in homeotherms. *Evolution*, 9(1), 15-26. doi: 10.2307/2405354

Schrier, L., Ferns, S.P., Barnes, K.M., Emons, J.A., Newman, E.I., Nisson, O., et al. (2006). Depletion of resting zone chondrocytes during growth plate senescence. *Journal of Endocrinology*, 189(1), 27-36. DOI: 10.1677/joe.1.06489

Schwab, S.A. (1977). Epiphyseal injuries in the growing athlete. *Canadian Medical Association Journal*, 117(6), 626-630.

Senay, L.C. Jr, Prokop, L.D., Cronau, L., & Hertzman, A.B. (1963). Relation of local skin temperature and local sweating to cutaneous blood flow. *Journal of Applied Physiology*, 18(4), 781-785. doi: 10.1152/jappl.1963.18.4.781

Sengupta, P. (2013). The laboratory rat: relating its age with human's. *International Journal of Preventive Medicine*, 4(6), 624-630.

Serrat, M., King, D., & Lovejoy, C.O. (2008). Temperature regulates limb length in homeotherms by directly modulating cartilage growth. *Proceedings of the National Academy of Sciences*, 105(49), 19348-19353. doi: 10.1073/pnas.0803319105

Serrat, M. (2013). Allen's rule revisited: temperature influences bone elongation during a critical period of postnatal development. *The Anatomical Record*, 296(10), 726-731. doi: 10.1002/ar.22763

- Serrat, M.A., & Ion, G. (2017). Imaging IGF-I uptake in growth plate cartilage using in vivo multiphoton microscopy. *Journal of Applied Physiology*, 123(5), 1101-1109. doi: 10.1152/jappphysiol.00645.2017
- Serrat, M.A., Efaw, M.L., & Williams, R.M. (2014a). Hindlimb heating increases vascular access of large molecules to murine tibial growth plates measured by in vivo multiphoton imaging. *Journal of Applied Physiology*, 116(4), 425-438. doi: 10.1152/jappphysiol.01212.2013
- Serrat, M.A., Lovejoy, C.O., & King, D. (2007). Age- and site-specific decline in insulin-like growth factor-I receptor expression is correlated with differential growth plate activity in the mouse hindlimb. *The Anatomical Record: Advances in Integrative Anatomy and Evolutionary Biology*, 290(4), 375-381. doi: 10.1002/ar.20480
- Serrat, M.A., Schlierf, T.J., Efaw, M.L., Shuler, F.D., Godby, J., Stanko, L.M., et al. (2015). Unilateral heat accelerates bone elongation and lengthens extremities of growing mice. *Journal of Orthopaedic Research*, 33(5), 692-98. doi: 10.1002/jor.22812
- Serrat, M.A., Williams, R.M. & Farnum C.E. (2009). Temperature alters solute transport in growth plate cartilage measured by in vivo multiphoton microscopy. *Journal of Applied Physiology*, 106(6), 2016-2025. doi: 10.1152/jappphysiol.00295.2009
- Serrat, M.A., Williams, R.M., & Farnum, C.E. (2010) Exercise mitigates the stunting effect of cold temperature on limb elongation in mice by increasing solute delivery to the growth plate. *Journal of Applied Physiology*, 109(6), 1869-1879. doi: 10.1152/jappphysiol.01022.2010
- Serrat, M.A. (2014b). Environmental temperature impact on bone and cartilage growth. *Comprehensive Physiology*, 4, 621-655. doi: 10.1002/cphy.c130023
- Shapiro, F. (1982). Developmental patterns in lower-extremity length discrepancies. *The Journal of Bone & Joint Surgery*, 64(5), 639-651. doi: 10.2106/00004623-198264050-00001
- Shapiro, I.M., Adams, C.S., Freeman, T. & Srinivas, V. (2005). Fate of the hypertrophic chondrocyte: microenvironmental perspectives on apoptosis and survival in the epiphyseal growth plate. *Birth Defects Research Part C: Embryo Today: Reviews*, 75(4), 330-339. doi: 10.1002/bdrc.20057
- Sheng, M.H.C., Zhou, Z.D., Bonewald, L.F., Baylink, D.J., & Lau, K.H.W. (2013). Disruption of the insulin-like growth factor-1 gene in osteocytes impairs developmental bone growth in mice. *Bone*, 52, 133-144. doi: 10.1016/j.bone.2012.09.027
- Shim, K.S. (2015). Pubertal growth and epiphyseal fusion. *Annals of Pediatric Endocrinology & Metabolism*, 20(1), 8-12. doi: 10.6065/apem.2015.20.1.8

- Shinar, D.M., Endo, N., Halperin, D., Rodan, G.A., & Weinreb, M. (1993). Differential expression of insulin-like growth factor-I (IGF-I) and IGF-II messenger ribonucleic acid in growing rat bone. *Endocrinology*, 132(3), 1158-1167. doi: 10.1210/endo.132.3.8440176
- Silvestrini, G., Ballanti, P., Patacchioli, F.R., Mocetti, P., Di Grezia, R., Wedard, et al. (2000). Evaluation of apoptosis and the glucocorticoid receptor in the cartilage growth plate and metaphyseal bone cells of rats after high-dose treatment with corticosterone. *Bone*, 26(1), 33-42. doi: 10.1016/S8756-3282(99)00245-8
- Simpson, M.E., Asling, C.W., & Evans, H.M. (1950). Some endocrine influences on skeletal growth and differentiation. *Yale Journal of Biology and Medicine*, 23(1), 1-27.
- Sims, N.A., Clément-Lacroix, P., Da Ponte, F., Bouali, Y., Binart, N., Moriggl, et al. (2000). Bone homeostasis in growth hormone receptor-null mice is restored by IGF-1 but independent of Stat5. *The Journal of Clinical Investigation*, 106(9), 1095-1103. doi: 10.1172/JCI10753
- Sjögren, K., Liu, J.L., Blad, K., Skrtic, S., Vidal, O., Wallenius, V. et al. (1999). Liver-derived insulin-like growth factor I (IGF-I) is the principal source of IGF-I in blood but is not required for postnatal body growth in mice. *Proceedings of the National Academy of Sciences of the United States of America*, 96(12), 7088-7092.
- Smith, L.E., Shen, W., Perruzzi, C., Soker, S., Kinose, F., Xu, X., et al. (1999). Regulation of vascular endothelial growth factor-dependent retinal neovascularization by insulin-like growth factor-1 receptor. *Nature Medicine*, 5(12), 1390-1395. doi: 10.1038/70963
- Soerensen, D.D., & Pedersen, L.J. (2015). Infrared skin temperature measurements for monitoring health in pigs: a review. *Acta Veterinaria Scandinavica*, 57(1), 5. doi: 10.1186/s13028-015-0094-2
- Sonekatsu, M., Sonohata, M., Kitajima, M., Kawano, S., & Mawatari, M. (2018). Total hip arthroplasty for patients with residual poliomyelitis at a mean eight years of follow-up. *Acta Medica Okayama*, 72(1), 17-22. doi: 10.18926/AMO/55658
- Song, C.W., Chelstrom, L.M., Levitt, S.H., & Haumschild, D.J. (1989). Effects of temperature on blood circulation measured with the laser Doppler method. *International Journal of Radiation Oncology*Biophysics*, 17(5), 1041-1047. doi: 10.1016/0360-3016(89)90153-3
- Song, K.M., Halliday, S.E., & Little, D.G. (1997). The effect of limb-length discrepancy on gait. *The Journal of Bone and Joint Surgery (American Volume)*, 79(11), 1690-1698. doi: 10.2106/00004623-199711000-00011

- Spira, E., & Farin, I. (1967). The vascular supply to the epiphyseal plate under normal and pathological conditions. *Acta Orthopaedica Scandinavica*, 38(1-4), 1-22. doi: 10.3109/17453676708989615
- Stempel, J., Fritsch, H., Pfaller, K., & Blumer, M.J., (2011). Development of articular cartilage and the metaphyseal growth plate: the localization of TRAP cells, VEGF, and endostatin. *Journal of Anatomy*, 218(6), 608-618. doi: 10.1111/j.1469-7580.2011.01377.x
- Stevens, D.A., Hasserjian, R.P., Robson, H., Siebler, T., Shalet, S.M., & Williams, G.R. (2000). Thyroid hormones regulate hypertrophic chondrocyte differentiation and expression of parathyroid hormone-related peptide and its receptor during endochondral bone formation. *Journal of Bone and Mineral Research*, 15(12), 2431-42. doi: 10.1359/jbmr.2000.15.12.2431
- Stevens, P.M. (2016). The role of guided growth as it relates to limb lengthening. *Journal of Children's Orthopaedics*, 10(6), 479-486. doi: 10.1007/s11832-016-0779-8
- Stevenson, S., Hunziker, E.B., Hermann, W., & Schenk, R.K. (1990). Is longitudinal bone growth influenced by diurnal variation in the mitotic activity of chondrocytes of the growth plate? *Journal of Orthopaedic Research*, 8(1), 132-135. doi: 10.1002/jor.1100080117
- Su, N., Jin, M., & Chen, L. (2014). Role of FGF/FGFR signaling in skeletal development and homeostasis: learning from mouse models. *Bone Research*, 2, 14003. doi: 10.1038/boneres.2014.3
- Tahimic, C.G.T., Wang, Y., & Bikle, D.D. (2013). Anabolic effects of IGF-1 signaling on the skeleton. *Frontiers in Endocrinology*, 4, 6. doi: 10.3389/fendo.2013.00006
- Tattersall, G.J., & Milson, W.K. (2003). Transient peripheral warming accompanies the hypoxic metabolic response in the golden-mantled ground squirrel. *Journal of Experimental Biology*, 206(1), 33-42. doi: 10.1242/jeb.00057
- Tattersall, G.J. (2016). Infrared thermography: a non-invasive window into thermal physiology. *Comparative Biochemistry and Physiology Part A: Molecular & Integrative Physiology*, 202, 78-98. doi: 10.1016/j.cbpa.2016.02.022
- TenBroek, E.M., Yunker, L., Nies, M.F., & Bendele, A.M. (2016). Randomized controlled studies on the efficacy of antiarthritic agents in inhibiting cartilage degeneration and pain associate with progression of osteoarthritis in the rat. *Arthritis Research & Therapy*, 18(1), 24. doi: 10.1186/s13075-016-0921-5
- Tilkens, M.J., Wall-Scheffler, C., Weaver, T.D., & Steudel-Numbers, K. (2007). The effects of body proportions on thermoregulation: an experimental assessment of Allen's rule. *Journal of Human Evolution*, 53(3), 286-291. doi: 10.1016/j.jhevol.2007.04.005

- Todd, B.J., Fraley, G.S., Peck, A.C., Schwartz, G.J., & Etgen, A.M. (2007). Central insulin-like growth factor 1 receptors play distinct roles in the control of reproduction, food intake, and body weight in female rats. *Biology of Reproduction*, 77(3), 492-503. doi: 10.1095/biolreprod.107.060434
- Togrul, E., Bayram, H., Gulsen, M., Kalaci, A., & Ozabarlas, S. (2005). Fractures of the femoral neck in children: long-term follow-up in 62 hip fractures. *Injury*, 36(1), 123-130. doi: 10.1016/j.injury.2004.04.010
- Tritos, N.A. & Klibanski, A. (2016). Effects of growth hormone on bone. *Progress in Molecular Biology and Translational Science*, 138, 193-211. doi: 10.1016/bs.pmbts.2015.10.008
- Truesdell, E.D., (1921). Inequality of the lower extremities following fracture of the shaft of the femur in children. *Annals of Surgery*, 74(4), 498-500.
- Trueta, J. & Amato, V.P. (1960). The vascular contribution to osteogenesis. III. Changes in the growth cartilage caused by experimentally induced ischaemia. *The Bone and Joint Journal*, 42-B, 571-587.
- Trueta, J. (1968). *Studies of the development and decay of the human frame*. William Heinemann Medical Books, London.
- Tryfonidou, M.A., Hazewinkel, H.A., Riemers, F.M., Brinkhof, B., Penning, L.C., & Karperien, M. (2010). Intraspecies disparity in growth rate is associated with differences in expression of local growth plate regulators. *American Journal of Physiology-Endocrinology and Metabolism*, 299(6), E1044-52. doi: 10.1152/ajpendo.00170.2010
- Turner, T.A. (2001). Diagnostic thermography. *Veterinary Clinics of North America: Equine Practice*, 17(1), 95-113. doi: 10.1016/S0749-0739(17)30077-9
- Uchimura, T., Hollander, J.M., Nakamura, D.S., Liu, Z., Rosen, C.J., Georgakoudi, I., et al. (2017). An essential role for IGF2 in cartilage development and glucose metabolism during postnatal long bone growth. *Development*, 144(19), 3533-3546. doi: 10.1242/dev.155598
- Ueki, I., Ooi, G.t., Tremblay, M.L., Hurst, K.R., Bach, L.A., & Boisclair, Y.R. (2000). Inactivation of the acid labile subunit gene in mice results in mild retardation of postnatal growth despite profound disruptions in the circulating insulin-like growth factor system. *Proceedings of the National Academy of Sciences USA*, 97(12), 6868-6873. doi: 10.1073/pnas.120172697
- Ulici, V., Hoenselaar, K.D., Gillespie, J.R., & Beier, F. (2008). The P13K pathway regulates endochondral bone growth through control of hypertrophic chondrocyte differentiation. *BMC Developmental Biology*, 11(8), 40. doi: 10.1186/1471-213X-8-40.

- Vail, B., Prentice, P., Dunger, D.B., Hughes, I.A., Acerini, C.L., & Ong, K.K. (2015). Age at weaning and infant growth: primary analysis and systemic review. *The Journal of Pediatrics*, 167(2), 317-325.e1. doi: 10.1016/j.jpeds.2015.05.003
- van der Eerden, B.C.J., Karperien, M., & Wit, J.M. (2003). Systemic and local regulation of the growth plate. *Endocrine Reviews*, 24(6), 782-801. doi: 10.1210/er.2002-0033
- Vitale, M.A., Choe, J.C., Sesko, A.M., Hyman, J.E., Lee, F.Y., Roye, D.P., et al. (2006). The effect of limb length discrepancy on health-related quality of life: is the '2cm rule' appropriate? *Journal of Pediatric Orthopaedics B*, 15(1), 1-5. doi: 10.1097/01202412-200601000-00001
- Vortkamp, A., Lee, K., Lanske, B., Segre, G.V., Kronenberg, H.M., & Tabin, C.J. (1996). Regulation of rate of cartilage differentiation by Indian hedgehog and PTH-related protein. *Science*, 273(5275), 613-622. doi: 10.1126/science.273.5275.613
- Vu, T.H., Shipley, J.M., Bergers, G., Helms, J.A., Hanahan, D., Shapiro, S.D., et al. (1998). MMP-9/gelatinase B is a key regulator of growth plate angiogenesis and apoptosis of hypertrophic chondrocytes. *Cell*, 93(3), 411-422. doi: 10.1016/S0092-8674(00)81169-1
- Walker, K.V.R., & Kember, N.F. (1972). Cell kinetics of growth cartilage in the rat tibia. *Cell Proliferation*, 5(5), 409-419. doi: 10.1111/j.1365-2184.1972.tb00378.x
- Walzer, S.M., Cetin, E., Grübl-Barabas, R., Sulzbacher, I., Rueger, B., Girsch, W., et al. (2014). Vascularization of primary and secondary ossification centres in the human growth plate. *BMC Developmental Biology*, 14(1), 36. doi: 10.1186/s12861-014-0036-7
- Wang, E., Wang, J., Chin, E., Zhou, J., & Bondy, C.A. (1995). Cellular patterns of insulin-like growth factor system gene expression in murine chondrogenesis and osteogenesis. *Endocrinology*, 136(6), 2741-2751. doi: 10.1210/endo.136.6.7750499
- Wang, J., Zhou, J., & Bondy, C.A. (1999). Igf1 promotes longitudinal bone growth by insulin-like actions augmenting chondrocyte hypertrophy. *The FASEB Journal*, 13(14), 1985-1990. doi: 10.1096/fasebj.13.14.1985
- Wang, J., Zhou, J., Cheng, C.M., Kopchick, J.J., & Bondy, C.A. (2004). Evidence supporting dual, IGF-I-independent and IGF-I-dependent, roles for GH in promoting longitudinal bone growth. *Journal of Endocrinology*, 180(2), 247-255.
- Wang, L., Shao, Y.Y., & Ballock, R.T. (2010). Thyroid hormone-mediated growth and differentiation of the growth plate chondrocytes involves IGF-1 modulation of beta-catenin signaling. *Journal of Bone and Mineral Research*, 25(5), 1138-1146. doi: 10.1002/jbmr.5.

Wang, Q., Fong, R., Mason, P., Fox, A.P., & Xie, Z. (2014). Caffeine accelerates recovery from general anesthesia. *Journal of Neurophysiology*, 111(6), 1331-1340. doi: 10.1152/jn.00792.2013

Wang, Y., Cheng, Z., Elalieh, H.Z., Nakamura, E., Nguyen, M.T., Mackem, S., et al. (2011). IGF-1R signaling in chondrocytes modulates growth plate development by interacting with the PTHrP/Ihh pathway. *Journal of Bone and Mineral Research*, 26(7), 1437-1446. doi: 10.1002/jbmr.359

Wang, Y., Nishida, S., Sakata, T., Elalieh, H.Z., Chang, W., Halloran, B.P., et al. (2006). Insulin-like growth factor-I is essential for embryonic bone development. *Endocrinology*, 147(10), 4753-4761. doi: 10.1210/en.2006-0196

Wen, Z., Zeng, W., Jingxing, D., Zhou, X., Yang, C., Duan, F., et al. (2012). Paravertebral fascial massage promotes brain development of neonatal rats via the insulin-like growth factor 1 pathway. *Neural Regeneration Research*, 7(15), 1185-1191. doi: 10.3969/j.issn.1673-5374.2012.15.010

White, S.C., Gilchrist, L.A., & Wilk, B.E. (2004). Asymmetric limb loading with true or simulated leg-length differences. *Clinical Orthopaedics and Related Research*, 421, 287-292. doi: 10.1097/01.blo.0000119460.33630.6d

Wildemann, B., Schmidmaier, G., Ordel, S., Stange, R., Haas, N.P., & Raschke, M. (2003). Cell proliferation and differentiation during fracture healing are influenced by locally applied IGF-1 and TGF-beta1: comparison of two proliferation markers, PCNA and BrdU. *Journal of Biomedical Materials Research Part B: Applied Biomaterials*, 65(1), 150-156. doi: 10.1002/jbm.b.10512

Williams, R.M., Zipfel, W.R., Tinsley, M.L., & Farnum, C.E. (2007). Solute transport in growth plate cartilage: in vitro and in vivo. *Biophysical Journal*, 93(3), 1039-1050. doi: 10.1529/biophysj.106.097675

Wilsman, N.J., Bernardini, E.S., Leiferman, E., Noonan, K., & Farnum, C.E. (2008). Age and pattern of the onset of differential growth among growth plates in rats. *Journal of Orthopaedic Research*, 26(11), 1457-1465. doi: 10.1002/jor.20547

Wilsman, N.J., Farnum, C.E., Green, E.M., Leiferman, E.M., & Clayton, M.K. (1996a). Cell cycle analysis of proliferative zone chondrocytes in growth plates elongating at different rates. *Journal of Orthopaedic Research*, 14(4), 562-572. doi: 10.1002/jor.1100140410

Wilsman, N.J., Farnum, C.E., Leiferman, E.M., Fry, M., & Barreto, C. (1996b). Differential growth by growth plates as a function of multiple parameters of chondrocytic kinetics. *Journal of Orthopaedic Research*, 14(6), 927-936. doi: 10.1002/jor.1100140613

- Wilson, P.D., & Thompson, T.C. (1939). A clinical consideration of the methods of equalizing leg length. *Annals of Surgery*, 110(6), 992-1015. doi: 10.1097/00000658-193912000-00002
- Wirth, T., Syed Ali, M.M., Rauer, C., Süß, D., Griss, P., & Syed Ali, S. (2002). The blood supply of the growth plate and the epiphysis: a comparative scanning electron microscopy and histological experimental study in growing sheep. *Calcified Tissue International*, 70(4), 312-319. doi: 10.1007/s00223-001-2006-x
- Wit, J.M., & Oostdijk, W. (2015). Novel approaches to short stature therapy. *Best Practice & Research Clinical Endocrinology & Metabolism*, 29(3), 353-366. doi: 10.1016/j.beem.2015.01.003
- Woodall, S.M., Breier, B.H., O'Sullivan, U., & Gluckman, P.D. (1991). The effect of the frequency of subcutaneous insulin-like growth factor-1 administration on weight gain in growth hormone deficient mice. *Hormone and Metabolic Research*, 23(12), 581-584. doi: 10.1055/s-2007-1003760
- Woods, K.A., Camacho-Hubner, C., Savage, M.O., & Clark, A.J. (1996). Intrauterine growth retardation and postnatal growth failure associated with deletion of the insulin-like growth factor I gene. *New England Journal of Medicine*, 335(18), 1363-1367. doi: 10.1056/NEJM199610313351805
- Wray, J.B., & Goodman, H.O. (1961). Post-fracture vascular phenomena and long-bone overgrowth in the immature skeleton of the rat. *The Journal of Bone & Joint Surgery*, 43(7), 1047-1055. doi: 10.2106/00004623-196143070-00014
- Wu, S., Yang, W., & De Luca, F. (2015). Insulin-like growth factor independent effects of growth hormone on growth plate chondrogenesis and longitudinal bone growth. *Endocrinology*, 156(7), 2541-2551. doi: 10.1210/en.2014-1983
- Wu, Y., Sun, H., Basta-Pljakic, J., Cardoso, L., Kennedy, O.D., Jasper, H., et al. (2013). Serum IGF-1 is insufficient to restore skeletal size in the total absence of the growth hormone receptor. *Journal of Bone and Mineral Research*, 28(7), 1575-1586. doi: 10.1002/jbmr.1920
- Yakar, S., & Isaksson, O. (2016). Regulation of skeletal growth and mineral acquisition by the GH/IGF-1 axis: Lessons from mouse models. *Growth Hormone & IGF Research*, 28, 26-42. doi: 10.1016/j.ghir.2015.09.004
- Yakar, S., Courthland, H.W., & Clemmons, D. (2010). IGF-1 and bone: new discoveries from mouse models. *Journal of Bone and Mineral Research*, 25(12), 2267-2276. doi: 10.1002/jbmr.234

Yakar, S., Jiu, J.L., Stannard, B., Butler, A., Accili, D., Sauer, B., et al. (1999). Normal growth and development in the absence of hepatic insulin-like growth factor I. *Proceedings of the National Academy of Sciences USA*, 96(13), 7324-9. doi: 10.1073/pnas.96.13.7324

Yakar, S., Rosen, C.J., Beamer, W.G., Ackert-Bicknell, C.L., Wu, Y., Liu, J.L., et al. (2002). Circulating levels of IGF-1 directly regulate bone growth and density. *Journal of Clinical Investigation* 110(6):771-81. doi: 10.1172/JCI0215463

Yan, H., Mitschelen, M., Bixier, G.V., Brucklacher, R.M., Farley, J.A., Han, S., et al. (2011). Circulating IGF1 regulates hippocampal IGF1 levels and brain gene expression during adolescence. *Journal of Endocrinology*, 211(1), 27-37. doi: 10.1530/JOE-11-0200

Yin, M., Guan, X., Liao, Z., & Wei, Q. (2009). Insulin-like growth factor-1 receptor-targeted therapy for non-small cell lung cancer: a mini review. *American Journal of Translational Research*, 1(2), 101-114.

Zelzer, E., & Olsen, B.R. (2005). Multiple roles of vascular endothelial growth factor (VEGF) in skeletal development, growth, and repair. *Current Topics in Developmental Biology*, 65, 169-87. doi: 10.1016/S0070-2153(04)65006-X

Zhang, P., Hamamura, K., Turner, C.H., & Yokota, H. (2010). Lengthening of mouse hindlimbs with joint loading. *Journal of Bone and Mineral Metabolism*, 28(3), 268-275. doi: 10.1007/s00774-009-0135-x

Zhou, X., von der Mark, K., Henry, S., Norton, W., Adams, H., & de Cromburghe, B. (2014). Chondrocytes transdifferentiate into osteoblasts in endochondral bone during development, postnatal growth and fracture healing in mice. *PLoS Genetics*, 10(12), e1004820. doi: 10.1371/journal.pgen.1004820

Zhou, Y., Xu, B.C., Maheshwari, H.G., He, L., Reed, M., Lozykowski, M., et al. (1997). A mammalian model for Laron syndrome produced by targeted disruption of the mouse growth hormone receptor/binding protein gene (the Laron mouse). *Proceedings of the National Academy of Sciences*, 94(24), 13215-13229. doi: 10.1073/pnas.94.24.13215

Zipfel, W.R., Williams, R.M., & Webb, W.W. (2003). Nonlinear magic: multiphoton microscopy in the biosciences. *Nature Biotechnology*, 21(11), 1369-1377. doi: 10.1038/nbt899

Zoetis, T., Tassinari, M.S., Bagi, C., Walthall, K., & Hurtt, M.E. (2003). Species comparison of postnatal bone growth and development. *Birth Defects Research Part B: Developmental and Reproductive Toxicology* 68(2), 86-110. doi: 10.1002/bdrb.10012

APPENDIX A: INSTITUTIONAL REVIEW BOARD APPROVAL



Office of Research Integrity

July 16, 2018

Holly Racine
121 Howard Ave
Brownsville, PA 15417

Dear Ms. Racine:

This letter is in response to the submitted thesis abstract entitled "*Targeted Limb Heating Augments the Actions of IGF1 in the Growth Plate and Increases Bone Elongation in Growing Mice.*" After assessing the abstract it has been deemed not to be human subject research and therefore exempt from oversight of the Marshall University Institutional Review Board (IRB). The Institutional Animal Care and Use Committee (IACUC) has reviewed and approved the study under protocol #558. The applicable human and animal federal regulations have set forth the criteria utilized in making this determination. If there are any changes to the abstract you provided then you would need to resubmit that information to the Office of Research Integrity for review and a determination.

I appreciate your willingness to submit the abstract for determination. Please feel free to contact the Office of Research Integrity if you have any questions regarding future protocols that may require IRB review.

Sincerely,

Bruce F. Day, ThD, CIP
Director

WE ARE... MARSHALL.

One John Marshall Drive • Huntington, West Virginia 25755 • Tel 304/696-4303
A State University of West Virginia • An Affirmative Action/Equal Opportunity Employer

APPENDIX B: LIST OF ABBREVIATIONS

ABC...avidin-biotin complex

ALS...acid labile subunit

BMP...bone morphogenic protein

BrdU...bromodeoxyuridine

CD31...cluster of differentiation 31

DAPI...4',6-diamidino-2-phenylindole

EDTA...ethylenediaminetetraacetic acid

ERK...extracellular receptor kinase

FGF...fibroblast growth factor

GH...growth hormone

GHR^{-/-}...growth hormone receptor knockout

GnRH...gonadotropin releasing hormone

GP...growth plate

H₂O₂...hydrogen peroxide

HSP...heat-shock protein

HZ...hypertrophic zone of growth plate cartilage

IF...immunofluorescence

IGF1...insulin-like growth factor 1

IGF1R...insulin-like growth factor 1 receptor

IGF2...insulin-like growth factor 2

IGFBP...insulin-like growth factor binding protein

IHC...immunohistochemistry

Ihh...Indian hedgehog
LID...liver IGF1-deficient
LLD...limb length discrepancy
MAPK... mitogen-activated protein kinase
MPM...multiphoton microscopy
OTC...oxytetracycline
pAkt...phosphorylated Akt
PBS...phosphate buffered solution
PCNA...proliferating cell nuclear antigen
PECAM1 (CD31)...platelet endothelial cell adhesion molecule
PI-3...phosphatidylinositol-3
PI3K...phosphoinositide 3-kinase
pIGF1R...phosphorylated insulin-like growth factor 1 receptor
PTHrP...parathyroid hormone-related protein
PZ...proliferative zone of growth plate cartilage
RZ...reserve zone of growth plate cartilage
SD...standard deviation
SE...standard error
SQ...subcutaneous
T3...triiodothyronine
TKI...tyrosine kinase inhibitors
TR α 1...thyroid hormone receptor alpha 1
TR β ...thyroid hormone receptor beta

VEGF...vascular endothelial growth factor

WISP3...Wnt induced secreted protein 3

Wnt...wingless/integrated

APPENDIX C: CURRICULUM VITAE

Holly L. Racine (Tamski), BS

CURRENT POSITION:

PhD Candidate
Department of Biomedical Science
Joan C. Edwards School of Medicine
Marshall University

CONTACT INFORMATION:

121 Howard Ave
Brownsville, PA 15417
Phone: (724)-787-1141
Email: tamski@marshall.edu

EDUCATION:

2008 Hempfield Area High School
2008-09 Mercyhurst College, Major: Forensic Anthropology/Biochemistry
2009-12 Seton Hill University, BS, Biochemistry
Expect 2018 Marshall University, PhD, Biomedical Sciences (Dr. Maria Serrat, Mentor)

PROFESSIONAL/HONORARY MEMBERSHIP:

2013-pres Member of Sigma Xi, The Scientific Research Society
2013-pres Member of the American Physiological Society
2013-pres Member of the American Association of Anatomists
2012-pres Graduate Student Organization (Biomedical Sciences Program)
Marshall University- **Secretary** July 2013-August 2014
2009-12 Member of the American Chemical Society
2009-12 Chemistry Club, Seton Hill University
2010 Certified EMT (Pennsylvania)
2008-09 International Student Organization, Mercyhurst College
2006-07 National French Honor Society

AWARDS/HONORS:

2017 American Association of Anatomists Travel Award, Experimental Biology Meeting in Chicago, IL
2016 American Association of Anatomists Travel Award, Experimental Biology Meeting in San Diego, CA
2015 American Association of Anatomists Travel Award, Experimental Biology Meeting in Boston, MA
2014 American Association of Anatomists Travel Award, Experimental Biology Meeting in San Diego, CA
2012 Academic Achievement Award, Department of Chemistry, Seton Hill University
2008-09 Dean's List for Academic Achievement, Mercyhurst College
2008 Pennsylvania Certificate of Distinction, Advanced Level in Mathematics on PSSA

AWARDS/HONORS CONT'D:

- 2008 Pennsylvania Certification of Distinction, Advanced Level in Reading on PSSA
- 2008 Outstanding Scholar Award, Hempfield Area High School

TEACHING EXPERIENCE:

- 2017 Introduction of Cell Structure and Metabolism- Teaching graduate level Cytoskeleton lectures (3hrs)- Marshall University, Huntington, WV
- 2016 Introduction of Cell Structure and Metabolism- Teaching graduate level Cytoskeleton lectures (3hrs)- Marshall University, Huntington, WV
- 2013 Frontiers in Aging and Regenerative Medicine Course- Senior Teaching Assistant- University of Pittsburgh-Xavier University, New Orleans, LA
- 2011 Frontiers in Stem Cell and Regenerative Medicine Course- Teaching Assistant- University of Pittsburgh-MBL, Woods Hole, MA

EXPERIMENTAL TECHNIQUES:

- 1) Preparation of experimental slides for Immunocytochemistry
- 2) Cell culture
 - a. Bio-safety level 2
- 3) Cell counting using a hemocytometer
- 4) MTT cell viability assay
- 5) Flow cytometry
- 6) Microarray
 - a. Total mRNA extraction
 - b. cDNA synthesis
- 7) Western Blotting
- 8) Quantitative Reverse Transcription- PCR
- 9) Bone Histology
 - a. Safranin O/Fast Green staining
 - b. Immunohistochemistry
 - c. Immunofluorescence
- 10) Multiphoton microscopy
 - a. Stereoscopy
- 11) Fluorescent microscopy
- 12) Infrared thermal imaging
- 13) Mouse limb bone dissections
- 14) Live animal experiments with anesthesia
- 15) Subcutaneous injection in a mouse
- 16) Intraperitoneal injection in a mouse
- 17) Cardiac puncture for blood collection in a mouse
- 18) ELISA of blood serum
- 19) X-Ray imaging using IVIS In-vivo Imager
- 20) Incapacitance meter weight bearing measurements

Ph.D. DISSERTATION:

Marshall University, expected August 2018

GRANTS/FELLOWSHIPS:

1. Unilateral heating to increase IGF1 uptake and bone length in mice. NASA WV Space Grant Consortium, Graduate Research Fellowship. April 15, 2014- April 20, 2015. \$12,000.

PUBLICATIONS:

1. **Racine HL**, Meadows CA, Ion G, Serrat MA. 2018. Heat induced limb length asymmetry has functional impact on weight bearing in mouse hindlimbs. *Front of Endocrinol.* 9:289. doi:10.3389/fendo.2018.00289.
2. Serrat MA, Schlierf TJ, Efaw ML, Shuler FD, Gidby J, Stanko LM, **Tamski HL**. 2015. Unilateral heat accelerates bone elongation and lengthens extremities of growing mice. *J Orthop Res.* 33(5):692-8 doi:10.1002/jor.22812.
3. Fei J, **Tamski H**, Cook C, Santanam N. 2013. MicroRNA regulation of adipose derived stem cells in aging rats. *PLoS One.* 8(3). Epub: March 14, 2013

ABSTRACTS AND PRESENTATIONS: NATIONAL AND INTERNATIONAL:

1. **HL Racine**, CA Meadows, G Ion, MA Serrat. Inhibiting IGF1 Activity in the Proximal Tibial Growth Plate Attenuates the Bone-Lengthening Effects of Temperature in Hindlimbs of Growing Mice (6136). **Competitively Selected for Podium Presentation** at the American Association of Anatomists Annual Meeting at Experimental Biology in Chicago, IL. April 2017.
2. **HL Racine**, G Ion, JC Kerby, MX Gray, CA Meadows, MA Serrat. Thermal Imaging Reveals Temperature Retention in Hindlimbs of Mice Up to 4 Hours after Targeted Intermittent Limb Heating. Presented at the annual 2016 Experimental Biology Meeting in San Diego, CA. March 2016. Poster #1032.2.
3. M.A. Serrat, **H.L. Racine**, G. Ion, J.C. Kerby, C.A. Meadows. Low Dose IGF-1 Augments the Bone-Lengthening Effect of Targeted Heat in the Mouse Hindlimb. 2016 Experimental Biology Meeting in San Diego, CA. March 2016. Poster #1032.1.
4. Maria A. Serrat, Gabriela Ion, **Holly Racine**, and Jenna Kerby. 2015. Low dose IGF-1 augments the bone lengthening effect of targeted heat in the mouse hindlimb. 2015 ASBMR Meeting in Seattle, WA. October 2015. Poster #MO0416.
5. **HL Tamski**, M Gray and MA Serrat. Infrared Thermal Imaging to Collect Quantitative Surface Temperature from Mice in Unilateral Limb Heating Study. Presented at the annual 2015 Experimental Biology Meeting in Boston, MA. March 2015. Poster #869.2.
6. J. Kerby, M. Gray, **H. Tamski**, A. Heaberlin, N. Crow, G. Ion and M.A. Serrat. 2015. Temperature Enhanced Extremity Lengthening is Growth Rate Dependent. Presented at the annual 2015 Experimental Biology Meeting in Boston, MA. March 2015. Poster #686.5.

ABSTRACTS AND PRESENTATIONS: NATIONAL AND INTERNATIONAL CONT'D:

7. **Holly Tamski** and Maria A. Serrat. 2014. Validation of a unilateral heating model to increase hindlimb length in growing mice (342.4). **Competitively Selected for Podium Presentation** at the American Association of Anatomists Annual Meeting at Experimental Biology in San Diego, CA. April 2014. The FASEB Journal. 28(1).
8. Maria A. Serrat, Thomas J. Schlierf, Morgan L. Efaw, Franklin D. Shuler, Justin Godby, Laura M. Stanko, **Holly L. Tamski**. 2014. Unilateral Heat Accelerates Bone Elongation and Lengthens Extremities of Growing Mice. **Selected for Podium Presentation** at the 60th Annual Meeting of the Orthopedic Research Society in New Orleans, LA. March 2014.
9. Nalini Santanam, **Holly Tamski** and Carla Cook. 2013. Omega-6 Fatty Acid Modulates MiRNA Profile in Microgravity Cultured Adipocytes. Presented at the 2013 Endocrine Society Meeting in San Francisco, CA. June 2013. SUN 6490677-Adipocyte Biology
10. Nalini Santanam, Melissa Massie, Myriaha Selbe, Logan Efaw, Courtney Crain, Carla Cook, **Holly Tamski**. 2013. Omega3-Rich Diet Modulates Leptin through Lipid Sensing G-Protein Coupled Receptors in Catalase Transgenic Mice. Presented at the 2013 American Heart: Arteriosclerosis, Thrombosis, and Vascular Biology Meeting in Lake Buena Vista, FL. May 2013. Abstract #166.
11. **Holly Tamski**. 2012. L. Variegatus Immunocytochemistry: Effects of Anti-Cancer Drug Monastrol on Embryo Development. Presented at the 2012 American Chemical Society Meeting in San Diego, CA. March 2012.
12. Amanda K Leonard, Lauren Freeman, **Holly Tamski**, Demetra Czegan. 2012. Seton Hill University's outstanding chemistry club: Enriching campus and community. Presented at the 2012 American Chemical Society Meeting in San Diego, CA. March 2012. Poster #1491.

ABSTRACTS AND PRESENTATIONS: REGIONAL:

1. **HL Racine**, CA Meadows, G Ion, MA Serrat. Inhibiting IGF1 Activity in the Proximal Tibial Growth Plate Attenuates the Bone-Lengthening Effects of Temperature in Hindlimbs of Growing Mice. Presented at the Regional American Association of Anatomists Meeting in Pittsburgh, PA. November 2017. Poster #28.
2. **Holly L Racine**. 2017. Blocking IGF1 Activity in Skeletal Growth Plates Reduces Limb Lengthening Effects of Temperature in Growing Mice. **Selected for Oral Presentation** at the 29th Annual Research Day, Marshall University Medical Center Huntington, WV. March 2017.
3. **Racine HL**, Ion G, Kerby JC, Meadows CA, Serrat MA. 2016. Thermal imaging reveals temperature retention in hindlimbs of mice up to 4 hours after targeted intermittent limb heating. Presented at the 28th Annual Research Day, Huntington WV. March 2016.
4. **Holly Tamski**, Justin Godby, Laura Stanko and Maria A Serrat. 2014. Development of a unilateral heating model to increase hindlimb length in growing mice. Presented at Marshall University Research Retreat, Huntington WV. August 2014.

ABSTRACTS AND PRESENTATIONS: REGIONAL CONT'D:

5. **Holly Tamski**, L.M. Stanko, J. Gorby, M.A. Serrat. 2013. Unilateral Heat as a Potential Therapy for Limb Length Inequalities. Presented at the Appalachian Regional Cell Conference in Charleston, WV. November 2013.
6. **Holly Tamski**. 2013. MicroRNA Regulation of Adipose Derived Stem Cells. **Selected for Oral Presentation** at the 25th Annual Research Day, Marshall University Medical Center Huntington, WV. March 2013.

REFERENCES:

1. Maria Serrat, PhD, Associate Professor, Department of Biomedical Sciences, Marshall University, Phone: (304)696-7392, Email: serrat@marshall.edu
2. Todd Green, PhD, Associate Professor & Co-Director of Biomedical Sciences, Marshall University, Phone: (304)696-3531, Email: green@marshall.edu
3. Beverly Delidow, PhD, Associate Professor, Department of Biomedical Sciences, Marshall University, Phone: (304)696-7266, Email: delidow@marshall.edu
4. Richard Egleton, PhD, Associate Professor, Research Cluster Coordinator & Co-Director of Biomedical Sciences, Marshall University, Phone: (304)696-3523, Email: egleton@marshall.edu